Final Report

Award Number: DE-FG36-08GO88004

Recipient: University of Hartford
200 Bloomfield Avenue
West Hartford, CT

Project Title: Effect of Component Failures on Financial Status of Grid-Connected Photovoltaic Systems[1]

Principal Investigator: Barry T. Lubin, PhD, PE

Date of Report: February 28, 2012

[1] Title changed from: **Evaluation of Economic Benefits of Distributed Photovoltaic Systems**

Table of Contents

Acknowledgments

The following people participated in all or portions of this project.

University of Hartford

Can Algan
Jeffrey Cohen, PhD
Earl Hasselmark
Muhammad Ishaq
Kathy Kruse
Lou Manzione, PhD
Spring Raymond
Beth Richards
Hemchandra Shertuke, PhD

Consultants

Joel Gordes, Environmental Solutions
Joseph Quinn, Alstom Power, RPI Hartford
William Stillinger, CEO PV^2
Mike Prucker, Palmetto Group
Congressman John Larson

Advisory Committee

Joseph Debs, Connecticut Light & Power
Roddy Diotalevi, United Illuminating Co.
Dale Hedman, Connecticut Clean Energy Fund
Dominick Lauria, Connecticut Light & Power
Devang Patel, United Illuminating Co.
Joel Reinbold, Connecticut Center for Advanced Technology
Michael Roy, Hartford Steam & Boiler Insurance Co.

Principal Investigator

Barry T. Lubin, PhD, PE

Nomenclature

NOTATION	DEFINITION	UNITS
A	Availability	-
CDF=F(t)	Cumulative Distribution Function	
E	Energy	Watt-hours
ELCC	Electrical Load Carrying Capacity	-
F(t)	Failure	-
GCPVS	Grid Connected Photovoltaic System	-
IGBT	Insulated Gate Bipolar Transistors	-
MPP	Maximum Power Point	Watts
MTBF	Mean Time Before Failure	-
MTTF	Mean Time to Failure	Time
MTTR	Mean Time to Repair	Time
MultiC_Risk	Multiple Component Risk	-
NPV	Net Present Value	Dollars-Cents
NREL	National Renewable Energy Laboratory	-
OEM	Original Equipment Manufacturer	-
P	Power	Watts
P	Probability	-
PCU	Power Control Unit	-
PDF= f(t)	Probability Density Function	-
PSCAD	Power System Computer Aided Design	-
PV	Photovoltaic	-
R(t)	Reliability	-
SEMS	Solar Economics Modeling Spreadsheets	-
SNL	Sandia National Laboratory	-
TBF	Time Before Failure	Time
TTR	Time to Repair	Time
β	Weibull Shape parameter	-
η	Weibull Scale parameter	Time $^{-1}$
λ	Failure Rate	Time $^{-1}$
μ	Repair Rate	Time $^{-1}$
ϒ	Weibull Location parameter	Time
Q	Un-Availability	-
I_n	Current	Amps
Vn	Voltage	Voltage
Pn	Power	Watts
$T_K(N)$	Temperature Coefficient	%/^oC
f	Frequency	cycles/second
L	Inductance	henry (H)
C	Capacitor	farad (F)
i	Discount rate	%

Nomenclature, *continued*		
Co	Initial Investment	$
B_t	Benefits @ time=t	$

Subscripts

n	denotes subscript
p	maximum power
oc	open circuit
sc	short circuit
sh	shunt

Executive Summary

This report describes an applied research program to assess the realistic costs of grid connected photovoltaic (PV) installations. A Board of Advisors was assembled that included management from the regional electric power utilities, as well as other participants from companies that work in the electric power industry. Although the program started with the intention of addressing effective load carrying capacity (ELCC) for utility-owned photovoltaic installations, results from the literature study and recommendations from the Board of Advisors led investigators to the conclusion that obtaining effective data for this analysis would be difficult, if not impossible. The effort was then re-focused on assessing the realistic costs and economic valuations of grid-connected PV installations.

The 17 kW PV installation on the University of Hartford's Lincoln Theater was used as one source of actual data. The change in objective required a more technically oriented group. The re-organized working group (changes made due to the need for more technically oriented participants) made site visits to medium-sized PV installations in Connecticut with the objective of developing sources of operating histories. An extensive literature review helped to focus efforts in several technical and economic subjects. The objective of determining the consequences of component failures on both generation and economic returns required three analyses.

The first was a Monte-Carlo-based simulation model for failure occurrences and the resulting downtime. Published failure data, though limited, was used to verify the results. A second model was developed to predict the reduction in or loss of electrical generation related to the downtime due to these failures. Finally, a comprehensive economic analysis, including these failures, was developed to determine realistic net present values of installed PV arrays.

Two types of societal benefits were explored, with quantitative valuations developed for both. Some societal benefits associated with financial benefits to the utility of having a distributed generation capacity that is not fossil-fuel based have been included into the economic models. Also included and quantified in the models are several benefits to society more generally: job creation and some estimates of benefits from avoiding greenhouse emissions. PV system failures result in a lowering of the economic values of a grid-connected system, but this turned out to be a surprisingly small effect on the overall economics.

The most significant benefit noted resulted from including the societal benefits accrued to the utility. This provided a marked increase in the valuations of the array and made the overall value proposition a financially attractive one, in that net present values exceeded installation costs. These results indicate that the Department of Energy and state regulatory bodies should consider focusing on societal benefits that create economic value for the utility, confirm these quantitative values, and work to have them accepted by the utilities and reflected in the rate structures for power obtained from grid-connected arrays. Understanding and applying the economic benefits evident in this work can significantly improve the business case for grid-connected PV installations. This work also indicates that the societal benefits to the population are real and defensible, but not nearly as easy to justify in a business case as are the benefits that accrue directly to the utility.

Effect of Component Failure on Economics of Distributed Photovoltaic Systems

1 BACKGROUND

In the last ten years the use of photovoltaic (PV) systems has grown from owner roof-top units in the watt (W) and kilowatt (kW) range to utility owned and operated solar "farms" generating megawatts (MW). This growth in installation of grid-connected PV systems (GCPVS) has been driven by the reduction in price per W responding to economies of scale. Thus, there has been a steady progression from private homes (W) to big-box stores and corporate parks (kWs) to utilities (MW) serving cities and states as well as nationally through local spot markets.

Although improvements have been introduced, these installations are still based on the original silicon-based solar cells and the same cells-modules-arrays design configuration. However, as this expansion continues it is not unreasonable to expect continued improvements to be introduced such as different materials and/or higher efficiency for the solar cells. In some cases, these advances will lower the cost per W produced, meaning that larger installations can be realized with the same level of investment. The progress in increased efficiency will mean a smaller footprint and space required to realize a given capacity. The number of interconnects per kW produced will also decline as each array becomes more productive and fewer arrays are needed.

This report documents efforts to develop a procedure, using performance results from these improved units, to understand and quantify failures vs. operating time, which lead to loss of generation, which in turn lead to the effects of downtime on revenue and expenses.

1.1 SCOPE OF PROPOSED PROGRAM

The original scope of the proposed program sought to develop the relationship between both electrical generation performance and financial performance.

The proposal was based on the concept of electrical load carrying capacity (ELCC). This concept was first introduced by Garver [1-1] and developed further by Perez and Margolis [1-2]. Perez and Margolis introduced the use of solar energy to be considered in the generating capacity that utilities need to maintain. When considered, solar generation provides a number of monetary and nonmonetary benefits, or "values" [1-3, 1-4] to various sectors of the economy, e.g., private owners, third-party owners and publicly owned utilities, which in many states can now own and operate renewable generation.

A number of similar methods are used by utilities to credit renewable energy in their generation capacity. However, a lack of consensus by a cross-section of utilities in preferring one method over another [1-5] makes it difficult to use a single method, such as Perez's concept of taking credit for usable solar generated power, to produce an approach acceptable to utilities.

A review of the numerous references on GCPVS shows that the types of reliability problems have evolved. While early PV systems encountered reliability problems with components such as the solar cells and modules themselves, this eventually gave way to more failures with the components and subsystems in the inverters. Furthermore, although numerous studies were completed and results documented in journal and conference papers, particularly by Department of Energy National Renewable Energy Laboratory (NREL) and Sandia National Laboratory (SNL), much of the needed reliability data were unavailable.

1.2 CHANGE IN SCOPE

In addition to the lack of an available robust database, it became evident that causes of many problems—particularly related to the modules and inverters—were identified, and design improvements mitigated a number of these failures.

However, as systems become larger, future problems with these significantly larger arrays remain unknown. As with inverters, these failures can be assumed to be stochastic (random). Thus, over the long operating times of these passive systems, some classes of failures will emerge, and others may prove to be of little or no concern.

Although the probability of occurrence vs. time before failure may not follow the overused normal distribution, solar arrays will have values of time to failure (TTF) both longer and shorter than the mean time before failure (MTBF).

The shorter and longer times to failure will generally have low probabilities characteristic of a Gaussian, or normal, distribution of time to failure. Other failure profiles feature “infant mortality” where a significant fraction of devices fail soon after initial assembly or powering up. Yet another failure profile is “wear out” when there is little failure over most of the expected lifetime of the system, but then a rapidly increasing rate of failures as the wear-out time approaches.

These limiting values of failure rate depend on the cause of the failures. They can be small or large, and they all have some impact on time to repair.

Replacement or repair of failed components can result in long periods of suboptimal production and significant losses in solar generated power (W), and thus electrical generation in Watt-hours (Wh). The loss in energy due to the downtime while the repair is made can incur unanticipated costs, not only for labor and parts, but also for the need to purchase electricity on the spot market. These costs could impact the expenses, income, and payback period of the installation, resulting in changes in the balance sheets on which the decision to build the facility was made.

Advances in generation and control may accompany larger future installations as the price for solar cells is reduced. These low-probability events with significant impacts represent the so-called “black swans” where “improbable” events occur and have a major impact on either generation or financial performance, or both.

Of interest are two studies that concentrate on performance and failure. The first, a study by the Canadian Centre for Mineral and Energy Technology [1-6], is summarized as follows:

1. PV system “availability” (on-line and fully operational): 95% (90% of systems >90%, 55% of systems >99%; (inverters account for 63% of failures, modules 15%, and ”other” 23%)
2. PV system “performance ratio” (how much of the available solar energy is converted to electrical energy) = 0.7-0.8
3. PV system failure every 4.5 years, on average
4. For a large (3.5 MW) plant comprising 26 subsystems, there were 150 unscheduled maintenance events over 5 years (mean time between services = 7.7 months)
5. These “events” comprised failures in the data acquisition systems, inverter, junction boxes, PV array, and AC disconnect. Other causes included a lightning strike, high contact resistance, lack of auto reset in inverter, failure of module blocking diodes, and rodents.
6. The report also noted a 2003 study in Japan where 45% of system failures were due to inverter problems (such as component failure, instability, power failure, shift to power limit mode). In this study, it was found that the MTBF was 3.55 years, mean time to failure (MTTR) was 24.6 days, and overall system availability was 99.74%.

The second study is by Maish, et al. [1-7] of the SNL:

1. Availabilities ranged from 83.5 to 98.3%
2. Inverter problems accounted for 76% of failures
3. Mean time to repair (MTTR) ranged from 19 days to 173 days
4. System time to failure ranged from 1 to 16 years
5. An inverter failure occurred every 1.65 years

6. A monitoring of 126 systems showed 190 failure events, 12 of which were module problems due to ground faults, dead or shattered modules, and wiring problems. Maintenance costs ranged from 0.4 cents/kWh to 7.6 cents/kWh. A properly designed and maintained system, with MTBF in the 20-year range, should have operation and maintenance costs <1 cent/kWh.

Based on these data it would seem that failures do occur, but information on these failures is limited by commercial concerns. Although both the NREL and SNL have actively promoted a failure database, results of this effort are, apparently, limited to the participating original equipment manufacturers and the national laboratories.

Thus, while this project maintained the objective of relating generation performance to financial performance, the revised scope will not follow the ELCC approach but will concentrate on developing a method to relate economic performance to failures that result in the loss of or reduction in generation, the subsequent effect of these failures on repair/replacement, and the overall impact on expenses and revenue, that is: failures lead to loss of power, which leads to loss of energy, which leads to decreases in revenues and increases in expenses.

1.3 STATUS OF PHOTOVOLTAIC GENERATION

Between 1998 and 2008 (Figure 1-1)[2] PV-based electrical generation has seen a 10^3 increase in installed power. This increase has seen changes from generation in W, primarily residential units, to kW for both residential and commercial installations. Recently MW-rated units have evolved as public utilities follow state mandates to add renewable energy capacity to their base and to include specified percentages of renewable energy capacity (Figure 1-2). This increase is due in part to the reduction in cost of the manufacture of solar modules, the direct increases in income associated with lower investments per kW produced, and, in part, to increased reliability and accompanying increase in availability. Improvements in reliability are believed to be related to improvements in modules and inverters.

However, as installations continue to increase in capacity, it can be assumed that the introduction of new components, subsystems, and system configurations will continue to add complexity to PV installations. The improved efficiency of solar cells means that each cell/module will carry an increasing percent of the generated power. Thus failure of a module (e.g., an inverter component) will result in replacement cost for the lost power. In this case this process includes the following three actions: failure, generation rate change, and repair.

Figure 1-1: Growth in PV Installations and Capacity

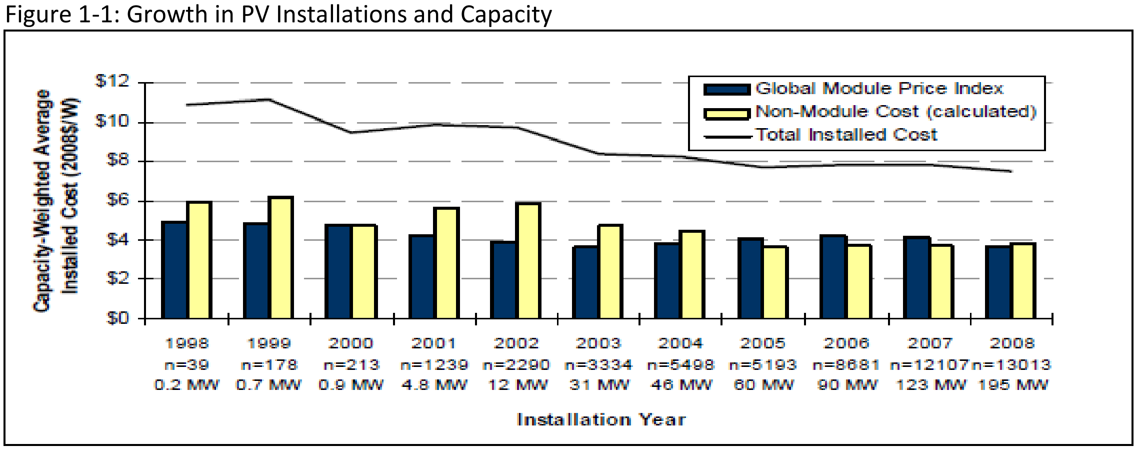

[2] "Module & Non-Module Cost Trends Over Time," Lawrence-Berkeley National Laboratory (Wiser et al., 2009).

Figure 1-2: Representation of Increase in Generation and Applications for PV Installations

Residential≈ Watts	Commercial≈ Kilowatts	Utilities≈ Megawatts

1.4 OBJECTIVE

Based on existing work on performance of PV cells/modules/arrays/systems, the objective of this program is to develop an analysis to determine the effect of component failures and societal benefits on the net present value (NPV) of a GCPVS.

1.5 PHASES OF THE WORK

Phase 1: Investigation of including the ELCC as part of a utility documented capacity [1-3]. This line of investigation was dropped based on lack of agreement on how different utilities credit or realize financial valuations based on ELCC, which would interfere with other methods already used to determine capacity.

Phase 2: The original objective of relating generation performance to economic performance, with minor changes, stayed the same. The method was changed to meet the objective by determining the influence of failures, subsequent loss of or reduction in generation, costs for repair and/or replacement, and purchase of replacement power on the installation's NPV. The effect of societal benefits was also considered and incorporated into the NPV analysis when defensible benefits were identified and quantified. Reviews of pertinent references were used to establish the calculation modules for failures, generation, and costs for repair and/or replacement.

Phase 3: Methods appropriate for the calculations in each module were completed. Output from each was the input for the following module. Demonstration cases were completed as a means of validating that the process worked and the results were acceptable. Documentation in this report is based on these results.

1.6 REFERENCES: BACKGROUND

1-1. Garver, L.L. "Effective Load Carrying Capability of Generating Units," *IEEE Transactions on Power*, v85, n8, 1966.
1-2. Perez, R., Margolis, R. "Update: Effective Load Carrying Capability of Photovoltaics in the United States," NREL/CP-620-40068, June 2006.
1-3. Hoff, T., Perez, R. "Photovoltaic Capacity Valuation Methods, SEPA Report 02-08, May 2008.
1-4. Robertson, C., Cliburn, J.K., "Utility-Driven Solar Energy as a Least-Cost Strategy to Meet RPS Policy Goals & Open New Markets," ASES Solar 2006 Conference, 2006.
1-5. Contreras, J.L., et al. "Photovoltaics Value Analysis," NREL/SR-581-42303, Feb. 2008.
1-6. Canmet Energy (Canadian Centre for Mineral and Energy Technology) Report 2010-122 (RP-TEC) 411-IEARES, March 31, 2010.
1-7. Maish, A.B., et al. "Photovoltaic System Reliability," Sandia National Laboratories, Proceedings of the 26th IEEE Photovoltaic Specialists Conference, Anaheim, CA, September 29-October 3, 1997.

2 ANALYSIS

2.1 CALCULATIONS

Predictions: There is sufficient evidence that failures, particularly of electronic components, are random. These predictions depend on detection of a failure, identification of the failed component/subsystem, and determination of the cause of the failure. From this, failure and repair rates can be determined, either from OEM-provided reliability data or calculations based on one of the standard techniques. Failing this, documentation of mean time before failure (MTBF) and, when available, mean time to repair (MTTR) was used.

Generation: Loss of or reduction in power due to this failure is the downtime multiplied by the predicted energy generated in that period of time, i.e., the power during downtime varies with time.

($Ti \leq t \leq Tf$) is:

$$E = \int_{Ti}^{Tf} P(t)dt \tag{1.}$$

Repair/Replacement: The driver impacting the income/expense number for the net present value (NPV) is the cost of the failed component(s) and labor costs for replacement of the failed components. The length of downtime includes both the identification of the failed component(s) as well as the planning, availability of the component(s), logistics of ordering a replacement, repair time if the service can be done in-house or for a contractor if it is outsourced, and the location of the failed component(s). All of these are included in the maintainability of the installation. Their influence on downtime is calculated, taking into account the types of component faults discussed below.

2.2 METHODS

2.2.1 Component Failure (MultiC_Risk)

Failure Predictions: Component failures are normally related to reliability, R (t), defined as the probability that the components will continue to perform their design functions for a specific time. However, although certain failures will result in a loss of power for one or more modules, others may result in a reduction in power of these modules [2-3, 2-6, 2-10].

The desired result would be the ability to detect the potential for a failure before it occurs. This includes inverter components, such as insulated gate bipolar transistors (IGBTs), lines between solar cells in series, and connections to junction boxes. While this has been studied for kW capacity arrays, the capability to build MW capacity systems makes it difficult, both theoretically and practically, to detect a change in current-voltage signature or power generation [2-1, 2-2, 2-15]. See Figures 2-1, 2-2, and 2-3.

With early systems, failures were dominated by inverter components such as electrolytic capacitors and transformers, and by subsystems, for example, power cooling [2-5]. Although one would expect components with low reliability to be most susceptible to failures, currently identifying the failed component involves a forensic inspection. Future efforts in identification of failed components could possibly be related to the “signature” of the component’s failure.

Figure 2-1: Normal Operation

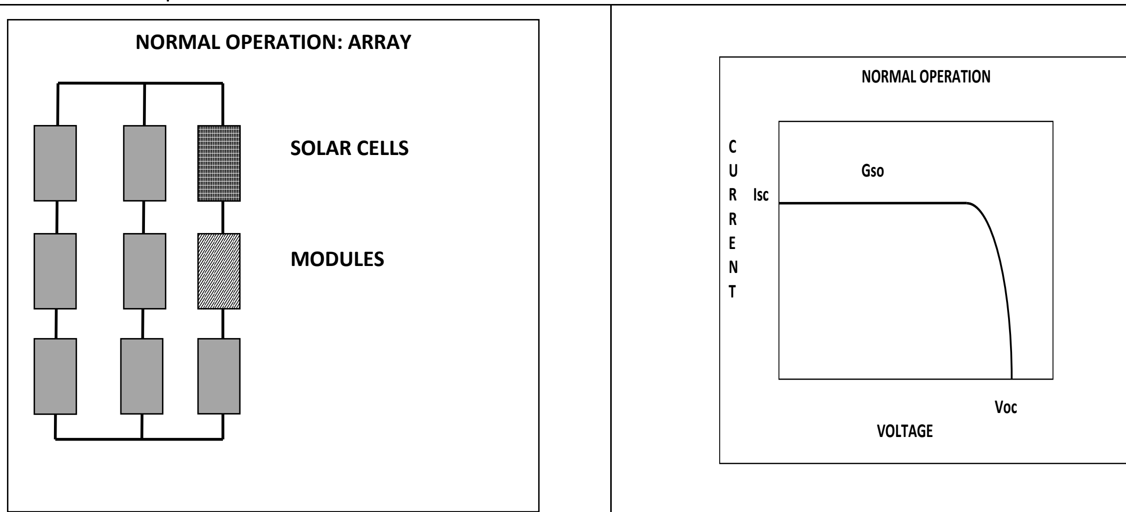

Figure 2-2: Low Resistance Faults

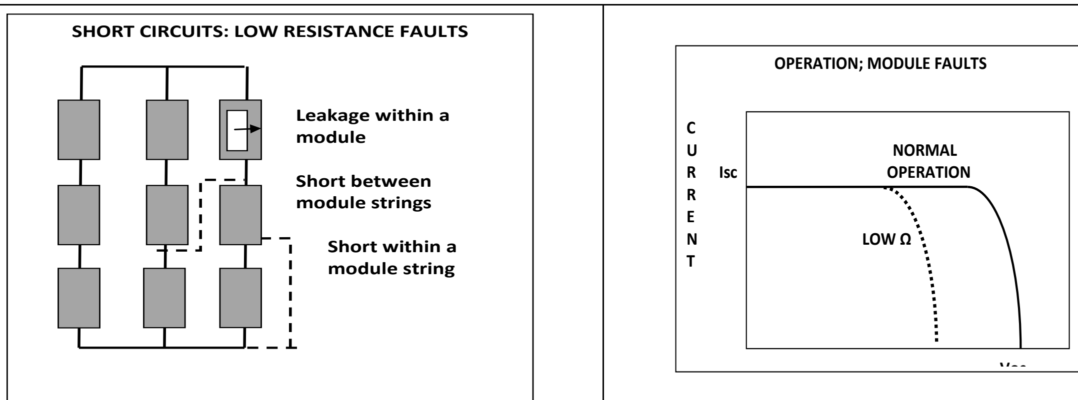

Figure 2-3: High Resistance Faults

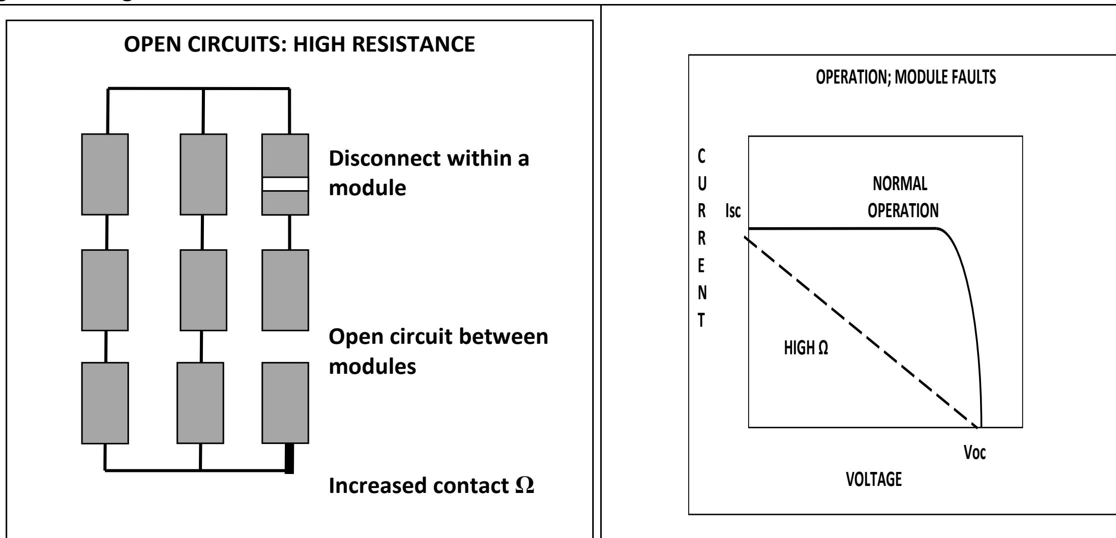

The component failure that can be verified by accelerated and performance tests is time before failure (TBF) and the time to replace or repair (TTR) the component(s) causing the failure. Based on these assumptions, the reliability is R(t) and failure, F(t), with R(t)+F(t)=1 and failure is F(t)=[1-R(t)]. The reliability, or probability of not failing, is related to the derivative of F(t); the probability density function (PDF) f(t) is f(t)=dF(t)/dt, so that R(t)=1-F(t).

For example, the reliability, based on degradation due to wear [2-16], is taken as a negative exponential function, $R(t)= \exp(-\lambda_F t)$, where λ_F is the failure rate. The failure is, then, $F(t)=1-R(t)= 1- \exp(-\lambda_F t)$. Thus the PDF is $f(t)=dF(t)/dt= -dR(t)/dt=-[- \lambda_F \exp(-\lambda_F t)]= [\lambda_F \exp(-\lambda_F t)]$.

The Weibull distribution, $f(t)=[\beta t^{\beta-1})/\eta^{\beta}][\exp[-(t/\eta)^{\beta}]$, where[3] $\beta>0$, $\eta>0$ and $t\geq 0$, is the most general PDF used since it is a good representation of failures and repairs.

The TBF and, to a lesser degree, TTR are assumed to be random. Calculations are based on the MTBF and MTTR of the components or systems. The expected, or mean, value is defined as $E(t) = \int \tau f(\tau)d\tau$. With limits on t of @t=0; τ=0 and @t=∞; τ=T, substitution for $f(\tau)= [\lambda_F \exp(-\lambda_F t)]$, and using integration by parts, E(t)=mean time $=1/\lambda_F$. Thus the mean values are equal to the inverse of the failure rate [2-14].

Reliability values, being random and not deterministic, are based on the assumption of a PDF, f(t), with a prior history of being a good approximation for similar components and conditions. A Monte-Carlo method, based on a random selection of the independent variable (in this case time) was used to calculate the probability. Simulations on the order of 10^4 are run until the distribution reaches steady state [2-14]. Ristow [2-8], evaluating one of a number of problems related to PV system's performance, used this procedure to predict mean times for the Georgia Tech Aquatic Center (GTAC) installation. This analysis and other problems were in a series of co-authored papers based on a range of topics, which included the performance of the GTAC facility [2-5, 2-7] and problems of optimizing the cost of manufacturing solar modules [2-6].

Based on input of values of MTBF and MTTR and using a Weibull distribution, a Monte-Carlo-based fault simulation program, MultiC_Risk, is used to determine the TBF and TTR.

2.2.2 Loss of or Reduction in Generation (PSCAD)

Failure of a component can result in failure of a module. Downtime to prepare for and then perform the repair or replacement means that no power or reduced power is produced—how much depends on atmospheric conditions and insolation at time of failure. Provided with information on initial and final times for downtime, a model was developed using the EMTDTC/PSCAD simulation code of the grid-connected photovoltaic system (GCPVS). Insolation data at the time of failure using the typical meteorological year (TMY2) database [2-15] for either of the two Connecticut locations (Hartford and Bridgeport) are used to calculate the lost energy.

Although this is only one of a number of similar electromagnetic transient codes, there is sufficient documentation to support this choice. Xue et al. [2-17] address the modeling of GCPVS. To accomplish this, the model includes the inverter, power controls, maximum power point tracking (MPPT), current controller, and protection hardware and software. Two cases are simulated: a single ground fault and a three-phase short circuit.

[3] η≡

Figure 2-4: Flow Chart of Input and Calculations

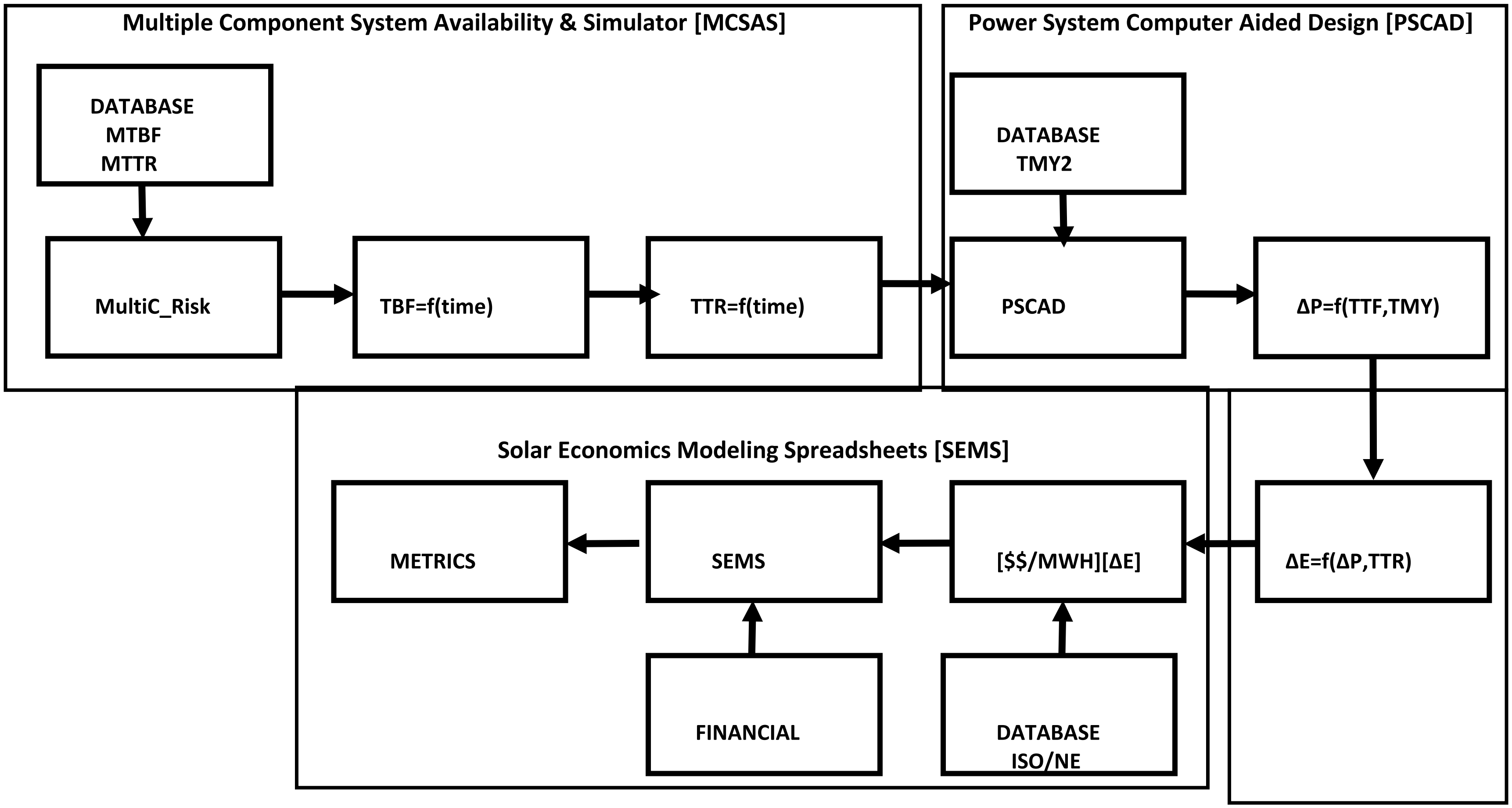

2.2.3 Evaluation of Economic and Societal Effects of PV Systems (SEMS)

The evaluation of the effect of failures and subsequent repairs on the bottom line is the objective of the economic evaluation. In keeping with generally accepted accounting methods, as with most projects, there are credits or income and debits or expenses. While the majority of these entries can be easily quantified, renewable energy presents a problem. Presently PV generation is yet to be competitive with fossil-fuel-based electrical generation. Economies of scale will continue to reduce the cost of silicon-based solar cells and continue the current trend of reduction in cost per W. This may eventually result in reducing solar power generation's present need to be subsidized. The question is how to quantify societal effects, e.g., reduction in pollution equivalent to reduction in related health [2-18, 2-19]. These effects have yet to be reflected in costs and thus in the bottom line.

In addition, while failures and subsequent repair or replacement costs are normally factored into operating budgets, increase in generation to MW-size plants could alter the costs of these failures, both in reduced generation and in hardware and labor costs.

Using data obtained from a 17kW GCPVS installed on the roof of the Lincoln Theater at the University of Hartford, performance and economic models were developed for such systems using realistic assumptions and data from the Lincoln Theater system. Attention will focus on several economic effects, societal benefits, and costs of failure that have not been emphasized in previous analyses of PV installations. These largely address the relatively new concept in industry of life cycle costing or whole life costing. The Solar Economics Modeling Spreadsheets (SEMS) are used to evaluate the economic and societal effects of PV systems.

2.3 CALCULATION MODULES

The objective of the calculations is to determine the economic impact as a function of the loss of power due to failure of one or more components. This procedure is divided into three modules:

Simulation of Failures: Failure and repair times over operating lifetime (MultiC_Risk)
Loss of Power: Loss of power and energy generated (PSCAD)
Economic Impact: Effect of this loss on economic results (SEMS)

These modules as part of the calculation procedure are shown in Figure 2-4. Key acronyms used in the three calculation modules, and elsewhere in the report, are listed in Table 2-1.

Table 2-1: Calculation Modules Acronyms

Acronym	Title	Content	Related Calculation
MTTF	Mean time to failure	Mean time until first equipment failure	
MTBF/MTTR	Mean time before failure/ Mean time to repair	Component mean times to next failure or repair	Input to MULTIC_RISK
MultiC_Risk	Multiple Component System Availability & Simulator	Monte-Carlo-based simulation of system	Failure vs. operating time
TMY2	Typical Meteorological Year	Database for solar radiation values for Connecticut	Input to PSCAD
PSCAD	Power System Computer Aided Design	Dynamic simulation of a GCPVS	GCPV response to failures
ΔP	Power Reduction	Power reduction due to component failure	PSCAD predictions based on TMY
TTR	Time to Repair	Values of random times to repair	Input to calculation of lost energy
ΔE	Energy Reduction	Lost energy due to repair of failed components	Input to financial models
ISO/NE	ISO/New England	Marginal prices for open market energy	Database marginal prices for Connecticut
SEMS	Solar Economics Modeling Spreadsheets	Effect of loss of energy on GCPVS financial projections	Energy replacement costs
METRICS	Parameters indicating the influence of failure	Expenses and income related to GCPVS performance	Influence on marginal prices

2.4 DEMONSTRATION CASES

A set of calculations will be performed to illustrate both the input and output for each of the calculation modules. Given that inverters are the major source of operational failures and subsequent loss of power, this study will focus, in spite of the lack of data on failures and repairs, on inverter components. In addition, for convenience, performance of inverter components is based on the 17kW GCPVS (Figure 2-5) installed on the roof of the Lincoln Theater at the University of Hartford, using SMA Solar Technology AG (SMA) inverters (Figure 2-6).

Figure 2-5: 17kW Lincoln Theater PV System

Figure 2-6: SMA SB-6000U Inverter Component Layout

Table 2-2 details the input and output for each of the calculation modules and their location in this report.

Table 2-2: Calculation Module Input and Output

Calculation Module	Input	Output	Comments	Section
Failure of Multiple Components	MTBF +/- ∆MTBF MTTR +/- ∆MTTR	Downtime [TBF+TTR]=f(time)	Repair is assumed to start immediately after failure	4
Modeling of GCPVS	Downtime [TBF+TTR]=f(time)	Energy Lost =∑∆P*[downtime] = f(time)	The power is based on the TMY2 data base for Hartford, CT	5
Economic Analysis	Energy Lost =∑∆P*[downtime] =f(time)	∑∆$ for replaced power	Use financial model to calculate the effect on net present value (NPV)	6

2.5 REFERENCES: ANALYSIS

2-1. Lashway, C. "Photovoltaic System Testing Techniques and Results," *IEEE Transactions on Energy Conversion*, v3, n3, Sept. 1988: 503-506.

2-2. Stellbogen, D. "Use of PV Circuit Simulation for Fault Detection in PV Array Fields," 23rd IEEE Photovoltaic Specialist Conference, 1993.

2-3. Pecht, M.G., et al. "Predicting the Reliability of Electronic Equipment," *Proceedings of the IEEE*, v82, n7, July 1994: 992-1004.

2-4. Maish, A.B., et al. "Photovoltaic System Reliability," 26th IEEE Photovoltaic Specialist Conference, Anaheim, CA, 1997: 1049-54.

2-5. Begovic, M., Pregeil, A., Rohatgi, A. "Four-year Performance Assessment of the 342kW PV System at Georgia Tech," 28th IEEE Photovoltaic Specialists Conference, Anchorage, AK, Sept. 15-22, 2000: 1575-78.

2-6. Ristow, A., Begović, M., Rohatgi, A. "Modeling the Effects of Uncertainty and Reliability on the Cost of Energy from PV Systems," 20th European Solar Energy Conference & Exhibition, Barcelona, Spain, June 6-10, 2005.

2-7. Begovic, M., Ghosh, S.R., Rohatgi, A. "Decade Performance of a Roof-Mounted Photovoltaic Array," Conference Record of the 2006 IEEE 4th World Conference, v2, May 2006: 2383-86.

2-8. Ristow, A.H. "Numerical Modeling of Uncertainty and Variability in the Technology, Manufacturing, and Economics of Crystalline Silicon Photovoltaics," PhD Thesis, Georgia Institute of Technology, August 2008.

2-9. Moore, L., Post, H., et al. "Five Years of Operating Experience at a Large, Utility-scale Photovoltaic Generating Plant," *Progress in Photovoltaics: Research and Applications*, v13, 2008: 249-59.

2-10. Collins, E., et al. "Reliability and Availability Analyses of a Fielded Photovoltaic System," IEEE 978-1 2950, Sept. 2009: 002316-2321.

2-11. Collins, E., et al. "Field Data Collection for Quantification of Reliability and Availability for PV Systems," 35th IEEE Photovoltaic Specialist Conference, June 10, 2010: SAND2010-3362-C.

2-12. Collins, E., et al. "A Reliability and Availability Sensitivity Study of a Large Photovoltaic System," Sandia National Laboratories, July 2010; 25th European Union Photovoltaic System Conference & Exhibition.

2-13. Firth, S.K., Lomas, K.J., Rees, S.J. "A Simple Model of PV System Performance and Its Use in Fault Detection," *Solar Energy*, v84, 2010: 624-35.

2-14. Andrews, J.D., Moss, T.R. *Reliability & Risk Assessment,* 2nd ed. ASME Press: 2002.

2-15. User's Manual for Typical Meteorological Year (TMY2), NREL, June 1995.

2-16. Suel, Ki Kim, et al. "Modeling and Simulation of a Grid-connected PV Generation System for Electromagnetic Transient Analysis," *Solar Energy* v83, n5, 2009: 664-78.

2-17. Xue, J., et al. "Design of PV Array Model Based on EMTDC/PSCAD," 2009 Asia-Pacific Power & Energy Engineering Conference Proceedings, March 28-31, 2009: 1-5.

2-18. Robertson, C., Cliburn, J. "Utility-Driven Solar Energy as a Least-Cost Strategy to Meet RPS Goals and Open New Markets," ASES Solar 2006 Conference.

2-19. Contreras, J., et al. "Photovoltaics Value Analysis," NREL/SR-581-42303, February 2008.

3 LITERATURE REVIEW

Entering "grid-connected photovoltaic systems" into Google produced a list of approximately $2x10^6$ documents. If nothing else, PV generation of electricity has provided gainful employment for a number of authors doing the work and publishing a large percentage of these numerous journal and conference papers. A review of a fraction of these publications noted that the great majority were produced by the Department of Energy's National Renewable Energy Laboratory (NREL) and Sandia National Laboratory (SNL).

Of the 100+ documents reviewed, the 15 most relevant to this study are summarized in this section, including relevant graphics and equations. This study looks toward the next generation of PV electrical generation. The papers, reports, and presentations included in this literature review provide a historical record of incremental improvements in the present state of the art for silicon-based solar cells, modules, and arrays.

REF	AUTHOR(S)	TITLE	PUBLICATION
A	Lashway, C.	Photovoltaic System Testing Techniques and Results	*IEEE Transactions on Energy Conversion*, v3, n3, Sept. 1988: 503-506

SUMMARY: For three years (1985-1988) the New Mexico Solar Energy Institute (NMSEI) measured and documented results of tests of eight flat-plate, silicon-based PV power plants, ranging from 20 to 1000 kW_{DC}, and in operation from one to 4 years. The objective was to determine which parameters could indicate the occurrence of component failures. Tests included recording of operating values of current-voltage characteristics and performance of a variety of components including the solar cells, connections, switches, bypass diodes, and modules. Instrumentation included a digital voltmeter, inductive current probe, pyranometer, and temperature sensors.

Tests indicated departures from usual data on current vs. voltage, particularly at conditions of maximum power. A reduction in current was associated with a problem related to the connections between modules and arrays and junction boxes. This connection also influences the current through the bypass diodes and can result in an open failure of the diode, reducing the power to zero. The faults in the power control system (PCS) were also found to influence the current vs. voltage characteristics although this can vary depending on the inverter design. Solar cells were found to continue to function, but breakage of the glass laminates were found to eventually reduce power.

Information and results for plants on tests performed are listed in the Table A-1 and Figure A-1 below.

Table A-1: Operating Information on Monitored Plants

PLANT	OPERATION		POWER[4] [kW]	MODULES	
	START	YEARS		TOTAL	FAULTS
A	Jan ‘81	4	20	576	3
B	March ‘81	4	117	3360	87
C	Sept. ‘81	4	112	3200	98
D	Feb. ‘82	4	53	1512	38
E	Aug. ‘84	3	49	1408	19
F	Aug. ‘84	2	1000	28672	14
G	Sept. ‘84	1	156	4464	96
H	July ‘85	1	683	19584	7

[4] Estimated assuming plant Fi is 1000kW=1MW

Figure A-1: Results for Non-Operating Modules and Component Failures for Monitored Plants

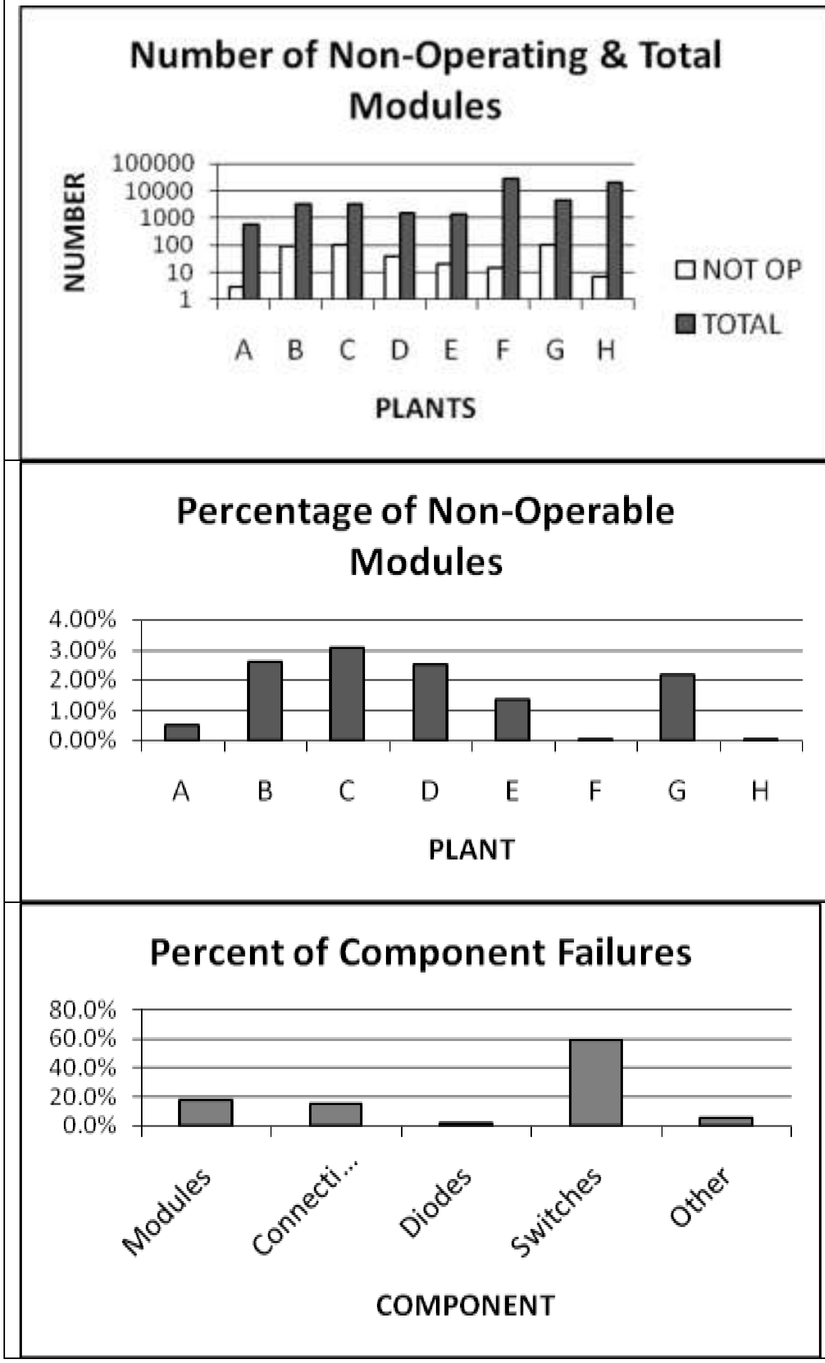

COMMENTS: From the conclusion: "The combination of these test techniques has been used by the NMSEI to successfully test many large-scale[5] PV systems in the United States and, therefore, begin the development of a database for use in tabulating PV system failures."

[5] Large-scale for the time the tests were done.

REF	AUTHOR(S)	TITLE	PUBLICATION
B	Stellbogen, D.	Use of PV Circuit Simulation for Fault Detection in PV Array Fields	23rd IEEE Photovoltaic Specialist Conference, 1993

SUMMARY: The objective of the paper was to develop a procedure for identifying potential loss of or reduction in generation due to faults related to the PV modules. This paper establishes the basis for this procedure using the PVNODE simulation program. Verification of the procedure was to be based on data from PV systems. Normal operation is represented in Figures B-1 through B-5. The representative I-V curves are based on the model, consisting of 5 strings of 6 modules each.

Faults: Reduction of or loss in power can be caused by ground faults, such as may occur in junction boxes, or current leakage from the module to the frame or faults within the modules. In general, faults can be divided into two categories:

- Low resistance connections (Figure B-2): Short circuits in a module string; leakage currents within a module; and short circuits between modules. Ground faults can be identified by monitoring power.
- High resistance connections (Figure B-3): Disconnection within a module string resulting in an open circuit, an open circuit within a module, and an increase in contact resistance. Module-related faults can be related to a departure from the normal current-voltage relationship (Figure B-1).

Detection: PV systems are usually operated at the maximum power point[6] (MPP). Current and voltage vs. time is monitored, as the system adjusts to changes in solar irradiation and cell temperature to maintain the MPP. Detection of faults is based on recording power, or voltage and current, vs. time. Examples in Figures B-4 and B-5 represent MPP monitoring vs. time, including shadowing and, for comparison, a module short circuit.

COMMENTS: The method is based on detection of the described faults and shadowing at the module level. For continuous monitoring this would need to be done at the module level, thus requiring the addition of locations between modules. For smaller units (e.g., one array) the inverter, which is usually connected to more than one parallel array, is connected to just one array. This presents another problem as to the “level” at which the monitoring is performed.

[6] Although not mentioned in the paper, the MPP hardware and software are usually part of the inverter.

Figure B-1: Normal Operation

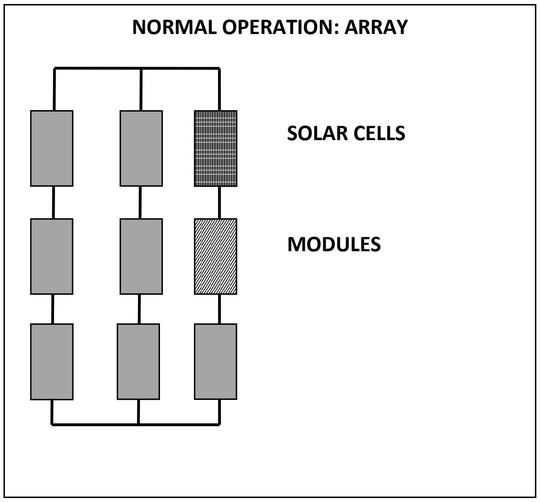

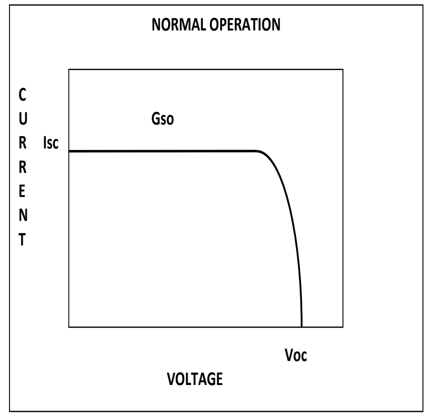

Figure B-2: Low Resistance Faults

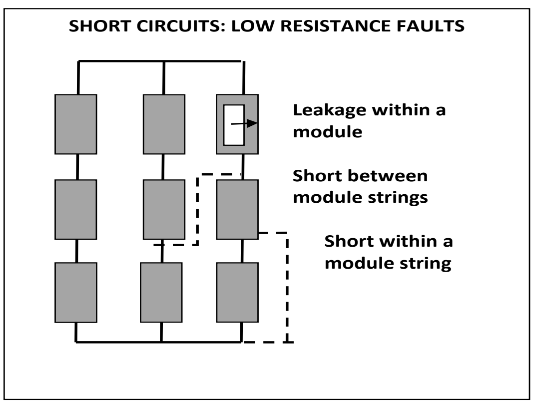

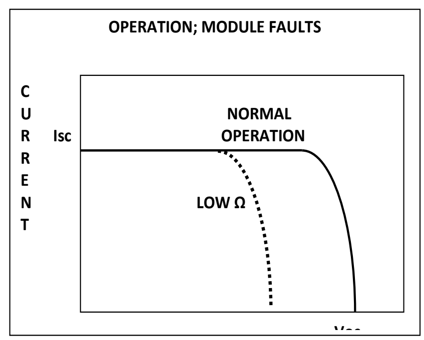

Figure B-3: High Resistance Faults

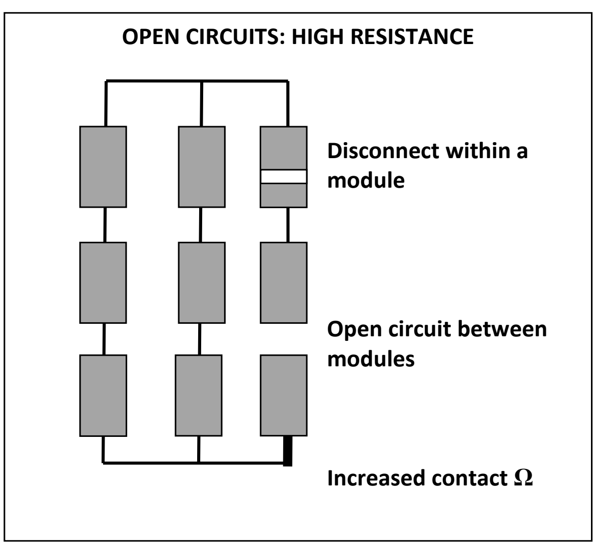

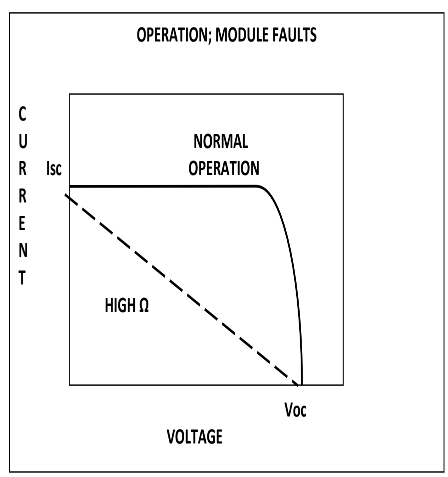

Figure B-4: MPP Monitoring: Voltage vs. Time

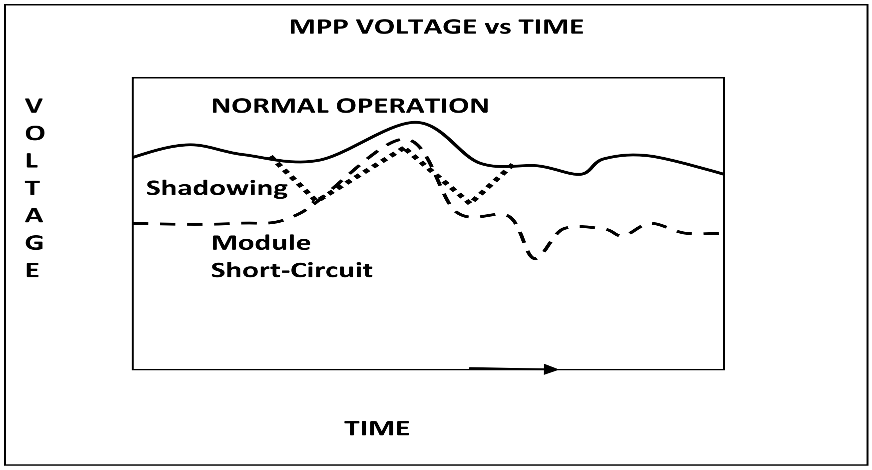

Figure B-5: MPP Monitoring: Current vs. Time

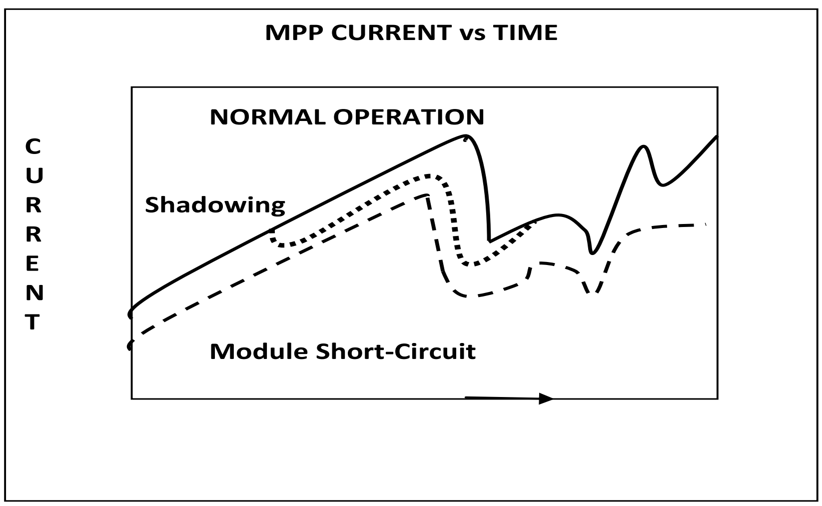

REF	AUTHOR(S)	TITLE	PUBLICATION
C	Pecht, M.G., et al.	Predicting the Reliability of Electronic Equipment	*Proceedings of the IEEE*, v82, n7, July 1994: 992-1004

SUMMARY: This article provides predictions for electronic components, particularly as related to reliability and increasing dependence on electronic control of missiles and other nuclear and conventional weapons. MIL-HDBK 217A (1965) was an early effort to develop a method, supported by test data, to predict reliability of electronic components and systems. Predictions for the most part were based on the assumption of constant failure rate. Methods were applicable to microelectronic devices, semiconductors, vacuum tubes, lasers, capacitors, relays, switches, connectors, and printed circuit boards.

In the effort to upgrade the data, methods were developed to consider how failure progresses and the factors influencing reliability. Three methodologies have been developed that account for these factors.

US MIL-HDBK-217F (Dec. 1991): This method neglects the time periods considered for initial operation and design life, based on the assumption that the time for normal operation is longer than either of these time periods.

The method, based on the assumption that the failures are random, considers categories of factors that can influence the failure rate expressed as "pi" factors, π_N, such as:

FACTORS	SYMBOLS
Temperature	π_T
Current	π_I
Duty Cycle	π_A
Loads	π_L
Environment	π_E
Base Failure Rate	λ_B=N/10^9 where N is failure with factors, π_N=1

FAILURE RATE: $\lambda = \lambda_B[\pi_T \bullet \pi_I \bullet \pi_A \bullet \pi_E] = \lambda_B \Pi[\pi_n \bullet \pi_{n+1I} \bullet\bullet\bullet \pi_N]$

Methodologies for categories and types of electronic components are listed in the latest issue of US MIL-HDBK-217[7]

Bellcore TA-TSY-000983 (Jan. 1990): The methodology developed by Bellcore is based on both the gradual degradation or degradation rate (DR) corresponding to initial operation and random failures in normal operation.

Gradual Degradation: The degradation rate of electronic components (Figure C-1) is attributed to the effects of temperature, and is expressed as $DR \propto \exp[\text{-Ea/kT}]$ where Ea is the thermal activation energy [eV], k the Boltzmann constant [eV/^{o}K], and T the absolute temperature [^{o}K] for the component of interest. Following the methodology the failure rate for gradual degradation is $\lambda_{GD} = (p/\tau_S)_{@25^o C}$ where P is the probability of failure at design time τ_S at reference temperature of @ 25^{o}C.

Random Failures: Failures during normal operation are assumed to involve manufacturing and assembly, e.g., dimensional accuracy or soldering. Per Figure C-2, unlike the gradual degradation, after ≈10^4 hours of operation, the failure rate is assumed to be constant. The failure rate is $\lambda_{RANDOM} = (1/\Sigma n_i t_i)\ln[1/(1-C)]$; where C= confidence level, ni=the aging time; ti=acceleration factors relative to the reference temperature of 25^{o}C.

[7] U.S. Department of Defense, Military Handbook for Reliability Prediction of Electronic Equipment, v. F (1991).

COMMENTS: The MIL-HDBK and Bellcore, along with Telcordia, have expanded the number of methods of calculating reliability. Even so, there are few data in the open literature that compare predicted failures with actual failures. Until this becomes available these data, if they exist, are proprietary to OEMs that are providing the data to the NREL and SNL.

Figure C-1: Electronic Components

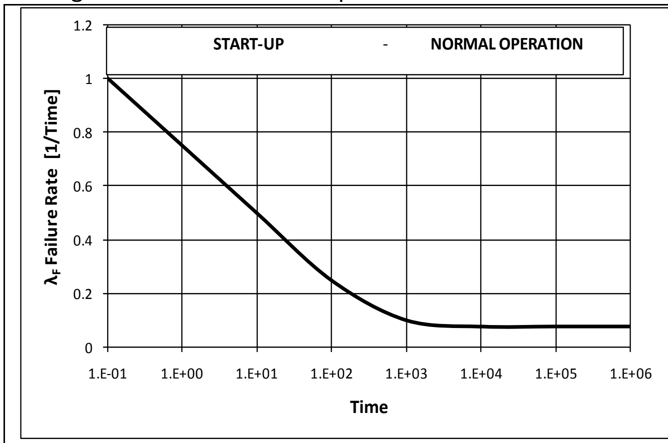

Figure C-2: Mechanical Components

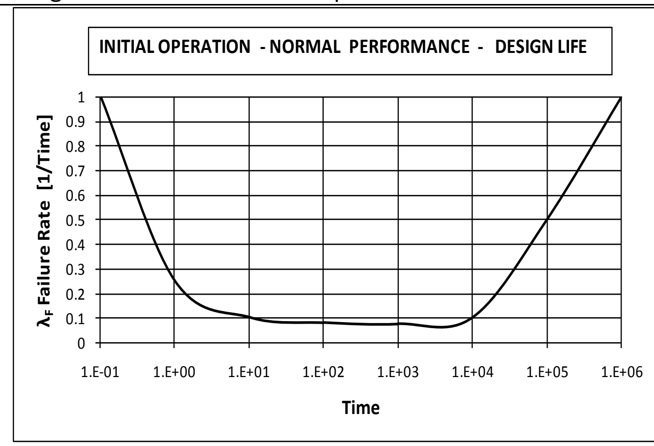

REF	AUTHOR(S)	TITLE	PUBLICATION
D	Maish, A.B., et al.	Photovoltaic System Reliability	26th IEEE Photovoltaic Specialist Conference, Anaheim, CA, 1997: 1049-54

SUMMARY: This paper is one of the first to document failures associated with PV systems. The work is based on earlier work done by Jet Propulsion Laboratory (JPL) and SNL. JPL procedure includes the following three phases: a) module testing, b) field exposure, and c) failure cause.

The objective of the SNL program was to determine the reliability of system components. The steps include: a) identification of a failure; b) forensic inspection for failed component; c) replacement or repair of the faulted component; and d) follow up to ensure acceptable operation. The information entered into the database includes: a) time to failure; b) time to repair; c) calculations for availability; and d) maintenance costs.

This approach was used in monitoring the six GCPVS installed from 1993 to 1997 as part of the Department of Energy's Million Solar Roof initiative, by the Sacramento Municipal Utility Department (SMUD). The total power rated at 1.43 MW has a total of 400 arrays. The installations were divided into subgroups monitored by SMUD and outside contractors. Based on this monitoring, though not listed in the paper, data on time before failure (TBF) and time to repair (TTR) were used to calculate mean time before failure[8] (MTBF) and mean time to repair (MTTR). It is noteworthy that this was one of the earliest documentations of repair times. A summary of MTTF and MTTR values are listed in Table A-1. Inverter-related failures, in which failed components are not identified, are shown in Figure D-1, and the mean times for failure and repair in Figure D-2.

Table D-1: SMUD Grid-Connected PV Systems

PLANTS	SMUD-S1	SMUD-S2	SMUD-R	SMUD-P	ACEN.	COLO.PRK	UNITS
YEAR	1993	1994	1995-R	1995-P	1994	1997	-
Start	Aug-96	Aug-96	Aug-96	Aug-96	Jul-93	Jan-97	-
End	Jul-97	Jul-97	Jul-97	Jul-97	Jun-96	Jul-97	-
Δ (end-start)	8.0160E+03	8.0160E+03	8.0160E+03	8.0160E+03	2.5584E+04	4.3440E+03	hours
MTBF	6.09E+04	1.39E+05	1.42E+05	9.81E+04	1.05E+04	1.18E+05	hours
MTTR	5.18E+03	1.87E+03	4.15E+03	2.59E+03	4.56E+02	1.58E+03	hours
MTTF	5.57E+04	1.37E+05	1.38E+05	9.55E+04	1.01E+04	1.17E+05	hours

COMMENTARY: Reliability is the probability of a component or system being able to provide the function for which it was designed. However, although the TTR information is useful, the paper does not identify what failed or why. Thus, although these may be related to inverter reliability, the contributions to this overall reliability cannot be identified.

[8] MTTF is used to avoid confusion as MTBF can mean either mean time before failure or mean time between failures. In this report MTBF is defined as mean time before failure.

Figure D-1: SMUD: Mean Times to Failure and Repair

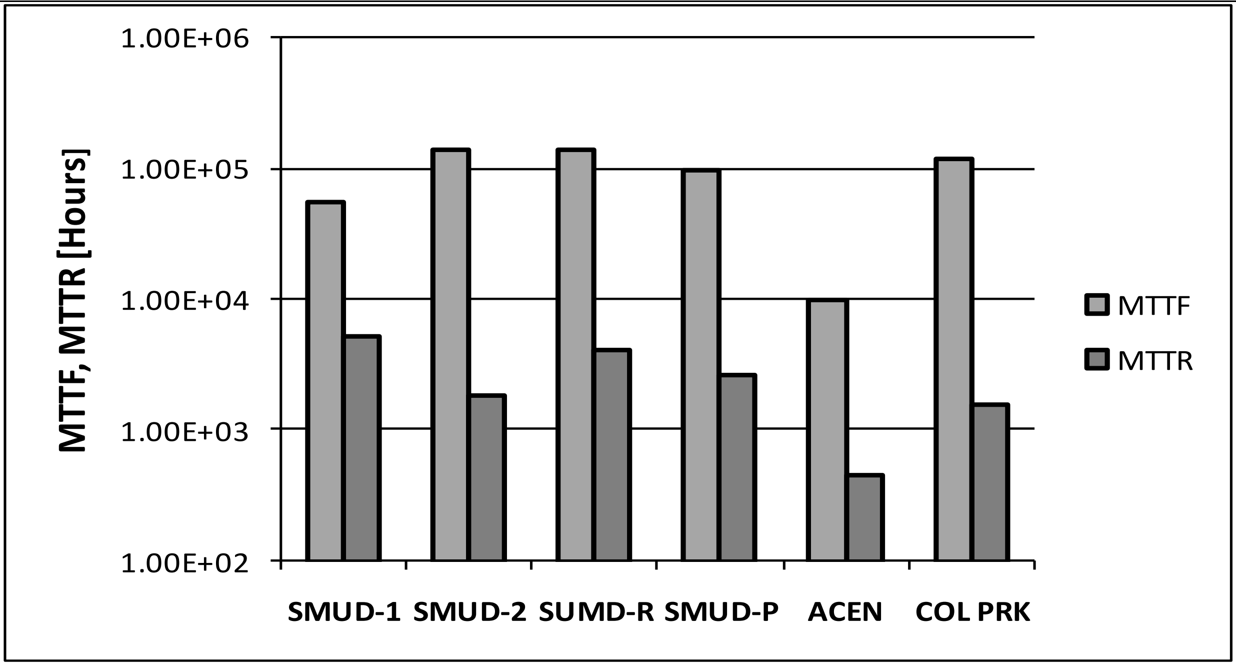

Figure D-2: SMUD: Ratio of MTTR to MTTF

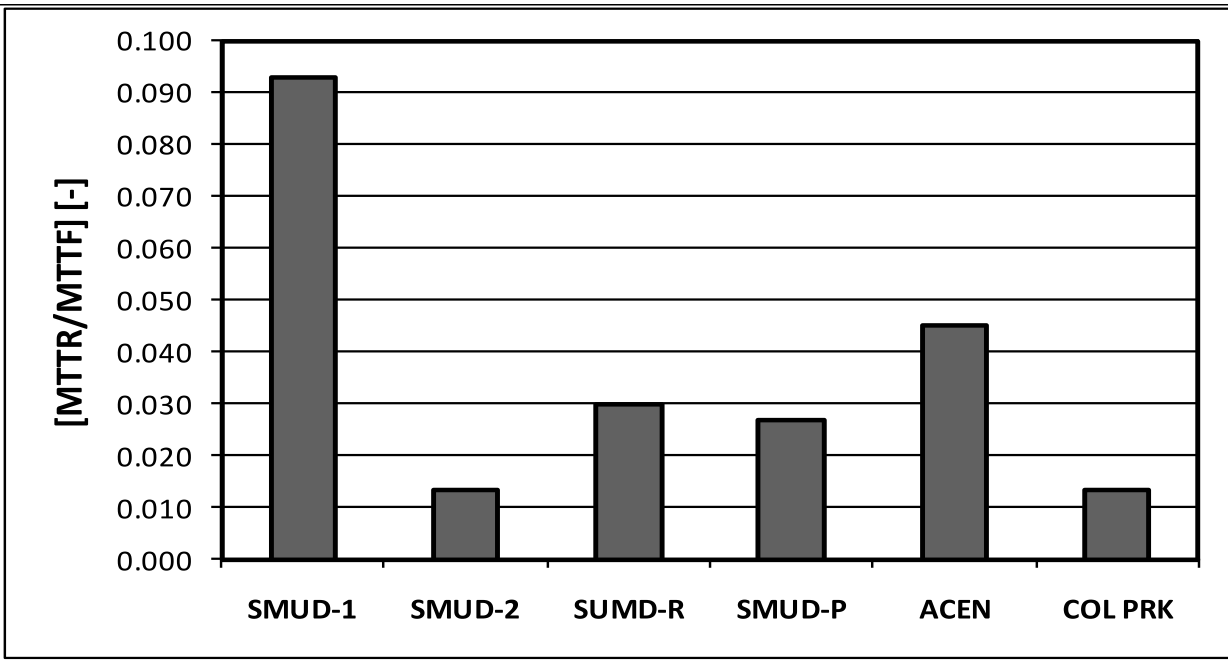

REF	AUTHOR(S)	TITLE	PUBLICATION
E	Begovic, M., Pregeil, A., Rohatgi, A.	Four-year Performance Assessment of the 342kW PV System at Georgia Tech	28th IEEE Photovoltaic Specialists Conference, Anchorage, AK, Sept. 15-22, 2000: 1575-78

SUMMARY: In 1996, the Georgia Institute of Technology completed installation of a 342 kW_{DC} PV system on the roof of its Aquatic Center. In 2000 a four-year review of the operating history was conducted to document performance and problems during this period of operation.

The system has 2,856 multi-crystalline silicon modules. Groups of 12 modules are connecting in series, making 238 strings connected in parallel.

Continuous monitoring is performed using a Campbell Scientific data acquisition system. The system documents performance parameters including DC power, real and reactive AC power, and voltage and current at various components. Meteorological data such as insolation, ambient and module temperatures, and wind speed were also recorded. In addition modeling using PVGRID was done, and performance predictions compared well to monitoring data.

Six of the eight failures (fault numbers 3-8) listed in Table E-1 were attributed to inverter components.

Table E-1: Five-Year Operational History of Downtime Due to Failures and Repairs

FAULT NO.	DATE	OPERATING TIME	TIME TO FAILURE	TIME TO REPAIR	CAUSE
Start	07/01/96	0	0	0	
1	07/15/96	14	14	15	Lightning
2	10/08/96	99	85	9	Plumbing
3	05/01/98	669	370	18	Transducer
4	06/02/98	701	32	31	PCU fan
5	06/28/99	1184	483	66	PCU fan
6	02/27/00	1336	152	32	PCU fan
7	06/08/00	1436	100	24	DC Matrix: IGBT
8	07/07/00	1467	31	17	PCU fan
		Mean time	183.375	26.5	
UNITS	-	DAYS	DAYS	DAYS	

TBF and TTR (Table E-1) indicate failure times are a factor of 1 to 10 larger than the repair times.

BACKGROUND: Reliability is a function of the probability density function (PDF), defined as f(t). The PDF is defined as equal to the derivative of the cumulative distribution function (CDF), where F(t), which has limits between zero and one ($0 \leq F(t) \leq 1$), is the probability that the free-variable, in this case time (t), has the value T between given limits, e.g., $P[t_1 \leq T \leq t_2]$. Equating the PDF to the derivative of the CDF:

$$f(t) = dF(t)/dt$$

Cross-multiplying both sides by dt and taking the integral of both sides and with $t_2=T$ and $t_1=0$, completion of the integration gives:

$$F(T)=\int f(t)dt$$

To complete the integration for F(T) a distribution for f(t) needs to be assumed. The two most frequently used are a) the negative exponential $f(t) = \lambda_F \bullet \exp[-\lambda_F \bullet t]$ where λ_F is the failure, or "hazard" rate, and b) the general Weibull function.

Weibull function: The advantage of the Weibull function as the PDF distribution is its flexibility in being able to approximate normal, log normal, and negative exponential functions. When used in MATLAB, for example, the exponents can be changed in the calculation to build a model that may more closely simulate the experimental results. The basic Weibull equations and values of β that result in approximations to the noted distributions are listed in Table E-2.

Table E-2: Equations for PDF and CDF for a Two-Parameter Weibull Function

	PDF	CDF	DISTRIBUTION
β	$f(t) = (\frac{\beta}{t})(\frac{t}{\eta})^{\beta} \bullet \exp[-(\frac{t}{\eta})^{\beta}]$	$F(T) = 1 - \exp[-(\frac{t}{\eta})^{\beta}]$ $R(T) = \exp[-(\frac{t}{\eta})^{\beta}]$	Weibull
1	$f(t) = (\frac{1}{\eta}) \bullet \exp[-(\frac{t}{\eta})]$	$F(T) = [1 - \exp[-(\frac{T}{\eta})]; R(T) = [\exp[-(\frac{T}{\eta})]$	Negative exponential
2	$f(t) = (\frac{2}{t})(\frac{t}{\eta})^{2} \bullet \exp[-(\frac{t}{\eta})^{2}]$	$F(T) = [1 - \exp[-(\frac{T}{\eta})^{2}]; R(T) = [\exp[-(\frac{T}{\eta})^{2}]$	Log normal

Representations of the PDF [f(t)] and CDF [F(t)] for functions used for failures (negative exponentials) and repairs (log normal) are shown in Figures E-1A and E1-B for negative exponential function, and Figures E-2A and E-2B for log normal functions.

Figure E-1A: PDF Failures

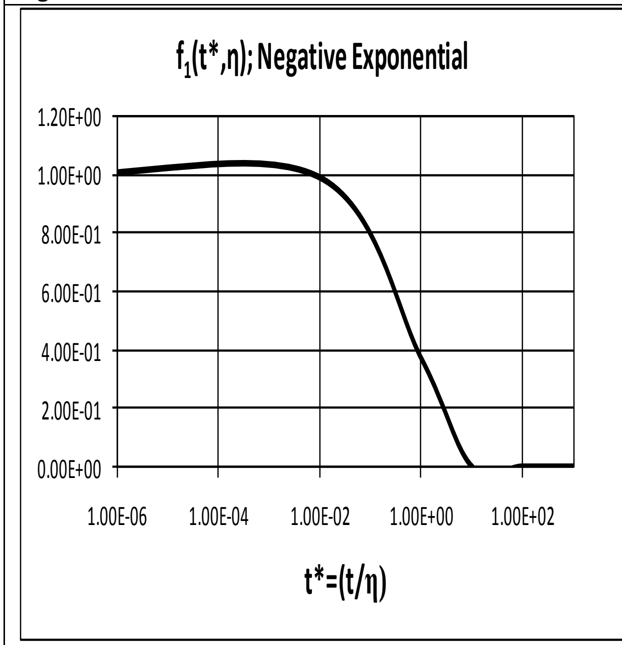

Figure E-2A: PDF Repairs

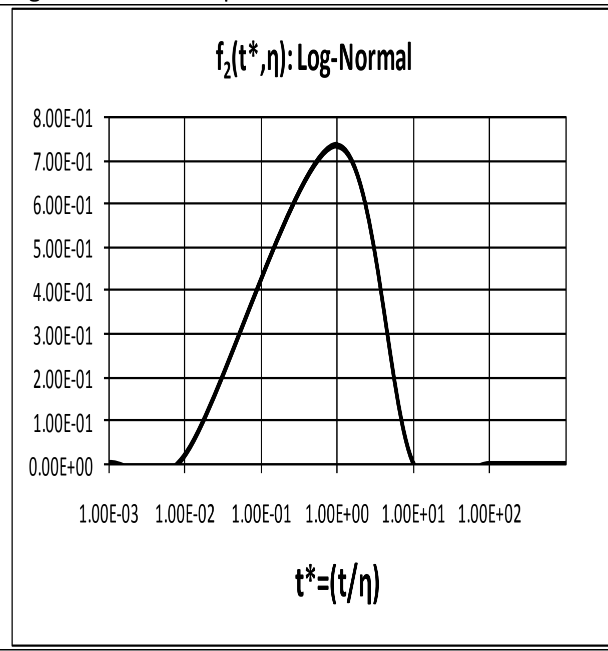

Figure E-1B: CDF Failures

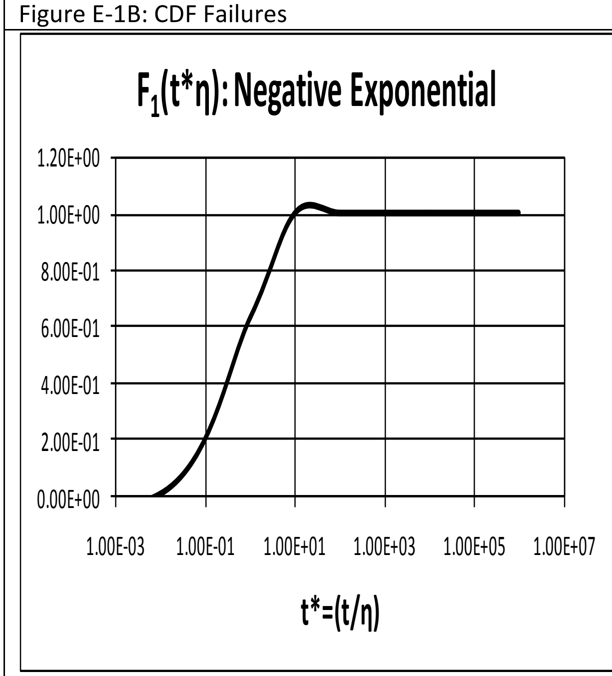

Figure E-2B: CDF Repairs

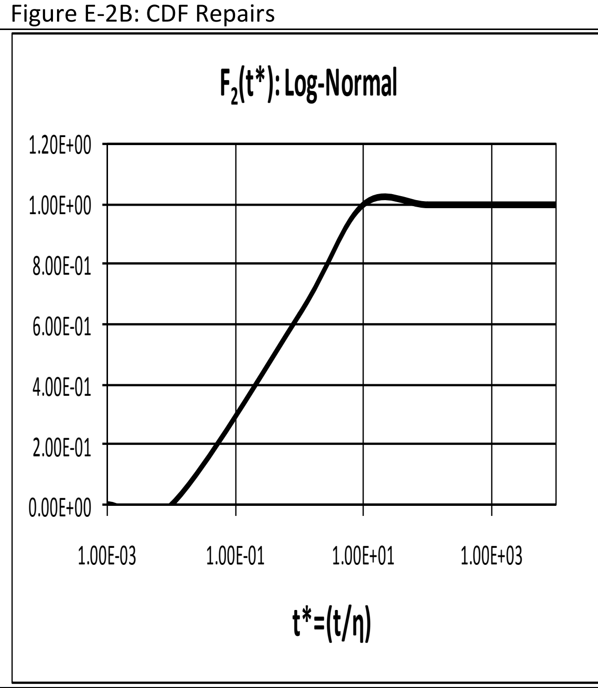

REF	AUTHOR(S)	TITLE	PUBLICATION
F	Ristow, A., Begović, M., Rohatgi, A.	Modeling the Effects of Uncertainty and Reliability on the Cost of Energy from PV Systems	20th European Solar Energy Conference & Exhibition, Barcelona, Spain, June 6-10, 2005

SUMMARY: This is one of a number of papers by Ristow, et al. covering problems related to reliability, cost of PV generation, use of multiple inverters, and performance of the 342 kW arrays installed at the Georgia Tech Aquatic Center (GTAC), based on Ristow's PhD thesis ("Numerical Modeling of Uncertainty and Variability in the Technology, Manufacturing and Economics of Crystalline Silicon Photovoltaics," Georgia Institute of Technology, 2008).

This paper introduces the use of a stochastic analysis, based on the assumption that both time before failure (TBF) and time to repair (TTR) are random. A record of failures and repairs, shown in Table F-1, are the basis of the ratios of repair times to failure times in Figure F-1.

Table F-1: Failure and Repair Times for the GTAC GCPV System

GTAC		Failure	Repair	Repair/Failure	Operating Time
DATE	FAULT	ΔTBF	ΔTTR	ΔTTR/ΔTBF	∑ΔTTF+ΔTTR
7/1/1996	Start	0	0	0	0
10/8/1996	Plumbing	2040	216	0.106	2952
5/1/1998	Current Transducer	13680	432	0.032	17064
6/2/1998	PCU Fan-1	768	744	0.969	18576
9/28/1999	PCU Fan-2	11592	1584	0.137	31752
2/27/2000	PCU Fan-3	3648	768	0.211	36168
6/6/2000	IGBT	2400	576	0.240	39144
7/7/2000	PCU Fan-4	744	408	0.548	40296
10/28/2003	Ground Fault	28992	168	0.006	69456
	Average=	MTBF (hrs)	MTTR (hrs)	MTTR/MTBF	YEARS OF OP
		7133.33	584.00	0.369	7.93

Figure F-1: Ratio of Times to Repair to Times to Failure

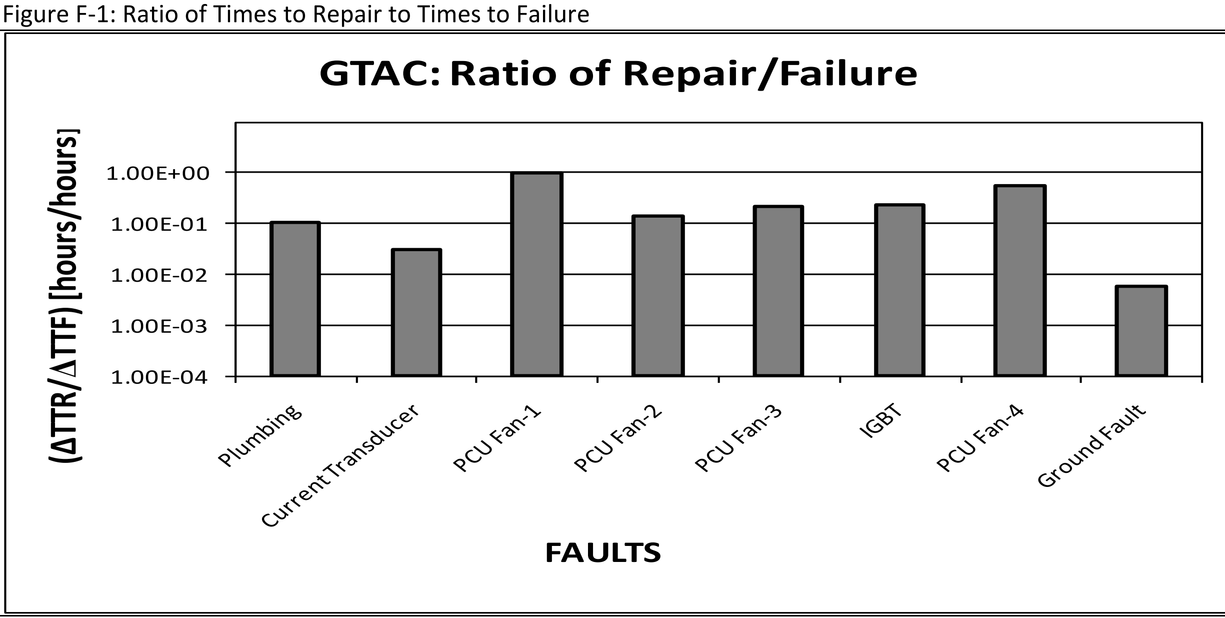

Note that the ratios of repair to failure times are a factor of about 100 larger than other available data.

COMMENTS: In contrast to many, the GTAC installations had multiple failures with the same component. The installation had PCS cooling fans that failed and were repaired four times during the seven-plus years of operation. Recognizing that these four points are insufficient to determine the mean values, the assumption was made that the average was acceptable as an approximation for MTBF and MTTR. Figure F-2 represents the operating time and downtime for these four failures.

Figure F-2: RCS Failure

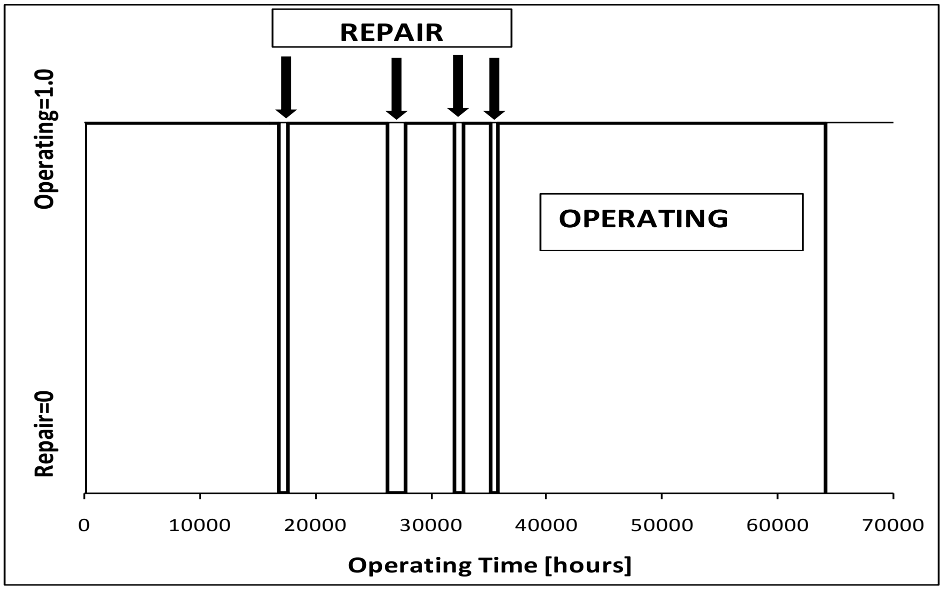

The equation based on the trend line is equated to the Weibull distribution (Table F-2) and assuming that the exponential terms in each are equal results in the following relationship between η, the mean times for failures or repairs, and the value of the power, β. $\eta = [(\Delta t)^{\beta-1}/(\text{Slope})]^{1/\beta}$.

Changing values of β it is noted that the predicted curve agrees with the GTAC results, as shown in Figures F-3 and F-4.

Table F-2: Calculation of Mean Time for Failures/Repairs for Weibull Distributions

FAILURE	PARAMETERS	GTAC Model	CALCULATE=η	
		$\exp[-(\Delta t/\eta)^{\beta}]$	$\eta=[(\Delta t)^{\beta-1}/(\text{Slope})]^{1/\beta}$	
	βF_F	1.052	VARY	1.00
	ηF_F=MTBF	1.32E+04		1.331E+04
	λF=1/ηF	7.57E-05		7.511E-05
REPAIR	PARAMETERS	GTAC Model	CALCULATE=η	
		$\exp[-(\Delta t/\eta)^{\beta}$	$\eta=[(\Delta t)^{\beta-1}/(\text{Slope})]^{1/\beta}$	
	βR_R	1.7397	VARY	1.70
	ηR_R=MTTR	7.18E+02		8.695E+02
	λR_R=1/ηR	1.39E-03		1.150E-03

Figure F-3: Failure

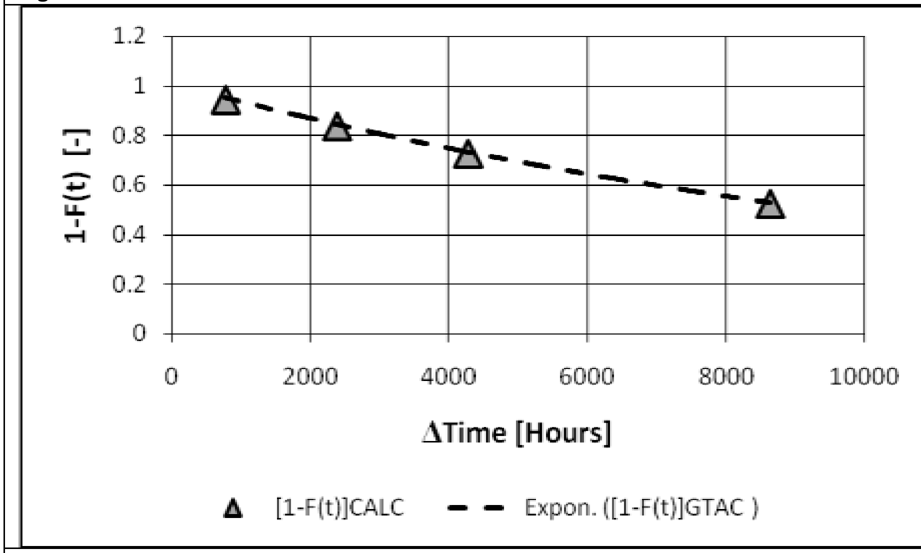

Figure F-4: Repair

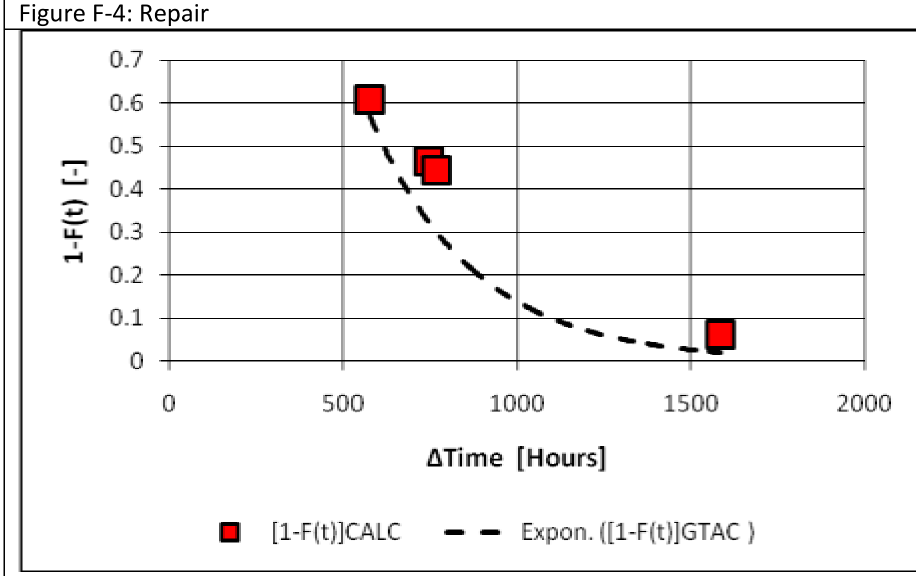

REF	AUTHOR(S)	TITLE	PUBLICATION
G	Begovic, M., Ghosh, S.R., Rohatgi, A.	Decade Performance of a Roof-Mounted Photovoltaic Array	Conference Record of the 2006 IEEE 4th World Conference, v2, May 2006: 2383-86

SUMMARY: In 1996, Georgia Institute of Technology completed installation of a 342 kW_{DC} PV system on the roof of its Aquatic Center. In 2006 a review of its operating history was performed to document performance for the 10-year period of operation.

Continuous monitoring is conducted using a Campbell Scientific data acquisition system. The system documents performance parameters including DC power, real and reactive AC power, voltage and current at various components. In addition meteorological data such as insolation, ambient and module temperatures, and wind speed are gathered.

Over this 10-year period there were 85,416 operational hours; unscheduled downtime, including construction, was 7,136 hours, for a downtime to generation time ratio of about 8%. Of this downtime 46%, or about 3,300 hours, was due to a period of construction on the Aquatic Center. Not counting the scheduled downtime due to construction, the downtime to operational time ratio is about 5%. The major contributors to the remaining downtime are listed in Table G-1.

Table G-1: Major Contributors to Downtime

FAILURES	CAUSE	NUMBER	PERCENT OF DOWNTIME	DOWNTIME (HRS)
PCU/Inverter	Fan failures	3	22%	1570
Construction	GTAC roof repair	3	46%	3303
“Other”	Not stated	24	32%	2263
	TOTAL	30	100%	7136

COMMENTS: The objective of the paper is to review the past 10 years of documenting performance, e.g., DC and AC power over the 10-year operation period. The primary reason for interest in this paper is its data (though limited) on the cause of failures that resulted in unscheduled or “other” downtime.

Details of these downtimes, e.g., failed components, time before failure (TBF), or time to repair (TTR), are not documented. Of note are the three over-temperature failures in the inverter due to repeated failures of the Power Control Unit (PCU) cooling fans. Also, during the 7th and 8th years of operation, construction work on the Aquatic Center resulted in interruptions of power generation. Also of note is the large percentage of downtime for the category labeled “other.” Figure G-1 is a compilation of the downtime over the 10 years of operation. Downtime due to construction and PCU fan failures is evident by the high percentages of the operating time per month attributed to these failures.

An approximation of the downtime based on this figure is shown in Table G-2. Although the majority of this “other” category is small, it totals about 32% of the downtime.

The additional data recorded between the evaluation after 4 years of operation and the current 10-year evaluation provide an opportunity to investigate the distribution function for repairs. Graphs of the construction- related outages, the PCU failures, and those attributed to “other” causes are shown in Figure G-2. Of note is the regular nature of the construction outages, possibly indicating that these were scheduled. On the other hand, the downtime due to PCS failures has appreciable differences between the 1st, 2nd, and 3rd failures.

Figure G-1: Record of Unscheduled Downtime

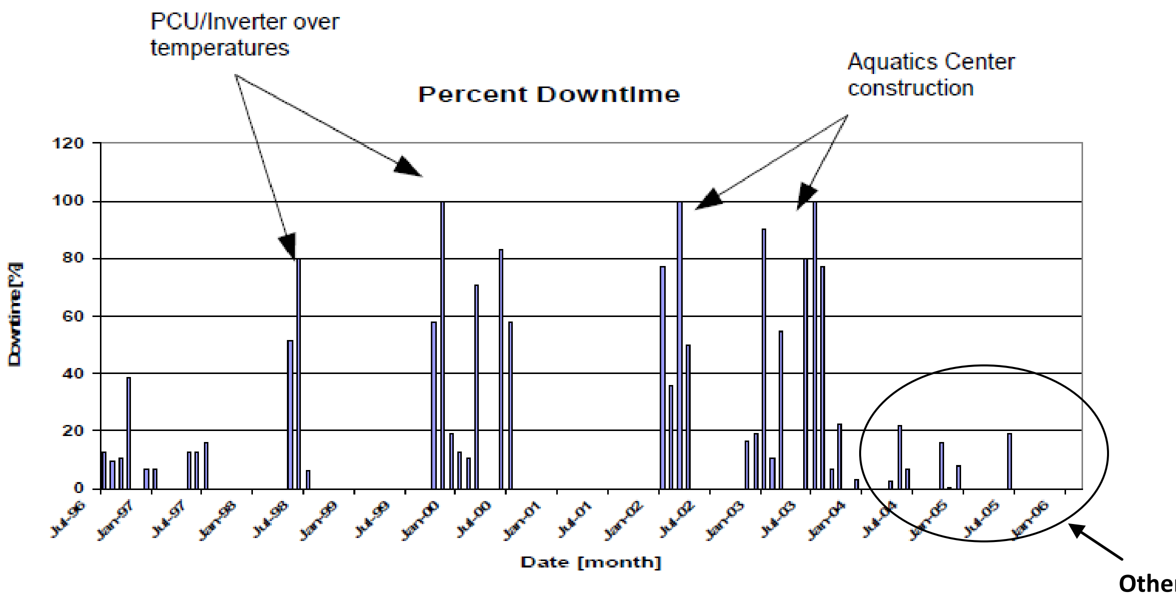

Table G-2: Primary Contributors to Downtime

ID	Year of Operation	"Other"	Construction	PCU	Downtime
1	7/96-7/97	912	-	-	912
2	7/97-7/98	474	-	-	474
3	7/98-7/99	-	-	37	37
4	7/99-7/00	-	-	1095	1095
5	7/00-7/01	-	-	438	438
6	7/01-7/02	621	1241	-	1862
7	7/02-7/03	-	584	-	584
8	7/03-7/04	-	1478	-	1478
9	7/04-7/05	255	-	-	255
	TOTALS	2263	3303	1570	7136
	UNITS	Hours	Hours	Hours	Hours

Figure G-2: Comparison of Major Contributors to Downtime

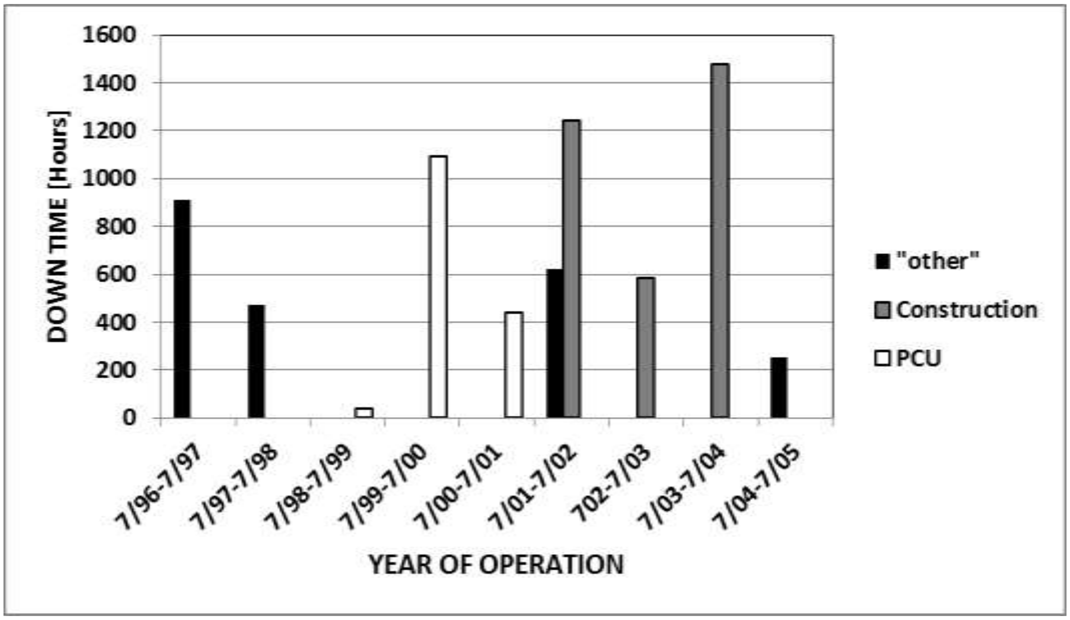

REF	AUTHOR(S)	TITLE	PUBLICATION
H	Ristow, A.H.	Numerical Modeling of Uncertainty and Variability in the Technology, Manufacturing, and Economics of Crystalline Silicon Photovoltaics	PhD Thesis, Georgia Institute of Technology, August 2008

SUMMARY: This thesis is a comprehensive analysis and evaluation related to the design and performance of a PV system. Of interest here is Chapter 6, "Modeling the Impact of System Reliability on Energy Production and Cost." The analyses assume failure and repair events are random. Thus, a stochastic Monte-Carlo-based analysis is used to determine reliability, availability, and serviceability.

The analysis used the 342 kW system installed at the Georgia Institute of Technology Aquatic Center (GTAC). The system began generation in July 1996 and had operated some 10 years by the time this work was done in March 2006. Operation was interrupted by 18 months of construction work on the GTAC (2002-2003). Otherwise performance was acceptable, experiencing nine downtimes, the majority due to failure of inverter subsystems (PCU fans, IGBTs), and the mean time between failures (MTBF), mean time to repair (MTTR), and mean time to failure[9] (MTTF). Failures are listed in Table H-1 (all tables and figures for this summary are located at the end of the summary).

Three metrics are needed to quantify the number and duration of these downtimes: availability, reliability, and serviceability. Availability requires that the component is working. Reliability ensures that the component will satisfy its design life. Should the component fail, serviceability can minimize the downtime.

AVAILABILITY: Availability, assuming the failure is repairable, is the fraction of the repairable system that is operational, defined as

$$A = \frac{MTBF}{MTBF + MTTR} \tag{1}$$

Where: MTBF is the mean time before failure, and MTTR the mean time to repair (Figure H-1).

Systems are composed of subsystems and subsystems contain individual components. Thus the availability for component "i" is,

$$A_i = \frac{1}{1+\sigma_i}\text{; Where: } \sigma_i = \frac{MTTR_i}{MTBF_i}\text{; so that } A_i = \frac{1}{1+\frac{MTTR_i}{MTBF_i}} = \frac{MTBF_i}{MTBF_i + MTTR_i}$$

The assumption is made that the PCUs and IGBTs are sufficient to result in failures of their independent subsystems. The availability, in this case, is the product of the availability of each subsystem.

$$A_{si} = \Pi_{i=1}^{i=N} A_i$$

In spite of delay in delivery of replacement components and the long delay due to contract work on the GTAC, the average availability over the 10 years of operation is 87% (Figure H-2).

[9] In certain instances MTTF is used as mean time to failure, if the component or subsystem has not or cannot be repaired. MTBF is used for repairable components and/or systems.

RELIABILITY: A component, subsystem, or system able to operate to meet its design function; reliability depends on its degradation with time.

SERVICEABILITY: Once a failure is detected, serviceability depends on location of the subsystem and/or that the components need to or can be repaired or replaced.

CALCULATIONS

The purpose of these calculations is to use the procedural steps in Ristow's study to calculate representative values of time between failures and repairs, reliability vs. time, and availability. Both failure and repair are assumed to be random. Thus the component of interest must either fail with time limits $t \le T_f \le (t+dt)$, or be repaired within the time period limits; $t \le T_r \le (t+dt)$.

Failures: Two inverter subsystems have been subject to failure. These components are storage electrolytic capacitors, IGBTs in the power stage drivers (1 failure), and cooling fans in PCUs (4 failures). It is assumed that these components represent two different subsystems. To determine subsystem failures and repairs, the failures and repairs at the component level need to be calculated. Hence values for MTBF and MTTR, which are necessary for calculating the availability, need to be determined.

Assume a distribution for a plausible probability density function (PDF), f(t). The probability that the failure will occur before (t+dt) is given by F(t), the cumulative density function (CDF):

$$F(t) = \int_0^t f(t)dt$$

If F(t) is the probability of failure, at a design lifetime, @t=T. The reliability, R(t)=1-F(t), is then the probability of NOT failing @ t=T, and represents success.

$$R(t) = 1 - F(t)$$

The failure rate, λ(t), is related to the PDF and R(t) as,

$$\lambda(t) = \frac{f(t)}{R(t)}$$

The failure of multiple numbers ($1 \le n \le N$) of the same component is $\lambda(t)=\sum\lambda_n(t)$, whereas the failure of different ($1 \le i \le I$) components is $\lambda(t)=\Pi\lambda_i(t)$.

For electronics the failure rate can be calculated using one of the standard references: MIL-HDBK-217F, Telcordia SR332, Siemens Norm, IEEE 493, etc. The method is based on the failure rate being a base value, λb, multiplied by the infinite product of various "stresses $\equiv \pi_N$" the component may experience in service, e.g.:

$$\lambda=\lambda b\Pi\pi_1 * \pi_2 * \pi_3 .... \pi_N$$

Based on the number of assumptions, these can be difficult to determine. In addition, field data is normally classified as proprietary by the OEM, thus limiting comparisons of predictions and data.

With most electronics the failure rates are 10^{-6} failures/hour, or time to failure of 10^6 hours. Thus, accelerated testing, such as testing at higher than normal operating temperature, can be used to determine a scaled time to failure.

The mean time between failures is: $MTBF = \int_0^{\infty} R(t)dt$

Based the assumption that the PDF can be represented by a Weibull distribution, $f(t) = (\frac{\beta}{\eta})[\frac{t}{\eta}]^{\beta\text{-}1} \bullet \exp[-(\frac{t}{\eta})^{\beta}]$ values of failure and reliability are calculated as follows.

Using a two-parameter Weibull distribution, the failure probability is:

Failure: $$F(t) = 1 - R(t) = 1 - \exp[-(\frac{t}{\eta_f})^{\beta_f}]$$

Mean time between failures: $$MTBF = \int_0^{\infty} R(t)dt = \int_0^{\infty} \exp[-(\frac{t}{\eta_f})^{\beta_f} dt = \eta_f \bullet \Gamma[\frac{1}{\beta_f} + 1]$$

Failure rate, λ(t): $$\lambda(t) = \frac{\beta_f}{\eta_f}(\frac{t}{\beta_f})^{(\beta_f - 1)}$$

In the above equations ηf is the scale factor, and βf is the shape factor for the Weibull distribution, and Γ(n) is the gamma function. Values of scale and size factors for failure, using a maximum likelihood estimation (MLE) procedure, are listed in Table H-3.

The repair time includes the following: Detect the failure; personnel (plant employees or outside repairs: contractors); diagnosis of the problem; order or take spare parts from stock; complete the repair; test the system; return to service.

Again assuming the repair PDF can be approximated by the Weibull distribution, the counterpart to failure, the following are defined for repair:

Reliability: $$R(t) = 1 - F(t) = 1 - (1 - \exp[-(\frac{t}{\eta_r})^{\beta_r}]) = \exp[-(\frac{t}{\eta_r})^{\beta_r}$$

Mean Time to Repair: $$MTTR = \int_0^{\infty} R(t)dt = \int_0^{\infty} \exp[(\frac{t}{\eta_r})^{\beta_r}]dt = \eta_r \bullet \Gamma[\frac{1}{\beta r} + 1]$$

Repair Rate, μ(t): $$\mu(t) = \frac{\beta_r}{\eta_r}(\frac{t}{\beta r})^{(\beta_r - 1)}$$

Where: ηr is the scale factor and βr the size factor for repairs. Assume that the PDF of a negative exponential distribution, where βr=1:

$$f(t) = (\frac{\beta}{\eta})(\frac{t}{\eta})^{\beta\text{-}1} \bullet \exp[-(\frac{t}{\eta})^{\beta}] = (\frac{1}{\eta})(\frac{t}{\eta})^{(1\text{-}1)}) \bullet \exp[-(\frac{t}{\eta})^{1}] = (\frac{1}{\eta}) \bullet \exp[-(\frac{t}{\eta})]$$

With η=μ; the function becomes

$$f(t) = (\frac{1}{\mu_r}) \bullet \exp[-(\frac{t}{\mu_r})]$$

Reliability: $$R(t) = 1 - F(t) = 1 - (1 - \frac{1}{\mu_r}\exp[-(\frac{t}{\mu_r})]) = \frac{1}{\mu_r}\exp[-(\frac{t}{\mu_r})]$$

Mean Time to Repair:

$$MTTR = \int_0^{\infty} R(t)dt = \int_0^{\infty} \frac{1}{\mu_r}) \exp[-(\frac{t}{\mu_r})dt = \frac{1}{\mu_r} \bullet [-\exp[-(\frac{t}{\mu_r})]_{t=0}^{t=\infty} = \frac{1}{\mu_r} \bullet [-0+1] = \frac{1}{\mu_r}$$

Repair Rate: $$\mu_r = \frac{\beta_r}{\eta_r}(\frac{t}{\beta r})^{(\beta_r - 1)} = \frac{1}{\eta_r}(\frac{t}{1})^{(1-1)} = \frac{1}{\eta_r} = \mu_r = \frac{1}{MTTR}$$

The calculation uses the following values in Tables H-3 and H-4, the reliability (repair completed in scheduled time) and the repair rates, Figures H-3A and H-3B, failure (repair not completed in scheduled time), and failure rates, Figures H-4A and H-4B.

AVAILABILITY AND UNAVAILABILITY

Availability is the fraction of time the system is available or currently in service.

Based on component failures, results in subsystem failure, $_i$

$$A_i = \frac{1}{1+\sigma i} = \frac{1}{1+\frac{MTTR_i}{MTBF_i}} = \frac{MTBF_i}{MTBF_i + MTTR_i}$$

For different subsystems; A_{Si} is product of the availabilities of the individual subsystems.

$$A_{si} = \Pi_{i=1}^{i=N} A_i$$

Unavailability: The time the subsystem or component is out of service, or the downtime:

Operating Time:

$$Q_i = \frac{1}{1+\frac{MTBF_i}{MTTR_i}} = \frac{MTTR_i}{MTBF_i + MTTR_i}$$

Downtime= Q_I*(8760 hours/year).Calculations of availability, unavailability, and downtime are shown in the tables and figures below.

Table H-1: Failures History of GTAC PV System

FAULT	DATE	TBF		TTR		CAUSE
Start up	07/01/96	-	-	-	-	-
1	07/15/06	14	336	15	360	Lightning strike
2	10/08/96	85	2040	9	216	Plumbing failure
3	05/01/98	570	13680	18	432	Current transducer
4	06/02/98	32	768	31	744	PCU fan
5	09/28/99	483	11592	66	1584	PCU fan
6	02/27/00	152	3648	32	768	PCU fan
7	06/06/00	100	2400	24	576	IGBT
8	07/07/00	31	744	12	288	PCU fan
9	10/28/03	1208	28992	7	168	Ground fault
	UNITS	days	hours	days	hours	

Table H-2: Inverter Components Weibull Distribution Parameters

COMPONENTS	SCALE=η		SHAPE=β	
PCUs	η_{RPCU}	995	β_{RPCU}	2.18
IGBTs	η_{RIGBT}	576	β_{RIGBT}	1.0
Capacitors	η_{RC}	576	β_{RC}	1.0
UNITS		hours		-

Table H-3: Failure and Repair Rates for Inverter Components

COMPONENT	FAILURE RATE (λ)		REPAIR RATE(μ)	
Capacitors	λ_C	3.03×10^{-6}	μ_C	1.7×10^{-3}
IGBTs	λ_{IGBT}	0.90×10^{-6}	μ_{IGBT}	1.7×10^{-3}
PCUs	λ_{PCU}	1.35×10^{-6}	μ_{IPCU}	1.03×10^{-3}
		1/hour		1/hour

Table H-4: Failure of Components within Cooling and Power Subsystems

AVAILABILITY						
COMP	FAILURE		REPAIR		σi	Ai=1/[1+σi]
PCU	MTTF	16752	MTTR	3384	0.2020	0.8319
IGBT	MTTF	2400	MTTR	576	0.2400	0.8065
SUBSYSTEM	-	hours	-	hours	-	0.6709
UNAVAILABILITY						
COMPONENT	FAILURE		REPAIR		σi	Qi=1/[1+1/σi]
PCU	MTTF	16752	MTTR	3384	0.2020	0.1681
IGBT	MTTF	2400	MTTR	576	0.2400	0.1935
SUBSYSTEM	-	hours	-	hours	-	0.0325

Figure H-1: Representation of Mean [M] Times: To First Failure (TTFT), Between Failures (MTBT), To Repairs (MTTR).

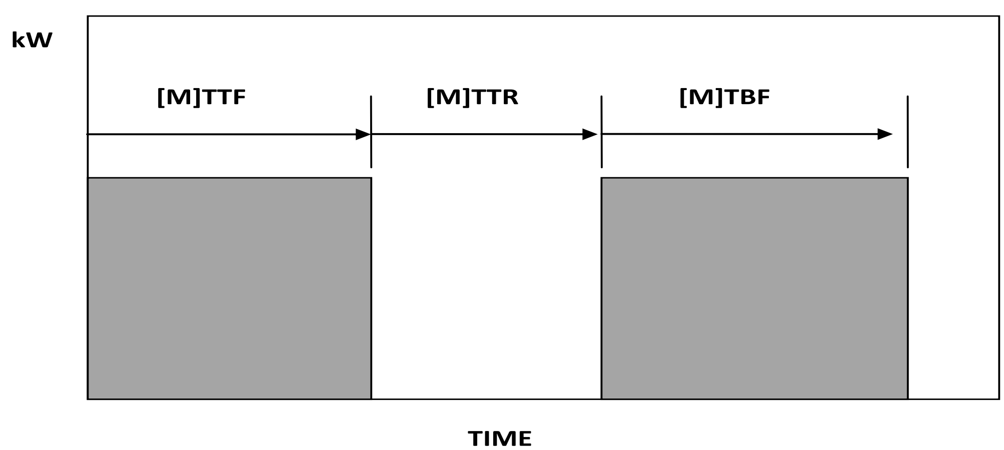

Figure H-2: GTAC Availability for 10 Years of Operation

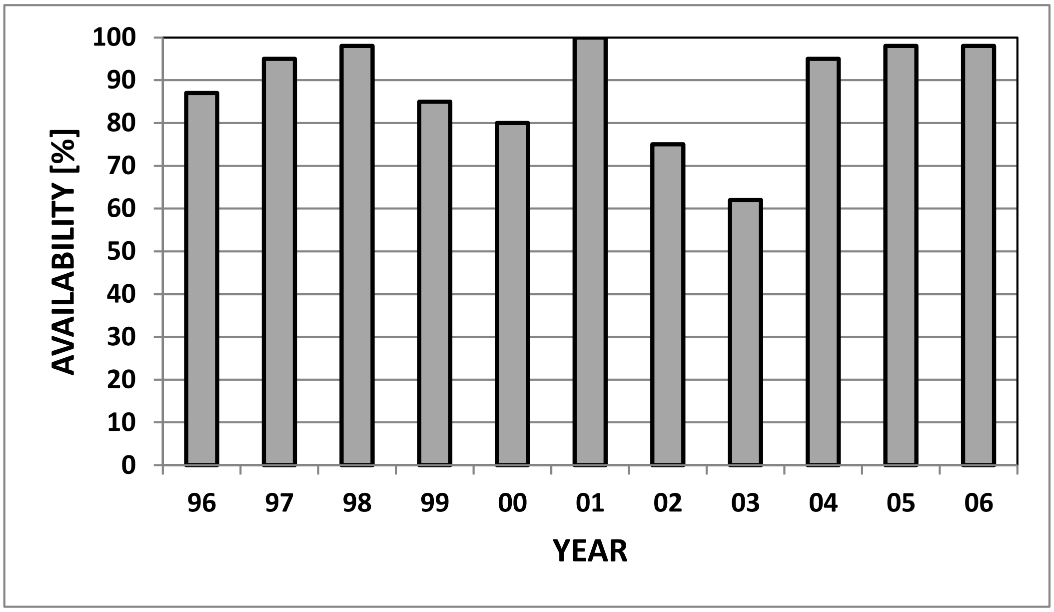

Figure H-3A: Probability **of Completing** Repair on Time

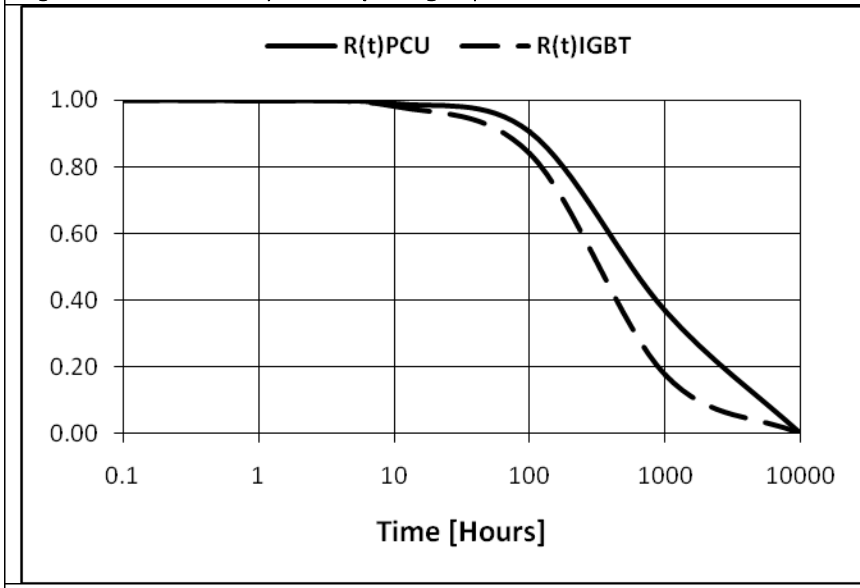

Figure H-4A: Probability **of Not Completing** Repair on Time

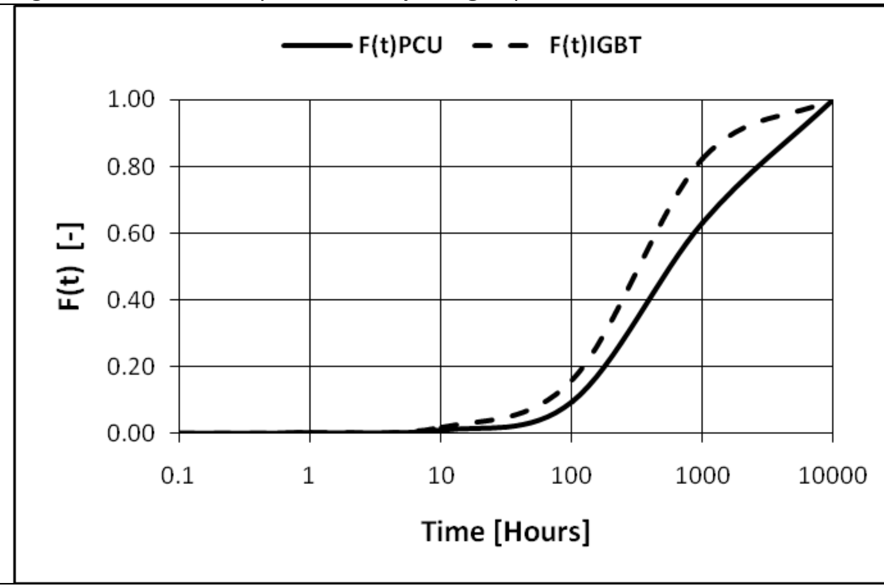

Figure H-3B: Repair Rate

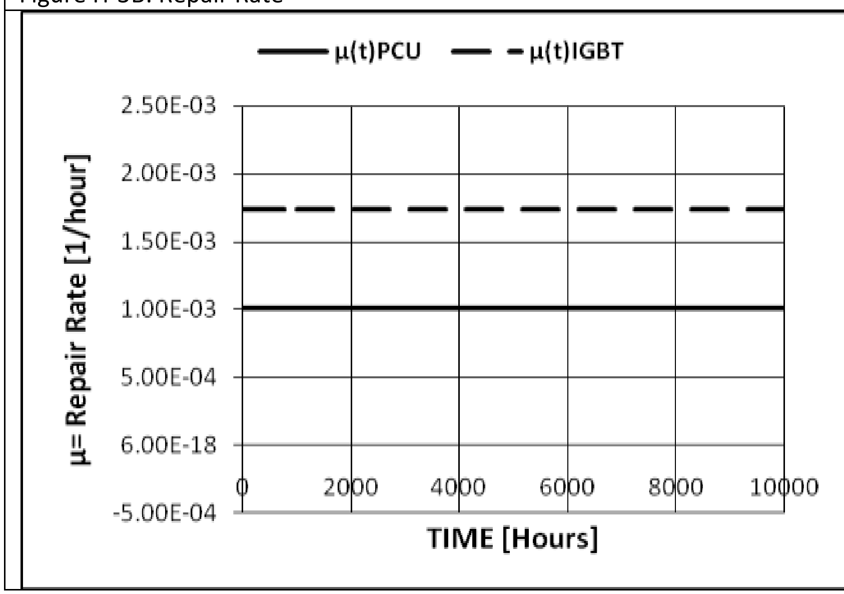

Figure H-4B: Failure Rate

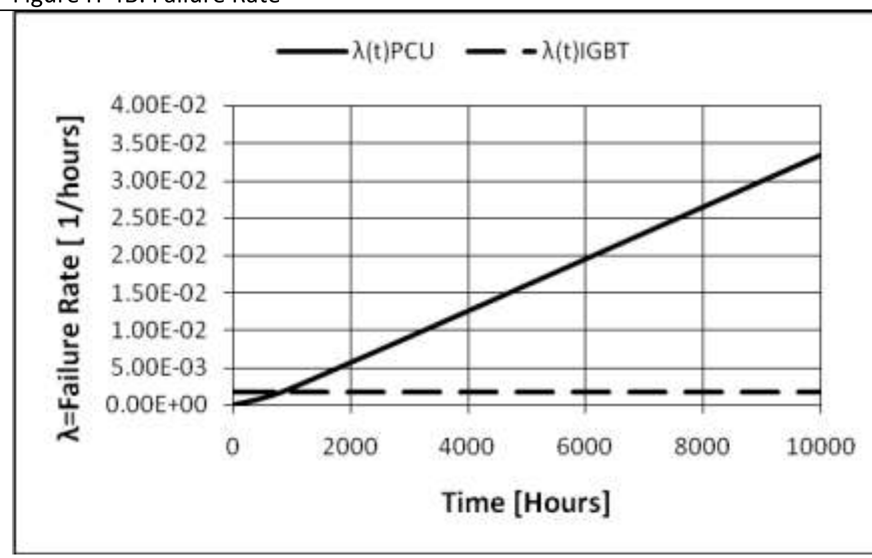

REF	AUTHOR(S)	TITLE	PUBLICATION
I	Moore, L., Post, H., et al.	Five Years of Operating Experience at a Large, Utility-scale Photovoltaic Generating Plant	*Progress in Photovoltaics: Research and Applications*, v13, 2008: 249-59

SUMMARY: Tucson Electric Power Company (TEP), from July 2001 to July 2004, installed a total of 26 crystalline silicon-based modules, grid-connected photovoltaic systems[10] at their Springerville, AZ facility. The 26 identical systems are designed to generate 135 kW_{DC} for a total generation of 3.51 MW_{DC}. Each system has 9 modules, each having 50 strings.

Test equipment consists of: DC and AC clamp-on ammeters, low and high range voltmeters; integral ohmmeters; optical temperature sensors, inverters including DC and AC current and voltage, AC frequency, and IGBT temperatures.

Systems were continuously monitored for changes in inverter performance, fault resets, IV curves, and diagnostic testing, e.g., current/voltage/ohms at specific locations; and performance, e.g., solar insolation, and power and energy vs. time.

The performance program was done from installation and operation of all 26 systems in 2004 to 2006. The program was conducted in accordance with the International Energy Agency Photovoltaic Systems Program documented in IEC Standard 6174.

Although the reference concentrates on the effect of the cost of unplanned outages due to component failures, of particular interest are the data reported on system failures and failures of inverter components. Systems were divided into the following categories: number of failures and percentage of these failures compared to the 156 unscheduled maintenance events (Table I-1).

Table I-1: Failures in TEP Systems

SYSTEM	FAILURES	PERCENTAGE
Data acquisition system (DAS)	11	7.0%
Inverter	58	37.2%
Junction boxes	19	12.2%
Arrays (PV)	23	14.7%
Balance of plant (systems)	12	7.8%
AC disconnects (ACD)	33	21.1%
TOTALS	156	100%

A high percentage of the DAS, Inverter, and ACD failures were attributed to lightning strikes in 2003 to 2005.

The highest number and percentage of failures were related to components in the inverters, as summarized in Table I-2.

[10] Installation History: 2001: 6 systems; 2002: 6 systems; 2003: 8 systems; 2004: 6 systems.

Table I-2: Failures Related to Inverters

COMPONENTS	FUNCTIONS	FAILURES	PERCENT
Interlock	DC disconnects alarm circuitry	13	22.4%
Controller	Components to control power conversion and protection	20	34.4%
Design	Cabinets weather protection	5	8.6%
Internal	Faults within inverter but not identified	6	10.3%
Matrix	Power controller switching transistors, capacitors, heat sink, cooling fans	4	6.9%
Other	Wiring, switches	10	17.4%
	TOTAL	58	100%

COMMENTS: Though the program appears to be thorough and comprehensive, the information published and its concentration on maintenance costs, while important to the TEP, does not document the monitoring that indicated failures, when these failures occurred, e.g., all at the same time and in the same modules, or spread over time and in different modules.

A record of the signal(s) vs. time that indicated a failure would be valuable information for monitoring, particularly for large MW systems.

REF	AUTHOR(S)	TITLE	PUBLICATION
J	Collins, E., et al.	Reliability and Availability Analyses of a Fielded Photovoltaic System	IEEE 978-1-2950, Sept. 2009: 002316-002321

SUMMARY: This article reviews the performance of the Tucson Electric Power PV array at Springerville, AZ. Twenty-six arrays are composed of 450 crystalline silicon modules. Arrays were installed in stages starting in July 2001 and completed in July 2004 for a total generation capacity of 4.6 MW_{DC}. The review documented component failures, data on mean time to failure (MTTF), and mean time to repair (MTTR).

This paper is a qualitative review describing a comprehensive program to develop estimates of reliability and availability for large GCPV systems. The analysis is based on a hierarchical reliability model defined as a reliability block diagram (RBD), for example, the inverter (Figure J-1), composed of components necessary to provide power to the grid. The higher level RBDs start with an overall representation of the arrays followed by division to small functional components. Commercial software ReliaSoft BlockSim 7™ was used to develop the RBDs. Evaluations of failures and repairs were based on operating reports for 2003-2007.

The program included the following objectives:

1. FAILURE OF SYSTEM COMPONENTS: 237 failures were recorded in the five years of operation. The inverter, with 125 failures most likely due to component faults, contributed about 50% of the failures.

2. FAILURE AND REPAIR DISTRIBUTIONS: Commercial software used was ReliaSoft Weibull++™. Monitoring results, operational records, and use of software ReliaSoft Weibull++™ determined acceptable models and scale (η), shape (β) and location (γ) parameters needed to define the distribution functions, f(t).

General distributions were based on failure and repair data (Table J-1). Substitution of values of η, β, and γ results in models for component failures are shown in Table J-2 and repairs in Table J-3. An example of calculations based on f(t) for the row box failure and repairs are in Figure J-2.

Note that this step is vital in estimating the time before failure (TBF) and time to repair (TTR).

Reliability, R(t), is a measure of useful life. With R(t)+F(t)=1, where F(t) is the unreliability, or failure, R(t)=1-F(t). With F(t)=∫f(t)dt, the reliability is R(t)=1-∫f(t)dt.

As an example, with $f(t) = \left(\frac{\beta_1 \bullet t^{(\beta_1 - 1)}}{\eta^{\beta_1}}\right) \bullet \mathrm{Exp}\left[-\left(\frac{t}{\eta}\right)^{\beta_1}\right]$

$$R(t) = 1 - \int_0^t \left[\frac{\beta_1 \bullet t^{(\beta_1 - 1)}}{\eta^{\beta_1}}\right] \bullet \mathrm{Exp}\left[-\left(\frac{t}{\eta}\right)^{\beta_1}\right] d\left(\frac{t}{\eta}\right)$$

, which, for β_1=1 becomes:

$$R(t) = 1 - \int_0^t \exp\left[-\left(\frac{t}{\eta}\right)\right] \bullet d\left(\frac{t}{\eta}\right) = 1 - \left[\mathrm{Exp}\left[-\left(\frac{t}{\eta}\right)\right]\right]\Big|_0^t = 1 + \left\{\mathrm{Exp}\left[-\left(\frac{t}{\eta}\right)\right] - \mathrm{Exp}[-(0)]\right\} = \mathrm{Exp}\left[-\left(\frac{t}{\eta}\right)\right]$$

Examples for the same components are in Figures J-2 and J-3.

Availability (A) is either a measure of the operational status or a ratio of energy produced (kWh) compared to the maximum energy that could have been produced (kWh_{MAX}), which can be recorded as a function of operating time.

Availability, as a measure of operational condition, is defined as $A = [\frac{MTTF}{MTTF + MTTR}] \leq 1$, where MTTF and MTTR are mean time to failure and mean time to repair.

Availability, as an indication of performance, is defined as $A(t) = [\frac{kWh}{kWh_{MAX}}] \leq 1.$

This can include effects of weather, evidence of reduction in power due to component failure or malfunction (Figure J-4).

Recorded and Predicted Failures: Once the distribution functions are known, a stochastic analysis, normally using a Monte-Carlo procedure, is used to determine the failure and repair times. Failures based on operating history are shown in Figure J-5 and predictions in Figure J-6: on average there is a 17% error between predicted and measured values.

Figure J-1: Example of a Reliability Block Diagram (RBD), Level 3: Arrays and Inverter

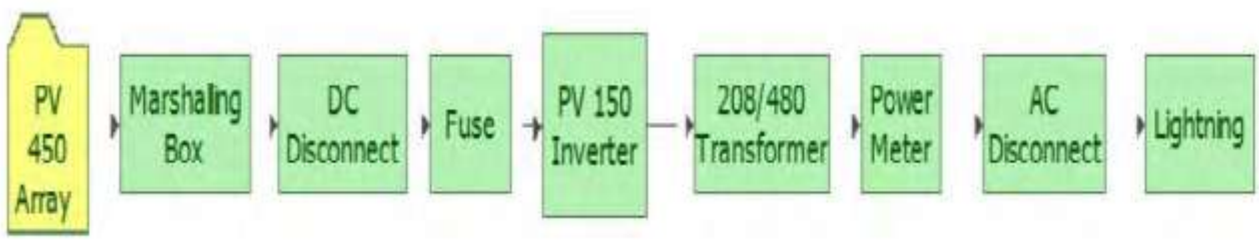

Table J-1: Generic Form of Equations for Distributions of Failed Components

FUNCTION	SCALE	SHAPE	LOCATION	PDF
Exponential-1	η_1	β_1	0	$f(t) = (\frac{\beta_1 \bullet t^{(\beta_1 - 1)}}{\eta^{\beta_1}}) \bullet Exp[-(\frac{t}{\eta})^{\beta_1}]$
Weibull-2	η_2	β_2	0	$f(t) = (\frac{\beta_2 \bullet (t)^{(\beta_2 - 1)}}{\eta^{\beta_2}}) \bullet Exp[-(\frac{t}{\eta})^{\beta_2}]$
Weibull-3	η_3	β_3	$\gamma_3 \leq t$	$\mathbf{f(t) = (\frac{\beta_3 \bullet (t - \gamma_3)^{(\beta_3 - 1)}}{\eta^{\beta_3}}) \bullet Exp[-(\frac{t - \gamma_3}{\eta})}$
Log Normal-2	μ_4	σ_4	0	$\mathbf{f(t)} = \frac{1}{\mathbf{t}\sqrt{2\pi\sigma_4}} \bullet \mathbf{Exp[} -\frac{(\ln\lvert t \rvert - \mu_4)^2}{2\sigma_4^2}\mathbf{]}$

Table J-2: Distributions and Parameters for Failed Components

COMPONENT	DISTRIBUTION	β=SHAPE	η=SCALE	γ= LOCATION
AC disconnect	Weibull-3	0.35	11000	3.9
Lightning	Exponential-1		λ=.00022	
Row box	Weibull-2	0.51	1.2E+06	
Marshalling box	Log Normal-2	2.3	10	
			Days	Days

Table J-3: Distributions for Repaired Components

COMPONENT	DISTRIBUTION	SHAPE	SCALE
AC disconnect	Weibull-2	β_1=0.71	η_1=1.4
Row box	Log Normal-2	σ_2=2.07	μ_2=-0.98
Marshalling box	Weibull-2	β_3=.35	η_3=3.55

Figure J-2: Distributions for Failed and Repaired Components

FAILURE: DISTRIBUTIONS=f(t)			DESCRIPTION	REPAIR: DISTRIBUTIONS=f(t)		
Row Box			Component	**Row Box**		
Weibull-2			Distribution	**Log Normal**		
$f(t) = (\frac{\beta \bullet (t)^{(\beta-1)}}{\eta^{\beta}}) \bullet Exp[-(\frac{t}{\eta})^{\beta}]$			PDF	$f(t) = \frac{1}{t\sqrt{2\pi\sigma}} \bullet Exp[-\frac{(ln\|t\|-\mu)^2}{2\sigma^2}]$		
Scale	**Shape**	**Location**	Parameters	**Scale**	**Shape**	**Location**
η =1.2E+06	**β =0.51**	**γ =0**		**μ=-0.98**	**σ=2.07**	**γ =0**
$f(t) = (\frac{.51 \bullet (t)^{(.51-1)}}{1.2E+06^{.51}}) \bullet Exp[-(\frac{t}{1.2E+06})^{.51}]$			Equation	$f(t) = \frac{1}{t\sqrt{2\pi(2.07)}} \bullet Exp[-\frac{(ln\|t\|+.98)^2}{2(2.07)^2}]$		
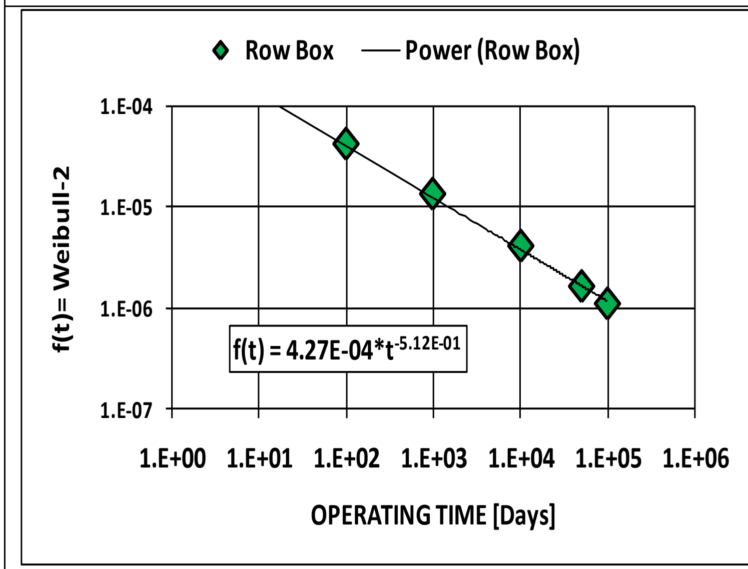			Figure	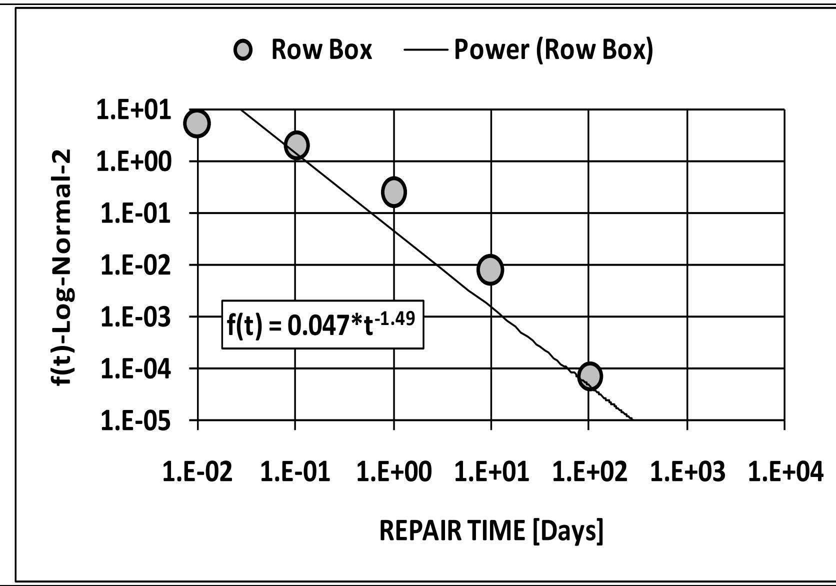		

Figure J-3: Reliability for Failed and Repaired Components

FAILURE: RELIABILITY=R(t)			DESCRIPTION	REPAIR: RELIABILITY= R(t)		
Row Box			Component	Row Box		
Weibull-2			Distribution	Log Normal		
$R(t) = Exp[-(\frac{t}{\eta})^{\beta 2}]$			CDF	$R(t)=\int f(t)dt \approx \Sigma\{\frac{1}{t\sqrt{2\pi\sigma_1}} \bullet Exp[-\frac{(\ln\lvert t\rvert-\mu_1)^2}{2\sigma_1^2}]\}\Delta t$		
Scale	**Shape**	**Location**	Parameters	**Scale**	**Shape**	**Location**
η =1.2E+06	**β =0.51**	**γ =0**		**μ_2=-0.98**	**σ_2=2.07**	**γ =0**
$R(t) = Exp[-(\frac{t}{1.2E+06})^{.51}]$			Reliability	$R(t) \approx \Sigma \frac{1}{t\sqrt{2\pi(2.07)}} \bullet Exp[-\frac{(\ln\lvert t\rvert+.98)^2}{2(2.07)^2}]\Delta t$		
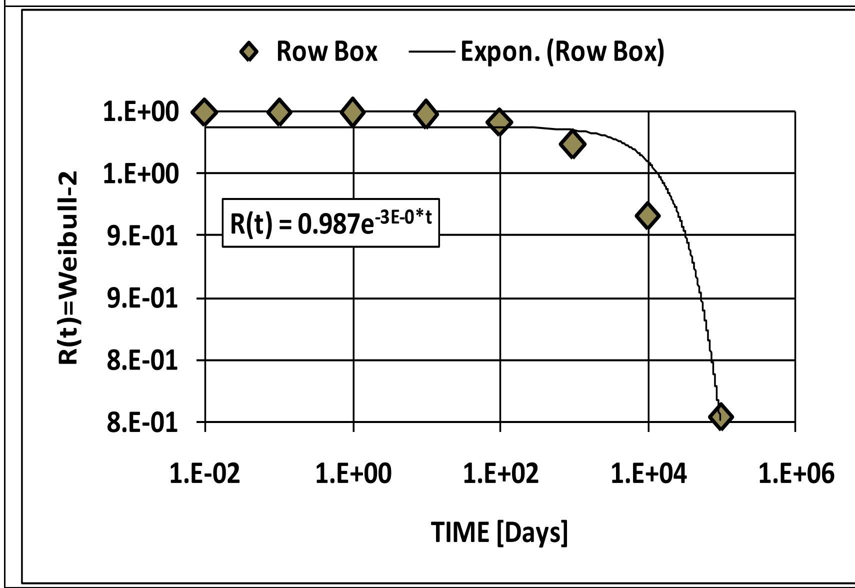			**Figure**	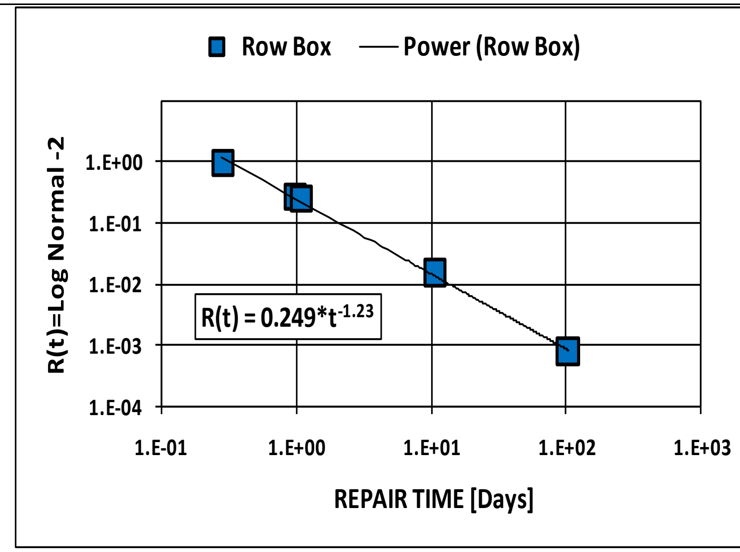		

Figure J-4: Availability

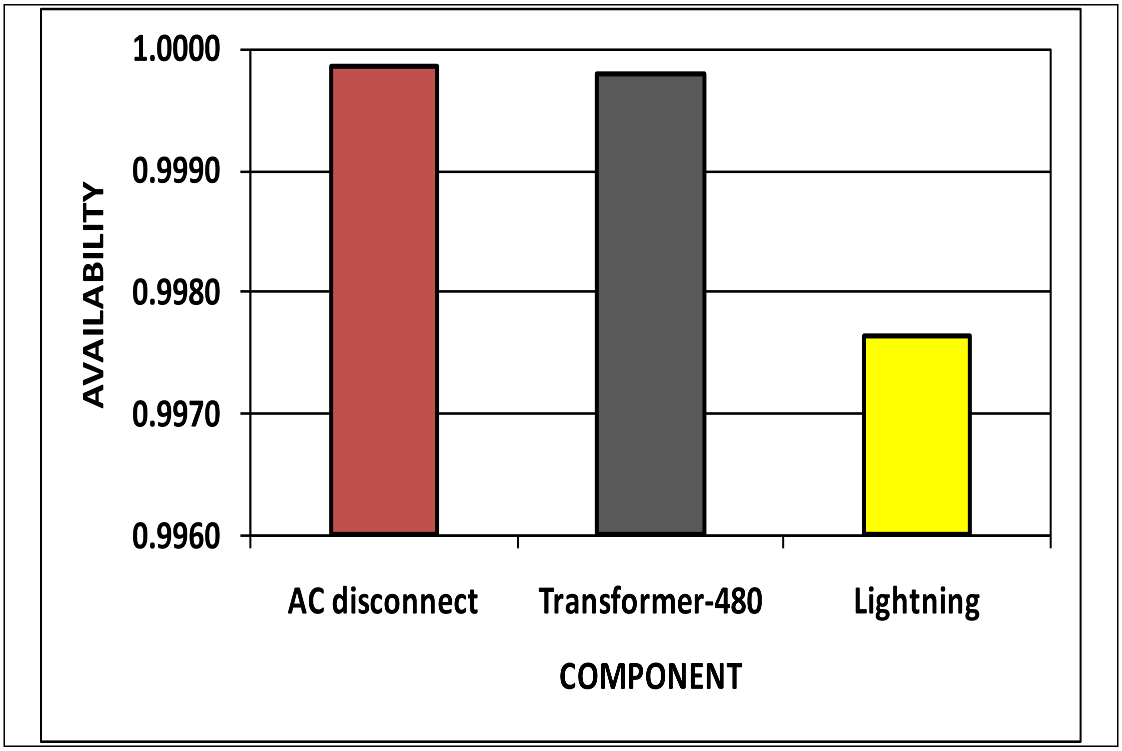

Figure J-5: Recorded Failures

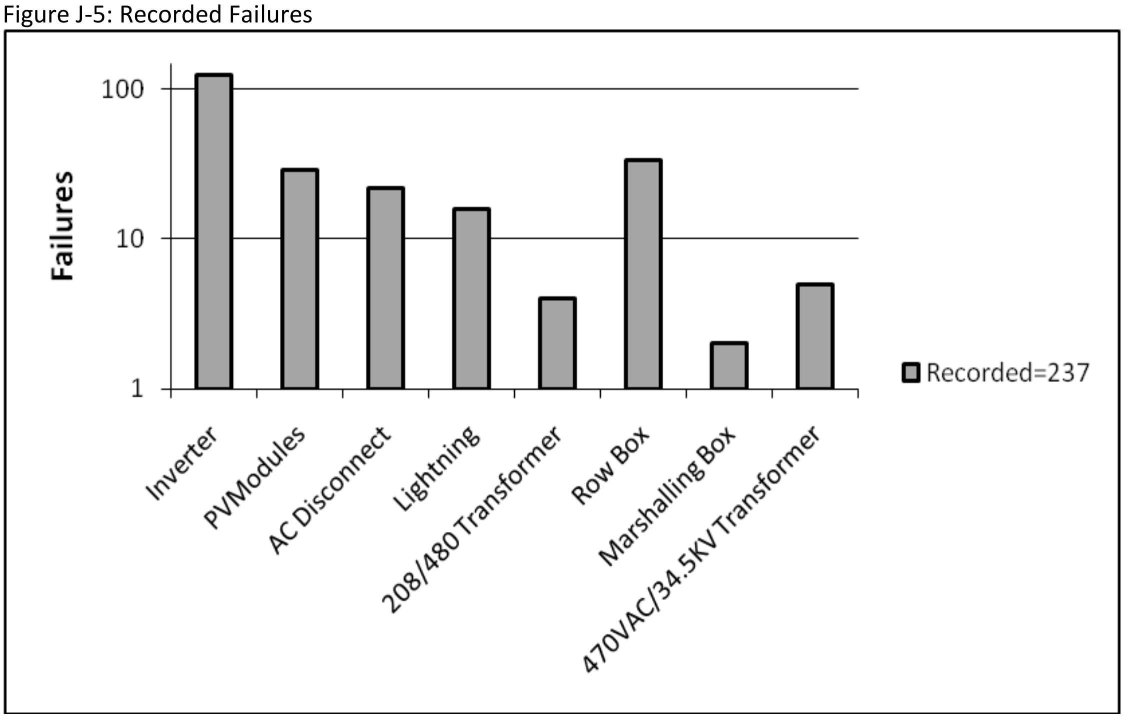

Figure J-6: Predicted and Recorded Failures

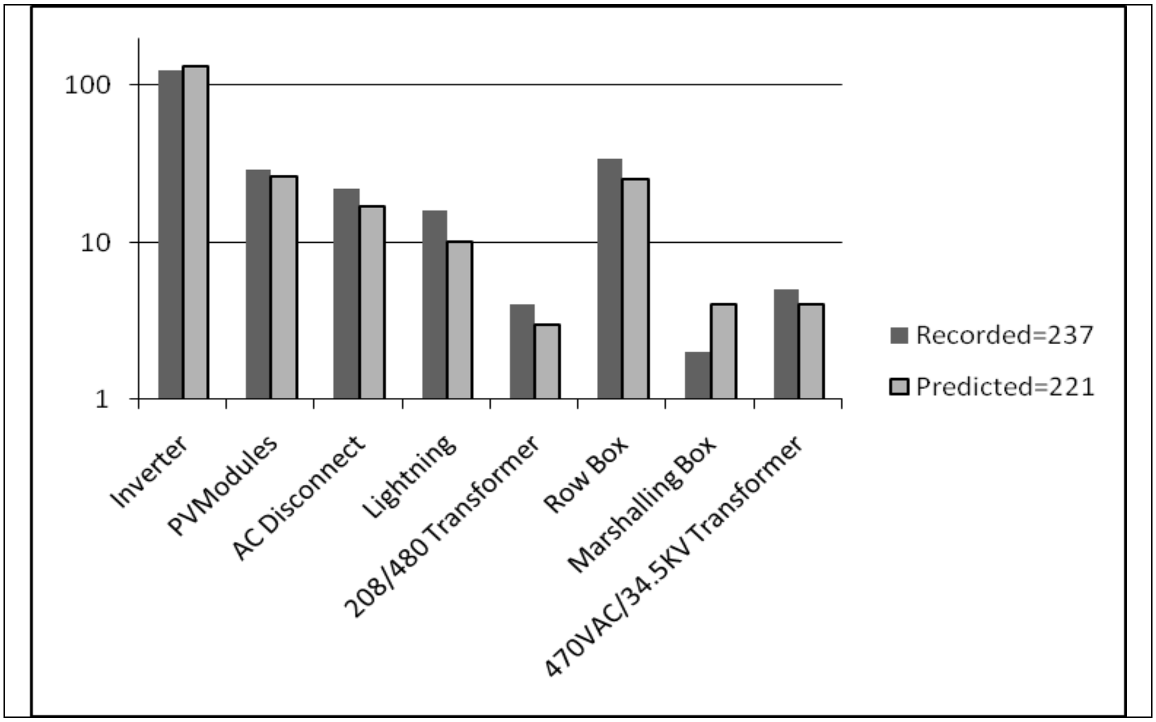

REF	AUTHOR(S)	TITLE	PUBLICATION
K	Seul-Ki Kim, et al.	Modeling and Simulation of a Grid-connected PV Generation System for Electromagnetic Transient Analysis	*Solar Energy*, v83, n5, 2009: 664-78

SUMMARY: The paper addresses the modeling and simulation of a grid-connected photovoltaic system (GCPVS) to analyze the interface between the grid and control of the GCPVS. The model and simulation of PV system responses to a range of control functions is based on the power transient software PSCAD/EMTDC.

CONTROL: This includes the PV array, a grid connected inverter, power control and anti-islanding control, which are integrated into the inverter enclosure. Figure K-1 is a model of the arrays, inverter, and grid. Figure K-2 is a model of a solar cell used in the analysis. The inverter, aside from conversion of DC to AC, also includes the measurement and calculations, power control, maximum power point tracking (MPPT), current controller, and protection. The functions of these subsystems are represented in Figure K-3 and are summarized in Table K-1. Representative results are as follows.

FAULTS: Figure K-4A shows values of GCPVS parameters for a single ground fault. Figure K-4B represents a three-phase short circuit fault.

GCPVS PARAMETERS: Figure K-5 shows variations in a number of parameters with the addition of the results for changes in solar irradiation. The model is used to calculate the response to the two major types of faults: a single line to ground fault and a three-phase short circuit fault. Responses to these faults are shown in Figures K-1 and K-2.

Table K-1: GCPVS Control Systems and Functions		
PV ARRAY		
Model consists of ideal current source; diode parallel with current source; series resistance		
GRID INVERTER		
DC to AC conversion; also performance for the following control functions		
GCPVS POWER CONTROL		
Measurement & Calculation		
	Measurements	PV current; inverter voltage; grid side current
	Calculations	Inverter V,I,Q, IPV, Vdc, phase, monitoring
Power Controller		Maximum power point
	Maximum Power	@Pmax, dP/dV algorithm
Current Controller		Grid side voltage; inverter side voltage
	Gating Signals	Pulse width modulation of DC power
Protection		O/U voltage, frequency; MC disconnect from grid
ANTI-ISLANDING CONTROL		
Disconnect from grid; array generation continues to generate DC power. SNL frequency shift algorithm used to de-energize inverter to load.		

Figure K-1: Model of GCPVS

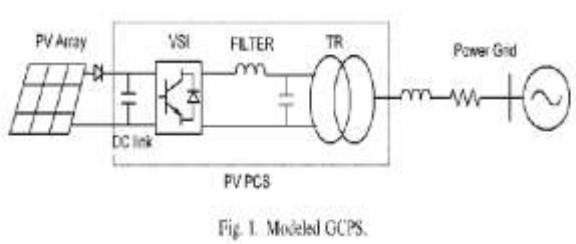

Figure K-2: Solar Array Model L

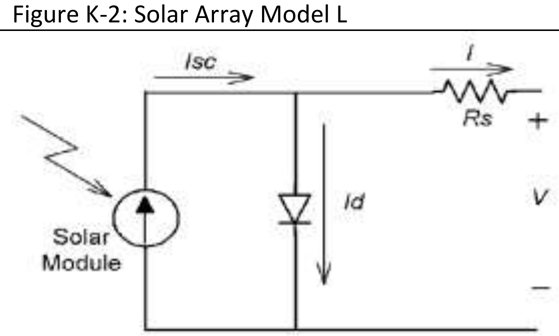

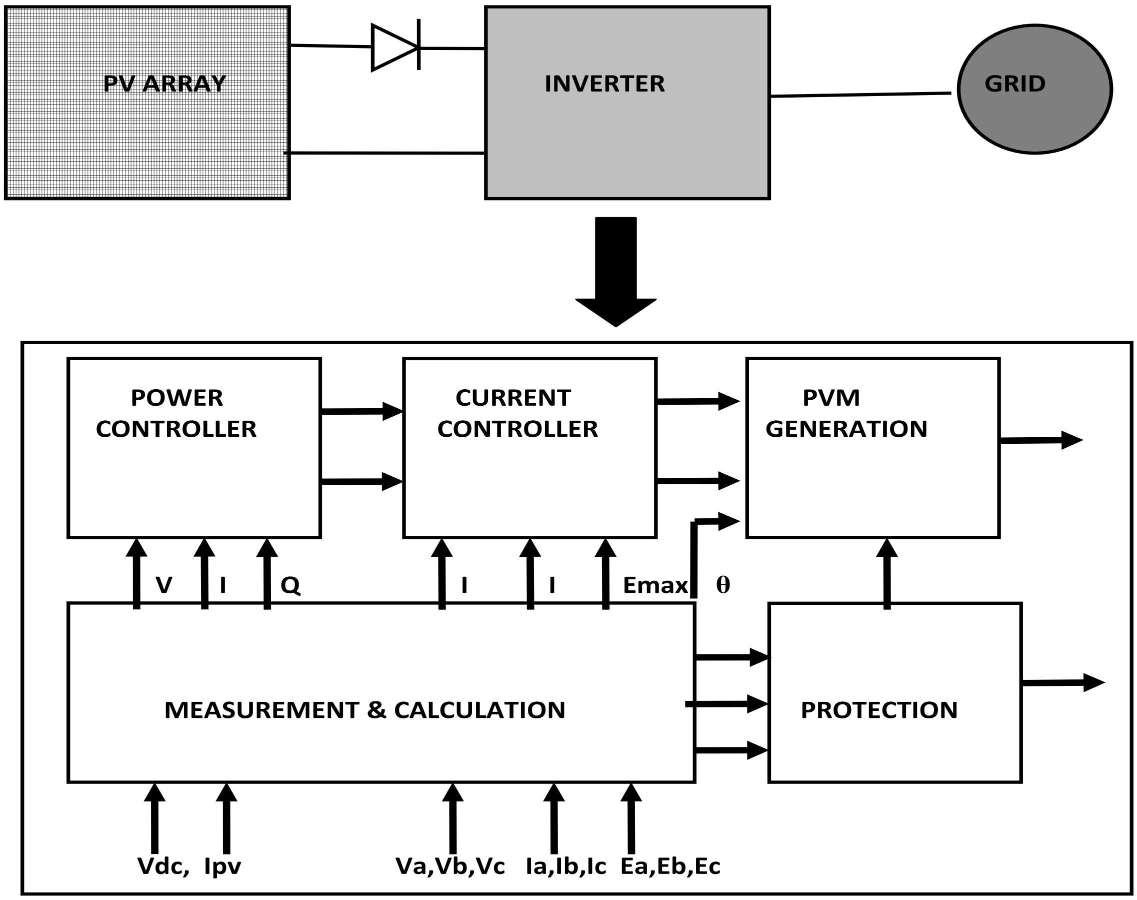

Figure K-3: Block Diagram of GCPVS Control

Figure K-4A: Single Line Ground Fault

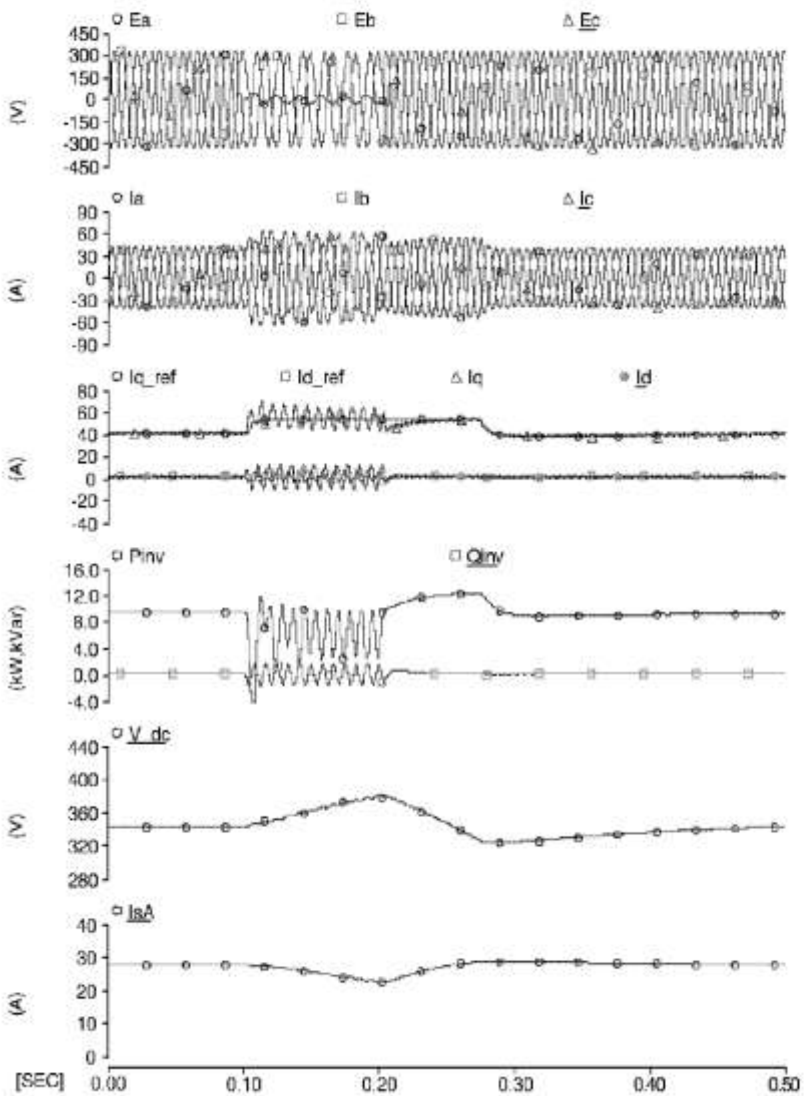

Figure K-4B: Three-Phase Short Circuit Fault

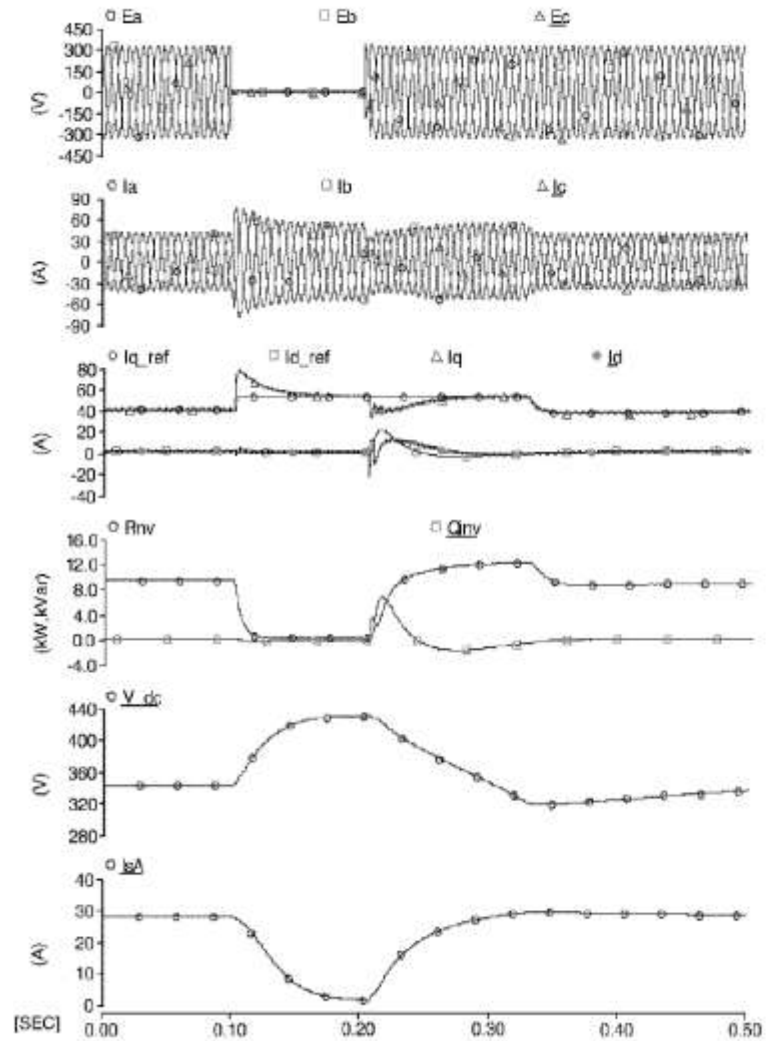

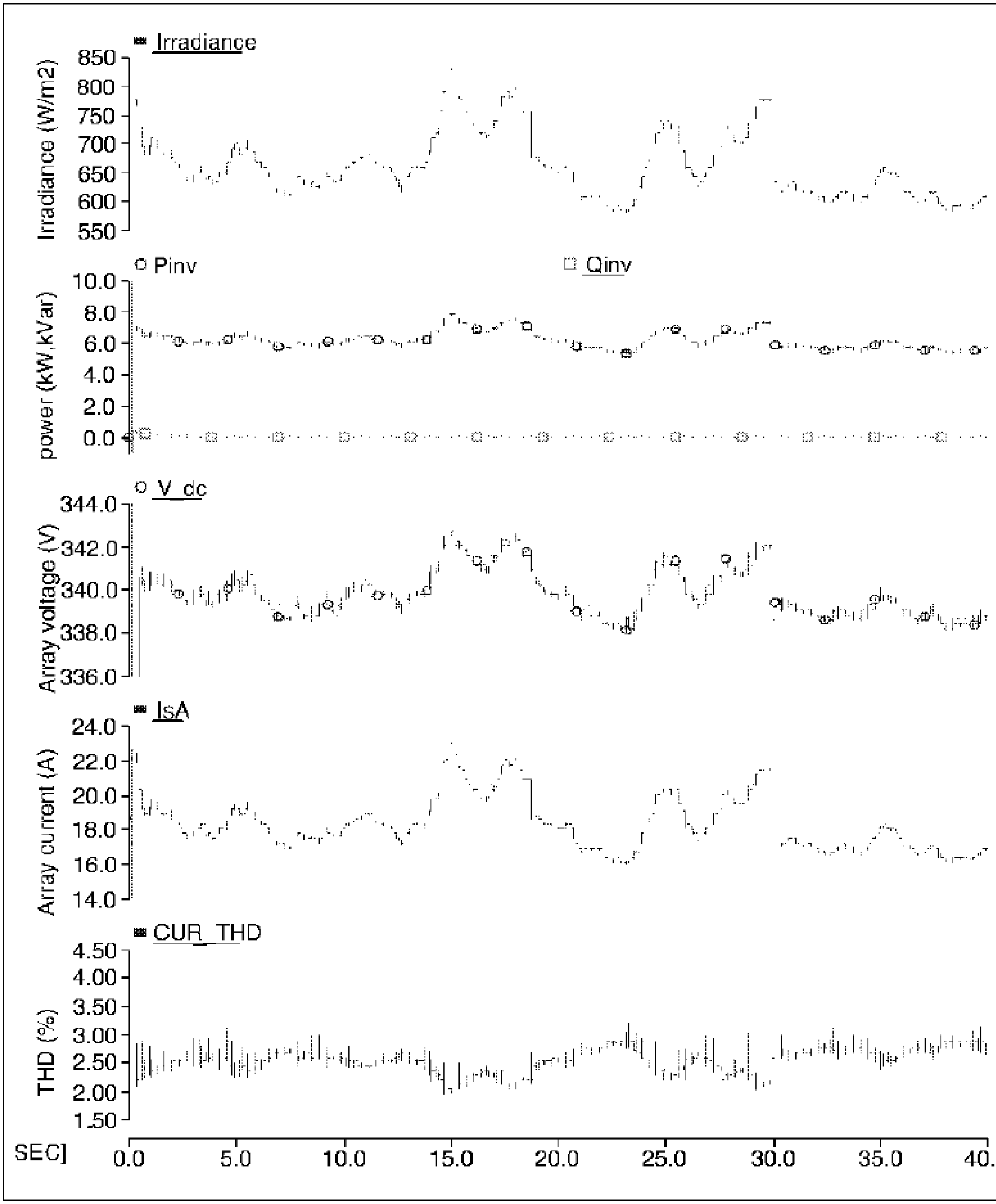

Figure K-5: GCPVS Performance

I=solar irradiance; Pinv=real power; Qinv=reactive power; Vdc=array voltage; IsA=array current; CUR-THD=total harmonic distortion, inverter output current

REF	AUTHOR(S)	TITLE	PUBLICATION
L	Kuei, H, et al.	Modeling and Fault Simulation of Photovoltaic Generation Systems Using Circuit-based Model	Sustainable Energy Technologies, 2008 ICSET-2008, Singapore, Jan. 2009: 290-294

SUMMARY: Numerous publications, both conference papers and texts, present models of a solar cell. For example Kuei et al. use a detailed model in PSIM to simulate the response of a PV system to various faults. However, this paper is not clear in defining all the terms. The expanded model, Figure L-1, adds the shunt, or parallel, resistance to account for losses in the branch with the diode. Table L-1 lists the definitions of the various terms and values.

Figure L-1: Silicon Solar Cell Equivalent Circuit

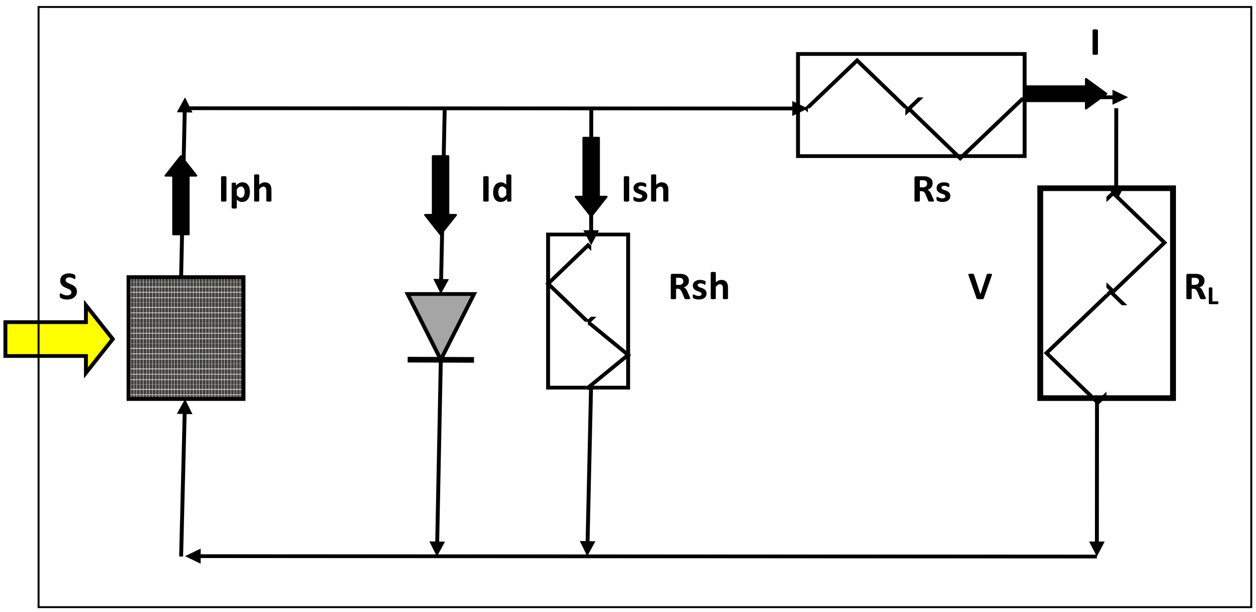

The model for a PV cell is derived as follows:

Based on summing the currents at each node, the load current, I, is, $I = Iph - Id - Ish$ (1)

Where:

$$\text{Cell}: Iph = [Isc + K_T(T - Tref)] \bullet \frac{S}{1000[w/m2]}$$

$$\text{Diode}: Id = Io[\exp(\frac{Q}{kA} \bullet \frac{Vd}{Tref}) - 1] \qquad (2)$$

$$\text{Shunt}: Ish = Vsh/Rsh$$

$$\text{Load}: I[R_S + R_L] = IsRs + V = IshRsh$$

Substitution into the summation of currents:

$$I = Iph - Id - Ish$$

$$I = [Isc + K_T(Tj - Tref)] \bullet (\frac{S}{1000}) - Io[\exp(\frac{q}{kA} \bullet \frac{Vd}{Tj}) - 1] - [\frac{(IRs + V)}{Rsh}] \quad (3)$$

With the diode voltage equal to the voltage across that of the series resistor and load, Vd = IRs + V. Substitution into equation 3:

$$I = [Isc + K_T(T - Tref)] \bullet (\frac{S}{1000}) - Io[\exp(\frac{q}{kA} \bullet \frac{I(Rs + V)}{Tj}) - 1] - [\frac{(IRs + V)}{Rsh}] \quad (4)$$

With the load voltage given by $V=IR_L$ equation (4) for current becomes:

$$I = [Isc + K_T(Tj - Tref)] \bullet (\frac{S}{1000}) - Io[\exp(\frac{q}{kA} \bullet \frac{I(Rs + R_L)}{Tj}) - 1] - I \bullet [\frac{(Rs + R_L)}{Rsh}] \quad (5)$$

It is obvious in this form that the equation is non-linear.

The author suggests the following procedure to solve for current, voltage and power:

a) Assume: Value of Vd
b) Calculate I:

$$I = [Isc + K_T(Tj - Tref)] \bullet (\frac{S}{1000}) - Io[\exp(\frac{q}{kA} \bullet \frac{Vd}{Tj}) - 1]]/[1 + \frac{(Rs + RL)}{Rsh}]$$

c) Calculate: V=(Vd-IRs)

d) Calculate: power: P=V*I

Results of current vs. voltage and power vs. voltage are shown in Figures L-3A and L-3B.

Table L-1: Definition of Terms and Values for Example Problem

COMPONENTS	SYMBOL	VALUE	UNITS
Parallel (shunt) Resistor	Rsh	6.6	Ohms
Series Resistor	Rs	0.005	Ohms
Load Resistance	R_L	0.01	Ohms
Reference Temperature	Tref	298	$^oC+273=^oK$
Junction Temperature	Tj=25^{o}C	298	$^oC+273=^oK$
Saturation Current	Io	6.00E-10	amps
Short Circuit Current	Isc	3.4	Amps
Diode Current	Id	TBD	Amps
Diode Voltage	Vd	ASSUME	Volts
Solar Insolation	S	1000	w/m^2
Temperature Coefficient	K_T	2.060E-03	Amps/oC
Electron Charge	q	1.6021E-19	Coulomb
Boltzmann Constant	k	1.3805E-23	Joules/oK
• Coulomb	C	2.777E-04	amp-hour
• Joule/^{o}K	J/^{o}K	1.000	watt-sec/^{o}K
Ideal factor	A	1.5	-
(q/k)* units conversion	(q/k)	11602.218	^{o}K/Volts
(q/kTj)	(q/k)(1/Tj)	38.933618	1/Volts

Current vs. voltage (Figure L-3A) and power vs. voltage (Figure L-3B) are the expected functional relationship between current, voltage and power for this example.

Figure L-3A: Current vs. Voltage

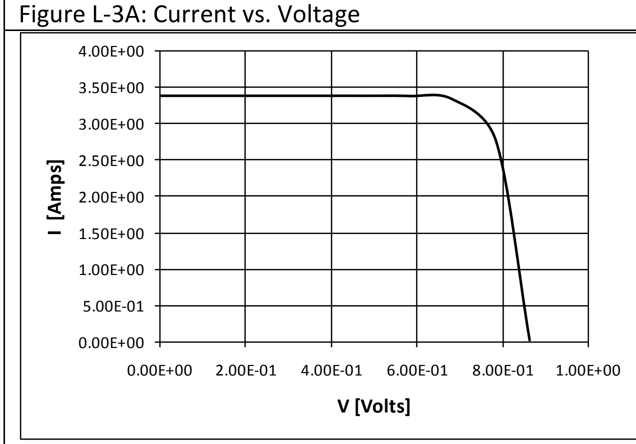

Figure L-3B: Power vs. Voltage

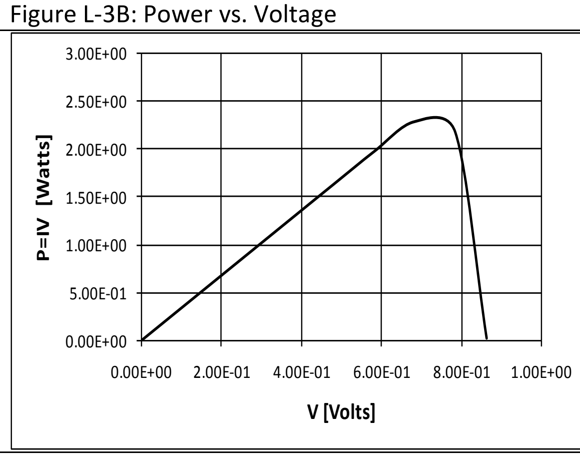

REF	AUTHOR(S)	TITLE	PUBLICATION
M	Collins, E., et al.	Field Data Collection for Quantification of Reliability and Availability for PV Systems	35th IEEE Photovoltaic Specialist Conference, June 10, 2010: SAND2010-3362-C

SUMMARY: There are approximately 50 module manufacturers[11] and some 50 designers and manufacturers of DC-AC inverters, plus numerous systems contractors and installers. Many started with residence-sized units with kW capacity and, to meet increased interest in GCPVS, are expanding to MW capacity. Although these units are similar in design there is currently no comprehensive database that consistently documents operating history, particularly component failures.

Sandia National Laboratories (SNL) with the support of the National Renewable Energy Laboratories (NREL) has developed the elements of a working database, the Photovoltaic Reliability Operation and Maintenance (PVROM) database. Any database needs to meet the following criteria:

Monitoring: ability to capture data at its source

Organization: capability to order information in format for standard reliability R(t) and availability A(t) analyses; time to failure (TTF) and time to replace (TTR) (downtime) for each subsystem and its major components

The following commercially available programs are used in these analyses:

- Weibull++TM and RGA to fit the scale, shape, and location parameters to a range of standard distributions;
- BlockSim-7TM: Divides the GCPVS into reliability block diagrams (RBDs) ranging from the overall system, e.g., collector-power generation (Level 1) to details of the inverters.

Access: provide ease of access to a wide range of users

Data: ease of input and retrieval as listed in Table M-1.

To meet these criteria, the database has been configured around ReliaSoft XFRACAS™.

Table N-1 lists the major information documented in the listed “Reports.” An example of the bill of materials input, in this case on the inverter, is found in Figure M-1.

COMMENTS: Access to the database is limited to OEMs that have a “partnership” relationship with the SNL. While understandable since the information is considered proprietary, this limits access to data that could be used to improved designs and, thus, possible reduction in downtime. One possibility would be to allow, for example, access to the database by universities, contingent on their providing the necessary legal processes to protect commercial concerns of the OEMs willing to participate.

[11] Of the 50, 17 are in the United States.

Table M-1: Database Reports

REPORTS	DESCRIPTION	INFORMATION
BILL OF MATERIALS	Inventory of components including a line diagram of system and subsystems	System or Subsystem
		Major components
		OEM
		Serial numbers
		Installation date
INCIDENT REPORTS	Current event that interrupts system operation	Date, time of event
		Event description
		Category
SERVICE RECORD	Current event related to current incident	Service provider
		Response; date/time
		Completion; date/time
		Return to operation
LEGACY DATA	Operating history including BOM information on repair or replaced components	Component
		Date
		Event(s)
		Repaired/Replaced
PERFORMANCE	Energy lost due to downtime	Downtime loss of kWh
EXPORT TO ANALYSIS	Use of software to calculate the information in the third column.	Distribution
		Reliability: $R(t)=1-F(t)$
		Availability: $A(t)=kWh/kWh_{MAX}$

Figure M-1: Example of Bill of Materials for an Inverter

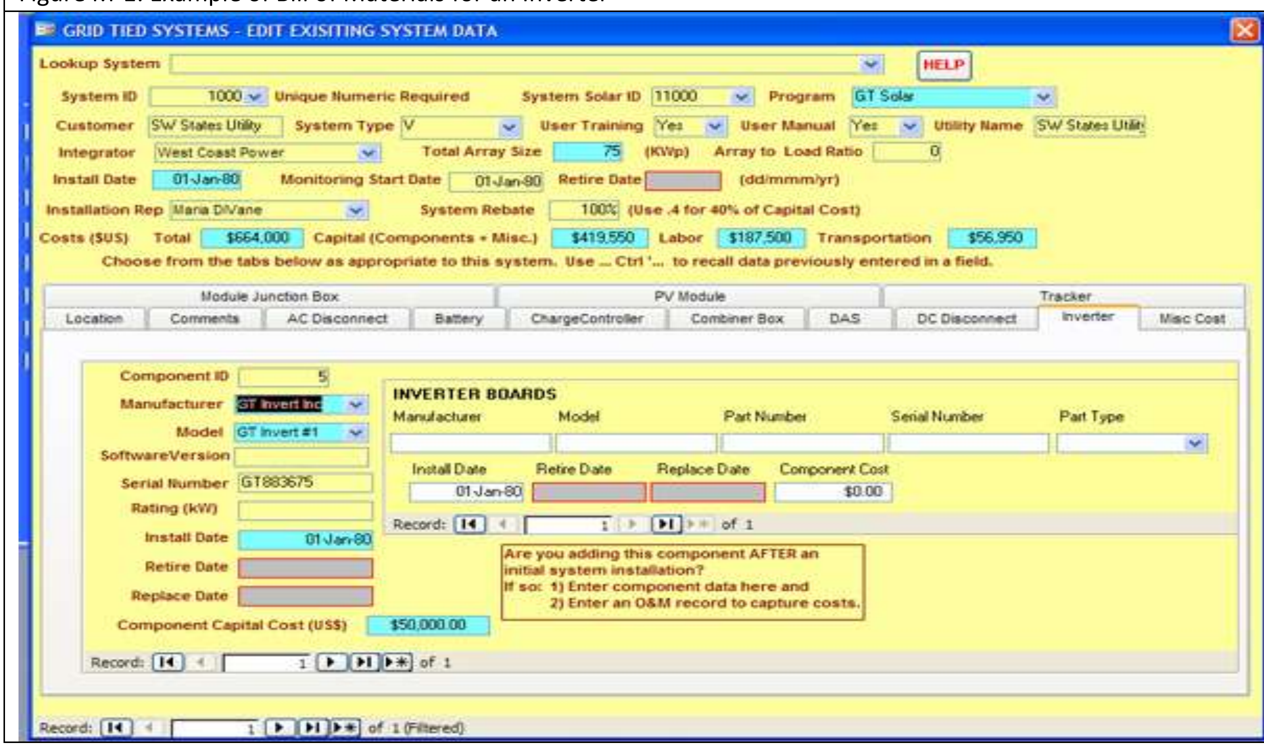

REF	AUTHOR(S)	TITLE	PUBLICATION
N	Collins, E. et al.	A Reliability and Availability Sensitivity Study of a Large Photovoltaic System	Sandia National Laboratories, 25th European Union PV System Conference & Exhibition, July 2010

SUMMARY: This paper was an extension of the database effort documented in the previous reference. The objective was to determine the variations in generating capacity due to weather, module degradation, system configuration, and plant location.

A simulation program was written (see flow chart in Figure N-1) that incorporated solar irradiance, module performance, and equipment availability. Model predictions and data were based on selected arrays of the Tucson Electric Power GCPVS in Springerville, AZ, with a total generating capacity of 4.6 MW_{DC}.

Variation in field data for 2003 to 2007 was compared to a normal distribution; the data has a mean of 229,645 kWh and a standard deviation of 5193 kWh.

Table N-1 lists results based on linear degradation of 0.50%/year, for 5 years of operation compared to field data. Differences between data and predictions were attributed to:

- Use of irradiance data for Flagstaff, AZ since this data was not available for Springerville.
- Influence on predictions of assumptions in weather model, based on TMY2.
- Year-to-year variations in weather, for Springerville, were not reliable.
- The 5 years of operation did not provide sufficient data to accurately define times for failure, repair, and reasons for these failures.

Availability is normally associated with the ratio of mean time between failure (MTBF) divided by mean time between failure plus mean time to repair (MTTR). The study uses availability as a measure of the generation divided by the maximum possible generation at specific locations, e.g., assuming weather conditions, no inverter component failures, etc., $A(t)= (kWh)/(kWh)_{max}$.

Per Figure N-2 the average availability is, as nearly as can be read, between 100% and 98%.

Data taken from Figure N-2 are in good agreement with predictions of reliability from Figure N-3, based on a negative exponential distribution. Of note is that the reliability asymptotically approaches zero after about 3 years of operation.

Figure N-1: Procedure for Calculating System Generation with Variations in Performance

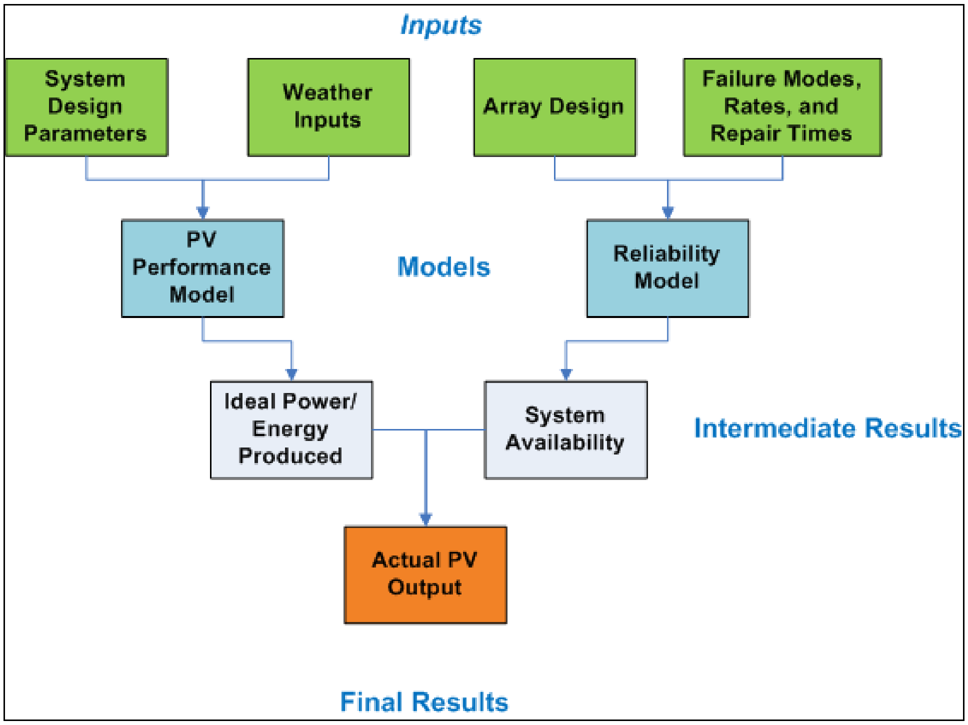

Table N-1: Comparison of Field Data and Predictions for Degrading of Power

PERCENTILE	DATA	PREDICTION	(Prediction-Data)/Prediction
5	221,300	229,900	3.7%
50	229,800	247,700	7.2%
95	238,400	263,600	9.6%
Percent	kWh	kWh	

Figure N-2: Availability and Reliability vs. Time

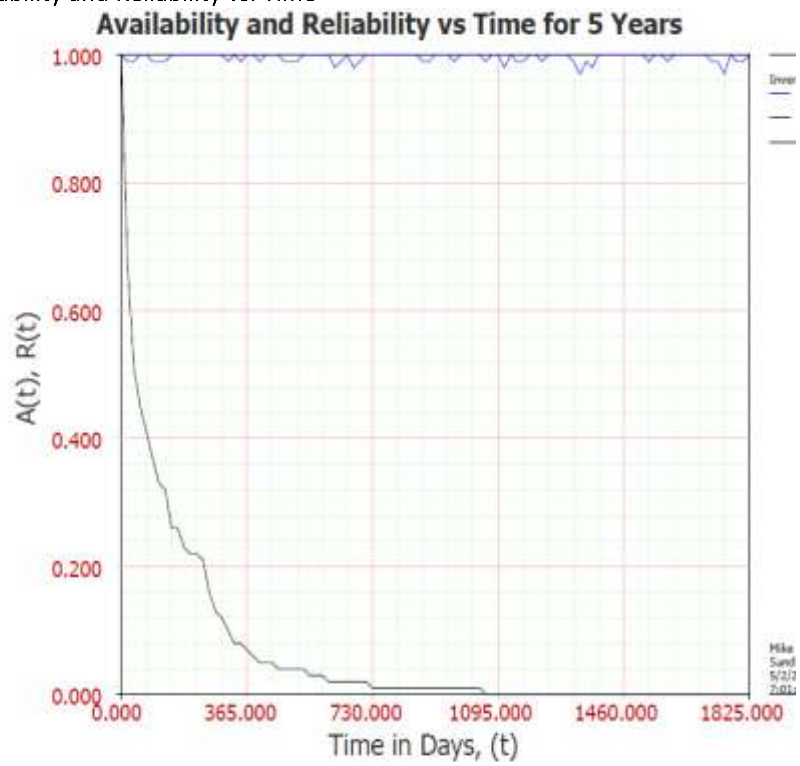

Figure N-3: Trend Line for Reliability

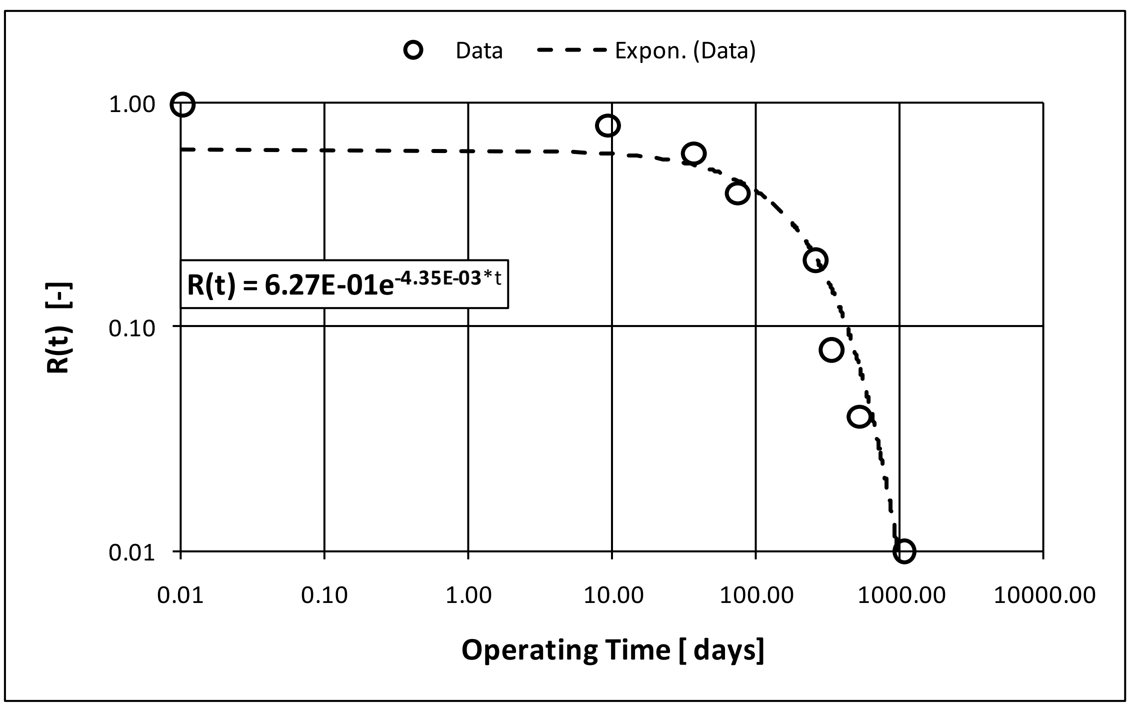

REF	AUTHOR(S)	TITLE	PUBLICATION
O	Firth, S.K., Lomas, K.J., Rees, S.J.	A Simple Model of PV System Performance and Its Use in Fault Detection	*Solar Energy*, v84, 2010: 624-35

SUMMARY: This paper presents a simple, straightforward method of fault detection. The method is based on a definition of efficiency based on the ratio of the AC power, P_{AC}, produced by the PV system divided by the insolation, G, incident on the plane of the module multiplied by the module surface area, A: $\eta = P_{AC}/GA$ (see Figure O-1).

In the region identified as normal operation, there is a dense set of points for the efficiency versus GA. The data spread in this region is attributed to changes in insolation and weather, and variations in solar cell temperatures. Data below this band are, in part, representative of faults in the performance.

These points are formed into a histogram of values of efficiency with a given range, vs. the number within that range divided by the total number of points within that range. Since data would be dominated by the normal operating points that fell below the normal operation-fault line, each range would have 300 points.

Thus a range of efficiency would be divided into ranges, or bins. The result, the data being random, would approximate a normal distribution between the mean and ($n\sigma$), where (σ) is the standard deviation and (n) the number of standard deviations. Values < ($n\sigma$), at lower values of probability, represent faulted operation, while values > ($n\sigma$) signify normal operation (see Figure O-2).

COMMENTS: Systems for which the data were taken were small, in the power range of 1-2 kW, consisting of one array and containing 10 to 20 modules. The series-connected "strings" of modules were then connected to the inverter.

- Lincoln Theater PV array (17kW) at the University of Hartford is divided into 3 sets of 3 arrays each (Figure O-3). With this larger number of modules and arrays, changes due to faults could be more difficult to identify.

- PSCAD could be used to simulate loss of solar cells, or modules.

- Monitoring at Lincoln Theater would be limited to the inverter. Faults might be easier to detect if the current from each of the strings was monitored before the inverter, to determine if any failures had occurred. The efficiency would then have to be based on the DC power.

Figure O-1: Limits for Normal Operation and Operation with Faults

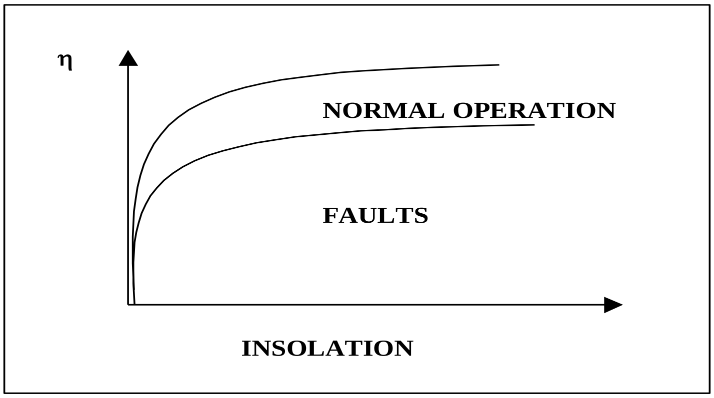

Figure O-2: Histogram for Operation Without and With Faults

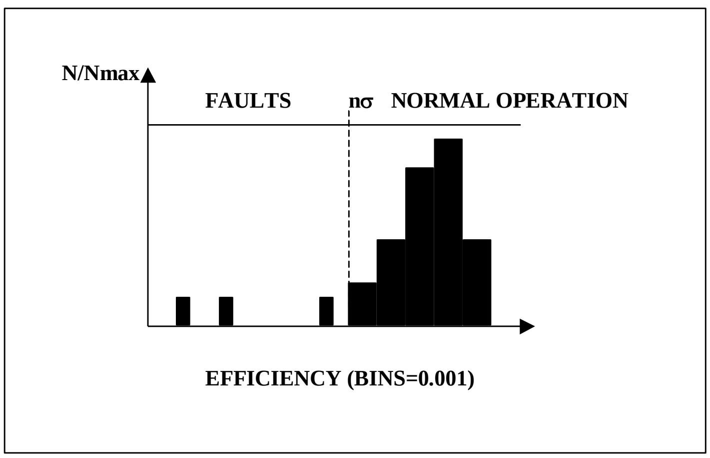

Figure O-3: PV System Monitored by Firth and Lincoln Theater PV System

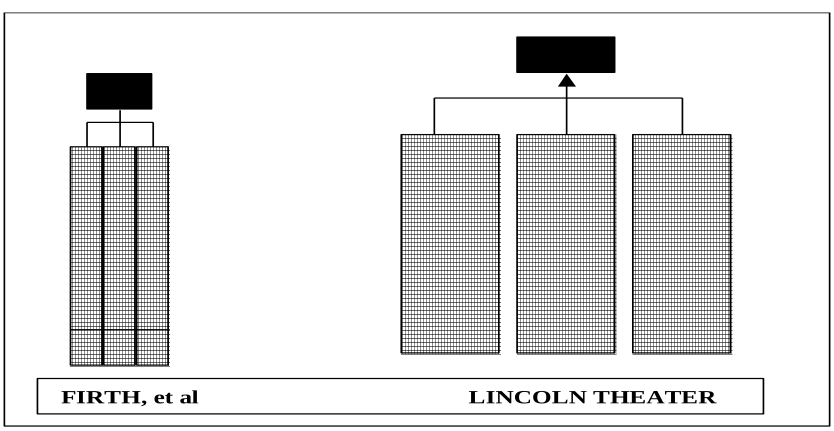

4 SIMULATION OF FAILURE OF MULTIPLE COMPONENTS

4.1 BACKGROUND

The precise outcome of a "random" process is unknowable prior to the actual outcome. However, through long observation and in some cases understanding the characteristic parameters of the process, the randomness can be estimated. The three key random process functions typically determined are the mean, variance, and probability density function (PDF). Mean and variance are single point values while the PDF is a function of probability vs. outcome. From these three values the probability of any given outcome from a random process event "trial" can be established.

Mean: The mean, or perhaps more correctly termed the "expectation value," provides the most probable value. For example if we repeat a trial observation of the process outcome for a large number of trials and we segregate all of the outcomes, then the number of times a particular outcome is observed, ratioed to the total number of trials, is the probability of that particular outcome. As the number of trials increases, the stability of the probability estimate also increases.

Once the probability of an outcome is determined, for any further experimentation the expected number of observations of the "i-th" outcome is:

Expected number of "i-th" outcomes = number of trials X "i-th" probability
For example, a simple fair coin toss p-tails = 0.5
Number of trials =1000
Expected number of tails = 500
M value = 500

The extent to which the above example outcome deviates from the expected value is also a vital random process variable.

Variance: The variance or $\sqrt{\sigma}$ where σ is the standard deviation is a second power parameter that measures how much the actual observation can deviate from the expected value. Often labeled as process "dispersion," it measures the magnitude of expected deviation from the mean value.

The example above establishes the number of tails "expected" from 1,000 trial experiments. The variance tells us how much we should expect the number of tails to deviate from 500 if the experiment is run a number of times. Thus, the variance is nothing more than a sum of the square of the deviation between the number of tails from all of the experiments and the constant mean value of a single experiment. For the above example if we had performed the 1,000 coin toss experiment 1,000 times and each time noted the actual number of tails that occurred, we could estimate the random process variance from the equation:

$$\frac{1}{1000}\left[\sum_{i=1}^{1000}\left(O_i - O_{expected}\right)\right]^2$$

Based on the probability of an event we can compute both the expected (mean) number of outcomes and also the variance about that mean outcome.

The mean and variance are collectively referred to as the "moments" of a random process.

Probability Density Function: The third random process characteristic is the probability density function (PDF). Mathematically, the PDF is the most important descriptive function for a random process. From the PDF all moments and any estimate about the probability of the occurrence of a range of outcomes can be calculated.

These three random process values are all that is required to determine the number of outcomes from a particular number of trials.

Random Process Simulation

As the above discussion shows, it is possible to determine the mean number of outcomes that should occur, as well as the variance of that number, but it does not provide any indication as to when such outcomes *could* occur.

One might make the case that for the 1,000 fair coin toss example above it does not matter in which order the expected 500 tails are produced. This is a valid point but the conditions under which the experiment is run impact the significance of outcome order.

For example, in the 1,000 fair coin toss, what if for every time a "tails" outcome occurred the experimenter received one unit of credit, but for every time a "heads" outcome occurred the experimenter forfeited a unit of credit? Further, what if a rule of the experiment stipulated that the both the credit receipt and forfeiture must be made immediately after each coin toss. And what if there is a rule that the number of credits in hand must be one or greater?

These rules highlight the need for some way to simulate the actual arrival order of the experiment's "tails." Such a simulation is important because it provides the participant with a sobering indication of the "extreme" possibilities that can occur.

For example it is possible to produce exactly 500 tails and 500 heads. But what about the rare situation where the 500 heads all occur in the first 500 trials, and the experimenter does not have at least 501 credits to start play? The experimenter's reserve would be exhausted and the experimenter would be eliminated from the experiment, even though the experiment would, at its full 1,000-trial completion, require no player reserve.

This is the value of random event simulation. It illustrates that reliable statistical characteristics speak only to aggregate output and that very unusual "runs" of outcomes can occur during the experiment, triggering unexpected results—just as unusual runs of failures can occur in PV arrays, which impact the owner's economic and technological reserves and ability to continue "playing the solar generation game."

4.2 SIMULATION OF THE FAILURE OF MULTIPLE COMPONENTS

Simulation for a GCPVS: On first inspection using the mean time between failure (MTBF) and mean time to repair (MTTR) appears to be sufficient to predict the availability of the GCPVS. However, since the installation does not produce the same amount of power during different times of the year and different times of day, a failure's power production impact differs even though the probability of that failure is constant.

The MultiC_Risk program was developed to investigate the possible failure scenarios of a multiple-component GCPVS. MultiC_Risk provides output of the operability status of each component in the simulation at a user-specified time interval.

MultiC_Risk does not provide any new information on the expected number of failures in the course of the simulation. MultiC_Risk produces on average the same number of failures as the standard statistical mean. The simulation does, however, permit the PV analyst to observe a time history of possible patterns of component failures and from this time history assess the impact of component failures on the system's power production.

Each execution of MultiC_Risk is a new experiment. By viewing the GCPVS component scenarios from a large number of MultiC_Risk runs, the full range of power production impact possibilities can be observed. Simply put, if a component's failure probability predicts two failures per year, MultiC_Risk will give the PV engineer the opportunity to realize there is an economic difference between those two failures occurring consecutively on a high production summer day at noon as opposed to singly in the morning during winter.

4.3 MULTIC_RISK INPUT AND OUTPUT

MultiC_Risk is a multiple component failure simulation function written using MATLAB® script. The duration of the simulation is one year. The computer program is listed in Appendix 4-A.

Input: The user provides input to MultiC_Risk in the form of direct inputs and the identification of a component filename.

Table 4-1: Case Input

% read the number of components in the system
N =components = input ('Enter the number of system components ');
C =filename = input ('Enter Component Filename ','s') ;
T =step = input ('Enter time step in hours ') ;
N =components = number of components in the simulation
C =filename = filenames of the component failure and repair probability s
T =step = = the simulation time step in hours

This can be put into a table, for example, the C file name component is a simple ASCII text file that contains the specific details of each simulation component.

Table 4-2: MultiC_Risk Calculation Parameters for Components

Component 1, 180, 1.002, 1, 1.0, .2
Component 2, 365, 1.002, 2, 1.0, .3
Component 3, 250, 1.002, 1, 1.0, .5
Component 4,500, 1.002, 10,1.0,.8

The component file has six fields for each component:

Table 4-3: Failure and Repair Parameters

1^{st} field = for the component's name
2^{nd} field = Mean Time Before Failure (MTBF) in days
3^{rd} field = Weibull "β" exponent for the failure rate
4^{th} field = Mean Time to Repair (MTTR) in days
5^{th} field = Weibull "β" for the probability of repair
6^{th} field = Impact of component failure on overall system

Note that the values are selected to demonstrate the effect of each set of failures and repair times for the length of time the solar-based generation is reduced.

Table 4-4: Component Failure and Repair Times

COLUMNS	1	2	3	4	5	6
TITLES	COMPONENT	MBTF	$\beta_{FAILURE}$	MTTR	β_{REPAIR}	IMPACT
VALUES	1	180	1.002	1	1.0	.20
	2	365	1.002	2	1.0	.30
	3	250	1.002	1	1.0	.50
	4	500	1.002	10	1.0	.80
UNITS	-	DAYS	-	DAYS	-	-

Failures: For the inverter, failures of the components depend on the failure rate and the interaction of the failed component. The failure rates, interaction, and failure mode are documented in Table 4-5.

Table 4-5: Failure Rates, Type and Effects on Operation and Other Inverter Components

#	Component	$\lambda_p/10^6$hrs	Mode	Failure Effect	Effect on Other Components
1	IGBT	300.96	short (85%)	power decrease/shutdown	overheating/failure of other IGBTs
2	Relay	2.075	open (80%)	shutdown	none
3	cap, elect.	9.54	open (90%)	power decrease/shutdown	none
4	microproc.	1.097	inoperative	power decrease/shutdown	possible failure
5	board supply	.522	inoperative	power decrease/shutdown	possible failure
6	cap, film	.274	open (90%)	output power decrease	none
7	cap, film	.274	open (90%)	output power decrease	none
8	transformer	.2058	open (80%)	shutdown	none
9	inductor	.000252	open (80%)	shutdown	none
10	inductor	.000252	open (80%)	shutdown	none

Repairs: Failed components are then "repaired" starting on the next simulation time step. Here again the probability of repair is also assumed to be exponential and the repair probability is assumed to be constant. The determination of a repaired component is based on the comparison of a randomly generated, uniformly distributed number compared with the repair probability. Once repaired the status flag for the component is returned to "OK"; on the next time step the failure of the component is evaluated. The failure and repair states of all the components in the simulation are evaluated for each time step during the simulation year. Neither a constant failure rate nor a constant repair rate is truly realistic. Older components have a higher probability of failure than new components, and the probability of repair should increase with older components if in fact they can be repaired.

Failure and Repair Distribution

The current version of MultiC_Risk is based on a Weibull distribution as the PDF, f(t), and the basis for the cumulative distribution function (CDF) for the reliability, R(t) and failure, F(t)=1-R(t). The general two-parameter Weibull distribution is a function of a "shape" factor, β, and "scale" η. Of these parameters, shape factor β is used as an approximation of the PDF and CDF for failure and repair (see Table 4-6).

Table 4-6: Probability Density and Cumulative Distribution Functions for a Weibull Distribution

	PDF	CDF	DISTRIBUTION	REPRESENT
β	$f(t) = (\frac{\beta}{t})(\frac{t}{\eta})^{\beta} \bullet \exp[-(\frac{t}{\eta})^{\beta}]$	$F(t) = 1 - \exp[-(\frac{t}{\eta})^{\beta}] \quad R(t) = \exp[-(\frac{t}{\eta})^{\beta}]$	2-parameter Weibull	Failure or Repair
1	$f(t) = (\frac{1}{\eta}) \bullet \exp[-(\frac{t}{\eta})]$	$F(t) = [1 - \exp[-(\frac{t}{\eta})]; R(t) = [\exp[-(\frac{t}{\eta})]$	Negative exponential	Failure
2	$f(t) = (\frac{2}{t})(\frac{t}{\eta})^{2} \bullet \exp[-(\frac{t}{\eta})^{2}]$	$F(t) = [1 - \exp[-(\frac{t}{\eta})^{2}]; R(t) = [\exp[-(\frac{t}{\eta})^{2}]$	Log Normal	Repair

The parameter β acts as an exponent of the constant probability values for failure and repair. If β = 1, no change in the exponential failure/repair rates occurs over time. For β > 1 the probability of failure increases for each time step until the component fails. A value of β > 1 for the repair probability will increase the probability of repair the longer a component has a "failed" state status. The MultiC_Risk simulation output is a text file (file extension .rsk) with a comma-separated values (CSV) structure for easy import to Excel.

Output: The output file has a summary header section, as shown in Table 4-7:

Table 4-7: Results of MultiC_Risk Calculation

COMPONENT	MTBF	$\beta_{FAILURE}$	MTTR	β_{REPAIR}
1	180	1.000	1.0	1.000
2	30	1.000	2.0	1.000
3	90	1.000	1.0	1.000
4	500	1.000	10.0	1.000
…..	…..	…..	…..	…..
UNITS	Days	-	Days	-

Results (Component Status): Following the information header, the status of each component is reported at every user-specified time step over a 365-day simulation year:

Availability*:* This parameter has a range of 0-1. A value of 1 means the system fails when the component fails. A value of 0 means component failure has no impact on system availability. Table 4-8 shows a sample output.

Table 4-8: Availability = 1, Operating; Availability =0, Being Repaired

Day	Time	Comp 1	Comp 2	Comp 3	Comp 4
28	12	1	1	1	1
29	0	1	1	1	1
29	12	1	1	1	1
30	0	1	1	1	1
30	12	1	0	0	1
31	0	1	0	0	1
31	12	1	1	0	1
32	0	1	1	0	1
32	12	0	1	0	1
33	0	0	1	0	1
33	12	1	1	1	1
34	0	1	1	1	1

Components 2 and 3 both fail at the start of the 30th day of the year. Component 2 is repaired in one day, but the Component 3 repair requires three full days. Figure 4-1 shows the downtime for Component 1 and no failures for Component 2.

Figure 4-1: Component Failure and Repair

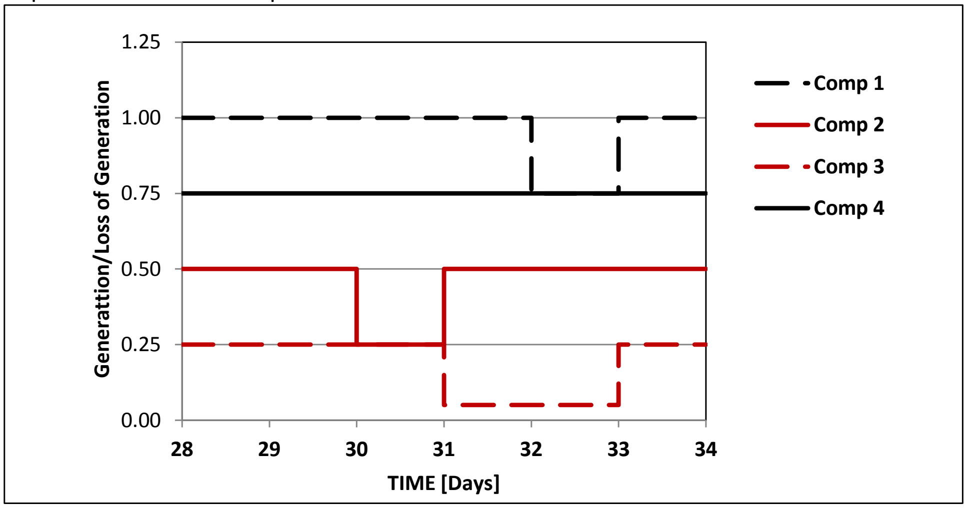

The full-year simulation is input to another application that evaluates the power production output during the year and determines the economic impact of the component failure.

Observations Regarding MultiC_Risk Simulator: While there is no need to have a component failure simulator to determine the number of expected component failures a GCPVS will experience in a year, MultiC_Risk provides a unique perspective on the kinds of component failure scenarios that can occur. Multiple MultiC_Risk runs provide a range of equally possible annual failure histories for design and economic assessments.

For a situation in which a number of component failures per year are expected, MultiC_Risk can identify the arrival sequences of these component failures (for example, evenly spaced vs. failure clusters). This makes MultiC_Risk a useful simulation for assessing the economic impact of PV power generation reliability.

Appendix 4-A shows the MultiC_Risk program.

MultiC_Risk Calculation Procedure

The calculation procedure starts with the Monte-Carlo-based analysis to determine the time before failure (TBF) and time to [complete] repair (TTR). Insight into results of the calculation procedure is gained by considering the result based on variations in failure and repair rates. The analysis assumes relative values rather than actual values of TTF and TTR. These are classified as (a) “high” as TTF and/or TTR >1, and (b) “low” as TTF and/or TTR <1. Results based on these combinations (Table 4-9) can provide insight into performance.

Table 4-9: Combinations of Time Before Failure and Time to Repair

COMPONENT	TIME BEFORE FAILURE (TBF)	TIME TO REPAIR (TTR)
A	TBF >1	TTR <1
B	TBF <1	TTR >1
C	TBF >1	TTR >1
D	TBF <1	TTR <1

The results shown in Figure 4-2 would, after a number of runs, provide information on the occurrences of failure and subsequent repair on the “dead-time” required to calculate the lost power generation (which continues in Section 5 of this report). Note that the values are representative and not related to actual failure or repair rates. Since the failure and repair times are random, sufficient cases must be run to show how the failure/repair times vary. If sufficient cases are run, a probability density distribution can be created. This would result in the mean values.

Figure 4-2: Representative Availability of Four Components at Conditions in Table 4-9 (above)

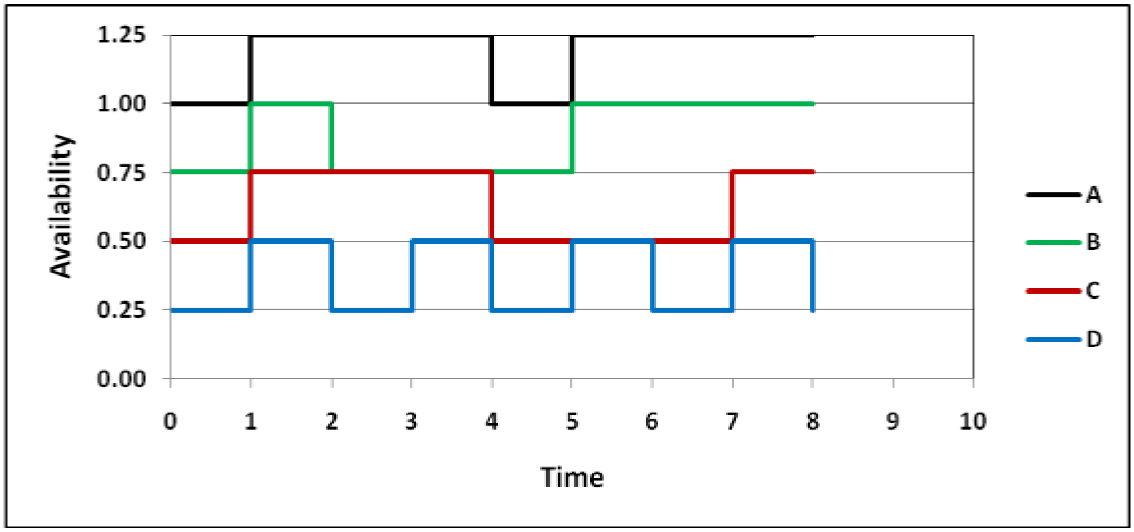

The failure patterns not only forecast when one of the components may fail but also, for multiple components, indicate when a surplus or deficit of power may occur and/or provide information that helps define an effective maintenance program.

4.4 FAILURE AND REPAIR

Failures: Failure and reliability are related. Reliability is the probability that a component will fail. Reliability depends on the design, manufacture, and loads on the component. Low reliability will result in frequent failures followed by repair or replacement.

Failure rates can be calculated in a variety of ways. Two frequently used methods are the Military Handbook and Telcordia, which updated the Bellcore version of the Military Handbook. A summary of each follows.

- *Reliability Prediction of Electronic Equipment* (MIL-HDBK-217F) issued by the U. S. Department of Defense in December 1991. Lambda Predict supports both the Part Stress and Parts Count calculation methods for electronic components in commercial and military applications. Note that high failure rates result in low values of time to reach this limit, while low failure rates result in high values of time to reach the design life.

- *Reliability Prediction Procedure for Electronic Equipment* (SR-332 Issue 2) issued by Telcordia Technologies in September 2006. This standard provides reliability prediction models for electronic components in commercial applications. Lambda Predict also supports two previous versions of the standard: TR-332 Issue 6, issued by Bell Communications Research in 1997 and SR-332 Issue 1, issued by Telcordia Technologies in 2001.

Results for the SMA SB-6000U Lincoln Theater inverter, based on the MIL-HDBK-217F and Telcordia SR-332 Issue 2 software, are shown in Tables 4-10A and 4-10B, and in Appendix 4-B.

Note that the failure rate data given by the MIL-HDBK is, for the IGBTs that have the highest failure rates, about 25 times higher than that of the more recent standards. Perhaps this is not surprising in view of statements by Bellcore, which previously used the MIL-HDBK for predictions but found they were getting very pessimistic results. This led to the development of their own model to more accurately reflect their field experience. Telcordia has continued development of the Bellcore procedure. Most commercial electronic product companies now use the Telcordia SR-332 handbook for reliability predictions.

Table 4-10A: Failure Rates of Inverter Components Based on Low Stress Values (MIL-HDBK-217F)

ID	COMPONENTS	MFR/MODEL NUMBER	QTY	$\lambda_p/10^6$hrs	FUNCTION
1	IGBT	IXYS/K30N60	8	37.62	PWM bridge switching device
2	relay	PB/T9AS1D12-9	1	2.075	AC disconnect
3	cap, elect.	EPCOS/B43504	20	9.54	DC filter
4	microprocessor	TI/MCUM3	1	1.097	PWM/control
5	board supply	DC/DC converter	1	.522	low voltage DC supply
6	capacitors, film	EPCOS/B32231	1	.274	PWM high frequency filter
7	capacitors, film	EPCOS/B32231	1	.274	AC filter
8	transformer		1	.2058	AC isolation
9	inductor	EPCOS/B82726	2	.000252	PWM high frequency filter
10	inductor	EPCOS/B82726	2	.000252	AC filter

Table 4-10B: Failure Rates for Inverter Components Based on Telcordia SR-332, Issue 2

ID	COMPONENTS	MFR/MODEL	QTY	$\lambda_p/10^6$hrs	FUNCTION
1	IGBT	IXYS/K30N60	8	1.452	PWM bridge switching device
2	relay	PB/T9AS1D12-9	1	.322	AC disconnect
3	microprocessor	TI/MCUM3	1	.365	PWM/control
4	board supply	dc/dc converter	1	.262	low voltage DC supply
5	capacitors	EPCOS/B43504	20	.107	DC filter
6	capacitors, film	EPCOS/B32231	1	.087	PWM high frequency filter
7	capacitors, film	EPCOS/B32231	1	.087	AC filter
8	transformer		1	.049	AC isolation
9	inductor	EPCOS/B82726	2	.000028	PWM high frequency filter
10	inductor	EPCOS/B82726	2	.000028	AC filter

Repair: Values of TTR are required to complete the stochastic analysis. The objective of this section is, based on published information on simulating the performance of a variety of components, to use this data to determine the difference in time between failure and repair. These values are then applied to corresponding components in the University of Hartford inverters for its 17kW GCPVS. Failure rates are identified for major components of the SMA SB-6000U inverter, using the Lambda Predict (Version 3) reliability software. These analyses were performed according to the published standards provided by the Lambda Predict software.

Repairs are usually treated as random. Unlike failure, which is related to deterioration of the various components (the solar modules as well as the inverter's electronic components), repair depends on activities leading up to the actual repair or replacement, for example: failure detection, identification of the cause, preparing work and purchase orders, training, gaining access to the failed component, the actual repair or replacement and, finally, confirmation of operation. As with failure, repair (including the intervals for preparation and return to service) is assumed to start at the time before failure (TBF). Thus while the number of repair rates is related to these times, the repair rate can include time for organization and preparation.

The time before failure (TBF) represents the time repair is completed and time of the next failure, while the time to repair (TTR) is the downtime during which the inverter, or other system or subsystem, is inoperable and no power is generated (Figure 4-3).

Figure 4-3: Time Before Failure and Time To Repair

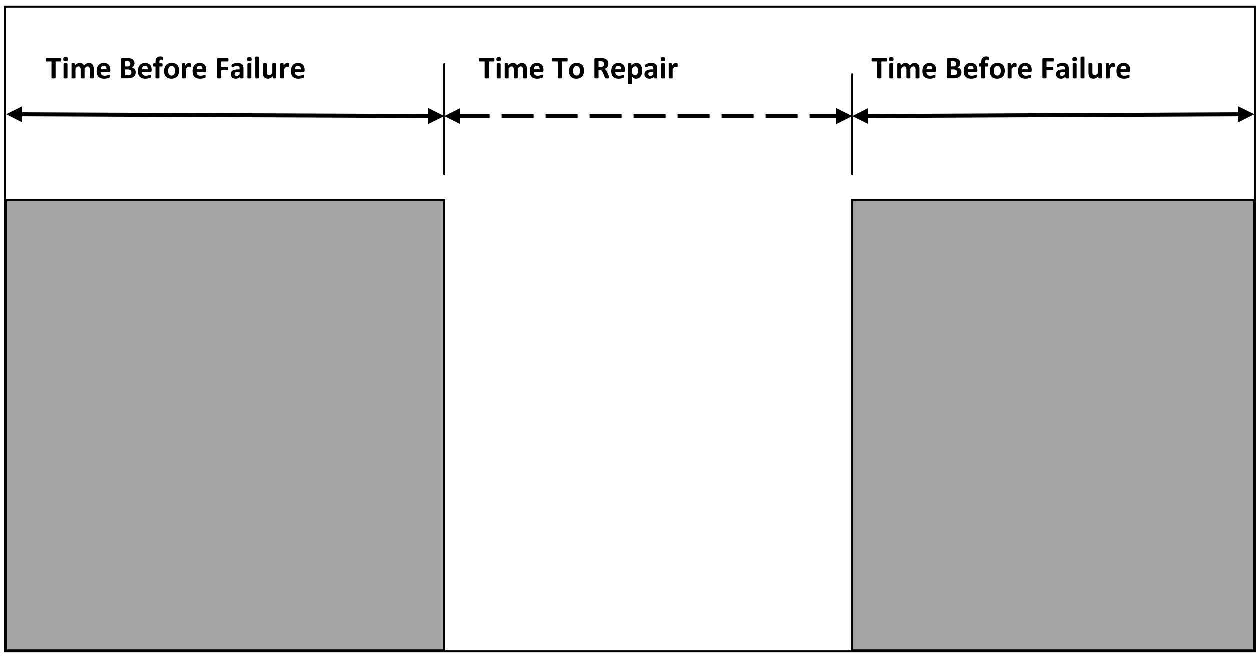

In many cases the IGBT failure rate is the dominant reason for failures and repairs. Values are listed in Table 4-11. Note that Ristow values for the system [4-1, 4-2] are in reasonable agreement with the Telcordia value.

Table 4-11: Failure Rates for IGBTs

MIL-HDBK		Telcordia	Ristow	Ristow, et al.
High Stress	Low Stress	SR-332	[4-2]	[4-1]
300.96	37.62	1.452	.90	.0017
$\lambda_p/10^6$hrs	$\lambda_p/10^6$hrs	$\lambda_p/10^6$hrs	$\lambda_p/10^6$hrs	$\lambda_p/10^6$hrs

Failure and Repair Rates: While a large bibliography exists on failure rates, there are far fewer studies on repair rates. This is partly due to the activities required before and after the actual repair activity. However, this downtime represents an interval when power generation is reduced. Aside from costs related to the repair, expense also can be incurred by the need to purchase replacement power.

Appendix 4-C lists failure rates for reference conditions, operating conditions, and components at operating conditions values, comparing MTBF using MIL-HDBK-217F, Bellcore (TR-332), Telcordia (SR-332, Issue 1), and Telcordia (SR-332, Issue 2).

Example of Failure and Repair Calculations: Ristow, et al. [4-1] assume that the the inverter's failure and repair probability density functions (PDF) can be represented by two parameters, the scale (η) and shape (β) Weibull function. Based on the data from the Georgia Tech Aquatic Center (GTAC) installation, η and β parameters were derived. Weibull functions and parameter values for the IGBTs are shown in Table 4-12.

Table 4-12: Parameters for Weibull Functions Based on GTAC Data

PDF			CDF
$f(t) = (\frac{\beta}{t})(\frac{t}{\eta})^{\beta} \bullet \exp[-(\frac{t}{\eta})^{\beta}]$			$F(t) = 1 - \exp[-(\frac{t}{\eta})^{\beta}]$
FAILURE (F)			
0≤ β≤1	Negative Exponential	$f(t) = (\frac{1}{\eta}) \bullet \exp[-(\frac{t}{\eta})]$	$F_F(t) = 1 - \exp[-(\frac{t}{\eta_F})]$
η_F	13213	Hr	
λ_F=1/ η_F	7.57E-05	failures/hr	
β_F	1.052	-	
REPAIR (R)			
1 ≤β≤2	Log Normal	$f(t) = 2(\frac{t}{\eta}) \bullet \exp[-(\frac{t}{\eta})^2]$	$F_R(t) = 1 - \exp[-(\frac{t}{\eta_R})^2]$
η_R	718.4	Hr	
λ_R=1/ η_R	1.39E-03	repairs/hr	
β_R	1.7397	-	

The failure and repair vs. time are shown in Figures 4-4A and 4-4B. As expected, repair requires less time than failure. This observation will be the basis of determining the ratio of repair to failure times.

Figure 4-4A: Failure and Repair (IGBT)

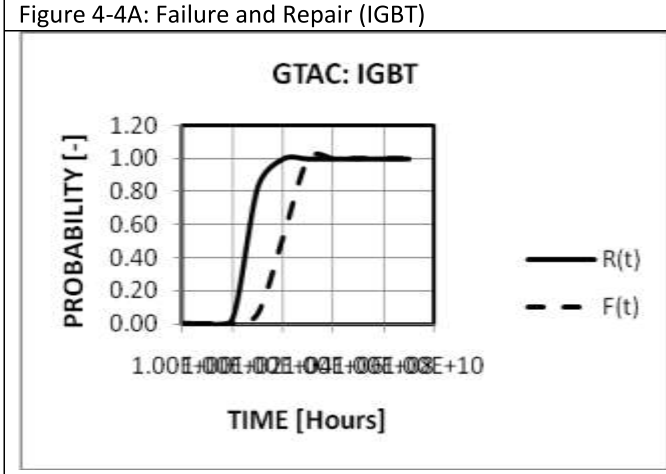

Figure 4-4B: Failure and Repair (PV Modules)

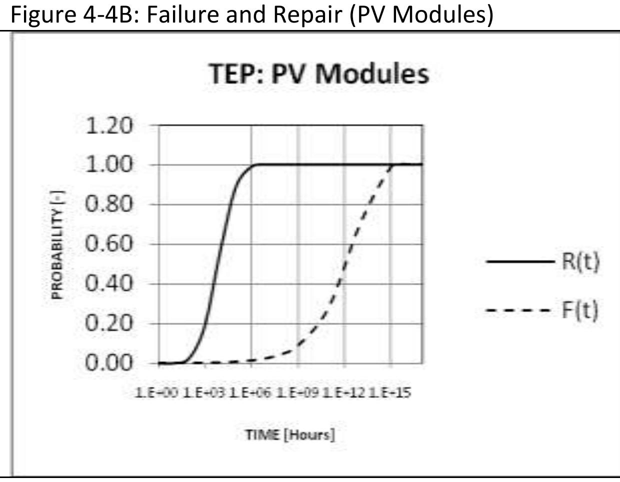

BTL to fix axis overlap

Failure and Reliability

Failure F(t), and reliability, R(t), are related: Components with low reliability tend to have a large number of failures. Appendix 4-D is a sample calculation using the website[12] calculator provided by the University of Massachusetts' electrical and computer engineering department. Per Andrews [4-4] series-parallel reliability calculations were accomplished by use of this software. System configuration information was entered at the nodes and connection points of modules. The reliability values were calculated using a "mission time," T = 20 years (1.753×10^5 hours). Results of these calculations, for the University of Hartford Lincoln Theater inverter, are as follows:

- Five DC filter capacitors in parallel: R(T) = 0.99999
- Four parallel DC filter capacitor groups (Figure 4-D1, Appendix): R(T) = 1
- Eight IGBTs in series: R(T) = 0.96961
- Three paralleled components of the PWM and AC filters: R(T) = 0.99999

Reliability for the complete inverter system of the system is $R_s(T) = 0.87079$. The corresponding failure rate of the complete system is $\lambda_s = -\ln[R_s(T)]/T = (-\ln 0.87079)/0.1753 = 0.78924$ FPMH (failures per million hours).

Time to Repair

Ristow's doctoral thesis [4-2] covered a number of areas ranging from cost of manufacturing solar cells to distribution functions for the Georgia Tech Aquatic facility. The method used to calculate repair times is documented in the literature review (section 3 of this report). Examples of the Failure , F(t) and repair, R(t) are shown in Figures 4-4A and 4-4B, above. Collins, et al. [4-5] used the operational data from Tucson Electric Power's (Springerville, AZ) 26 identical systems with a total generation capacity of 4.6 MW_{DC}.

Values of the two- and three-parameter Weibull functions are given for failure (Table 4-13A) and repair (Table 4-13B). The ratios of values of TBF and TTR are then used to calculate the ratio of repair to failure times (Table 4-14).

Note that this is based on the assumption of a relationship between component failure and repair. However, while failure depends on reliability being "built" into the component, repair depends on repairability being one of the design requirements; for example ease of access, etc.

[12] www.ecs.umass.edu/ece/koren/FaultTolerantSystems/simulator/NonSerPar/nsnpframe.html

Table 4-13A: Weibull Function Parameters for Failure

REFERENCES	FACILITY	COMPONENT	WEIBULL	ηF=SCALE	βF=SHAPE	ˈϒF=LOCATION	TBF@prob=1
4-1	GTAC	System	Weibull-2	1.32E+04	1.05	0.00	1.00E+05
4-2	GTAC	IGBT	Weibull-2	1.11E+06	1.00	0.00	1.00E+05
		PCU	Weibull-2	9.95E+02	2.18	0.00	1.00E+07
		Capacitors	Weibull-2	5.76E+02	1.00	0.00	1.00E+07
4-3	TEP	AC Disconnect	Weibull-3	1.10E+04	0.35	3.90	1.00E+06
		Row Box	Weibull-2	1.20E+06	0.51	0.00	1.00E+08
		PV Module	Weibull-3	5.20E+12	0.28	17.00	1.00E+16
		480 Transformer	Weibull-2	7.10E+03	0.58	0.00	1.00E+07
		208/480	Weibull-3	1.00E+01	2.30	0.00	1.00E+07
			LOG NORMAL	**Σ**	**μ**		
		Marshall Box	Log Normal	2.30E+00	10.00		1.00E+07

Table 4-13B: Weibull Function Parameters for Repair

REFERENCES	FACILITY	COMPONENT	WEIBULL	ηR=SCALE	βR=SHAPE	ˈϒR=LOCATION	TTR@prob=1
4-1	GTAC	System	Weibull-2	7.18E+02	1.74	0	1.00E+04
4-2	GTAC	IGBT	Weibull-2	5.76E+02	1.00	0	1.00E+04
		PCU	Weibull-2	9.95E+02	2.18	0	1.00E+04
		Capacitors	Weibull-2	5.76E+02	1.00	0	1.00E+07
4-3	TEP	AC Disconnect	Weibull-2	1.40E+00	0.71	0	1.00E+02
		480 Transformer	Weibull-2	1.36E+00	0.53	0	1.00E+03
		Marshalling Box	Weibull-2	3.50E-01	3.55	0	1.00E+02
			LOG NORMAL	**μ**	**σ**		
		Row Box	Log Normal-2	-0.98	2.07	0	1.00E+03
		PV Module	Log Normal-2	-1.37	3.11	0	1.00E+06
		208/480	Log Normal-2	-2.33	1.6	0	1.00E+01

Table 4-14: Ratios of Repair to Failure Times

Component	References	TBF@prob=1	TTR@prob=1	TTR/TBF
System	4-1	1.00E+05	1.00E+04	1.00E-01
IGBT	4-2	1.00E+05	1.00E+04	1.00E-01
PCU	4-2	1.00E+07	1.00E+04	1.00E-03
Capacitors	4-2	1.00E+07	1.00E+04	1.00E-03
AC Disconnect	4-3	1.00E+06	1.00E+02	1.00E-04
PV Module	4-3	1.00E+16	1.00E+06	1.00E-01
480 Transformer	4-3	1.00E+07	1.00E+03	1.00E-04
208/480	4-3	1.00E+07	1.00E+01	1.00E-06

Note that row and marshalling boxes, which are not part of the inverter, have been omitted.

4.5 DEMONSTRATION CASES

The objective of the following is to document the input and output of the MultiC_Risk analysis.

Table 4-15 lists the components of the SMA SB-6000U Inverter. Comparison of the components was used to determine the Weibull functions; it is clear that not all components are in the inverters. Table 4-15 also lists the SMA SB-6000U components and the corresponding components used in the prior analysis.

Five components selected for the table are assumed to be similar, if not identical, to the components fitted to Weibull functions. Based on this it is assumed that values of repair times are close to those of the components documented in Table 4-15.

A summary of the MTBF values and, using the calculated ratios, the MTTR is listed in Table 4-15 for components common to the Lincoln Theater inverter and the inverters studied in the references.

The objective of this demonstration case is to use predictions based on the MIL-HDBK-217F of mean time before failure (MTBF) and mean time to repair (MTTR) for Lincoln Theater inverter components. The Monte-Carlo-based MultiC_Risk program is used to calculate the availability of generation up to failure and the time for repair of the failure. System availability to generate power is denoted by “1.” Alternately, the repair time and thus no (or reduced) generation is denoted by an availability of “0” as discussed in previous sections.

MultiC_Risk is able simultaneously to consider the performance of multiple components. As structured, the program is not limited in the length of time the system is expected to operate; in this case it is assumed to be 20 years.

Table 4-15: Repair Times for Components in SMA SB-6000U Inverter and Times for Similar Components

COMPONENTS: LINCOLN THEATER INVERTER				COMPONENTS EQUIVALENT TO LINCOLN THEATER INVERTER		CALCULATED VALUES OF MEAN TIME TO REPAIR	
Component	Mfr/model number	qty	MTBF	Function	Components	MTTR/MTBF	MTTR
IGBT	IXYS/K30N60	8	1.38E+02	PWM bridge switch	IGBT	1.00E-01	13.84
capacitor, elec.	EPCOS/B43504	20	4.37E+03	DC filter	capacitors	1.00E-03	4.37
relay	PB/T9AS1D12-9	1	2.01E+04	AC disconnect	AC disconnect	1.00E-04	2.01
capacitor, film	EPCOS/B32231	1	1.52E+05	AC filter	filter	1.00E-03	152.07
480/208	not accessible	1	2.02E+05	step down transf.	480/208 trans	1.00E-06	.20
	Units		Days	-	-	-	Days

Power System Computer-Aided Design (PSCAD) has three limitations:

1. **Multiple Component Failures:** Currently PSCAD can consider only one component at a time. Thus, although MultiC_Risk can perform availability calculations for more than one component at a time, the limit on the number of components (the one component at a time limitation) in PSCAD results in having to consider each component separately. There being a total of 5 similar components, this would require 100 sets of MultiC_Risk calculations, at best, for 20 years.

2. **Time Limits:** MultiC_Risk is not limited by time. However, limits imposed by available RAM memory result in a limit of approximately 60 seconds of simulation time. This can be overcome by scaling the 20 years of expected operation. Scaling for 20 years, or 1.05×10^7 minutes for 1 minute of run time, however, results in an unreasonable reduction in time. The result was that a scaling of one year, or 5.2×10^5 minutes = 1.0 minute of run time was used. The result is that, if all components are considered, 31 one-year cases would have to be done.

3. **Insolation:** PSCAD uses the TMY2 insolation database for calculating power generation. This requires that each day of the month would need 24 hours, or 8,760 total hours per year, or 175,200 data points for 20 years or, for 31 components, 5.4×10^6 calculated values. Based on this, and having the highest value of MTBF, the demonstration cases were limited to the IGBTs. There are 8 separate IGBTs, or four IGBT pairs: IGBT-1/2, IGBT-3/4, IGBT-5/6, IGBT-7/8. This reduces the calculation to 4 sets of IGBTs for 20 one-year sets of calculations.

MultiC_Risk Calculations: The following tables show the steps from A (the values of failure and repair based on data or calculations) to D (distributions of failure and repair times) as reviewed in Section 4-2.

Table 4-16: Data

		Failure rate	Repair rate	Mean Time Before Failure	Mean Time To Repair	Ratio of Repair Time to Time Before Failure
COMPONENT	ID	λF	μR	MTBF	MTTR	MTTR/MTBF
IGBT		300.96	30.096	138.45	13.845	.10
		$\lambda_p/10^6$hrs	$\lambda_p/10^6$hrs	days	days	Note: Rounded off

Table 4-17: Values

FIELDS	1	2	3	4	5	6
TITLES	COMPONENT	MTBF	β[13] $_{FAILURE}$	MTTR	β_{REPAIR}	IMPACT[14]
VALUES	IGBT-1/2	138.4	1	13.84	1	1
	IGBT-3/4	138.4	1	13.84	1	1
	IGBT-5/6	138.4	1	13.84	1	1
	IGBT-7/8	138.4	1	13.84	1	1
UNITS	-	days	-	days	-	-

[13] Both failure and repair are based on Weibull models. With β =1 the model is a negative exponential function.
[14] Impact, which has values from 1-0, is defined as the consequence of this failure: It compromises the operation of other components (≈ 1), or it does not affect the operation of other components (≈ 0.10), etc.

Table 4-18: MultiC_Risk Output for TBF and TTR

TIME			AVAILABILITY			
Year	Day	**Hour**	**IGBT 1/2**	**IGBT 3/4**	**IGBT 5/6**	**IGBT 7/8**
1	1	1	1	1	1	1
1	1	2	1	1	1	1
1	1	3	1	1	1	1
1	1	4	1	1	1	1
1	1	5	1	1	1	1
1	1	6	1	1	1	1
1	1	7	1	1	1	1
1	1	8	1	1	1	1
1	1	9	1	1	1	1
1	2	10	0	0	1	1
1	2	11	0	0	1	1
1	2	12	0	0	1	1
1	2	13	0	0	1	1
1	2	14	0	0	1	1
1	2	15	0	0	1	1
1	2	16	0	0	1	1
1	2	17	0	0	1	1
1	2	18	0	0	1	1
1	3	19	0	1	1	1
1	3	20	0	1	1	1
1	3	21	0	1	1	1
1	3	22	0	1	1	1
1	3	23	0	1	1	1
1	3	0	0	1	1	1
1	3	1	0	1	1	1
1	3	2	0	1	1	1
1	3	3	0	1	1	1
1	3	1	0	0	1	1
1	3	2	0	0	1	0
1	3	3	0	0	1	0
1	3	4	0	0	1	0
1	44	5	0	0	1	0
1	44	6	0	0	1	0
1	44	7	1	0	1	0
1	44	8	1	0	1	0
1	44	9	1	0	1	0

Table 4-19: MultiC_Risk Output in Excel Spreadsheet Format

IGBT 1/2	Hours	Availability	Hours	Hours	Hours	Hours	Days	Days
Year	**Day**	**Hour**	**Op Time**	**IGBT 1/2**	**FAILURE**	**REPAIR**	**FAILURE**	**REPAIR**
1	1	1	1	1	1	0		
1	1	2	2	1	2	0		
1	1	3	3	1	3	0		
1	1	4	4	1	4	0		
1	1	5	5	1	5	0		
1	1	6	6	1	6	0		
1	1	7	7	1	7	0		
1	1	8	8	1	8	0		
1	1	9	9	1	**9**	0	**0.375**	
1	1	10	10	0	0	1		
1	1	11	11	0	0	2		
1	1	12	12	0	0	3		
1	1	13	13	0	0	4		
1	1	14	14	0	0	5		
1	1	15	15	0	0	6		
1	1	16	16	0	0	7		
1	1	17	17	0	0	8		
1	1	18	18	0	0	9		
1	1	19	19	0	0	**10**		**0.4167**
1	1	20	20	1	1	0		
1	1	21	21	1	2	0		
1	1	22	22	1	3	0		
1	1	23	23	1	4	0		
1	2	0	24	1	5	0		
1	2	1	25	1	6	0		
1	2	2	26	1	7	0		
1	2	3	27	1	8	0		
1	2	4	28	1	9	0		
1	2	5	29	1	10	0		
1	2	6	30	1	11	0		
1	2	7	31	1	12	0		
1	2	8	32	1	13	0		
1	2	9	33	1	14	0		
1	2	10	44	1	25	0		
1	2	11	45	1	26	0		
1	2	12	46	1	**27**	0	**1.9167**	

Table 4-20: Summary of IGBT 1/2 Failures and Repairs vs. Operating Time

Year	Time	TBF	TTR
1	0	0	0
	3	1.92	-
	49	-	46.13
	366	316.92	-
2	431	64.75	-
	432	-	1.71
	567	134.92	-
	570	-	2.67
	609	39.46	-
	648	-	38.13
	731	83.33	-
3	767	35.92	-
	778	-	10.88
	871	93.54	-
	886	-	14.46
	959	73.54	-
	962	-	2.38
	1096	134.25	-
4	1254	158.00	-
	1286	-	31.88
	1410	123.83	-
	1420	-	10.38
	1461	40.88	-
5	1484	22.79	-
	1493	-	9.50
	1600	107.17	-
	1620	-	19.25
	1826	206.25	-
6	1889	63.04	-
	1890	-	1.50
	1920	29.88	-
	1937	-	17.25
	1978	40.92	-
	1992	-	13.96
	2191	198.42	-
7	2486	295.25	-
	2516	-	29.875
	2556	39.83	-
YEAR	**DAYS**	**DAYS**	**DAYS**

Year	Time	TBF	TTR
8	2563	7.25	-
	2568	-	4.71
	2583	15.17	-
	2597	-	14.46
	2628	30.42	-
	2638	-	10.50
	2753	114.58	-
	2773	-	20.21
	2851	77.75	-
	2872	-	21.13
	2921	48.79	-
9	2984	63.46	-
	3009	-	24.58
	3202	193.58	-
	3221	-	18.42
	3235	14.58	-
	3238	-	3.21
	3286	47.13	-
10	3380	94.46	-
	3388	-	7.83
	3464	75.83	-
	3467	-	3.17
	3474	7.17	-
	3500	-	26.25
	3651	150.25	-
11	3880	229.42	-
	3893	-	13.17
	3930	36.54	-
	3931	-	0.92
	4016	84.92	-
12	4041	25.79	-
	4052	-	10.42
	4141	89.46	-
	4162	-	20.96
	4210	48.33	-
	4217	-	6.71
	4267	49.54	-
	4287	-	19.88
	4333	46.08	-
	4342	-	8.83
	4380	38.96	-

Year	Time	TBF	TTR
14	4873	127.79	-
	4882	-	8.58
	4939	57.63	-
	4967	-	27.54
	5074	107.17	-
	5076	-	1.75
	5110	34.50	-
15	5166	55.63	-
	5172	-	6.42
	5232	59.50	-
	5253	-	20.79
	5267	14.71	-
	5292	-	24.21
	5475	183.71	-
16	5529	53.88	-
	5541	-	11.96
	5593	52.17	-
	5611	-	17.42
	5705	93.83	-
	5709	-	4.00
	5840	131.71	-
17	5888	48.00	-
	5914	-	25.29
	5916	2.25	-
	5920	-	4.29
	6205	285.13	-
18	6570	364.9583	-
19	6604	34.13	-
	6624	-	19.17
	6712	88.33	-
	6729	-	16.67
	6935	206.67	-
20	7011	75.83	-
	7019	-	7.79
	7129	110.29	-
	7150	-	20.50
	7300	150.54	-
YEAR	**DAYS**	**DAYS**	**DAYS**

Table 4-21: Distribution of Failures and Repairs

FAILURE				REPAIR			
ΔN	N	ΔN/2	Failure	ΔN	N	ΔN/2	Repair
-20	7	10	10.14%	0-10	20	5	40.00%
20-40	11	30	15.94%	10-20	16	15	32.00%
40-60	13	50	18.84%	20-30	11	25	22.00%
60-80	7	70	10.14%	30-40	2	35	4.00%
80-100	7	90	10.14%	50-60	1	55	2.00%
100-120	4	110	5.80%	Sum=	50		100.00%
120-140	6	130	8.70%				
140-160	3	150	4.35%				
160-180	0	170	0.00%				
180-200	3	190	4.35%				
200-220	2	210	2.90%				
220-240	2	230	2.90%				
240-260	0	250	0.00%				
260-280	0	270	0.00%				
280-300	2	290	2.90%				
300-320	1	310	1.45%				
320-340	0	330	0.00%				
340-360	0	350	0.00%				
360-380	1	370	1.45%				
380-400	0	390	0.00%				
Sum=	69		100.00%				
Days	Days	Days		Days	Days	Days	

Figure 4-5: Availability for IGBT-1/2

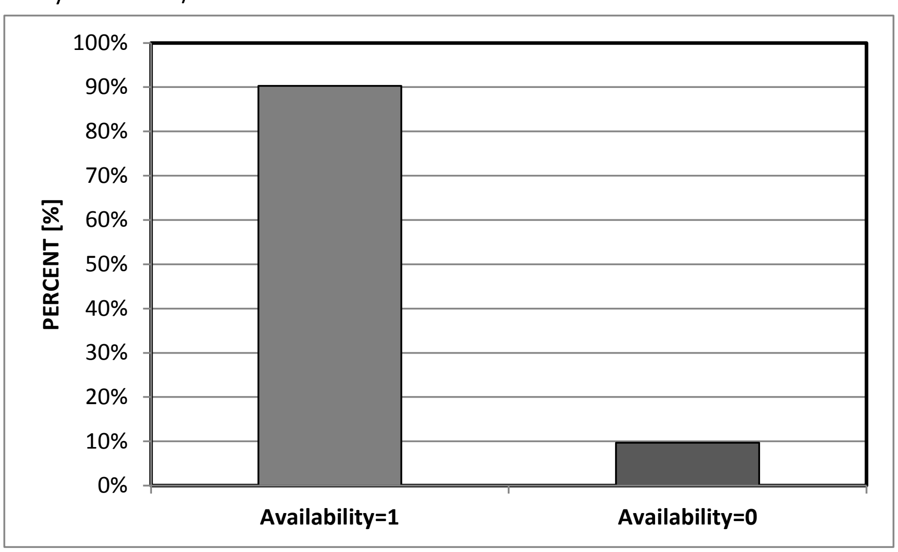

Figure 4-6: Distribution of Time Before Failure and Time to Repair vs. Time

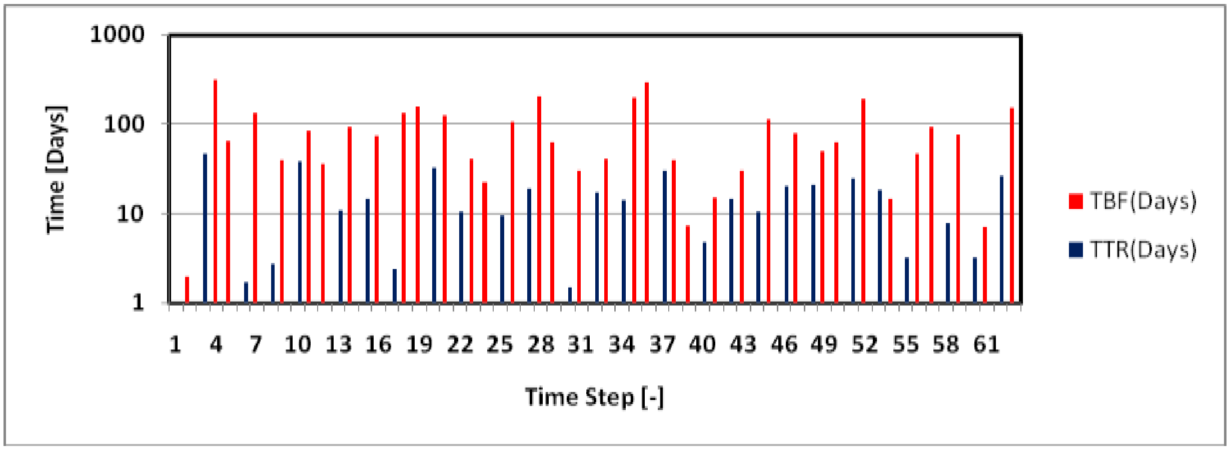

Figure 4-7: Failure Distribution

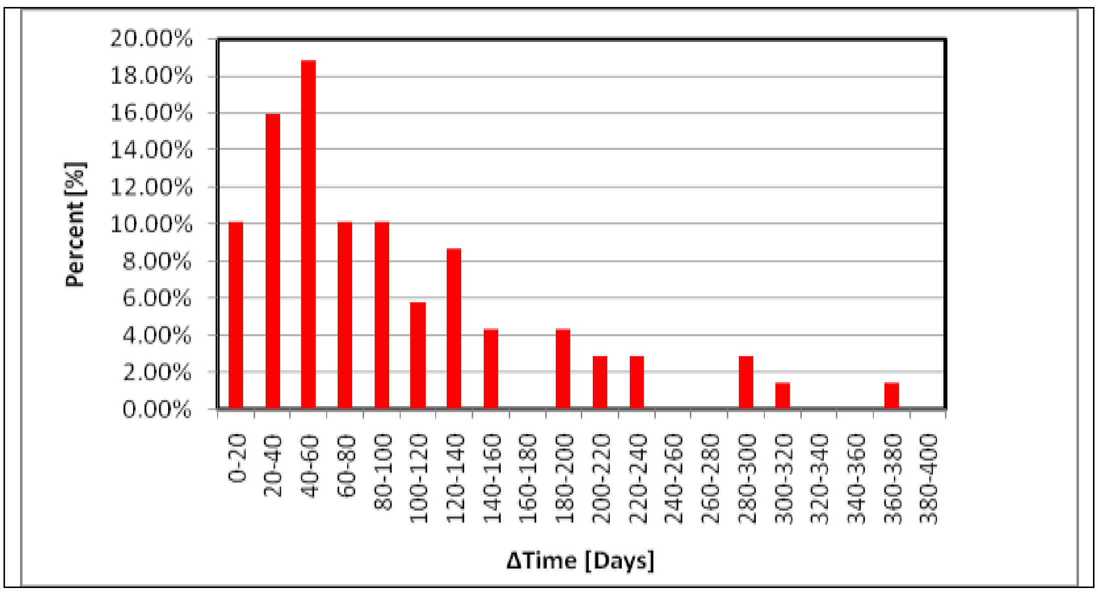

Figure 4-8: Repair Distribution

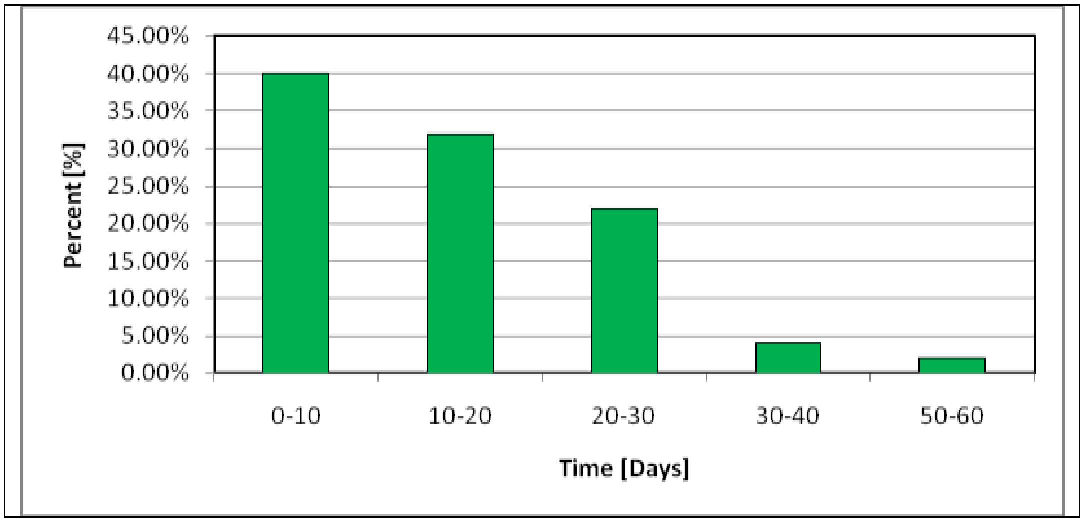

Discussion of Tables and Figures

Data

Failure and repair rates are based on either OEM information or values based on MIL-HDBK-217F, or one of the commercially available computer programs, e.g., Telcordia.

Values

- **Column 1: All the components** are assumed to experience failure during the design lifetime.
- Column 2: Based on OEM documentation or commercial computer program.
- Columns 3 & 5: Assuming that a Weibull function is used to represent failure and repair, the current version for both failure and repair is based on a negative exponential model. Thus, βF=1 and βR=1.
- Column 4: Repair times are not readily available. Values used herein are a model assuming the difference in repair-failure times are proportional to the difference in times at which the repair cannot be completed and the time that failure occurs, i.e., F(t)=[1-exp(tF/MTBF)βF]→1 and
  R(t)=[1-exp(tR/MTTR)βR]→0.
- Column 6: Impact is the effect of inverter component failure on other inverter components and other PV systems. The impact is a number > 0 (low impact) to < 1.0 (high impact) that reflects the consequences of a failure. The consequences can be divided into four primary categories:
  1) frequency of failure,
  2) loss of or reduction in power,
  3) causes failures in other inverter components, and
  4) failures or reduced performance of other systems.

The following table is a more comprehensive description of the failures and consequences.

Table 4-22: Guidelines for Values of Impact

CATEGORY	CRITERIA	DESCRIPTION	IMPACT	
Failure	MTBF	High failure rates	≤ 1	≥0
Power	KWh	High % reduction	≤ 1	≥0
Inverter	Failures	Occurs a short time after initial failure	≤ 1	≥0
Systems	Shutdown	Loss of module power	≤ 1	≥0

The effects of failures on inverter and system components that need to be considered in setting impact values are listed in Table 4-23 on the following.

Table 4-23: Effect of Inverter Component Failures on Other Inverter Components

INVERTER COMPONENT FAILURE MODES					EFFECT OF FAILURES ON OTHER INVERTER COMPONENTS AND SYSTEMS	
#	Component	$\lambda_p/10^6$hrs	Function	Failure mode	Effect on system	Effect on other inverter components
1	IGBT	300.96	PWM switching device	short (85%)	power decrease/shutdown	overheating/failure of other IGBTs
2	relay	2.075	AC disconnect	open (80%)	shutdown	none
3	cap, elect.	9.54	DC filter	open (90%)	power decrease/shutdown	none
4	microproc.	1.097	PWM/control	inoperative	power decrease/shutdown	possible failures
5	board supply	.522	low voltage DC supply	inoperative	power decrease/shutdown	possible failures
6	cap, film	.274	PWM high freq. filter	open (90%)	output power decrease	none
7	cap, film	.274	AC filter	open (90%)	output power decrease	none
8	transformer	.2058	AC isolation	open (80%)	shutdown	none
9	inductor	.000252	PWM high freq. filter	open (80%)	shutdown	none
10	inductor	.000252	AC filter	open (80%)	shutdown	none

Output

The output of Version 1 of MultiC_Risk documents the N design operating years, the day of each month, and the hour of each day. The availability, A, is either of two values: A = 1 denotes that the system is or can be operating; A=0 denotes that the system is not producing power but is most likely being repaired. Figure 4-5 (above) shows that the availability is about 90% and the unavailability about 10%.

Following the MultiC_Risk output is an Excel file that contains, in addition to the same information, the number of days before failure and the days required for repair. The example is for one pair of IGBTs.

Distributions of Failure and Repair Times

Failures and repairs, over a period of operating time (Figure 4-6) show their random character. Thus it makes sense to determine the mean times, as compared to the assumed values used in the predictions.

Failures and repairs, over a period of operating time, show their random character. Mean times depend on the PDFs, which can be compared to failure and repair predictions. The limited data, 69 points for failure and 50 for repair, are insufficient to make accurate statements as to the distributions. However, the failure histogram (Figure 4-7) appears to approximate a Weibull function with ($2 \le \beta F \le 3$), while the repair histogram (Figure 4-8) is closer to an exponential with ($1 \le \beta R \le 2$).

4.6 CONCLUSIONS

Figure 4-4A documents the failure and repair rates based on Ristow [4-1, 4-2] and Collins [4-3]. Although there is a similar trend of the ratio of MTTR/MTBF it is difficult to substantiate support for the trend. The reasons are:

1) MTTR and MTBF are taken as random, which argues against a functional relationship;
2) The removal, repair or replacement of the failed component would have to be from the same OEM, have the same design and location within the inverter, etc.;
3) Downtime would have to include the same nonreplacement activities; and
4) Availability of the replacement component.

Failure is more likely to be random than repair, which depends on a number of accumulating, small random failure activities. Thus the variations both in the predictions and on the limited data may be acceptable. Based on all the caveats it seems reasonable to assume the ratio of MTTR to MTBF, depending on the component, to be a value of .0001-.001, or a factor of 10^{-4} -10^{-3} smaller than the failure time.

Again, a detailed database would be a vital source for documenting these failures and repair times [4-5].

4.7 REFERENCES: SIMULATION OF FAILURE OF MULTIPLE COMPONENTS

4-1. Ristow, A., Begović, M., Rohatgi, A. "Modeling The Effects of Uncertainty and Reliability on the Cost of Energy from PV Systems," 20th European Solar Energy Conference & Exhibition, Barcelona, Spain: June 6-10, 2005.

4-2. Ristow, A.H. "Numerical Modeling of Uncertainty and Variability in the Technology, Manufacturing, and Economics of Crystalline Silicon Photovoltaics," PhD Thesis, Georgia Institute of Technology: August 2008.

4-3. Collins, E., et al. "Reliability and Availability Analyses of a Fielded Photovoltaic System," *IEEE* 978-1-2950, Sept. 2009 002316-2321.

4-4. Andrews, J.D, Moss, T.R. *Reliability and Risk Assessment,* ASME Press, 2nd ed., 2002.
A: Chapter 1: An Introduction in Reliability and Risk Assessment, pp. 1-20.
B: Chapter 5: Quantification of Component Failure Probabilities, pp. 115-64.
C: Chapter 6: Reliability Networks, p. 165-99.
D: Chapter 11: Simulation, p. 341-61.

4-5. Collins, E., et al. "Field Data Collection for Quantification of Reliability & Availability for PV Systems," 35th IEEE Photovoltaic Specialist Conference, June 10, 2010: SAND2010-3362-C.

4-6. Andrews, J.D., Moss, T.R. *Reliability and Risk Assessment*, ASME Press 2nd ed., 2002. Chapter 6: Reliability Networks, pp. 165-99.

APPENDIXES: SECTION 4

Appendix 4-A: MultiC_Risk Version 1.0

```
% Multi component Exponential failure simulation
% Joe Quinn
% One year simulation
% February 2011
Clc
Clear
% read the number of components in the system
N_components    =   input('Enter the number of system components   ')   ;
C_filename = input("Enter Component Filename : 's')
T_step          =   input('Enter time step in hours  ')                ;
cd E:\BRisk\Config\
 % read the rest of the component file
[c_title,mtbf,mtrpr,impact]  =   textread(C_filename,'%20s %10f %10f %10f ','delimiter',',') ;
titles        =    char(c_title)                              ;
for j = 1:N_components
O_stat(j)       =   1                                        ;
SM_mtbf(j)      =   mtbf(j)   *24/T_step                        ;
SM_mtrpr(j)     =   mtrpr(j)  *24/T_step                        ;
% the probability having survived until now and failing in the next interval
P_fail(j)       =   1- exp(-1/SM_mtbf(j))                       ;
P_repr(j)       =   1- exp(-1/SM_mtrpr(j))                      ;
End
%
% compute the number of steps
Steps           =   fix(365*24/T_step)                          ;
%
% seed the failure and repair generator
clk         =   clock                                           ;
seed        =   clk(6)                                          ;
rand ('seed',seed)                                              ;
% fill both the failure and repair arrays at the beginning
%
RN          = rand(N_components,Steps,2)                            ;
% Create the output file name
    out_file        = strrep(C_filename, 'txt', 'rsk')                ;
    cd E:\BRisk\Results                                             ;
    fid_results     =   fopen(out_file,'a+')                        ;
    count   =   fprintf(fid_results, '   Title,     MTBF(days),   MTR(days),    Impact  \r\n' )              ;
% Output component info
  for k     =    1:N_components
   count    =   fprintf(fid_results, '%10s,',titles(k,:))                  ;
   count    =   fprintf(fid_results,'     %5.1f , ', mtbf(k))              ;
   count    =   fprintf(fid_results,'   %5.1f , ', mtrpr(k))               ;
   count    =   fprintf(fid_results,'   %5.2f     \r\n', impact(k))        ;
```

Appendix 4-A: MultiC_Risk Version 1.0 (continued)

```
  End
%
% Data file header
   count   =   fprintf(fid_results,'   Day,     Hour,   Availability     \r\n')  ;
% outer time step loop
for t       =   1: Steps
    Days    =   fix((t*T_step)/24)                                   ;
    Hours   =   fix((t*T_step) - (Days * 24))                        ;
    TotLoss =   0                                                    ;
 % inner component loop
 for c      =   1:N_components
     Loss(c)   =   impact(c)                                         ;
     if O_stat(c) == 1                                               ;  % test for failure
         if RN(c,t,1) < P_fail(c)
            O_stat(c)  =   0                                         ;
            Else
            Loss(c)       =   0                                      ;
         End
  Else
          if RN(c,t,2) < P_repr(c)
             O_stat(c)  =   1                                        ;      % test for repair
             Loss(c)    =   0                                        ;
     End
     End
     TotLoss    =   TotLoss + Loss(c)                                ;
 End
 % end of the inner component list
 if TotLoss > 1.0
     TotLoss    =   1.0                                              ;
 End
 Avail      =   1-TotLoss                                            ;
 % print out the results
 count    =   fprintf(fid_results,'  %5i,%5i,%5.2f     \r\n', Days, Hours, Avail)           ;
End
% end of the outer time step loop
% close the results file
fclose(fid_results)
End
```

Appendix 4-B: Failure of Lincoln Theater Inverter Components

Table 4-B1 identifies the major electronic components for the SMA SB-6000U inverter in order of decreasing failure rate. Components are assigned identification numbers (left column). Component type, function, manufacturer/model number, quantity (in the inverter assembly), and failure rate (MIL-HDBK 217) are given.

Table 4-B1: Electronic Components for the Inverter in Order of Decreasing Failure

#	Component	Mfr/model Number	Qty	$\lambda_p/10^6$hrs	Function
1	IGBT	IXYS/K30N60	8	300.96	PWM bridge switching device
2	Relay	PB/T9AS1D12-9	1	2.075	AC disconnect
3	cap, elect.	EPCOS/B43504	20	9.54	DC filter
4	microproc.	TI/MCUM3	1	1.097	PWM/control
5	board supply	dc/dc converter	1	.522	low voltage dc supply
6	cap, film	EPCOS/B32231	1	.274	PWM high frequency filter
7	cap, film	EPCOS/B32231	1	.274	AC filter
8	transformer		1	.2058	AC isolation
9	inductor	EPCOS/B82726	2	.000252	PWM high frequency filter
10	inductor	EPCOS/B82726	2	.000252	AC filter

Table 4-B2 identifies the major electronic components for the SMA SB-6000U inverter in order of decreasing failure rate. Component identification numbers are identical to Table 4-B1. Component type, function, manufacturer or model number, and quantity (in the inverter assembly) are given, but failure rates are based on Telcordia SR-332 Issue 2.

Table 4-B2:Failure Rates for SMA SB-6000U Inverter Components Based on Telcordia SR-332 Issue 2

ID	Components	Mfr/model Number	Qty	$\lambda_p/10^6$hrs	Function
1	IGBT	IXYS/K30N60	8	1.452	PWM bridge switching device
2	relay	PB/T9AS1D12-9	1	.322	AC disconnect
3	microprocessor	TI/MCUM3	1	.365	PWM/control
4	board supply	dc/dc converter	1	.262	low voltage DC supply
5	capacitors	EPCOS/B43504	20	.107	DC filter
6	capacitors, film	EPCOS/B32231	1	.087	PWM high frequency filter
7	capacitors, film	EPCOS/B32231	1	.087	AC filter
8	transformer		1	.049	AC isolation
9	inductor	EPCOS/B82726	2	.000028	PWM high frequency filter
10	inductor	EPCOS/B82726	2	.000028	AC filter

Note that the transistor (IGBT) failure rate prediction is much improved according to the more recent Bellcore/Telcordia standards. This change is likely supported by significant improvements in power semiconductor technology in recent years.

Table 4-B3 lists the failure mode for these major components. This failure mode information came from the BSI document “Draft–BS EN 61709 Electronic Components; Annex A,” p. 50. Data listed in the “failure effect” and “effect on other components” columns are “best guesses” based on knowledge of component function in the SMA SB-6000U inverter.

Table 4-B3: Expected Failure Mode and Effect

#	Failure Mode	Failure Effect	Effect on Other Components
1	short (85%)	output power decrease/shutdown	overheating/failure of other IGBTs
2	open (80%)	shutdown	none
3	open (90%)	output power decrease/shutdown	none
4	inoperative	output power decrease/shutdown	possible failure of other components
5	inoperative	output power decrease/shutdown	possible failure of other components
6	open (90%)	output power decrease	none
7	open (90%)	output power decrease	none
8	open (80%)	shutdown	none
9	open (80%)	shutdown	none
10	open (80%)	shutdown	none

Table 4-B4: GCPVS Component Failure Modes

Component	Failure Mode	Failure Effect
Module	open	output power decrease
Array	open (ex: blown fuse)	output power decrease
DC breaker	open	shutdown
Inverter	partial or total shutdown	output power decrease/shutdown
Combiner	open	shutdown
kWh meter	open	shutdown
AC breaker	open	shutdown

Appendix 4-C: Failure Rates

This section documents the formulation of a prediction model for the reliability of the University of Hartford Lincoln Theater PV system inverter. Component failure rates are identified for major components of the SMA SB6000U inverter, using Lambda Predict version 3 reliability software. These analyses were performed according to the following major published standards provided by Lambda Predict software:

Reference Failure Rates: Table 4-C1 documents the reference failure rates (FPMH, FIT)[15], MTBF, and contribution factors for the major individual components of the SB-6000U inverter, as identified by Lambda Predict. These reference failure rates do not account for specific stress factors that may be present for components. The major blocks (headings) are the specific standards employed; in order top to bottom they are: MIL-HDBK-217F, Bellcore TR-332, Telcordia SR-332 Issue 1, and Telcordia SR-332 Issue 2. The components are listed in order of decreasing failure rate, top to bottom under each heading.

Failure Rates at Operating Conditions: Components in equipment do not always operate under reference conditions. The operational environment may differ from the reference environment, requiring conversion of failure rate data to reflect the actual operating conditions. The application of stress factors (ambient temperature, electrical stress, etc.) in this conversion results in a more accurate and realistic prediction.

Major Components: Table 4-C2 shows the reference failure rates (FPMH, FIT), MTBF, and contribution factors for the major individual components of the SMA SB-6000U inverter, using stress factors that may be present for the inverter components. The major blocks (headings) are the specific standards employed. In order, top to bottom they are: MIL-HDBK-217F, Telcordia SR-332 Issue 2, Bellcore TR-332, and Telcordia SR-332 Issue 1. The components are listed in order of decreasing failure rate, top to bottom under each heading.

Lincoln Theater Inverter: Table 4C-3 lists the failure rates based on the number of the identified components, for example for 8 transistors (IGBTs). Note that the higher the mean time before failure (MTBF) the longer the time before failures and thus, for a fixed operating time, the fewer the number of failures.

Table Overview, Appendix 4-C					
MBTF: TRANSISTORS; NUMBER = 8					
Table	CONDITIONS	MIL-HDBK-217F	Bellcore TR-332	Telcordia SR-332 Issue 1	Telcordia SR-332 Issue 2
4-C1	Reference	$7.47X10^5$	$3.22X10^6$	$3.33X10^7$	$4.33X10^7$
4-C2	Operating	$3.06x10^5$	$5.87X10^7$	$4.49X10^8$	$1.48X10^9$
4-C3	Operating SB-6000U	$4.63x10^4$	$5.62X10^6$	$1.87X10^7$	$7.3X10^6$
UNITS		hours	hours	hours	hours

[15] FPMH = Failures Per Million Hour ; FIT = Failures in Time

Table 4-C1: Base (Reference) Failure Rates

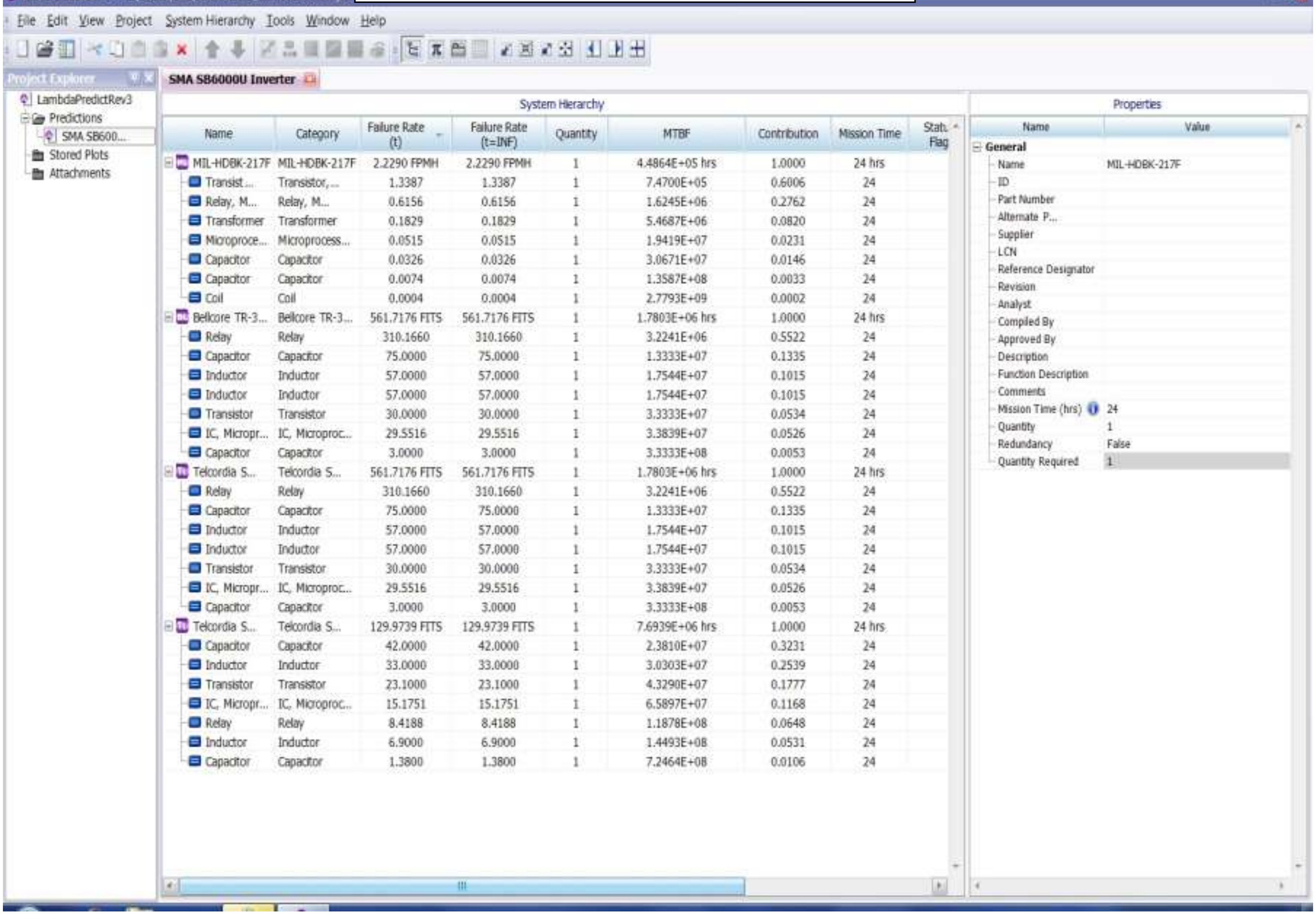

Name	Category	Failure Rate (t)	Failure Rate (t=INF)	Quantity	MTBF	Contribution	Mission Time	Stat. Flag
MIL-HDBK-217F	MIL-HDBK-217F	2.2290 FPMH	2.2290 FPMH	1	4.4864E+05 hrs	1.0000	24 hrs	
Transist...	Transistor,...	1.3387	1.3387	1	7.4700E+05	0.6006	24	
Relay, M...	Relay, M...	0.6156	0.6156	1	1.6245E+06	0.2762	24	
Transformer	Transformer	0.1829	0.1829	1	5.4687E+06	0.0820	24	
Microproce...	Microprocess...	0.0515	0.0515	1	1.9419E+07	0.0231	24	
Capacitor	Capacitor	0.0326	0.0326	1	3.0671E+07	0.0146	24	
Capacitor	Capacitor	0.0074	0.0074	1	1.3587E+08	0.0033	24	
Coil	Coil	0.0004	0.0004	1	2.7793E+09	0.0002	24	
Bellcore TR-3...	Bellcore TR-3...	561.7176 FITS	561.7176 FITS	1	1.7803E+06 hrs	1.0000	24 hrs	
Relay	Relay	310.1660	310.1660	1	3.2241E+06	0.5522	24	
Capacitor	Capacitor	75.0000	75.0000	1	1.3333E+07	0.1335	24	
Inductor	Inductor	57.0000	57.0000	1	1.7544E+07	0.1015	24	
Inductor	Inductor	57.0000	57.0000	1	1.7544E+07	0.1015	24	
Transistor	Transistor	30.0000	30.0000	1	3.3333E+07	0.0534	24	
IC, Micropr...	IC, Microproc...	29.5516	29.5516	1	3.3839E+07	0.0526	24	
Capacitor	Capacitor	3.0000	3.0000	1	3.3333E+08	0.0053	24	
Telcordia S...	Telcordia S...	561.7176 FITS	561.7176 FITS	1	1.7803E+06 hrs	1.0000	24 hrs	
Relay	Relay	310.1660	310.1660	1	3.2241E+06	0.5522	24	
Capacitor	Capacitor	75.0000	75.0000	1	1.3333E+07	0.1335	24	
Inductor	Inductor	57.0000	57.0000	1	1.7544E+07	0.1015	24	
Inductor	Inductor	57.0000	57.0000	1	1.7544E+07	0.1015	24	
Transistor	Transistor	30.0000	30.0000	1	3.3333E+07	0.0534	24	
IC, Micropr...	IC, Microproc...	29.5516	29.5516	1	3.3839E+07	0.0526	24	
Capacitor	Capacitor	3.0000	3.0000	1	3.3333E+08	0.0053	24	
Telcordia S...	Telcordia S...	129.9739 FITS	129.9739 FITS	1	7.6939E+06 hrs	1.0000	24 hrs	
Capacitor	Capacitor	42.0000	42.0000	1	2.3810E+07	0.3231	24	
Inductor	Inductor	33.0000	33.0000	1	3.0303E+07	0.2539	24	
Transistor	Transistor	23.1000	23.1000	1	4.3290E+07	0.1777	24	
IC, Micropr...	IC, Microproc...	15.1751	15.1751	1	6.5897E+07	0.1168	24	
Relay	Relay	8.4188	8.4188	1	1.1878E+08	0.0648	24	
Inductor	Inductor	6.9000	6.9000	1	1.4493E+08	0.0531	24	
Capacitor	Capacitor	1.3800	1.3800	1	7.2464E+08	0.0106	24	

Name	Value
General	
Name	MIL-HDBK-217F
ID	
Part Number	
Alternate P...	
Supplier	
LCN	
Reference Designator	
Revision	
Analyst	
Compiled By	
Approved By	
Description	
Function Description	
Comments	
Mission Time (hrs)	24
Quantity	1
Redundancy	False
Quantity Required	1

Table 4-C2: Failure Rates at Operating Conditions

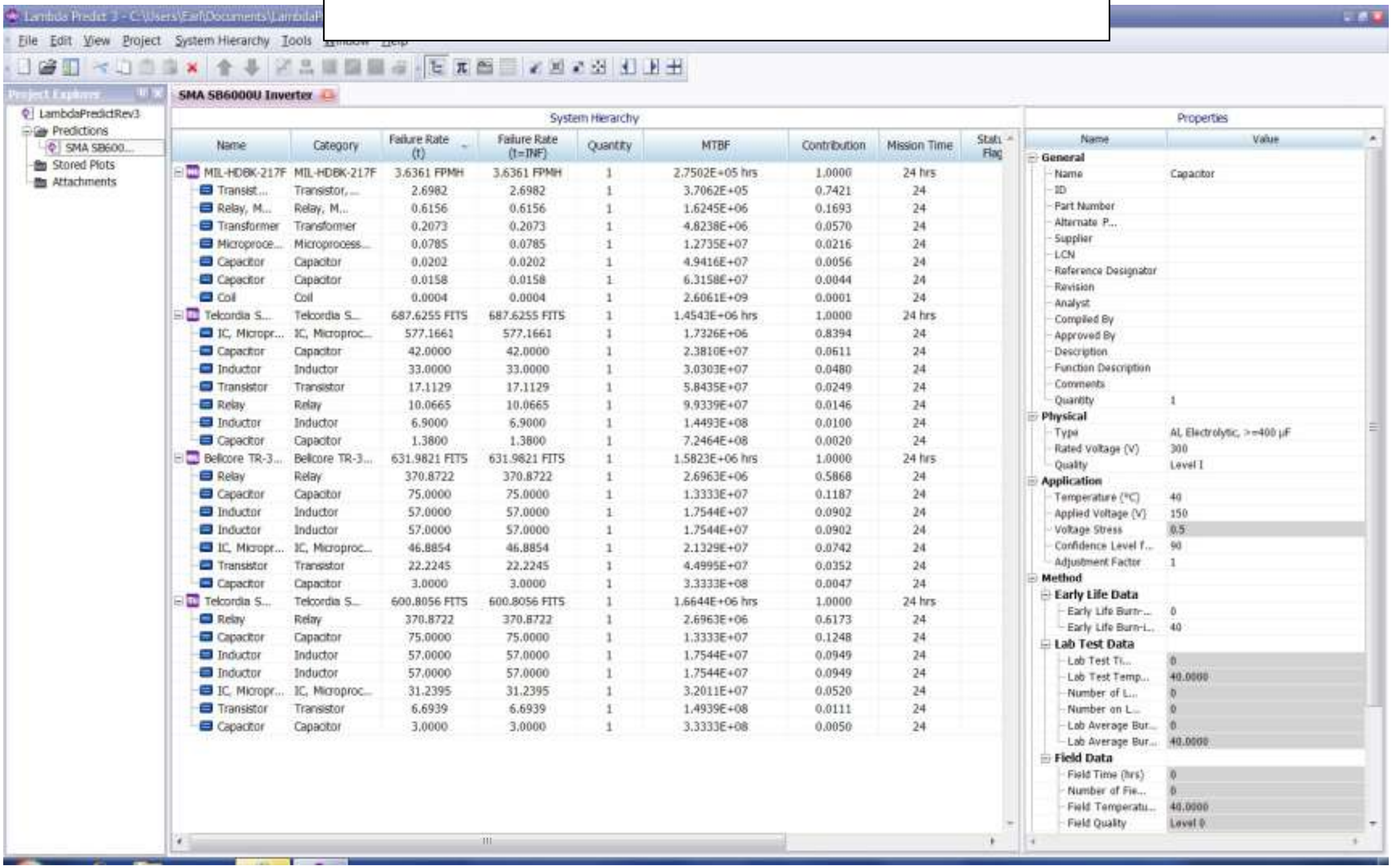

Name	Category	Failure Rate (t)	Failure Rate (t=INF)	Quantity	MTBF	Contribution	Mission Time	Stat. Flag
MIL-HDBK-217F	MIL-HDBK-217F	3.6361 FPMH	3.6361 FPMH	1	2.7502E+05 hrs	1.0000	24 hrs	
Transist...	Transistor, ...	2.6982	2.6982	1	3.7062E+05	0.7421	24	
Relay, M...	Relay, M...	0.6156	0.6156	1	1.6245E+06	0.1693	24	
Transformer	Transformer	0.2073	0.2073	1	4.8238E+06	0.0570	24	
Microproce...	Microprocess...	0.0785	0.0785	1	1.2735E+07	0.0216	24	
Capacitor	Capacitor	0.0202	0.0202	1	4.9416E+07	0.0056	24	
Capacitor	Capacitor	0.0158	0.0158	1	6.3158E+07	0.0044	24	
Coil	Coil	0.0004	0.0004	1	2.6061E+09	0.0001	24	
Telcordia S...	Telcordia S...	687.6255 FITS	687.6255 FITS	1	1.4543E+06 hrs	1.0000	24 hrs	
IC, Micropr...	IC, Microproc...	577.1661	577.1661	1	1.7326E+06	0.8394	24	
Capacitor	Capacitor	42.0000	42.0000	1	2.3810E+07	0.0611	24	
Inductor	Inductor	33.0000	33.0000	1	3.0303E+07	0.0480	24	
Transistor	Transistor	17.1129	17.1129	1	5.8435E+07	0.0249	24	
Relay	Relay	10.0665	10.0665	1	9.9339E+07	0.0146	24	
Inductor	Inductor	6.9000	6.9000	1	1.4493E+08	0.0100	24	
Capacitor	Capacitor	1.3800	1.3800	1	7.2464E+08	0.0020	24	
Bellcore TR-3...	Bellcore TR-3...	631.9821 FITS	631.9821 FITS	1	1.5823E+06 hrs	1.0000	24 hrs	
Relay	Relay	370.8722	370.8722	1	2.6963E+06	0.5868	24	
Capacitor	Capacitor	75.0000	75.0000	1	1.3333E+07	0.1187	24	
Inductor	Inductor	57.0000	57.0000	1	1.7544E+07	0.0902	24	
Inductor	Inductor	57.0000	57.0000	1	1.7544E+07	0.0902	24	
IC, Micropr...	IC, Microproc...	46.8854	46.8854	1	2.1329E+07	0.0742	24	
Transistor	Transistor	22.2245	22.2245	1	4.4995E+07	0.0352	24	
Capacitor	Capacitor	3.0000	3.0000	1	3.3333E+08	0.0047	24	
Telcordia S...	Telcordia S...	600.8056 FITS	600.8056 FITS	1	1.6644E+06 hrs	1.0000	24 hrs	
Relay	Relay	370.8722	370.8722	1	2.6963E+06	0.6173	24	
Capacitor	Capacitor	75.0000	75.0000	1	1.3333E+07	0.1248	24	
Inductor	Inductor	57.0000	57.0000	1	1.7544E+07	0.0949	24	
Inductor	Inductor	57.0000	57.0000	1	1.7544E+07	0.0949	24	
IC, Micropr...	IC, Microproc...	31.2395	31.2395	1	3.2011E+07	0.0520	24	
Transistor	Transistor	6.6939	6.6939	1	1.4939E+08	0.0111	24	
Capacitor	Capacitor	3.0000	3.0000	1	3.3333E+08	0.0050	24	

Name	Value
General	
Name	Capacitor
ID	
Part Number	
Alternate P...	
Supplier	
LCN	
Reference Designator	
Revision	
Analyst	
Compiled By	
Approved By	
Description	
Function Description	
Comments	
Quantity	1
Physical	
Type	Al, Electrolytic, >=400 µF
Rated Voltage (V)	300
Quality	Level I
Application	
Temperature (°C)	40
Applied Voltage (V)	150
Voltage Stress	0.5
Confidence Level f...	90
Adjustment Factor	1
Method	
Early Life Data	
Early Life Burn-...	0
Early Life Burn-i...	40
Lab Test Data	
Lab Test Ti...	0
Lab Test Temp...	40.0000
Number of L...	0
Number on L...	0
Lab Average Bur...	0
Lab Average Bur...	40.0000
Field Data	
Field Time (hrs)	0
Number of Fie...	0
Field Temperatu...	40.0000
Field Quality	Level 0

Table 4-C3: Failure Rates at Operating Conditions, with Component Quantities

SMA SB6000U Inverter

System Hierarchy

Name	Category	Failure Rate (t)	Failure Rate (t=INF)	Quantity	MTBF	Contribution	Mission Time	Stat. Flag
MIL-HDBK-217F	MIL-HDBK-217F	22.8457 FPMH	22.8457 FPMH	1	4.3772E+04 hrs	1.0000	24 hrs	
Transist...	Transistor,...	21.5856	21.5856	8	4.6327E+04	0.9448	24	
Relay, M...	Relay, M...	0.6156	0.6156	1	1.6245E+06	0.0269	24	
Capacitor	Capacitor	0.3167	0.3167	20	3.1579E+06	0.0139	24	
Transformer	Transformer	0.2073	0.2073	1	4.8238E+06	0.0091	24	
Microproce...	Microprocess...	0.0785	0.0785	1	1.2735E+07	0.0034	24	
Capacitor	Capacitor	0.0405	0.0405	2	2.4708E+07	0.0018	24	
Coil	Coil	0.0015	0.0015	4	6.5152E+08	6.7184E-05	24	
Bellcore TR-3...	Bellcore TR-3...	2386.5540 FITS	2386.5540 FITS	1	4.1901E+05 hrs	1.0000	24 hrs	
Capacitor	Capacitor	1500.0000	1500.0000	20	6.6667E+05	0.6285	24	
Relay	Relay	370.8722	370.8722	1	2.6963E+06	0.1554	24	
Inductor	Inductor	228.0000	228.0000	4	4.3860E+06	0.0955	24	
Transistor	Transistor	177.7964	177.7964	8	5.6244E+06	0.0745	24	
Inductor	Inductor	57.0000	57.0000	1	1.7544E+07	0.0239	24	
IC, Micropr...	IC, Microproc...	46.8854	46.8854	1	2.1329E+07	0.0196	24	
Capacitor	Capacitor	6.0000	6.0000	2	1.6667E+08	0.0025	24	
Telcordia S...	Telcordia S...	2246.6629 FITS	2246.6629 FITS	1	4.4510E+05 hrs	1.0000	24 hrs	
Capacitor	Capacitor	1500.0000	1500.0000	20	6.6667E+05	0.6677	24	
Relay	Relay	370.8722	370.8722	1	2.6963E+06	0.1651	24	
Inductor	Inductor	228.0000	228.0000	4	4.3860E+06	0.1015	24	
Inductor	Inductor	57.0000	57.0000	1	1.7544E+07	0.0254	24	
Transistor	Transistor	53.5512	53.5512	8	1.8674E+07	0.0238	24	
IC, Micropr...	IC, Microproc...	31.2395	31.2395	1	3.2011E+07	0.0139	24	
Capacitor	Capacitor	6.0000	6.0000	2	1.6667E+08	0.0027	24	
Telcordia S...	Telcordia S...	1627.4958 FITS	1627.4958 FITS	1	6.1444E+05 hrs	1.0000	24 hrs	
Capacitor	Capacitor	840.0000	840.0000	20	1.1905E+06	0.5161	24	
IC, Micropr...	IC, Microproc...	577.1661	577.1661	1	1.7326E+06	0.3546	24	
Transistor	Transistor	136.9032	136.9032	8	7.3044E+06	0.0841	24	
Inductor	Inductor	33.0000	33.0000	1	3.0303E+07	0.0203	24	
Inductor	Inductor	27.6000	27.6000	4	3.6232E+07	0.0170	24	
Relay	Relay	10.0665	10.0665	1	9.9339E+07	0.0062	24	
Capacitor	Capacitor	2.7600	2.7600	2	3.6232E+08	0.0017	24	

Properties

Name	Value
General	
Name	MIL-HDBK-217F
ID	
Part Number	
Alternate P...	
Supplier	
LCN	
Reference Designator	
Revision	
Analyst	
Compiled By	
Approved By	
Description	
Function Description	
Comments	
Mission Time (hrs)	24
Quantity	1
Redundancy	False
Quantity Required	1

Appendix 4-D: Reliability of Inverter Components

This section describes the procedure followed in establishing and processing a reliability model for the Lincoln Theater SMA SB-6000U inverter. Results are presented for the individual reliabilities [$R_i(T)$] and failure rates [λ] fa1ilures per million hours (FPMH) of the major components of the inverter, along with the reliability and failure rate of the complete inverter system.

Process: Figure 4-D1 (following) shows a series-parallel "ladder" arrangement of the major inverter/PV system components. Components in series comprise the "sides" of the ladder, whereas components in parallel comprise the "rungs" of the ladder. Components are arranged from left to right in power flow sequence, from the source (PV module array) to the load (AC grid). A component is declared either series or parallel, based on its actual wiring and function in the inverter. Component I.D. numbers are given in parentheses in each block so they can be correlated with the listings in Tables 4-B1 and 4-B2 in Appendix 4-B. Note that the microcontroller is neither series nor parallel but is shown in an overall sense: receiving and processing data (DC and AC voltage/current, etc.), operational functions, e.g., maximum power point tracking (MPPT), pulse width modulation (PWM, current control), safety requirements (anti-islanding, ground fault detection, etc.), and data transmission (web box).

The reliability block diagram of the inverter (Figure 4-D1) comprises the major components arranged in series-parallel configuration to represent the failure modes. A series system is a configuration such that, if any one of the system components fails, the entire system fails. A series system is as weak as its weakest link. Accordingly, the microprocessor, DC board supply, IGBT power semiconductors, isolation transformer, and relay are depicted in series because if any one of these components fails the whole system is expected to shut down.

In a parallel system configuration, as long as not all of the system components fail, the entire system works. In a parallel configuration, the total system reliability is higher than the reliability of any single system component. Therefore the inverter DC filter capacitors and PWM filter/AC filter capacitors/inductors are arranged in parallel to represent the fact that if one or even several of these components fails, the system is expected to continue to operate.

The method chosen to obtain the reliability of the complete SMA SB-6000U inverter system is to break the total system configuration into homogeneous subsystems, consider the parallel subsystems separately as units, and calculate their reliabilities. The final step is to put these units back into a single system (via series recombination) and obtain its reliability. In Figure 4-D1 the failure rates (FPMH) are shown above each block, and the reliabilities are shown below each block. The reliability values are calculated using a "mission time" T = 20 years (1.753×10^5 hours).

Calculations: Series-parallel reliability calculations were accomplished using the website calculator provided by the Electrical and Computer Engineering Department of the University of Massachusetts: www.ecs.umass.edu/ece/koren/FaultTolerantSystems/simulator/NonSerPar/nsnpframe.html.

The user inputs the system configuration information via nodes and connection points of modules. After inputting the system description, the user clicks the RUN button to calculate the general expression for system reliability, along with numerical results.

Results of these calculations for the Lincoln Theater inverter are:

- Five DC filter capacitors in parallel: R(T) = 0.99999
- Four parallel DC filter capacitor groups (Figure 4-D1): R(T) = 1
- Eight IGBTs in series: R(T) = 0.96961
- Three paralleled components of the PWM and AC filters: R(T) = 0.99999

Results/Conclusions: The UMASS calculator results for the complete inverter system of 8 blocks in series is shown in Figure 4D-1, where the total reliability of the system $R_s(T) = 0.87079$. The corresponding failure rate of the complete system may then be identified:

$$\lambda_s = -\ln R_s(T)/T = (-\ln 0.87079)/0.1753 = 0.78924 \text{ FPMH}$$

It should be noted that the above assumptions and calculations employed only a limited number of major inverter components; other essential components of the PV system such as the PV modules, control components, circuit boards, cooling system, and interconnections were not included in this simplified reliability model. In addition, other effects that could cause system shutdown, such as electrical noise pick-up and grid monitoring, were not addressed.

Figure 4D-1: Inverter Reliability Block Diagram for Inverter

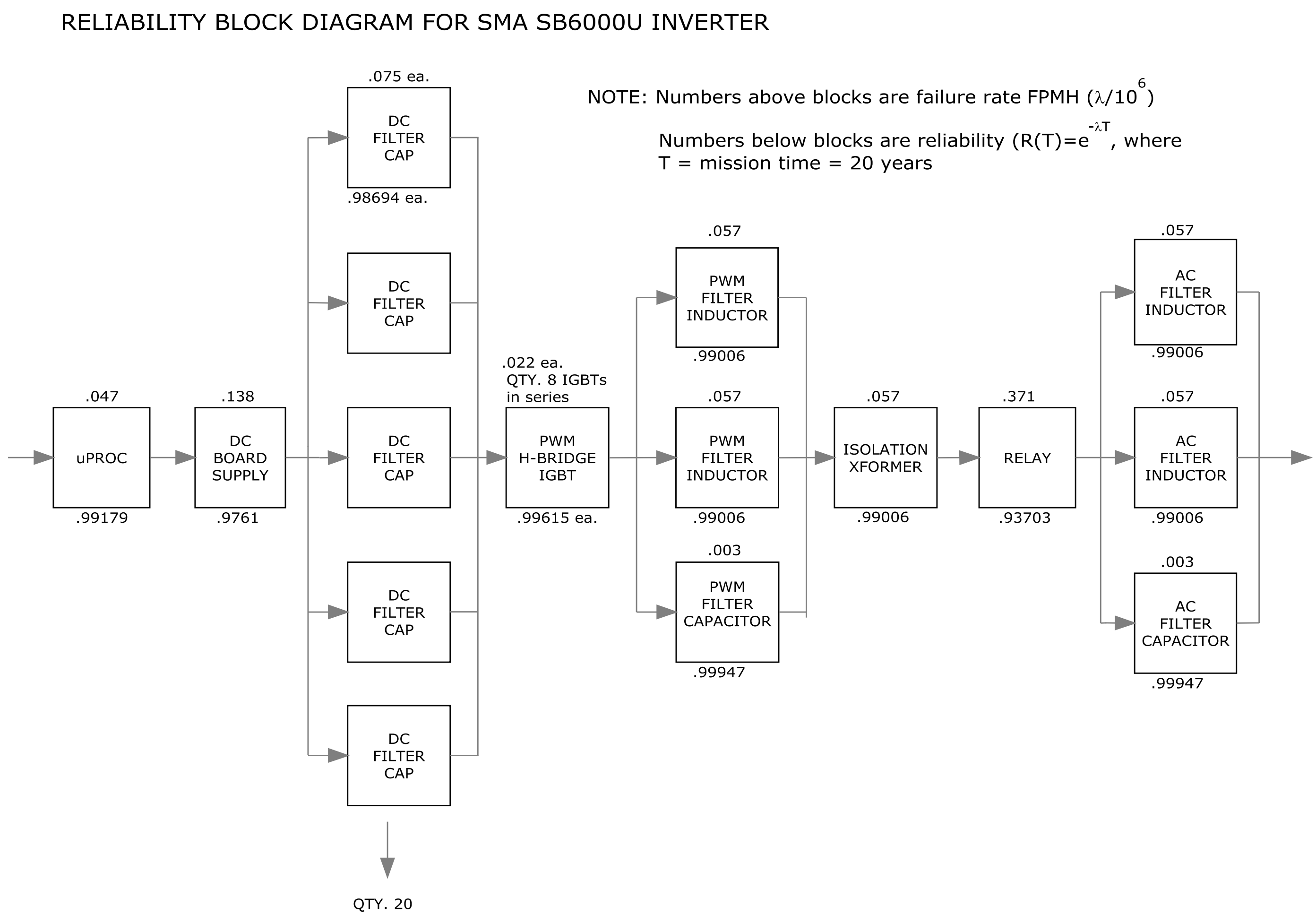

5 REDUCTION IN KWh DUE TO COMPONENT REPAIRS/REPLACEMENT

5.1 INTRODUCTION

Scope

This is the second of the calculation modules. The results of the first (Section 4) provided the failure time for the four components. The resulting downtime, primarily for repair or replacement of the failed component, results in a period of time that power and energy are not generated. The stochastic analysis provides the failure times. This calculation used the transient simulation Power Systems Computer Aided Design (PSCAD) code [5-1] to model the GCPV system, including the failure of components identified in Section 4. PSCAD has been used successfully to predict time behavior as the result of changes, or to introduce new topology or control modules [5-2, 5-3, 5-4].

The resulting downtime to repair or replace the failed component results in a loss in power and, depending on the duration of the downtime, loss of generation of DC electrical energy. The purpose of this section is to determine this lost generation.

Assumptions

The assumption made in the model in Section 4 is that the repair proceeds as soon as the failure ends. Thus loss in generation includes logistical activities as well as the actual repair. This assumption could result in errors in the repair time values taken from published documents.

A number of publications [5-5, 5-6, 5-7] conclude that failure of inverter components is the leading cause of loss of generation. Although there have been improvements in component reliability, lacking comprehensive data based on failures and subsequent repairs, the assumption is that failures considered are limited to inverter components.

Literature Review

The analyses herein are, for the most part, based on the 2011 master's thesis of M. Ishaq, at the University of Hartford: "Modeling of a Photovoltaic System Using PSCAD" [5-8]. However, this work was the extension of a number of journal papers and dissertations published in the early 2000s. These publications are divided into three categories, discussed below.

Simulations of Grid Connected Photovoltaic Systems

Papers by Kuei, et al. [5-2], Kim, et al. [5-3], Xuc, et al. [5-4]., and Villalva [5-9] use transient electromagnetic power system programs, with variations in models of the solar cells and other components and systems, to explore performance and/or control of a grid connected photovoltaic system (GCPVS).

The paper by Kim, et al. [5-3] addresses the modeling and simulation of a GCPVS to analyze the interface between the grid and control of the GCPVS. The model and simulation of the PV system responses to a range of control functions is based on the power transient software PSCAD/EMTDC. The model is used to calculate the response to the two major types of faults: a single line to ground fault and a three-phase short circuit fault. This model includes the PV array, a grid connected inverter, power control and anti-islanding control, which are integrated into the inverter enclosure. Simulated models include the arrays, inverter, and grid. The inverter, aside from conversion of DC to AC, also includes measurements and calculations, power control, maximum power point tracking (MPPT), current controller, and protection.

Both Kuei, et al. [5-2] and Xuc, et al. [5-4] present detailed solar cell models simulating the response of a PV system to various faults. Their expanded models add a shunt, or parallel, resistance to account for losses in the branch with the diode.

Villalva's work [5-9] presents a simplified model of PV arrays based on manufacturer's data sheets. Predictions based on a simulation code are validated with experimental measurements. The simplified models of the arrays as well as other systems and components were instrumental in using this approach for the models and simulations in this section.

Stochastic analyses related to performance

Ristow, et al. [5-10] notes that uncertainty in performance calculations can result in unexpected variations in costs associated with component prices and their relationship to installed costs of the system, and the effect of failure and resulting downtime. Based on the assumption that these variations are random, a stochastic model of system reliabilities used a Monte Carlo model to predict failures and subsequent downtimes. This economic model is then used to determine variations in installed costs and the effects of failure and resulting downtime on the generation costs of the system.

Ristow's 2008 dissertation [5-11] is a comprehensive analysis and evaluation of the design and performance of a PV system. The analyses assume that failure and repair events are random. A stochastic Monte-Carlo-based analysis is used to determine reliability, availability and serviceability.

Availability requires that the component is working. Reliability ensures that the component will satisfy its design life. Should the component fail, serviceability can minimize downtime.

The analysis used the 342kW system installed at the Georgia Institute of Technology Aquatic Center (GTAC). The system began generation in July 1966 and had operated some 10 years, when operation was interrupted by 18 months of construction work on the GTAC (2002-2003). Otherwise performance was acceptable, experiencing 9 down times, the majority due to failure of inverter subsystems (PCU fans, IGBTs), and the mean time between failures (MTBF) and mean time to repair (MTTR).

Using the data from these failures probability, based on a Weibull model, $f(t) = 1 - [\exp(-t/\eta)]^{\beta}$, was used to calculate the parameters η≡ and β≡.

Collins et al. [5-7] reviewed the performance of the Tucson Electric Power at Springerville, Arizona, of 26 arrays and 450 crystalline silicon modules, for a total generation capacity of 4.6 MW. Installation started in July 2001 and was completed in July 2004. The review documented component failures and data on mean time before failure (MTBF) and mean time to repair (MTTR).

A comprehensive program to develop estimates of reliability and availability for large GCPV systems included the following objectives

- **Failure of system components:** 237 failures were recorded in the five years of operation. The inverter with 125 failures (most likely due to component faults) contributed about 50% of the failures.

- **Failure and repair distributions:** Commercial software ReliaSoft Weibull++™: Based on monitoring results and operational records, and the software ReliaSoft Weibull++™ was used to determine acceptable models and scale (η), shape (β) and location (γ) parameters needed to define the distribution functions, f(t).

Substitution of values of η, β, and γ results in a series of comprehensive models for component failures and repairs, which are vital in estimating the times before failure (TBF) and time to repairs (TTR).

Distributed Generation Based on GCPS

Golder [5-12] examined the trend for distributed generation, which could include different sources of renewable energy, noting that this could have significant impact on distribution. Based on this a simulation model was developed for utility based distribution systems with PV power as the primary source of generation. The variation in local insolation and atmospheric conditions resulted in unbalanced distribution. Simulations were performed to study the effect of demand profiles, phase and feeder balancing, changes in power factor and increases in voltage. The results were then factored into operation of distribution where PVs are the main source of generation. While not directly applicable to the objectives of this project this information would be the next step in the design and operation of utility-based distribution systems.

Dzimano [5-13] focused on the impact of the effect of climate and environmental changes on the growth of alternative energy sources. A mathematical model, based on analysis and empirical data, was used to determine the effect of these changes on solar cells. Models used were based on existing models of solar cells. However, as with Golder [5-12], while not directly applicable to the scope of this project, these insights may well be the next step in adapting distributed PV generation to types of utility-based distribution systems.

5.2 TYPES OF PHOTOVOLTAIC SYSTEMS

Grid-Tied PV Topologies

There are two topologies in which the PV system can be connected to feed power into the grid. One topology connects the PV to the DC-DC converter to step up or step down the DC voltage to an appropriate voltage that provides the maximum power point tracking (MPPT), and then converts the DC into AC and feeds electrical power into the grid. This topology is shown in Figure 5-1. The second topology connects the PV to the inverter to convert DC into AC. This inverter also tracks maximum power point (MPP) and extracts maximum power from the PV modules.

Figure 5-1: PV Grid Topology without DC-AC Inverter

Grid-Connected Photovoltaic System

The main function of the inverter is to give as pure as possible sinusoidal output in desired phase, voltage, and frequency to match the grid.

Grid-connected photovoltaic systems (GCPVS) feed power to the local grid. The inverter converts the DC to AC, which is either consumed by the load or fed to the grid. During the day, the power produced by the PV system is used by the load and excess is fed to the grid and sold. In case of failure or at night, the GCPVS is shut off, and the load gets power from the local grid.

The inverter converts DC into AC. Figure 5-2 shows a single-phase inverter topology. It contains 4 power semiconductor switches, where 2 switches are connected in series with each other. The switching devices could be a bipolar junction transistor (BJT), metal oxide semiconductor field effect transistor (MOSFET), or insulated gate bipolar transistor (IGBT). The inverter also contains 4 freewheeling diodes across each switch. The purpose of the freewheeling diodes is to provide a path for the load current to flow when the two IGBTs in series are turned off.

Figure 5-2: Basic Components of a GCPVS

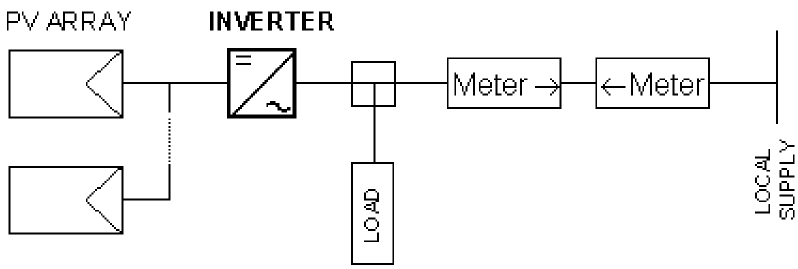

Basic components of a GCPVS are:

PV array: Several modules are connected in a series-parallel combination to produce DC power when exposed to sunlight.

Inverter: Converts DC power to AC power. The inverter output matches the technical requirements of the grid supplier.

Transformer: Steps voltage from the inverter up or down to the appropriate level to match the grid. It is also sometimes used for isolation and safety reasons.

Load: The appliance either fed by the inverter directly or the inverter feeds the grid and the grid feeds the load.

Load grid: The conventional utility the power company maintains to provide power to consumers.

5.3 LINCOLN THEATER PHOTOVOLTAIC SYSTEM

The University of Hartford's Lincoln Theater GCPVS employs the SMA SB-6000U inverter, a grid-tied string inverter for PV power generating systems developed in Germany by SMA Regel systems GmbH. String technology means that a number of PV modules are connected in series, i.e., a "string." One or more "strings" then serve as input to one or more inverters, resulting in a flexible building block for PV system design. The SB-6000U represents the classic inverter configuration most popular in the late 1990s and early 2000s: a single-stage, single-phase, 60 Hz transformer-based string inverter. These inverters have a high conversion efficiency and power factor (>90%) over a wide operating range and total harmonic distortion (THD) of less than 5%. Alternative inverter topologies include 3-phase, high frequency transformer-based, transformerless, battery-based, off-grid stand-alone, and lower power level inverters with a DC-to-DC converter front-end for increased efficiency. The Lincoln Theater installation (Figure 5-3) [16] employs three SB-6000U inverters, each receiving DC power from a PV module array comprising 3 paralleled sets of 7 series-connected modules. Each module consists of 216 individual semi-crystalline silicon cells.

[16] Source: Facilities Department, University of Hartford

Figure 5-3: Lincoln Theater One Line Diagram

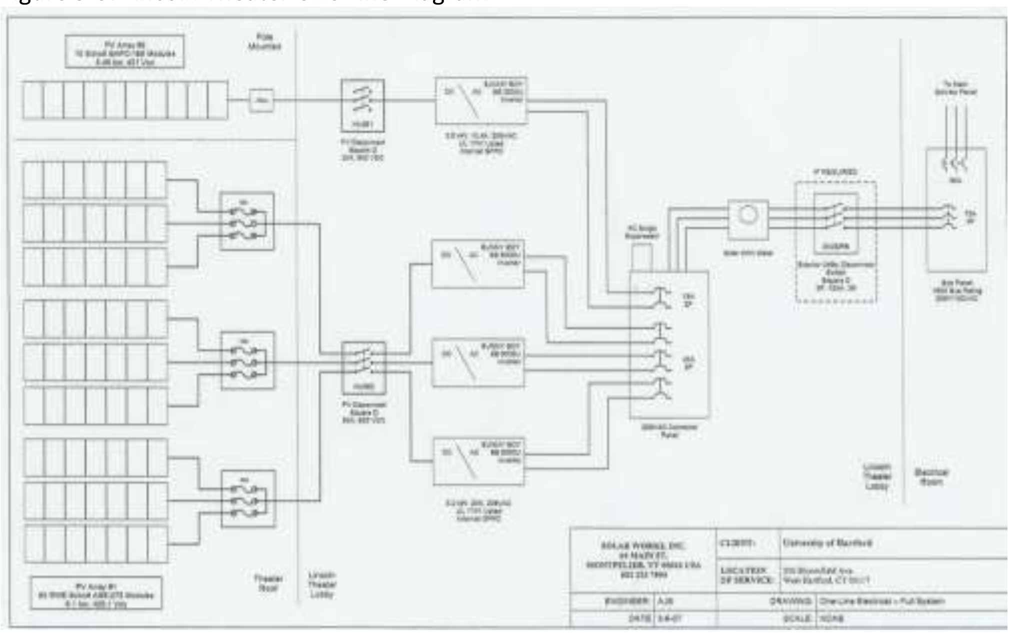

Note that the Lincoln Theater system also includes a fourth inverter (model SB2500U) for a tracking module array. All four inverter outputs are connected via a "combiner" box to the conventional three-phase Y AC power grid, with manual disconnect breakers on both the AC and DC side. A KWh meter monitors AC energy delivered to the grid.

Basic Functions

The grid-tied inverter installed at Lincoln Theater performs these basic functions:

- Converting DC from the PV array into AC power.
- Tracking MPP on the VI curve and adjusting PV voltage and current to transfer maximum power.
- Disconnecting the grid in case of grid voltage or frequency changes beyond the coded limits.
- AC and DC automatic and manual disconnection, EMI filtering, cooling, ground fault protection, communication busses, operational data display, and product packaging.

Inverter Components

The main components of the Lincoln Theater grid-tied, SMA SB-6000U inverter are as follows:

- DC filter
- PWM H-bridge
- PWM high frequency filter / AC filter
- Line isolation transformer
- Microcontroller
- MPPT
- 208 V line

Figure 5-4 is a schematic of the SMA SB-6000U inverter.

Figure 5-4: PV Inverter Schematic

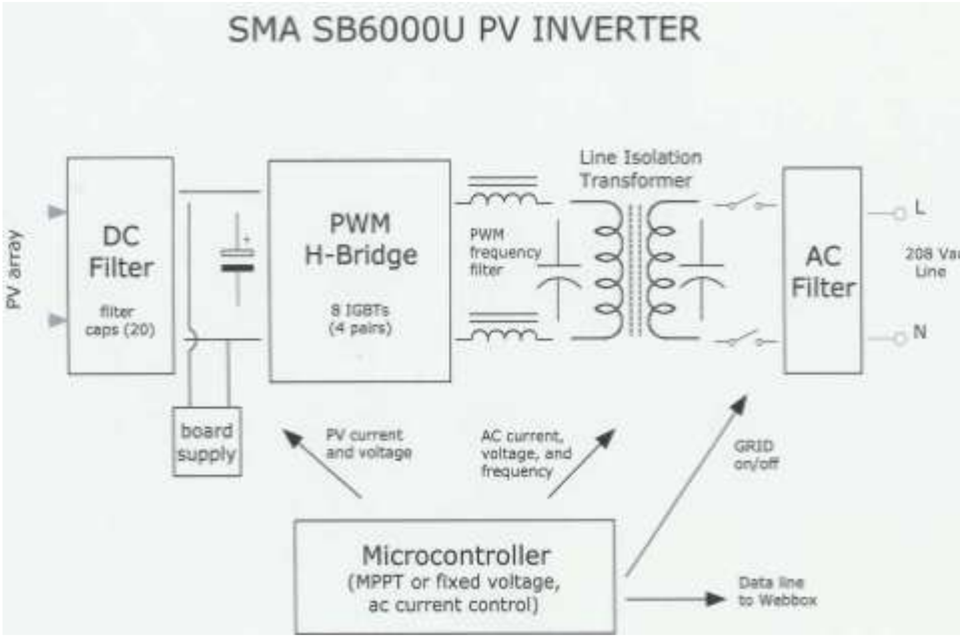

Details of the inverter design are documented in Appendix 5-A.

5.4 MODELING OF PHOTOVOLTAIC SYSTEMS

Photovoltaic Module and Array

A PV cell is a solid state device that converts sunlight into electricity. The basic principle involved in this conversion is the photoelectric effect. An ideal solar cell can be simply modeled as a DC current source connected in parallel with a diode, as shown in Figure 5-5. The current produced by the sunlight on the solar cell is represented by the current source while the diode gives typical characteristics of a solar cell. The magnitude of the current source is at a constant irradiance and constant temperature and has a linear relationship with increasing irradiance. In addition to the components of the ideal model, the model shown includes series R_S and shunt resistance R_{SH} to capture the behavior of a practical solar cell.

Several elements of the solar cell contain resistive properties, including the semiconductor material itself, the metal grid that collects current from the semiconductor material, the collector bus, and the internal wiring. It is assumed that these series losses can be modeled using a lumped resistor R_S. Several shunt-resistive losses can occur, such as localized shorts at the emitter layer of the semiconductor material and perimeter shunts at the cell borders. The combined effect of these shunts is modeled by a lumped parallel resistor R_{SH}. Usually the value of R_{SH} is very high whereas R_S is low. An ideal solar cell does not contain series and shunt resistances.

Figure 5-5: Solar Cell Equivalent Circuit

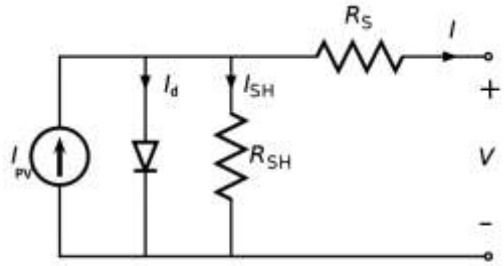

Source:http://upload.wikimedia.org/wikipedia/commons/9/92/SolarCell-EquivalentCircuit.PNG

Output current and voltage produced by the solar cell are related by the equation below:

$$I = I_{PV} - I_o \exp\left\{\frac{(qV + IR_s)}{n\,K\,T} - 1\right\} - \frac{V + I_{SH}R_s}{R_{SH}} \qquad (1)$$

Where:

I_{PV} is the PV current generated due to sunlight

I_O is the reverse saturation current

I_{SH} is current through the shunt resistor

q is charge on electron ($1.63\ x$ [$10^{\uparrow}(-19)$ C)

K is Boltzmann's constant $(1.38\ x\ 10^{-23} m^2 kg\ s^{-2} K^{-1})$

T is temperature in Kelvin

n is ideality factor (value usually between 1 and 1.5)

Voltage Current (VI) Characteristics of a PV Module

A module produces maximum current when the two PV output terminals are short circuited and thus there is no resistance in the circuit. At this point, the current is a maximum value and the voltage is zero. Conversely, maximum voltage and zero current result when the two PV output terminals are open circuited. Resistance values between zero and higher will get values of voltages and currents as depicted on the VI-curve graph (Figure 5-6).

This graph highlights four important points: $I_{SC}, V_{OC}, V_{mp}, I_{mp}$. I_{SC} is the short circuit current when the two PV output terminals are short circuited (voltage becomes zero). V_{OC} is the open circuit voltage when the two PV terminals are open (in that case, the current is equal to zero).

Figure 5-6: Typical VI Curve of P Module

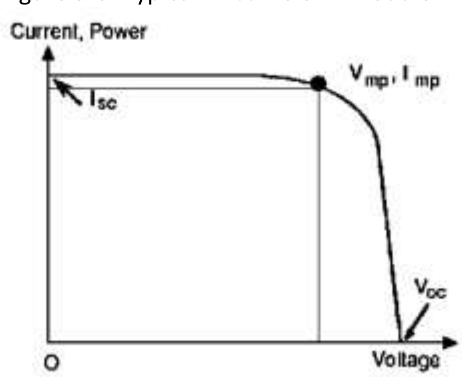

Between these two points (V_{oc} and I_{sc}), where the power is zero, there is a point on the "knee" of the curve indicating where the module is producing maximum power. V_{mp} and I_{mp} are the voltage and current at this maximum power point (MPP), the highest production of current and voltage. For the SCHOTT ASE-270 module employed in the University of Hartford's PV system, the MPP is at 49.1 volts and 5.5 amperes, providing 270.05 watts. Different manufacturers also call this the peak power point or the rated power point. In order to use the PV module at its maximum capacity—that is, to extract as much power as possible—the module needs to be operated at the MPP. This is called maximum power point tracking (MPPT). The PV system is made to operate at this point using a maximum point tracker circuit to actively monitor the array's voltage and current. This tracking will ensure that maximum power is extracted from the arrays at a certain insolation level. It should be noted that the VI curve is obtained under standard test conditions, assuming no shading on the module.

Impact of Temperatures and Irradiance on VI Curves

The VI characteristics of a solar module depend on the module's temperature and insolation.

Impact of Solar Irradiance: Current produced by the PV module is linearly proportional to the number of photons absorbed by the PV module material and thus proportional to incident light. At standard test condition (STC), the insolation level is 1000 W of solar energy per square meter, called one "sun." Manufacturer-provided VI curves are obtained at this insolation level. If a module produces 6.1 amperes current at STC, then at 500 (W/m^2) it should produce approximately half of 6.1 amperes. Figure 5-7 shows how PV current decreases with reduced insolation.

Various simulations at various insolation levels validate the linearity of solar insolation and produced current.

Figure 5-7: Impact of Decreasing Irradiance on VI Curve

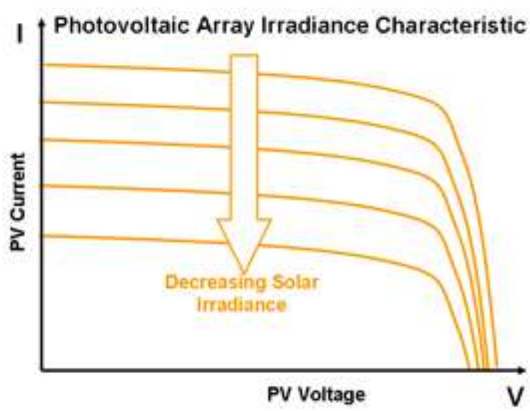

Source: http://www.mpoweruk.com/images/pv_insolation.gif

Impact of Temperature: The output voltage of the PV module decreases with increases in temperature while the short circuit current increases with increasing temperature. Manufacturers provide the module temperature coefficient on how much the current or voltage changes per degree change in temperature. Figure 5-8 shows the effect of temperature on VI curves.

Figure 5-8: Impact of Temperature on VI Curve

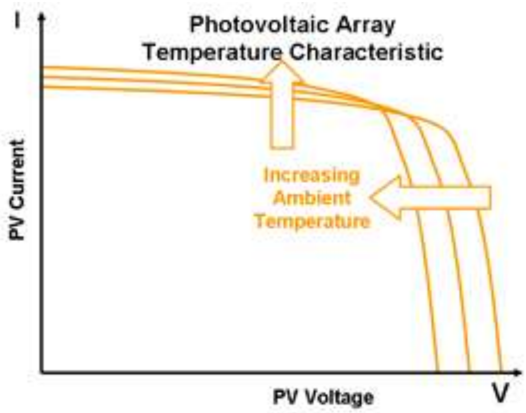

Source: http://www.mpoweruk.com/images/pv_temperature.gif

Air space of 4 to 7 inches is required to provide proper ventilation. Modules are installed with space underneath them for cooling, thus increasing their efficiency.

5.5 SIMULATION

PV Module Manufacturer Provided Parameters

Basic parameters provided by the manufacturer are short current I_{SC} , open circuit voltage V_{OC} , current at maximum power point I_{mp} , voltage at maximum power point V_{mp} , temperature coefficient of current K_I , temperature coefficient of voltage K_V , and number of cells in the module N_{cell} . These values are provided at STC of 1000 (W/m^2) and 298 K. Several curves provided by the manufacturer can be used to adjust the values of other parameters such as R_S and R_{SH} .

Modeling of PV Module Using Manufacturer-Provided Parameters

The high value of R_{SH} would be ignored for simplification. Since the value of R_S is very low and R_{SH} is very high, it is assumed that the short circuit current I_{SC} is equal to I_{PV} , the PV current. Assumptions are that $I_{sc} \approx I_{PV}$ and $R_{SH} \approx \infty$.

To verify the model, manufacturer-provided parameters of the SCHOTT ASE-270 module are used in the model and the results compared with the manufacturer-provided curves at different insolation and temperatures. The PV module modeled is connected across a variable resistor that exponentially increases with time. The modeled circuit was simulated and voltage vs. current and voltage vs. power curves obtained.

Table 5-1 shows the electrical parameters for a SCHOTT ASE-270 single module. The electrical parameters are tested at STC [5-14]. Irradiance and temperature level are 1,000 W/m^2 and 298 K, respectively.

Table 5-1: Electrical Parameters of SCHOTT ASE-270 Module

Power (max)	P_p (watts)	260 W	270 W
Voltage at maximum power point	V_p (volts)	48.7 V	49.1 V
Current at maximum power point	I_p (amps)	5.3 A	5.5 A
Open circuit voltage	V_{OC} (volts)	60.8 V	61.3 V
Short circuit current	I_{SC} (amps)	5.9 A	6.1 A

Table 5-2 provides cell temperature coefficients for the module.

Table 5-2: Cell Temperature Coefficients of SCHOTT ASE-270 Module

Power	T_K (P_p)	-0.47 % / ^{o}C
Open circuit voltage	T_K (V_{OC})	-0.38 % / ^{o}C
Short circuit current	T_K (I_{SC})	+10 % / ^{o}C

Figure 5-9 shows the VI curve characteristics for the module.

Figure 5-9: Manufacturer VI Characteristics of SCHOTT ASE-270 Module

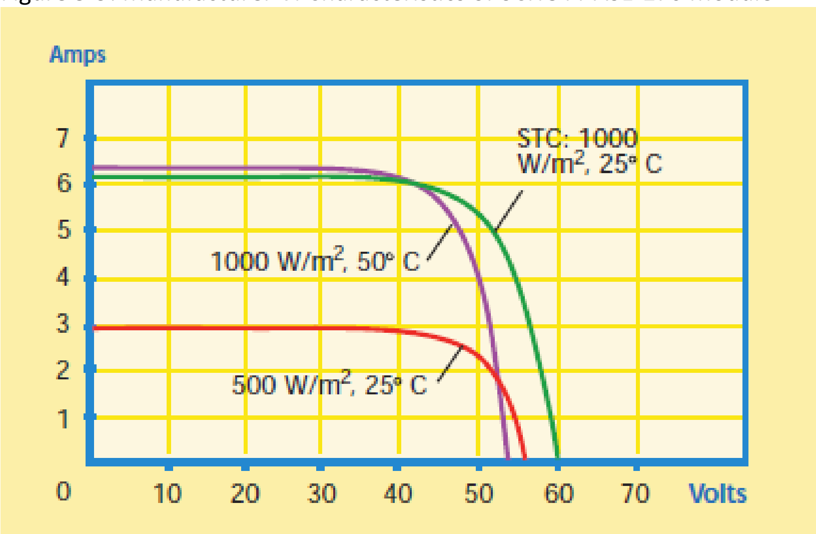

Source: http://energyoptions-wind.com/docs/Schott%20ASE_270.pdf

Details of the simulation model, based on manufacturer's parameters, are discussed in Appendix 5-B, while details of the PSCAD subsystems and GCPVS are detailed in Appendix 5-C.

Benchmark

The model predictions are verified by two methods. The first method is to compare predictions recorded by the software provided with the Lincoln Theater inverter and stored by SMA.

Simulations are run first without applying the failures; current injected into the grid multiplied by voltage (208 V) is observed and recorded in the form of kilowatt-hours per year (kWh/yr). A user-defined component is designed in PSCAD to record kWh at each time step using FORTRAN.

The simulation is again run with the same typical meteorological year (TMY) data and the availability/failures are applied to one leg of the inverter (see Figure 5-10) and KWh/Year is again measured and recorded[5-8].

Figure 5-10: Flow Chart of Simulation

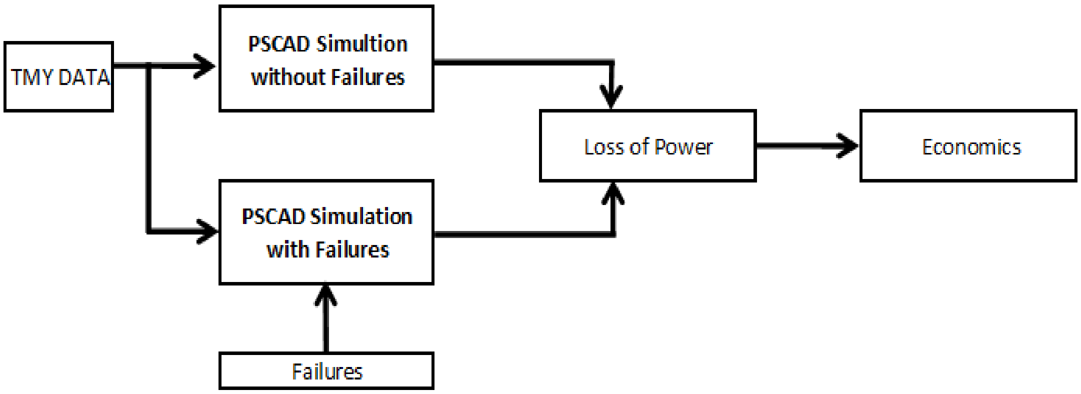

Table 5-3 documents the recorded values of grid current (Ireal) and voltage (Ereal) for November 10, 2011. Ignoring the value at sunrise, the average difference between the recorded power (Preal) and power calculated using PSCAD (Psimulated) is -11 %.

Table 5-3: Simulated and Real Current Values

Time	W/m2	Iac (Real)	Iac(Simulated)	Vac Real	Vac (Simulated)	Pac(Real)	Pac(Simulated)	Current Error
7:00	28	0.343	0.65	222.2	206	80	150	-89.50437318
8:00	183	3.63	4.5	220.3	206.4	800	958	-23.96694215
9:00	330	7.56	8.54	220.3	210	1670	1832	-12.96296296
10:00	450	10.58	11.78	219.6	209.5	2322	2556	-11.34215501
11:00	513	12.17	13.52	220.3	210.2	2680	2839	-11.09285127
12:00	522	12.23	13.66	219.7	209.6	2689	2863	-11.69255928
13:00	466	10.92	11.93	220.6	209.07	2405	2635	-9.249084249
14:00	366	8.37	9.4	220.9	209.54	1840	2041.2	-12.30585424
15:00	227	4.43	5.2	220.2	207.2	975	1210.2	-17.38148984
16:00	83	0.19	0.25	220.5	206.5	39	465	-31.57894737

The second model prediction method compares the values of a reference current injected into the grid with the values recorded by the Lincoln Theater software. Figure 5-11 shows that the recorded grid current (the jagged line due to the frequency at which the IGBTs alternate the DC current) and the reference current (the unbroken line imposed on the grid) are in good agreement.

Figure 5-11: Inverter Current Injected into Grid Following Reference Current

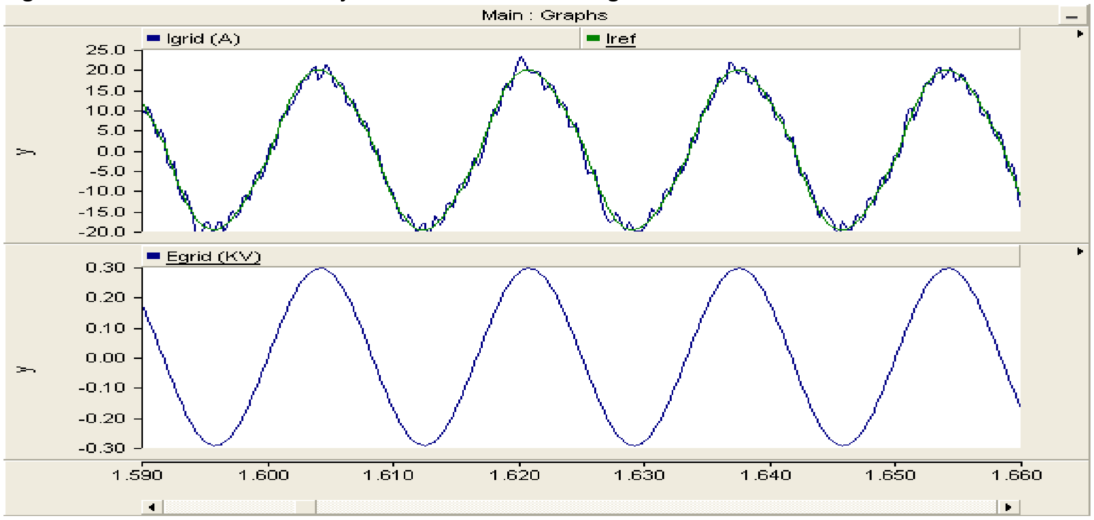

5.6 INTERFACING MULTIC_RISK WITH PSCAD GCPVS MODEL

The financial impact of failure is two-fold. First, if reduction in or loss of generation occurs during periods of high insolation, usually late spring to early autumn, the result could be higher prices for replacement power. Second, regarding replacement components being readily available or easily repaired, the time of year also could influence the availability of both hardware and qualified labor. The analysis is divided into three parts:

(1) Component failures with either partial or complete reduction of power: The first considers partial failures, e.g., failures that do not result in complete reduction of power, and complete failure, e.g., loss of IGBTs resulting in complete reduction of power from one or more of the inverters.

(2) Effect of mean time before failure (MTBF) and mean time to repair (MTTR) on failures and subsequent reduction of generation: Described is a series of cases that document the effect of MTBF and MTTR on failures and subsequent reduction of power generation. This involves introducing conditions that result in failure of a component, in this case the IGBT.

(3) Calculations based on failure rates calculated using MIL-HDBK 217F procedures and repair rates derived from published data for components similar to those in references [4-1] and [4-2]. In prior sections these are referred to as demonstration cases (section 4.5).

The results are used to establish the data needed for the economic analysis.

Observations on MultiC_Risk Simulator

While there is no need to have a component failure simulator to determine the number of expected component failures a PV system will experience in a year, MultiC_Risk does provide a unique perspective on the kinds of component-failure scenarios that can occur. Multiple MultiC_Risk runs provide a range of equally possible annual failure histories for design and economic assessments.

MultiC_Risk provides evidence for a situation in which a number of component failures per year are expected. The arrival sequences of these component failures (evenly spaced vs. failure clusters) make MultiC_Risk a useful simulation for assessing the economic impact of PV power generation reliability.

One-year simulation data of a component's availability or failure are produced by the MultiC_Risk simulator and put in appropriate order in Windows™ Notepad to be read by the file-reader component inside the PSCAD.

Similarly, TMY irradiance data are put in Notepad in appropriate order and fed to the PV module using the file reader.

The full-year simulation is input in another application that evaluates the power production output during the year and determines economic impact of any component failure.

5.7 COMPONENT FAILURES

This section considers two cases of fault simulation: partial failure and full failure.

Case 1: Partial failure in a single inverter. A loss of energy due to partial reduction in the current injected into the grid is observed and recorded, without considering the quality/shape of the output current.

Case 2: Full failure of the PV inverter when the fault occurs inside the inverter. In this case, the inverter is considered completely shut down. Loss of energy for the whole PV system (1 of 3 inverters) is observed and recorded.

Case 1: Partial Failure

At a given time, different pairs of mean time between failure (MTBF) and mean time to repair (MTTR) data for the inverter component are fed into the MultiC_Risk simulator. The simulator produces availability or failures of the selected component in the forms of 0s and 1s over one year.

A file reader in PSCAD reads the data from the notepad output file and the availability/failures data are applied to the breakers, which are connected in series with the components to be failed. This is shown in Figure 5-12 in which two breakers are connected in series with IGBTs (the first identified as IGBT 1/2 and the second as IGBT 3/4) in one leg of the inverter. When input to the breakers from the data file is 1, the breakers are closed (red) and the component, in this case IGBTs, is said to be working.

Figure 5-12: Inverter Showing IGBT and Breaker

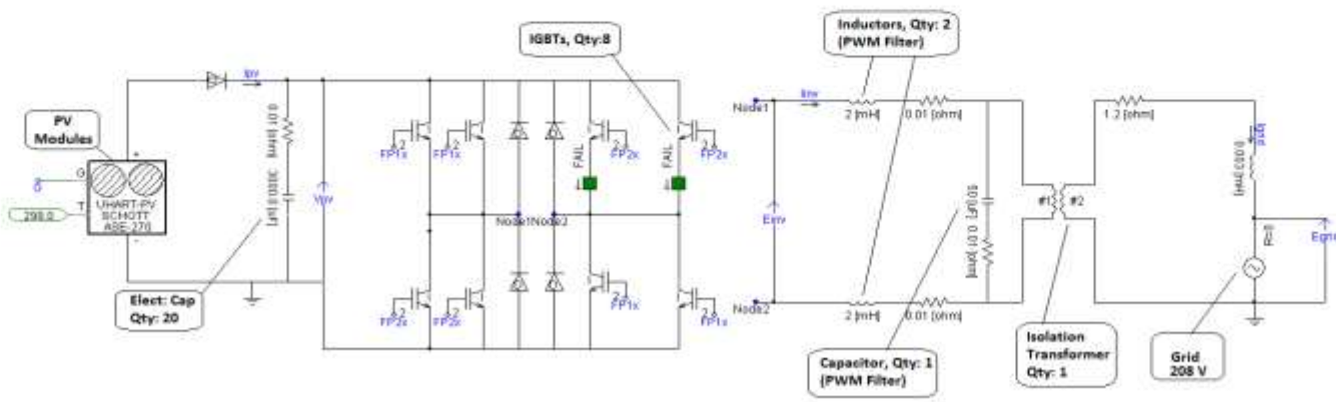

When input to the breaker from the data file is 0, the breakers are open and the IGBTs are said to be failed. Figure 5-13 shows availability/failures of MultiC_Risk simulator output data over the period of 1 year, imported into PSCAD.

Figure 5-13: Availability/Failure Data in PSCAD for 1 Year

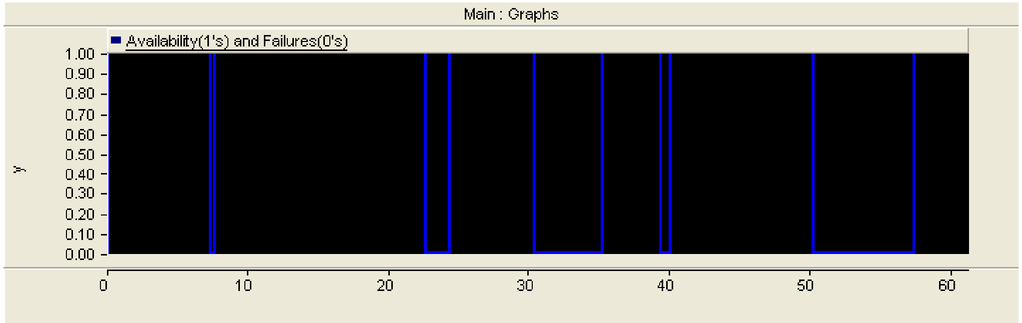

Case 2: Full Failure

In the case of complete or full failure, one of the 3 inverters is considered completely shut down when failure occurs. For this simulation, the availability and failure data are given to the breaker connected between the inverter and grid, and this breaker controls whether the current is being injected. Loss of energy for the whole PV system is observed and recorded by the KWh-meter. The simulation places a breaker between the AC portion of the inverter, on the high voltage side of the transformer, and the circuit on the low voltage side of the transformer (Figure 5-14). A failure of at least one IGBT pair will result in 0 current to the load (Figure 5-15).

Figure 5-14: Full Failure Due to IGBT Failure

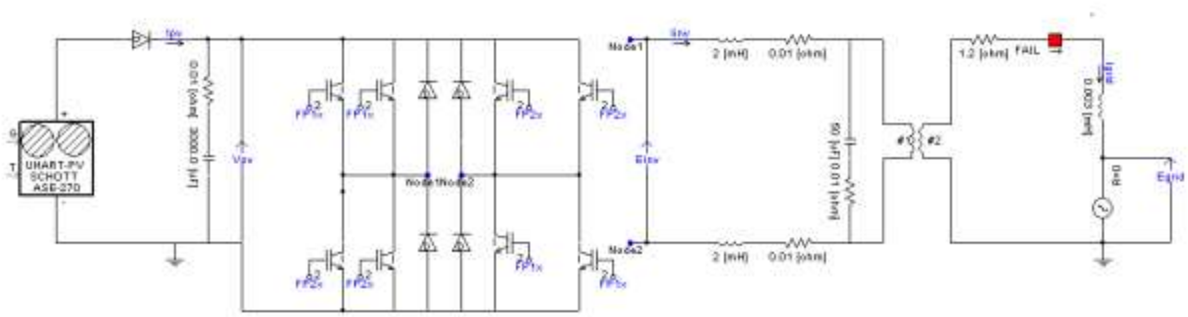

The energy produced without any failure per inverter per year is 8894.66 kWh/yr. For the Lincoln Theater GCPVS the energy produced by the 3 inverters is 3 × 8894.66 = 26683.98 kWh/yr. In case of failure of one of the inverters, total energy output by the 2 remaining inverters is 2 × 8894.66 = 17789.32 kWh/yr plus, upon completion of repair or replacement of the failed IGBT, minus the output of 1 inverter (8894.66 kWh/yr) multiplied by [1-(downtime)]/365 [days]. When one leg of the inverter is open-circuited (failed) the current produced is pulsating DC and harmonic character (no failure) when working (Figure 5-15).

Figure 5-15: IGBT Full Failure and Normal Operation

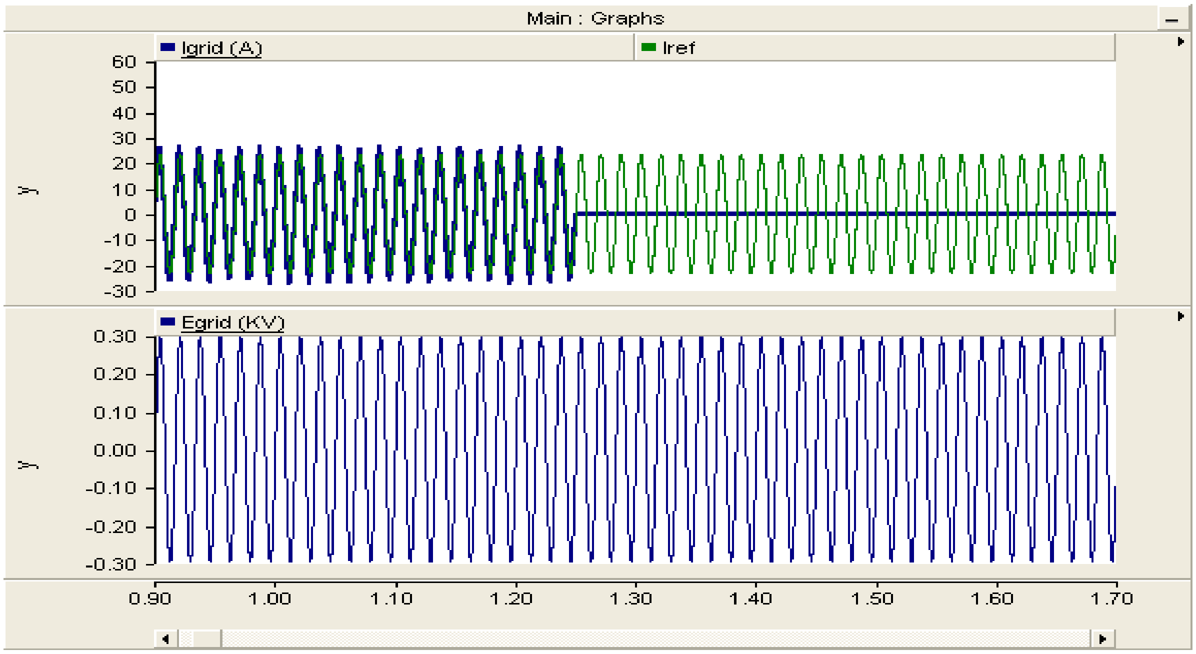

Effects of MTBF and MTTR: The purpose of these calculations is to investigate the impact of selected values of MTBF and MTTR on the energy decrease during repair time following failure of one or more components.

Different values for the pairs of MTBF, β for the Weibull function[17], based on the assumption that both failure and repair are a negative exponential function, MTTR, and Beta for repair and impact are input into MultiC_Risk. Table 5-4 lists the MTBF and MTTR values.

Table 5-4: Operating State as a Function of MTBF and MTTR

FIGURE	TITLE	MTBF (Days)	Beta_F	MTR(Days)	Beta_R	Impact	OPERATING STATE
5-16A	1 IGBT	90	1	10	1	1	No Failure
5-16B	1 IGBT	100	1	15	1	1	Failure-No power
5-17A	1 IGBT	100	1	10	1	1	No Failure
5-17B	1 IGBT	100	1	30	1	1	Failure-Reduced Power

In figures 5-16 and 5-17 the following information is listed:

Information	Units
Watt hours accumulated over one year	kWh/yr
Energy injected at the corresponding insolation	Energy Injected
Current into the grid at the corresponding insolation	Igrid
Input insolation	kW/m^2
Loss of energy due to repair	Availability = 0

Each time the MultiC_Risk simulation is run, it provides an output text file that shows component availability (based on input values) over one year. The availability data of a certain component over 1 year in Notepad is then

[17] Weibull function for a CPD $F(t)= 1\text{-}\exp[-(t/\eta)^{\beta}]$ where for the exponential function η=MTBF, for failure and MTTR for repair.

interfaced to PSCAD and simulations are run with and without applying the failures, and loss of kWhr/year is calculated. Values for Beta for failures and Beta for repair are taken as 1 all the time for all the cases.

Figures 5-16A and 5-16B are based on calculations for different values of MTBF and MTTR considering full failure of the whole PV system. In the first there are more frequent failures but short repair periods, resulting in minor power reduction. In the second, the failures are not as frequent and there are different repair periods. However, the loss of one inverter (represented by the long repair period), depending on the insolation, can result in significant reduction in system energy. Additional cases are documented in Appendix 5-D.

Frequency Limits: The prior cases deal with failures that result in loss of or reduction in generation. For a GCPVS the frequency of the AC fed into the grid must be within high and low limits. Frequency control is discussed in Appendix 5-E.

Figure 5-16A: Wh/yr, Energy, Irradiance, Current vs. Time, Availability (MTBF=90, MTTR=10)

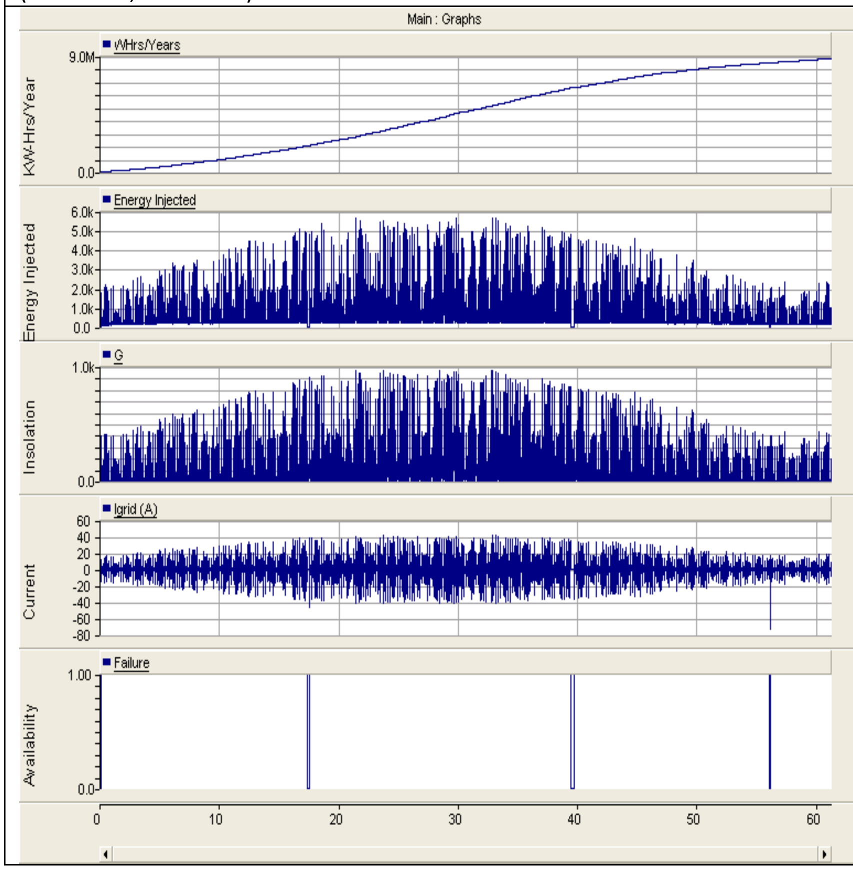

Figure 5-16B: Wh/yr, Energy, Irradiance, Current vs. Time, Availability (MTBF= 100, MTTR=15)

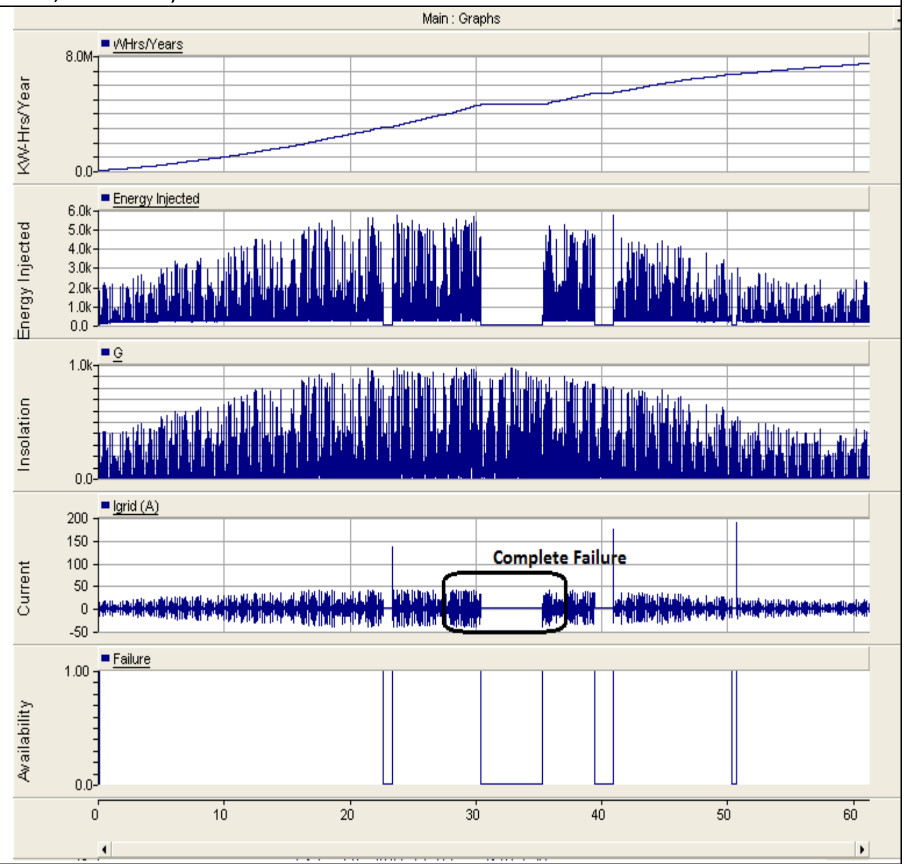

Figure 5-17A: Wh/yr, Energy, Irradiance, Current vs. Time (MTBF=100 and MTTR=10)

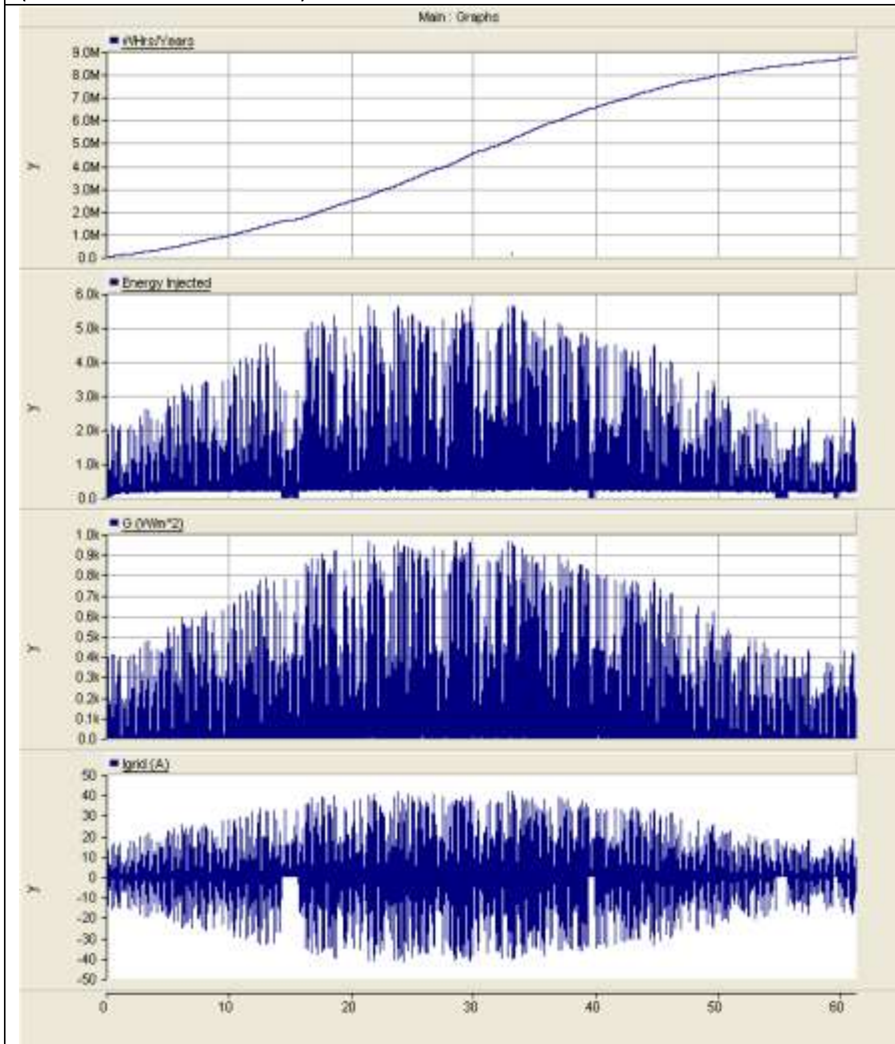

Figure 5-17B: Wh/yr, Energy, Irradiance, Current Verses Time (MTBF=100 and MTTR=30)

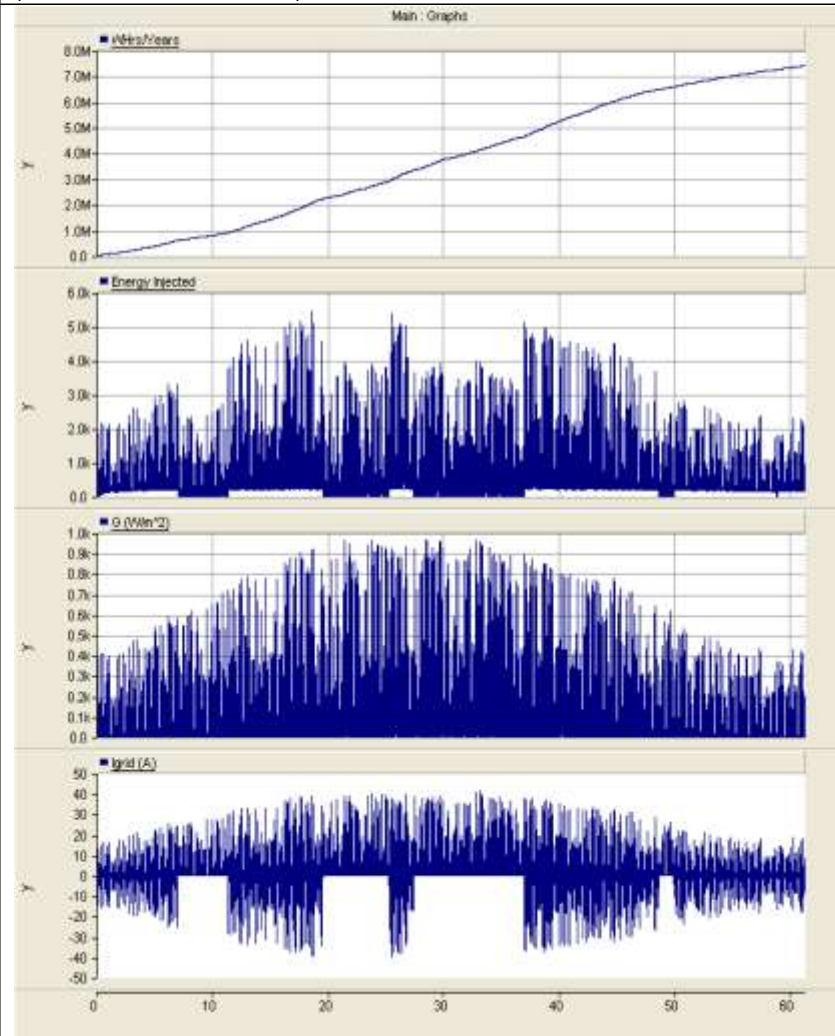

5.8 DEMONSTRATION CASES

Component Time Before Failure

MTBF are based on the MIL-HDBK-217 methodology.

Table 5-5: Electronic Components for the SB-6000U Inverter Based on High Stress Factors

#	Component	Mfr/model number	Qty	$\lambda_p/10^6$hrs	Function
1	IGBT	IXYS/K30N60	8	300.96	PWM bridge switching device
2	Relay	PB/T9AS1D12-9	1	2.075	AC disconnect
3	cap, elect.	EPCOS/B43504	20	9.54	DC filter
4	microproc.	TI/MCUM3	1	1.097	PWM/control
5	board supply	dc/dc converter	1	.522	low voltage DC supply
6	cap, film	EPCOS/B32231	1	.274	PWM high frequency filter
7	cap, film	EPCOS/B32231	1	.274	AC filter
8	transformer		1	.2058	AC isolation
9	Inductor	EPCOS/B82726	2	.000252	PWM high frequency filter
10	Inductor	EPCOS/B82726	2	.000252	AC filter

Simulation of Failures

The component is said to be failed when the breaker connected in series becomes open circuited and no current flows through the device. The breaker becomes open when we provide 1 to it and it becomes shorted circuit when we provide 0 to it as data. Figure 5-18 shows two breakers connected in series with their respective IGBTs to be failed. For the whole simulation, the status (short/open) of breaker changes with input data of 1s and 0s generated by the MultiC_Risk simulation.

Figure 5-18: One IGBT Pair

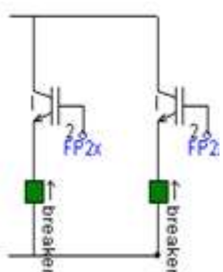

As detailed in Table 5-6, simulation of component failures, based on the guidelines for failure effects are generated by open circuits, specifically, by connecting a breaker in series with the selected component. The failure rates in Table 5-6 are per component. Thus failure rates are multiple components, e.g., 8 IGBTs and 20 electrolytic capacitors are, for the IGBTs, multiplied by (8-N) and the capacitors multiplied by (20-N) and the capacitance, assuming all capacitors are operating, should be divided by 1/(20-N), where N is the number of failed components.

Table 5-6: PV System Component Failure Effects

Component	Failure mode	Failure effect
Module	open	output power decrease
Array	open (ex: blown fuse)	output power decrease
DC breaker	open	shutdown
Inverter	partial or total shutdown	output power decrease/shutdown
Combiner	open	shutdown
kWh meter	open	shutdown
AC breaker	open	shutdown

Repair Times

The repair times (Tables 5-7 and 5-8), based on a negative exponential function, were used to calculate the reduction in power and energy, taken as the product of reduction or loss of power and the repair time. Figure 5-19 compares the times for failure and completion of repair for the Georgia Tech Aquatic Center [5-11].

Table 5-7: Repair Times for Similar Components from References and Lincoln Theater Inverters

LINCOLN THEATER INVERTER					**REFERENCES [5-7, 5-10, 5-11]**		
Component	**Mfr/model number**	**qty**	**MTBF**	**Function**	**Components**	**MTTR/MTBF**	**MTTR**
IGBT	IXYS/K30N60	8	1.38E+02	PWM	IGBT	1.00E-01	13.8
capacitor	EPCOS/B43504	20	4.37E+03	DC filter	Capacitors	1.00E-03	4.37
relay	PB/T9AS1D12-9	1	2.01E+04	AC disconnect	Disconnect	1.00E-04	2.01
capacitor	EPCOS/B32231	1	1.52E+05	High frequency	Filters	1.00E-03	152.7
transformer	480/208	1	2.02E+05	Step Down	Transformer	1.00E-06	0.20
			Days				Days

Figure 5-19: Time for Failure (F(t)=1) and Completion of Repair (R(t)=1) for IGBT

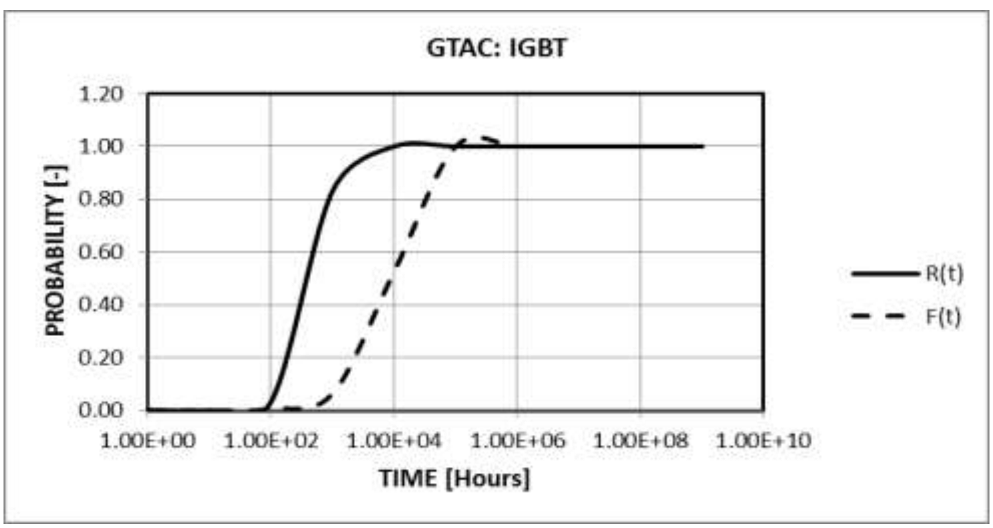

Table 5-8: Repair Times for Similar Components from References and Lincoln Theater Inverters

LINCOLN THEATER INVERTER					REFERENCES [2.3.2-8,9,10]		
Component	**Mfr/model number**	**qty**	**MTBF**	**Function**	**Components**	**MTTR/MTBF**	**MTTR**
IGBT	IXYS/K30N60	8	1.38E+02	PWM	IGBT	1.00E-01	13.8
capacitor,	EPCOS/B43504	20	4.37E+03	DC filter	Capacitors	1.00E-03	4.37
Relay	PB/T9AS1D12-9	1	2.01E+04	AC disconnect	Disconnect	1.00E-04	2.01
capacitor,	EPCOS/B32231	1	1.52E+05	High frequency	Filters	1.00E-03	152.7
transformer	480/208	1	2.02E+05	Step Down	Transformer	1.00E-06	0.20
			Days				Days

5.9 CALCULATIONS

As discussed in Section 4, PSCAD is limited to the calculation of performance due to the failure of one component at a time. Thus, the calculations are restricted to the IGBTs since their MTBF of 138 days is the highest failure rate value and hence there will be a sufficient number of failures over the 20-year operational lifetime. Thus, with the objective being to complete a sample calculation, considering only the IGBTs will satisfy the objective. Table 5-9 lists input for the four pairs of IGBTs.

Table 5-9: Input for Sample Calculation

LINCOLN THEATER INVERTER					REFERENCES [5-7-5-10, 5-11]		
Component	**Mfr/model number**	**qty**	**MTBF (days)**	**Function**	**Components**	**MTTR/MTBF**	**MTTR (days)**
IGBT	IXYS/K30N60	8	138	PWM	IGBT	1.00E-01	13.8

Procedure

Both partial and full failures result in the loss of the inverter containing the failed component. Thus, for example, Lincoln Theater has three inverters, based on the assumption that one inverter has a higher probability of failing at the same time as 2 or 3, resulting in the loss of one-third of the generation for the duration of the downtime**.**

Results

The purpose of this section is to determine the energy lost due to partial and total failure and subsequent repair. These calculations are based on 20 years of warranted service. No failures and the same set of global horizontal radiation values for Hartford, Connecticut from TMY2 [5-14] result in the maximum energy generated. PSCAD is capable of considering only one failed component or, in the case of the IGBTs, failure of one pair of IGBTs at a time. Thus simulations must be performed for each IGBT pair.

Partial Failures: Figure 5-20A shows the IGBT working conditions while Figure 5-20B represents the open circuit failure.

Figure 5-20A: Component (IGBTs) Working

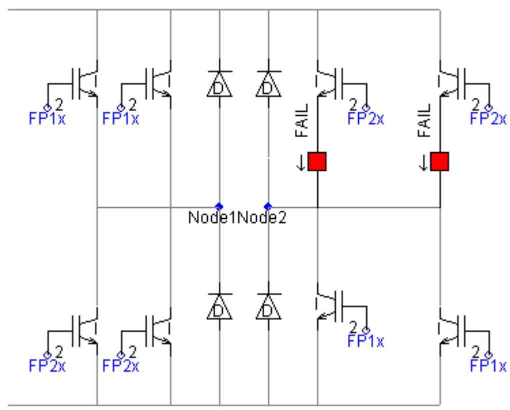

Figure 5-20B: Component (IGBTs) Failed

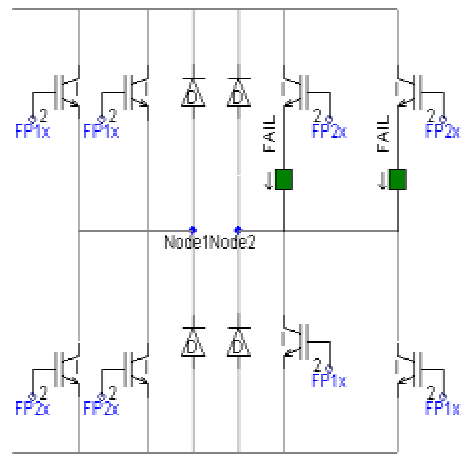

As stated in Section 5.7 failure of one pair of IGBTs results in an asymmetric, or nonharmonic, wave form that is detected by the microcontroller and, subsequently, isolates and effectively shuts down the failed IGBT pair.

The consequence is the loss or reduction of generation for the time it takes to repair or replace the faulty inverters. Assume that the IGBTs in the three inverters have identical MTBF. Based on the times before failure being random, IGBT failures in the three different inverters can occur at different times. Thus the subsequent failure and repair time, and loss or reduction of generation during this downtime, will differ from one pair of IGBTs to another (Figure 5-21).

Figure 5-21: Distribution of Availability

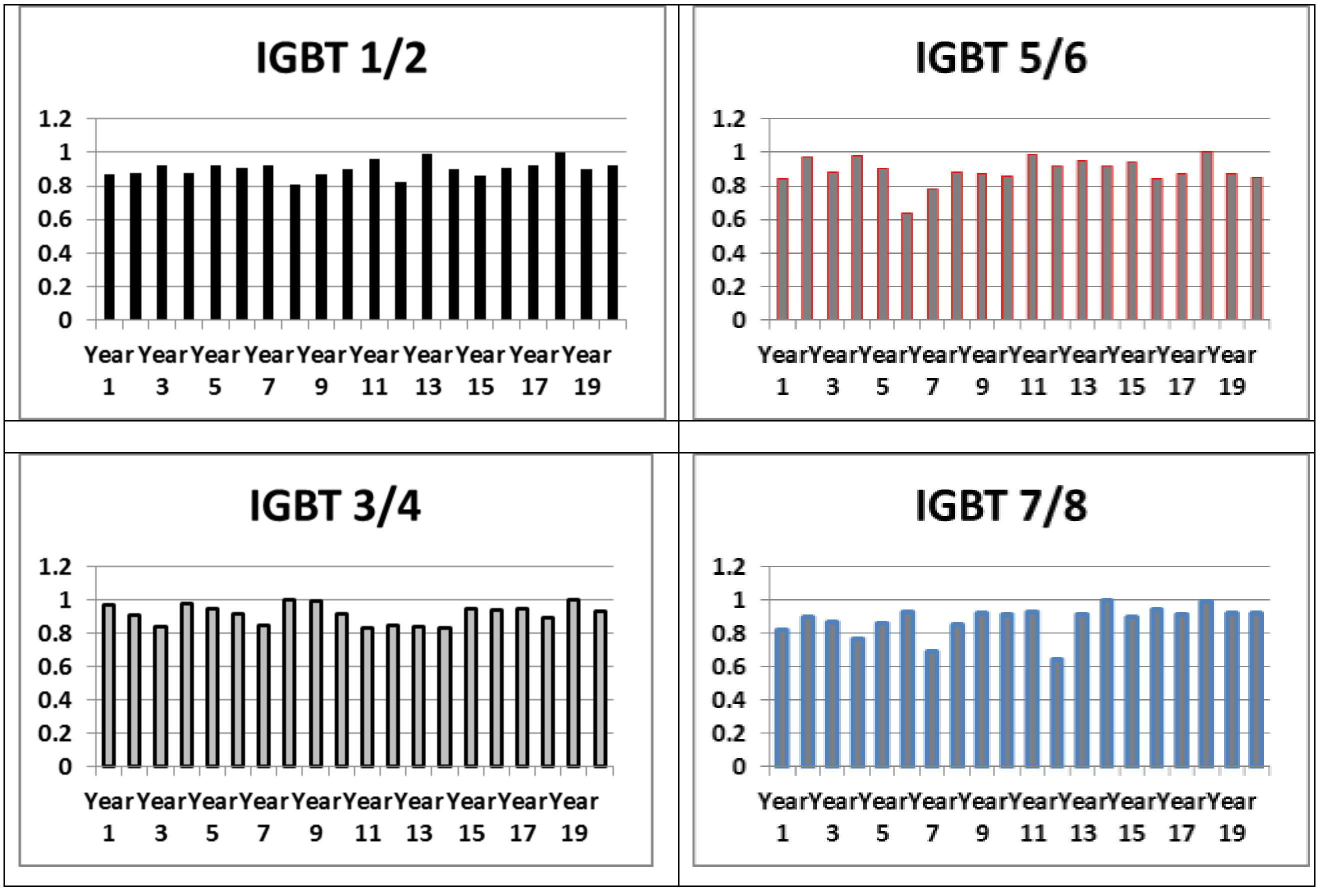

The Lincoln Theater installation has three inverters (referred to as A, B, and C). Since all are the same, it makes no difference which one of the failed IGBT pairs is installed. For calculations based on inverters A, B and C, inverters B and C do not fail, while A is assumed to fail due to the open circuit.

Results of the partial failures are documented in Appendix 5-F for both lost generation and availability. Values of energy generation and reduction or loss, based on 20 years of operation, are shown in Figure 5-22. Calculations of availability based on TBF and TTR are shown in Figure 5-23.

Figure 5-22: Energy Generated and Lost with Inverter A Failed, 20 Years of Operation

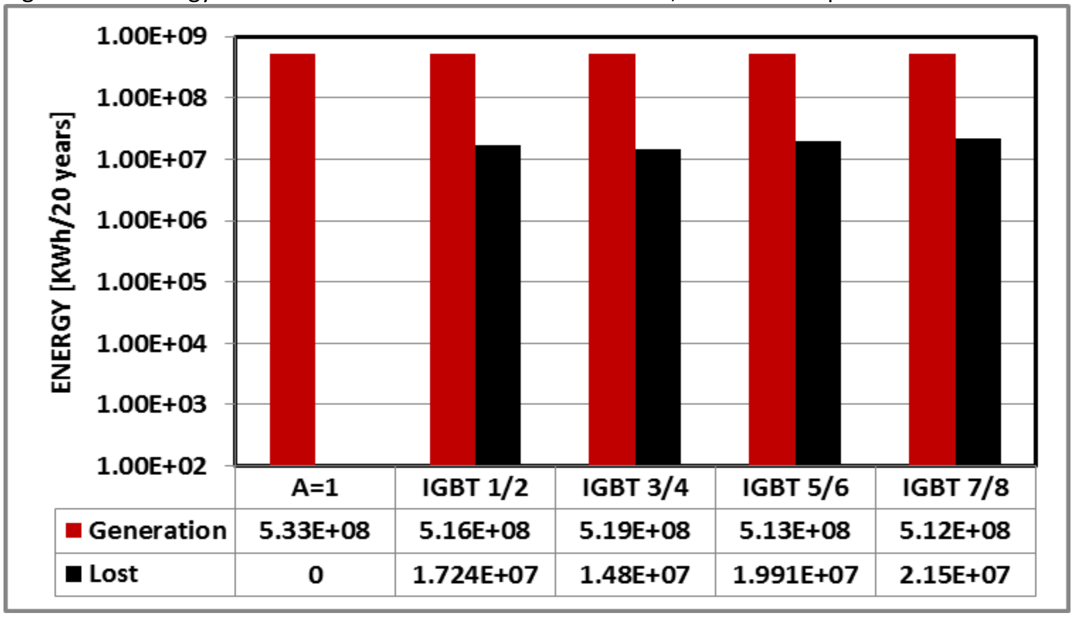

Figure 5-23: Average Availability for Failed Inverter A, Based on 20 Years of Operation

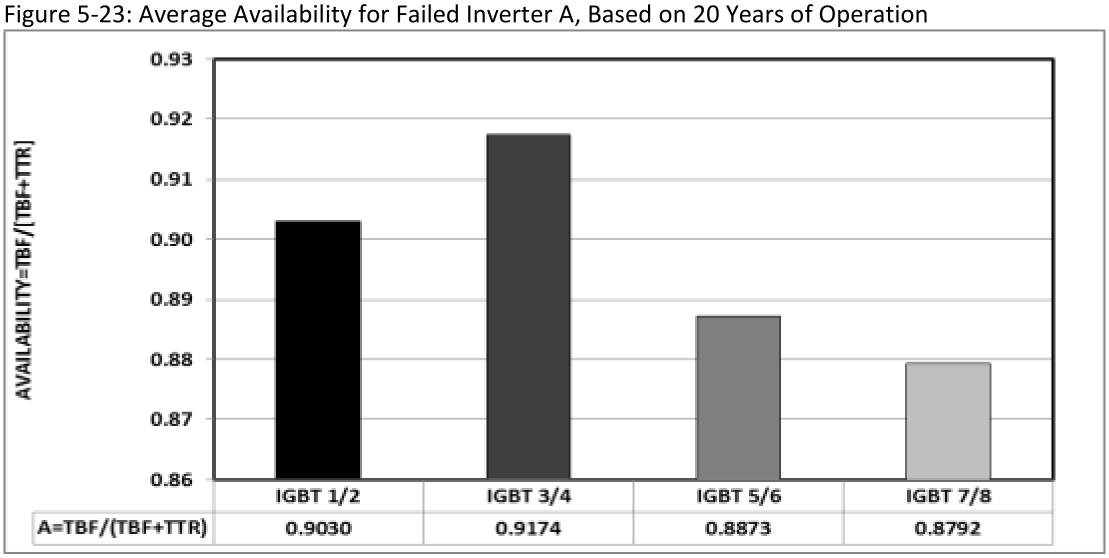

Full Failures: The failed inverter is incapable of converting the DC current from the solar cells to AC for the load. Thus the generation provided by this inverter is 0. Maximum energy is generated with all three inverters (A, B, and C) operational. The loss of generation is based on any one inverter not operating. The failures are based on one or more inverters shut down due to IGBT failures. The tables in Appendix 5-F are based on the fraction of downtime for the four pairs of IGBTs. The results are similar to the partial failure with the exception that, for use in the economic analysis, the failures includes inverters A, B, and C. Figure 5-24 shows the resulting yearly reduction in energy.

Figure 5-24: Energy/Year Lost Due to Inverter Failure

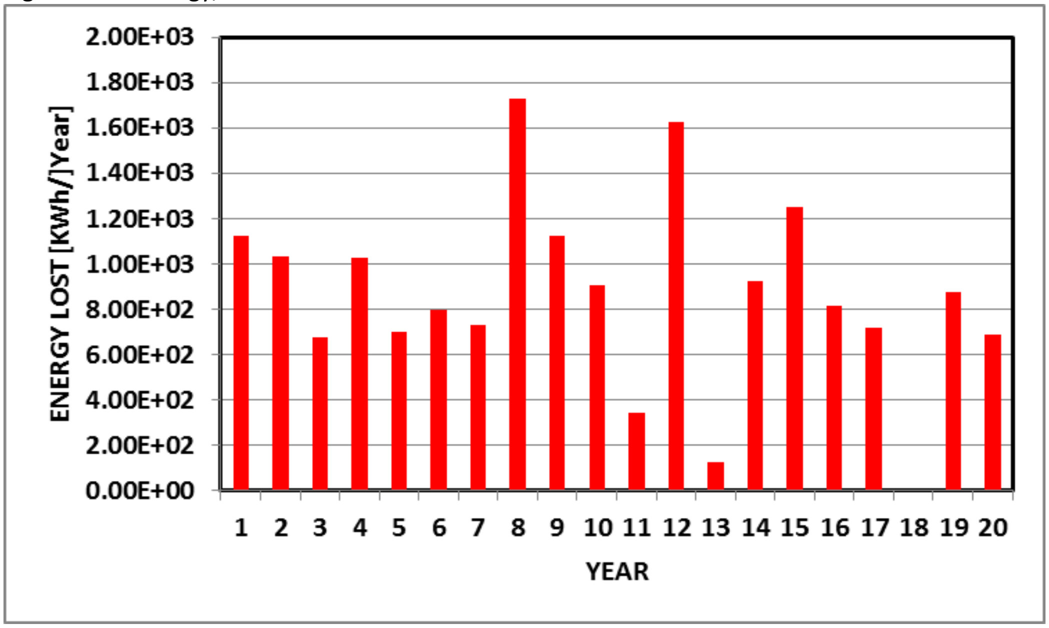

5.10 CONCLUSIONS

The example problem, while having some shortcomings, indicates that even with a high rate of failures, as was assumed for the IGBTs, the impact on performance may be limited. While the costs for this repair/replacement/power purchase may be minimal, they do provide an important answer to the impact on the many parameters that make up the financial predictions that indicate a system is profitable. Effects of the reduction or loss of generation on the installation's financial status are addressed in Section 6.

5.11 REFERENCES: REDUCTION IN KWH DUE TO COMPONENT REPAIR/REPLACEMENT

5-1. PSCAD User Manual. https://pscad.com/resource/File/PSCAD_Manual(1).pdf.

5-2. Kuei, H., et al. "Modeling and Fault Simulation of Photovoltaic Generation Systems Using Circuit-based Model," Sustainable Energy Technologies, Singapore, ICSET-2008.

5-3. Kim, Seul-Ki, et al. "Modeling and Simulation of a Grid-connected PV Generation System for Electromagnetic Transient Analysis," *Solar Energy* v83, n5, 2009: 664-78.

5-4. Xuc, J., et al. "Design of PV Array Model Based on EMTDC/PSCAD," 2009 Asia-Pacific Power & Energy Engineering Conference, Wuhan China: March 29-31, 2009.

5-5. Canmet Energy (Canadian Centre for Mineral and Energy Technology) Report 2010-122 (RP-TEC) 411-IEARES: March 31, 2010.

5-6. Maish A.B., et al. "Photovoltaic System Reliability," Sandia National Laboratories, Proceedings of the 26th IEEE Photovoltaic Specialists Conference, Anaheim, CA: September 29-October 3, 1997.

5-7. Collins, E., et al. "Reliability and Availability Analyses of a Fielded Photovoltaic System," IEEE 978-1-2950, Sept. 2009: 002316-002321.

5-8. Ishaq, Muhammad, "Modeling of Photovoltaic System Using PSCAD," master's thesis, University of Hartford, College of Engineering, Technology, and Architecture: 2011.

5-9. Villalva, M.G., Gazoli, J.R., Ruppert, E.F. "Modeling and Circuit Based Simulation of Photovoltaic Arrays," *Brazilian Journal of Power Electronics*, v14, 2009: 35-45.

5-10. Ristow, A., Begović, M., Rohatgi, A. "Modeling the Effects of Uncertainty and Reliability on the Cost of Energy from PV Systems," 20th European Solar Energy Conference & Exhibition, Barcelona, Spain: June 6-10, 2005.

5-11. Ristow, A.H. "Numerical Modeling of Uncertainty and Variability in the Technology, Manufacturing, and Economics of Crystalline Silicon Photovoltaics," PhD Thesis; Georgia Institute of Technology: August 2008.

5-12. Golder, A.S. "Photovoltaic Generator Modeling for Large Scale Distribution System Studies," master's thesis, Drexel University: 2006.

5-13. Dzimano, G. "Modeling of Photovoltaic Systems," master's thesis, The Ohio State University: 2008.

5-14. Farrett, F.A., Godoy-Simoes, M. "Integration of Alternative Energy Sources,"[18] Wiley-Interscience, 2006: 132-37.

5.15. User's Manual for Typical Meteorological Year (TMY2), NREL, June 1995.

[18] References for Standard Test Conditions (STC) for solar cells

Appendix 5-A: Lincoln Theater Inverter

System Description

The University of Hartford's SMA SB-6000U is a grid-tied string inverter for PV power generating systems developed in Germany by SMA Regel Systems GmbH. String technology means that a number of PV modules are connected in series, i.e., a "string." One or more "strings" then serves as input to one or more inverters, resulting in a flexible building block for PV system design. The SB-6000U represents the classic configuration most popular in the late 1990s and early 2000s: a single-stage, single-phase, 60 Hz transformer-based string inverter. These inverters have high conversion efficiency and power factor (>90%) over a wide operating range, and total harmonic distortion (THD) of less than 5%. Alternative inverter topologies include 3-phase, high frequency transformer-based, transformerless, battery-based off-grid stand-alone, and lower power level inverters with a DC-to-DC converter front end for increased efficiency.

The University of Hartford Lincoln Theater installation (Figure 5A-1) employs three 6000U inverters, each receiving DC power from a PV module array comprising 3 paralleled sets of 7 series-connected modules. Each module consists of 216 individual semi-crystalline silicon cells.

Figure 5-A1: Lincoln Theater One Line Diagram

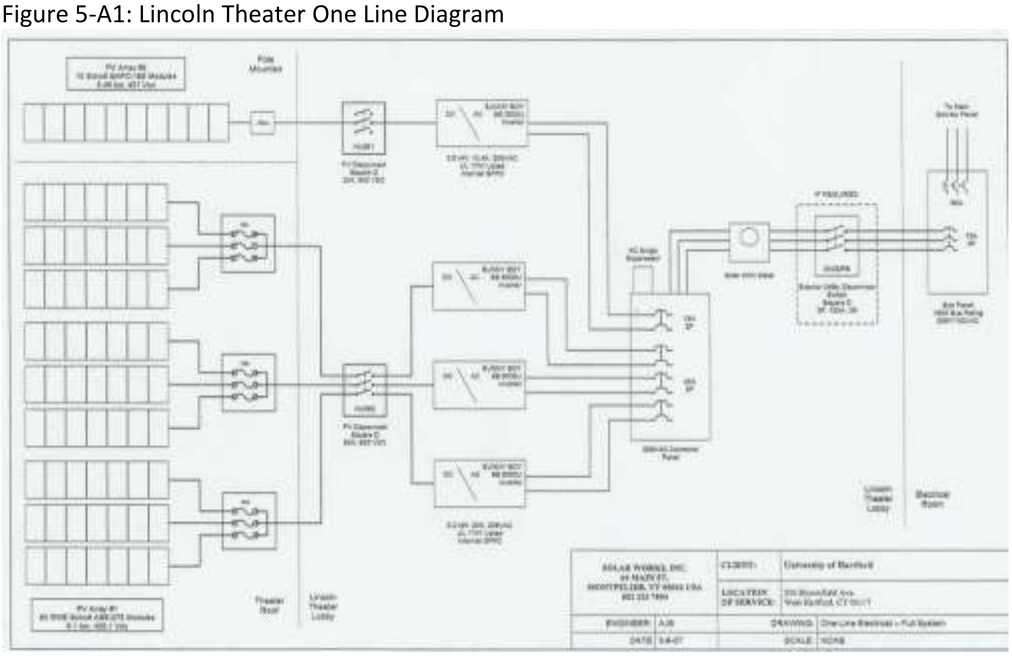

Note that the Lincoln Theater system also includes a fourth inverter (model SB-2500U) for a tracking module array. All four inverter outputs are connected via a "combiner" box to the conventional three-phase Y AC power grid, with manual disconnect breakers on both the AC and DC side. A kWh meter monitors AC energy delivered to the grid.

Basic Functions of Lincoln Theater Inverter

The grid-tied inverter installed at Lincoln Theater performs the following functions:

- Converting DC from the PV array into AC power.
- Tracking MPP on VI curve and adjust PV voltage and current to transfer maximum power.
- Disconnecting the grid in case of grid voltage or frequency changes beyond the coded limits.
- AC and DC automatic and manual disconnection, EMI filtering, cooling, ground fault protection, communication busses, operational data display, and product packaging.

SMA SB-6000U Inverter Specifications

The 6000U inverter is a DC-to-AC grid-tied utility interactive inverter for use with photovoltaic (PV), fuel cell, wind turbine and other sources of DC power. It represents the most common configuration for PV system inverters of lower power level (<30 kW) a decade ago: voltage source, PWM current control output, and low frequency transformer coupling to the grid. Protection functions include anti-islanding and PV ground fault detection and interruption.

Components of SMA SB-6000U Inverter:

The main components of the Lincoln Theater inverter are as follows:
- DC filter
- PWM H-Bridge
- PWM High frequency filter / AC filter
- Line isolation transformer
- Microcontroller
- MPPT
- 208 V line

The SMA SB-6000U inverter system block diagram is shown in Figure 5-A2.

Figure 5-A2: SB-6000 PV Inverter Schematic

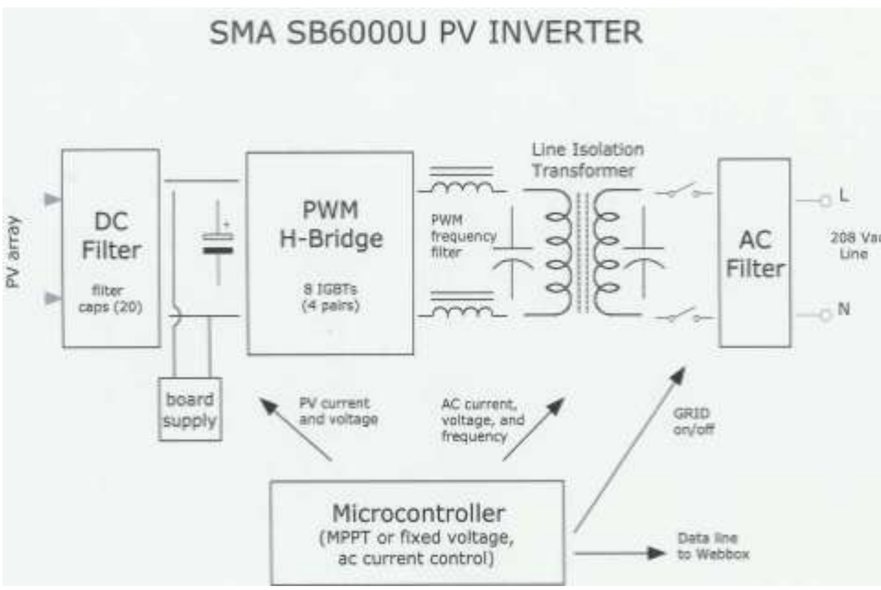

Basic component functions are described below (see Figure 5-A3).

DC filter: The function of the DC filter is to smooth the DC voltage and current at the input of the inverter for inverter operation. The filter is composed of 20 aluminum electrolytic capacitors of 300 microfarads each in a series-parallel combination, giving a total capacitance of 3000 microfarads. In the layout photo below, they are the blank cylindrical cans at the top of the inverter. In PSCAD, the DC filter is modeled simply as one capacitor of 3000 uF, component A.

PWM H-bridge: The function of the PWM H-bridge is to convert DC into AC by turning on the IGBT switches at the right instant. The inverter uses 4 pairs of IGBTs in a single phase H-bridge configuration. These high-speed IGBTs, manufactured by IXYS Corporation, have a maximum rating of 600 V and 55 A. They are shown at the top center in the layout photo as component B.

PWM high frequency/AC filters: The purpose of the PWM frequency filter and AC filter is to remove the high switching frequency components from the PWM H-bridge output, resulting in a smooth sine wave of AC current while providing isolation between the DC circuits and the AC grid. These components consist of high frequency inductors and high quality, non-electrolytic (film) capacitors. They are shown in the lower left of the layout photo as component C**.**

Line isolation transformer: Isolation between the PV system and the grid is required by safety operating standards and codes. The SB-6000U inverter employs a low frequency (60 Hz) transformer to provide isolation between the DC system and the grid. This prevents any DC current from flowing to the grid and causing power distribution transformers to overheat or large harmonic currents to occur. The isolation transformer for the inverter is behind the circuit board and is labeled as component D although it cannot be seen in the photo. The transformer leads and terminal connections, however, can be seen at center right.

Microcontroller: The SB-6000U employs a microcontroller (microprocessor or DSP) with algorithms to control the PWM switching, the interaction with the grid, voltage and current levels, controls and events required by safety standards and codes, the MPPT function, and communication/data monitoring.

208 VAC Line Output: The Lincoln Theater PV 17kW fixed array system comprises three single-phase 6000U 6kW inverters and a 2.5kW tracking inverter that connect independently to the 208 Y three-phase grid load. The tracking array inverter output sums into one of the three phases. A three-phase unit is thus formed from single-phase inverters, which is technically no different from a single three-phase inverter. A "power balancer" is not employed as it is not necessary for relatively small systems of fewer than 30kW.

Figure 5-A3: SMA SB-6000U Layout in Lincoln Theater

A=DC-filter capacitors
B=IGBT PWM H-bridge
C=Microcontroller board
D=AC line isolation transformer (rear of chassis)
E=High frequency PWM filters

The inverter is a self-commutated type, and the control strategy is current control. The PV DC side is treated as a voltage source and the bridge IGBTs are switched on and off, according to the current control scheme, providing a sine wave current at the output. The SB-6000U employs a ramp comparison current control scheme with a switching frequency of 16kHz. Figure 5-A4 shows the H-bridge model in PSCAD.

Figure 5-A4: PSCAD Simple Inverter Model

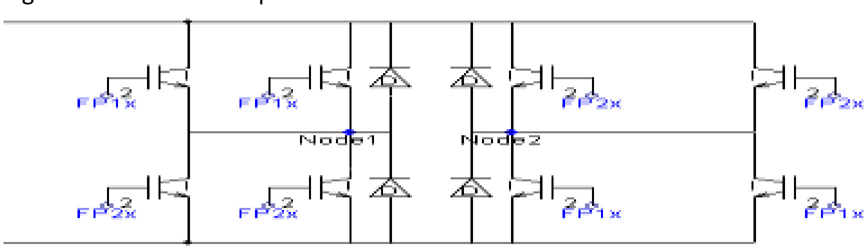

Figure 5-A5 shows the final single-phase PSCAD model for the complete PV system at Lincoln Theater.

Figure 5-A5: PSCAD Model of Lincoln Theater GCPVS

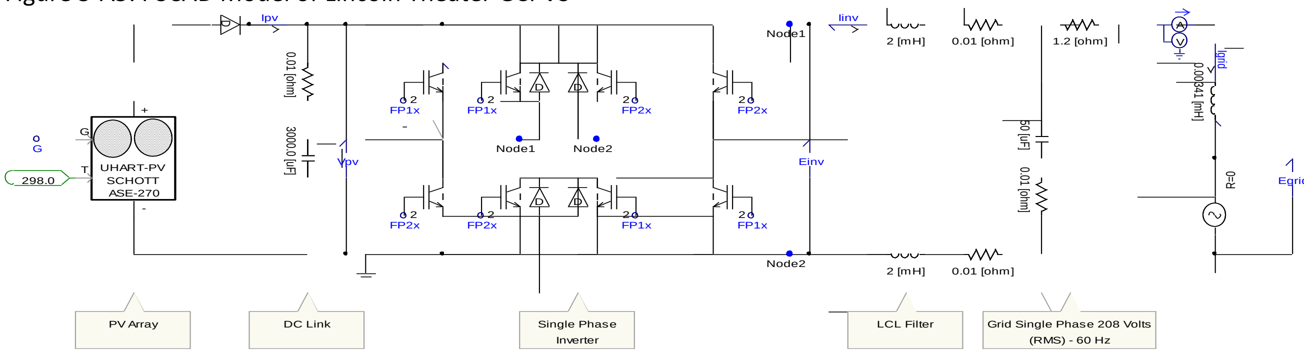

Appendix 5-B: PSCAD Model of Lincoln Theater GCPVS

Photovoltaic Module Manufacturer-Provided Parameters

Basic parameters provided by the manufacturer are short current I_{SC} , open circuit voltage V_{OC} , current at maximum power point I_{mp} ,voltage at maximum power point V_{mp} , temperature coefficient of current K_I , temperature coefficient of voltage K_V , and number of cell in module N_{cell} . These values are provided at standard test conditions of 1000 (W/m^2) and 298 K. Several curves provided by the manufacturer can be used to adjust the values of other parameters such as R_S and R_{SH} .

.

Figure 5-B1: Solar Cell Equivalent Circuit

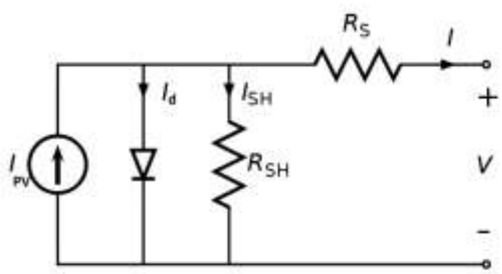

Source: http://upload.wikimedia.org/wikipedia/commons/9/92/SolarCell-EquivalentCircuit.PNG

Based on the circuit in Figure 5-B1, the equation for the output current and voltage produced by the solar cell is:

$$I = I_{PV} - I_o \exp\left\{\frac{(qV + IR_s)}{n\ K\ T} - 1\right\} - \frac{V + I_{SH}R_s}{R_{SH}} \tag{5B.1}$$

Where:

I_{PV} is the photovoltaic current generated due to the sunlight

I_O is the reverse saturation current

I_{SH} is current through the shunt resistor

q is charge on electron($1.63\ x\ 10^{-19}\ C$)

K is Boltzmann's constant $(1.38\ x\ 10^{-23} m^2 kg\ s^{-2} K^{-1})$

T is temperature in Kelvin

n is ideality factor and its value is usually between 1 and 1.5

Modeling of PV Module Using Manufacturer-Provided Parameters

The value of R_{SH} is very high and this value is ignored for simplification. Since the value of R_S is very small and R_{SH} is very high, it is assumed that the short circuit current I_{SC} is equal to I_{PV} , the PV current. Assumptions are: $I_{sc} \approx I_{PV}$ and $R_{SH} \approx \infty$.

Using these assumptions, equation 5B.1 can be expressed as equation 5B.2:

$$I = N_P I_{PV} - N_P I_o \exp\left\{\frac{(qV + IR_s)}{N_S N_{cell} n\ K\ T} - 1\right\} \tag{5B.2}$$

PV current I_{PV} varies linearly with the incident insolation. It also varies with the change in temperature of the solar cell and is shown by equation 5B.3:

$$I_{PV} = I_{SC-ref} + K_I(T - T_{ref}).\frac{G}{G_{ref}} \tag{5B.3}$$

Where I_{SC} is the short circuit current at STC provided by the manufacturer, K_I is the temperature coefficient of current, T_{ref} is the reference temperature (298 K), G_{ref} is the reference insolation of 1000 $\frac{W}{m^2}$. T and G are the working temperature and insolation of the PV module.

The reverse saturation current I_O can be expressed as equation 5B.4:

$$I_O = I_{O-ref}\left(\frac{T_{ref}}{T}\right)^3 \exp\left\{\frac{qE_g}{nK}\left(\frac{1}{T_{ref}} - \frac{1}{T}\right)\right\} \tag{5B.4}$$

I_{o-ref} is not provided by the manufacturer but can be found by solving equation 5B.4 and setting $V = V_{OC} = \mathbf{0}$, $I = \mathbf{0}$ and $I_{PV} \approx I_{SC-ref}$, equation 5B.5:

$$I_{O-ref} = \frac{I_{SC-ref}}{\exp\left(\frac{qV_{OC-ref}}{N_{cell} n\, K\, T}\right) - \mathbf{1}} \tag{5B.5}$$

This can be further improved by including the parameters K_I and K_V and thus the reverse saturation current can be found by equation 5B.6:

$$I_{O-ref} = \frac{I_{sc-ref} + K_I\boldsymbol{\Delta}T}{\exp\left(\frac{qV_{OC-ref} + K_V\boldsymbol{\Delta}T}{N_{cell} n\, K\, T}\right) - \mathbf{1}} \tag{5B.6}$$

To solve the implicit equation 5B.2 at a working temperature and insolation:

- I_{PV} can be found using equation 5B.3
- I_O can be found using equation 5B.4

Parameters at STC are provided by the manufacturer and can be used in equations 5B.3 and 5B.4. Since equation 5B.2 is a nonlinear implicit equation, the electric circuit is used to find its numerical solution. This is shown in Figure 5-B2:

Figure 5-B2: Electric Solution for Equation 5B.2

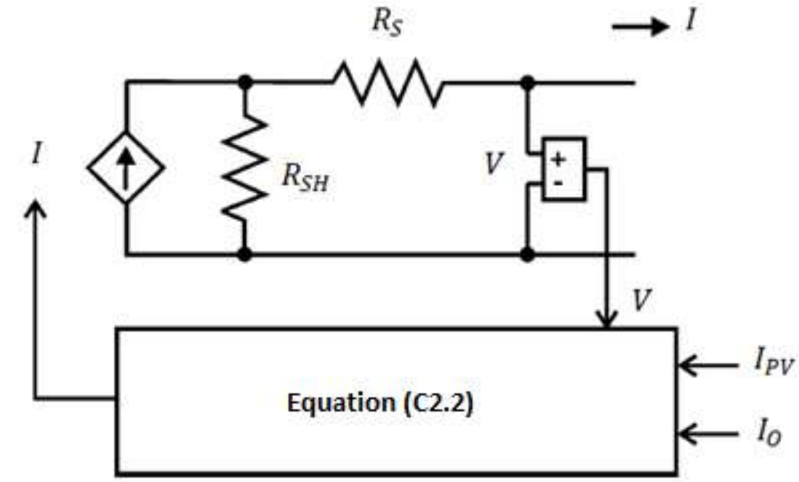

I_{PV} and I_O are calculated using equations 5B.3 and 5B.4 for working temperature and insolation. The measured value of voltage V from the circuit and calculated values of I_{PV} and I_O are inserted in equation 5B.2 to find the value of I. The value of I is the magnitude of the externally controlled current source. This is performed in PSCAD and shown in Figure 5-B2.

Figure 5-B2: Numerical Solution of Equation 5B.2 Using PSCAD

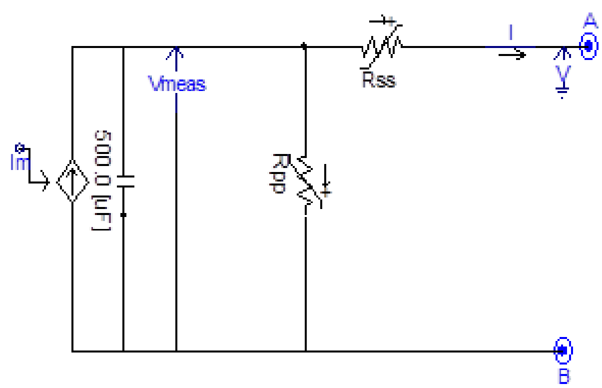

To verify the model, the manufacturer-provided parameters of the SCHOTT ASE-270 module are used in the model and compared with the manufacturer-provided curves at different insolation and temperatures. The PV module model is connected across a variable resistor that exponentially increases with time. The modeled circuit is simulated and voltage vs. current and voltage vs. power curves are obtained.

Table 5-B1 shows the electrical parameters for the SCHOTT ASE-270 module and VI characteristics curves for the single module.

Table 5-B1: Electrical Parameters of SCHOTT ASE-270 Module

Power (Max)	P_p (watts)	260 W	270 W
Voltage at maximum power point	V_p (volts)	48.7 V	49.1 V
Current at maximum power point	I_p (amps)	5.3 A	5.5 A
Open circuit voltage	V_{OC} (volts)	60.8 V	61.3 V
Short circuit current	I_{SC} (amps)	5.9 A	6.1 A

These electrical parameters are tested at STC. Irradiance and temperature levels are 1000 W/m2 and 298 K, respectively.

Table 5-B2: Cell Temperature Coefficients

Power	T_K (P_p)	-0.47 % / ^{o}C
Open circuit voltage	T_K (V_{OC})	-0.38 % / ^{o}C
Short circuit current	T_K (I_{SC})	+10 % / ^{o}C

Figure 5-B4: Manufacturer VI Characteristics Curves of SCHOTT ASE-270 Module

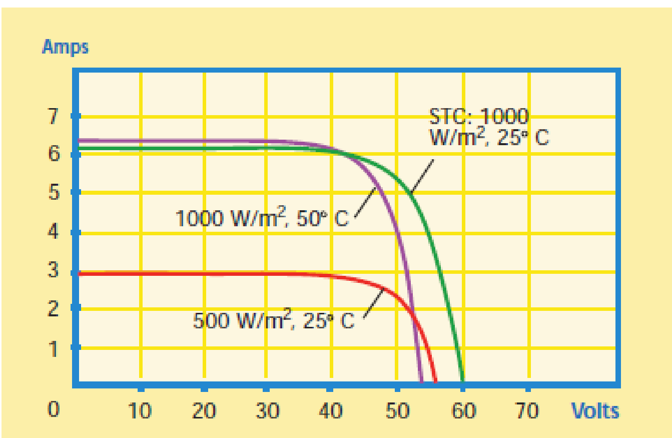

Source: http://energyoptions-wind.com/docs/Schott%20ASE_270.pdf

Simulations

Figure 5-B5: PV Module Equations Implementation

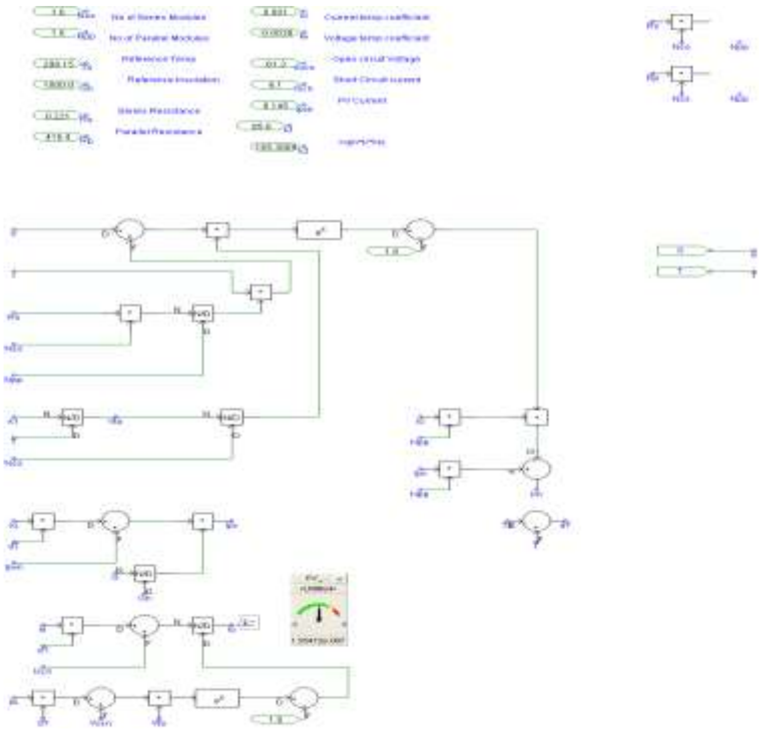

Figure 5-B6: PSCAD VI Characteristics of SCHOTT ASE-270 Module at Various Irradiances

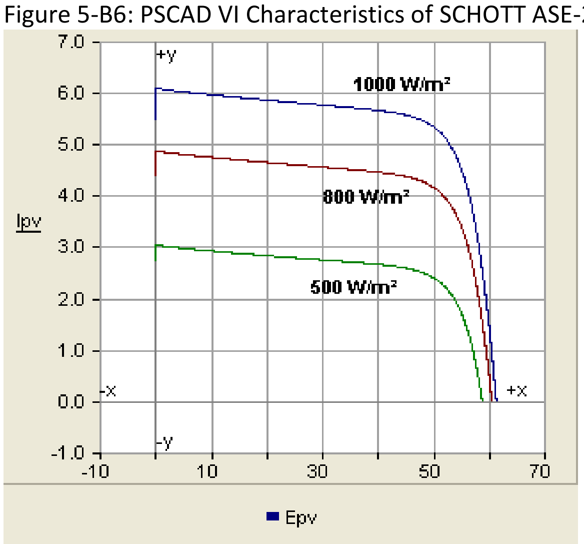

Figure 5-B7: PV Power at Various Irradiances

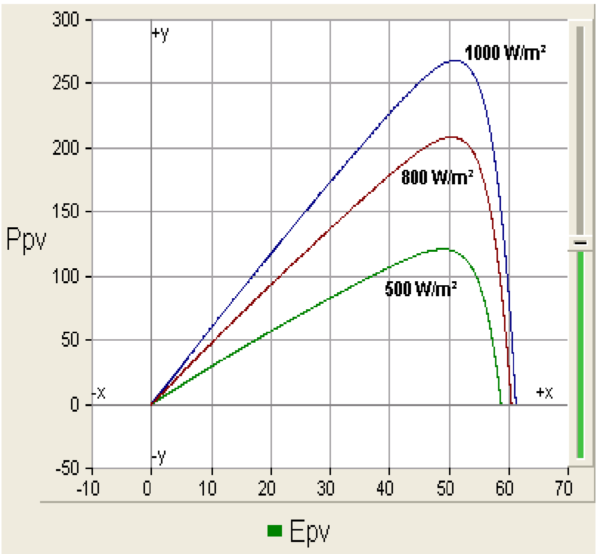

MPPT Algorithms

MPP can be tracked by controlling the duty cycle of the DC-DC converter or DC-AC inverter that is the interface between the PV and the load. It is important to vary the duty cycle and to know in which direction to vary it. Manual tracking of the duty cycle is not possible, but computer programs using certain algorithms can automatically track the correct duty cycle for the DC-DC converter. Some of the popular algorithms designed for this purpose are:

- Perturb and observe method
- Incremental conductance method
- Constant voltage method

Perturb and Observe: The perturb and observe method is the most commonly used algorithm for MPP tracking. It is widely employed in commercial PV products because of its simplicity. The PV tracker controller increases its reference voltage (or duty) and then perturbs the actual output power. If the output power is increased, then it keeps updating the reference voltage (or duty) until the output power starts to decrease. At this point the reference voltage or duty is decremented.

Figure 5-B8 shows the flowchart for this method. Operating values of voltage V(k) and current I(k) are measured and the present power calculated P(k). The present power is compared with the sampled power previously calculated. If power is positive the algorithm keeps the next voltage change (or duty change) in the same direction as the previous one; otherwise, it reverses the voltage change (or duty change) direction.

Figure 5-B8: Flowchart of Perturb and Observe Algorithm

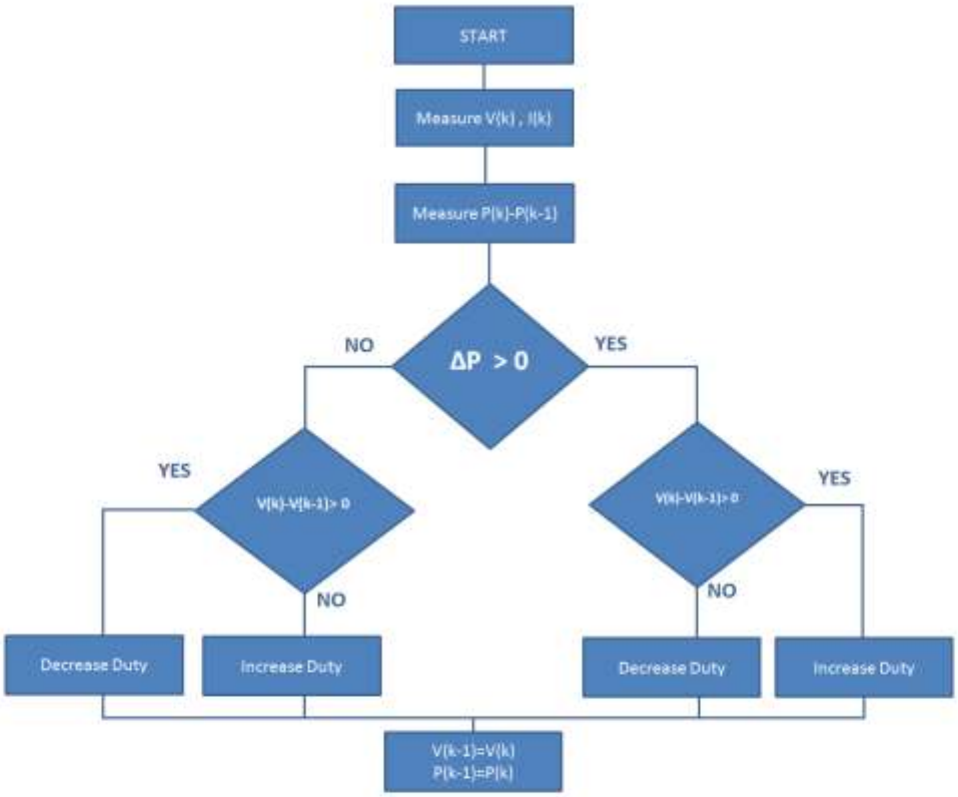

Incremental Conductance: In the incremental conductance algorithm, we find the derivative of PV output power with respect to output voltage. The dP/dV is evaluated and the algorithm keeps checking this value and changes the duty cycle such that dP/dV=- I/V = 0. This is the point at which maximum power is transferred. If dP/dV is greater than zero, it means the PV is operating to the left of the MPP. If dP/dV is less than zero, it means the PV is operating to the right of the MPP. This method holds an advantage over the perturb and observe method since it is fast and does not oscillate around MPP. However, the method could experience instability due the involvement of the derivative.

Figure 5-B9: Derivative of PV Power with Respect to Output Voltage

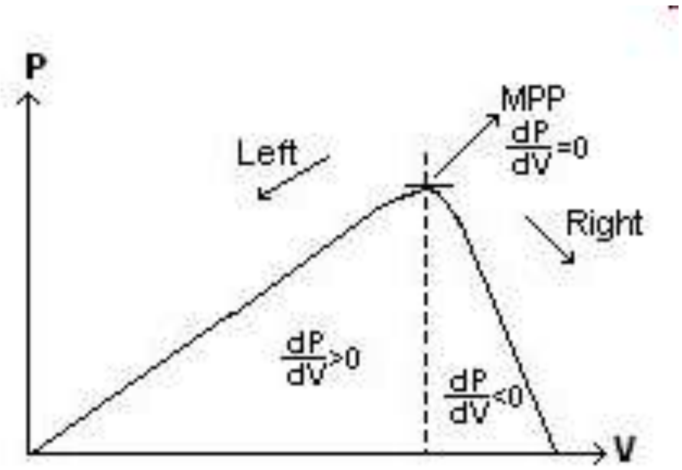

Source: http://students.sabanciuniv.edu/~erhandemirok/class_files/image004.jpg

Figure 5-B10: Flowchart for the Incremental Conductance Algorithm

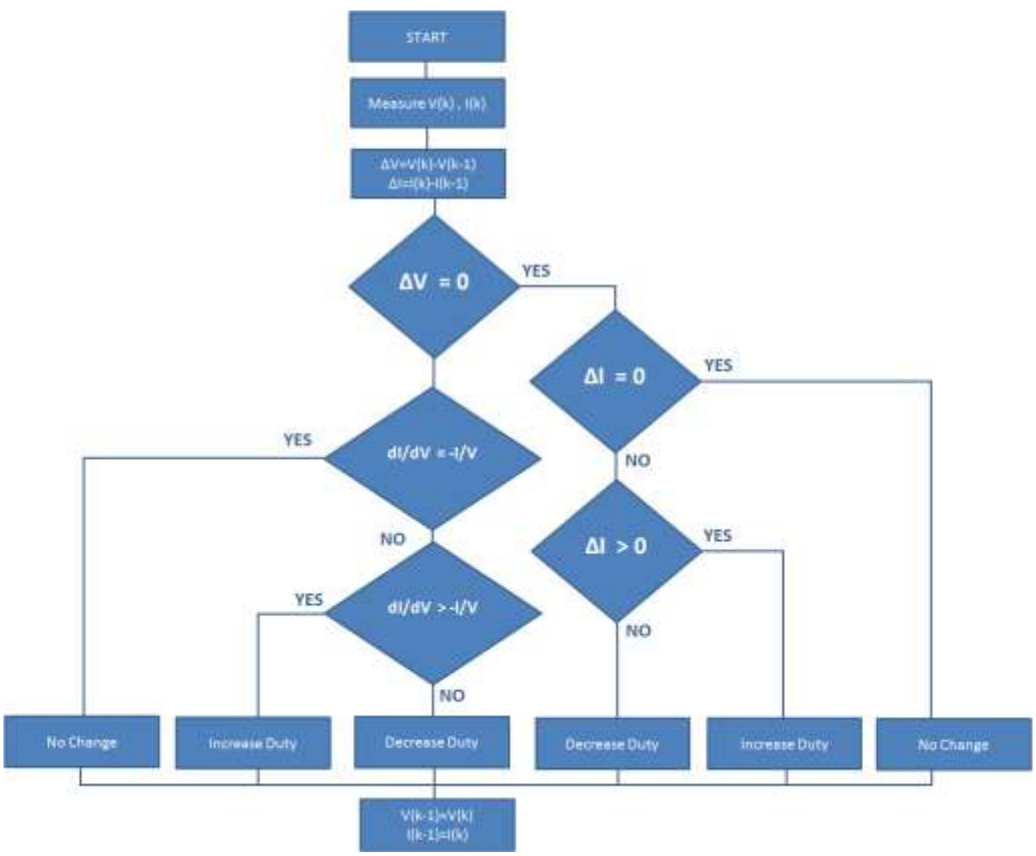

Constant Voltage Method: The constant voltage method is the simplest and most accurate simulation. In software or in simulation, the value of the open circuit voltage is calculated at a certain insolation and temperature given by the equation 5B.7:

$$V_{OC} = \ln\left(\frac{I_{pv}}{I_0} + 1\right) * \left(\frac{nKTN_{SS}}{q}\right) \qquad (5B.7)$$

In real practice, the PV module terminals are open circuited for a few seconds and the open circuit voltage is measured. It is assumed that the maximum voltage at which the maximum power occurs is 78% of the open circuit voltage.

Conclusion

For optimum power transfer, the system needs to track the MPP as the solar irradiance and ambient temperature change to provide a dynamic maximum reference current injected into the grid.

Appendix 5-C: Models, Performance, and Control of the Lincoln Theater GCPVS

Figure 5-C1: Lincoln Theater One Line Diagram

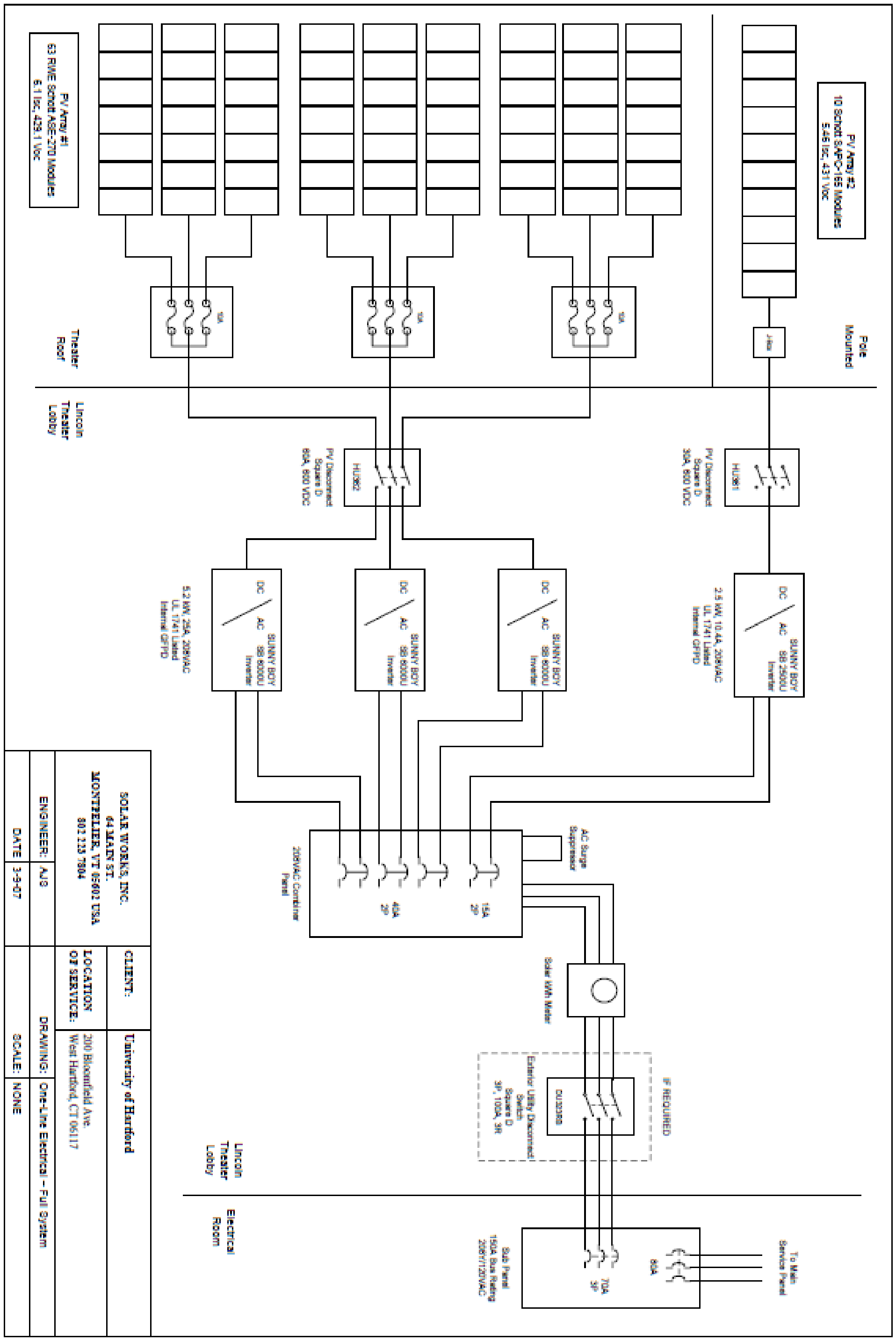

Voltage-Current (VI) Characteristics of the SCHOTT ASE-270 module:

Figure 5-C2: PSCAD VI Characteristics of SCHOTT ASE-270 Module at Various Irradiances

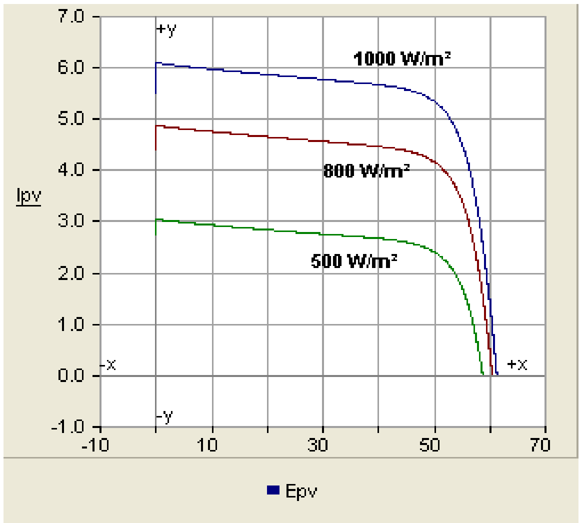

Figure 5-C3: PV Power at Various Irradiances

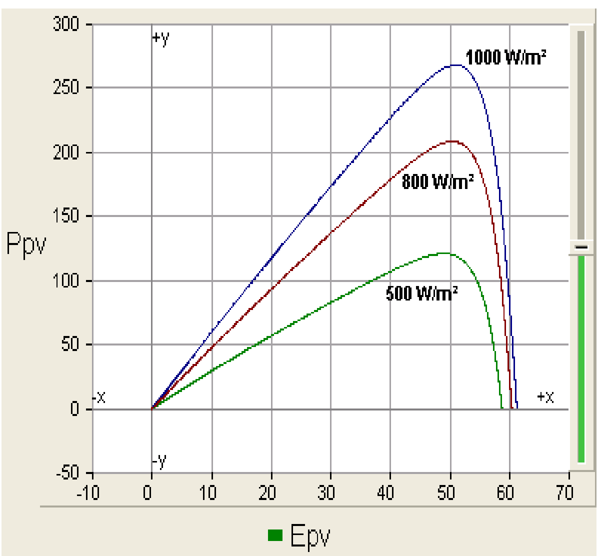

PSCAD Module Subsystem Implementation

Figure 5-C.4: Equations Implementation in PSCAD Photovoltaic Module

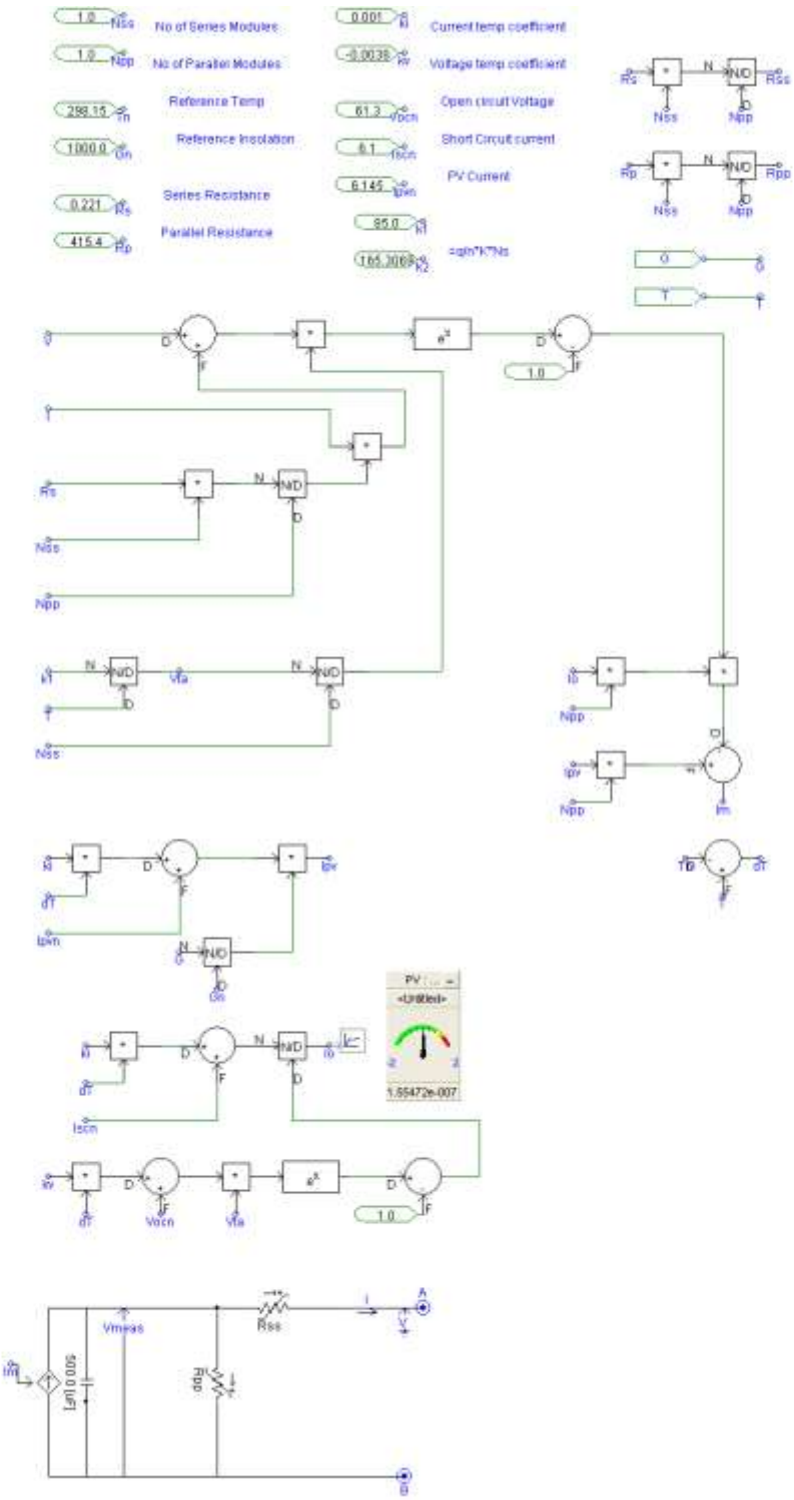

PSCAD Arrays-Inverter-Load

Figure 5-C5: PSCAD Schematic of PV-Array-Inverter and Grid

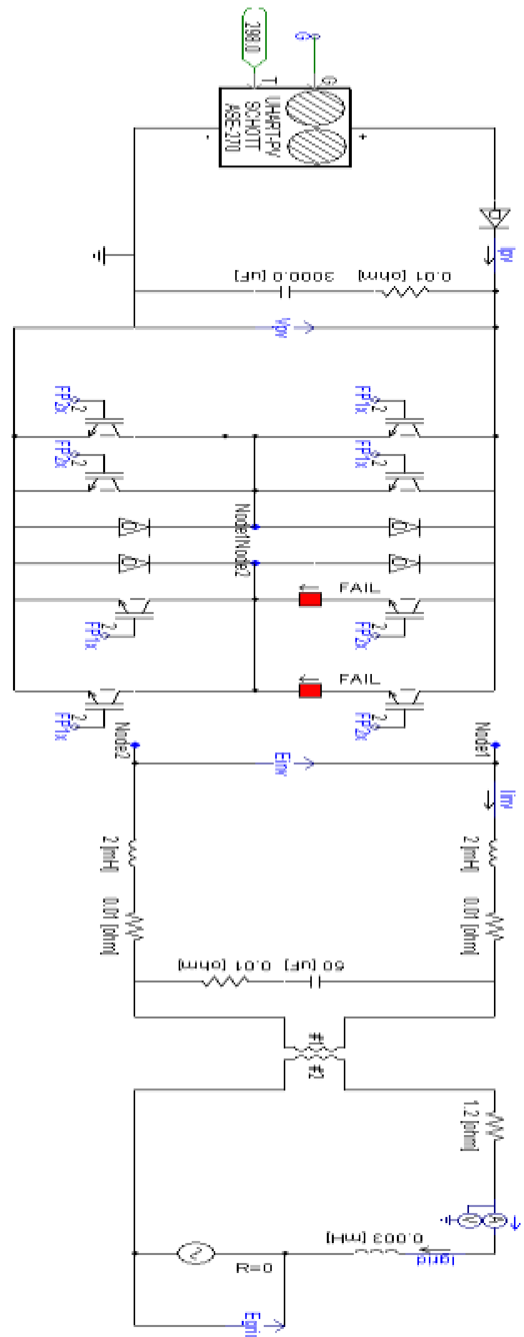

Figure 5-C6: Current Control PWM Scheme in PSCAD

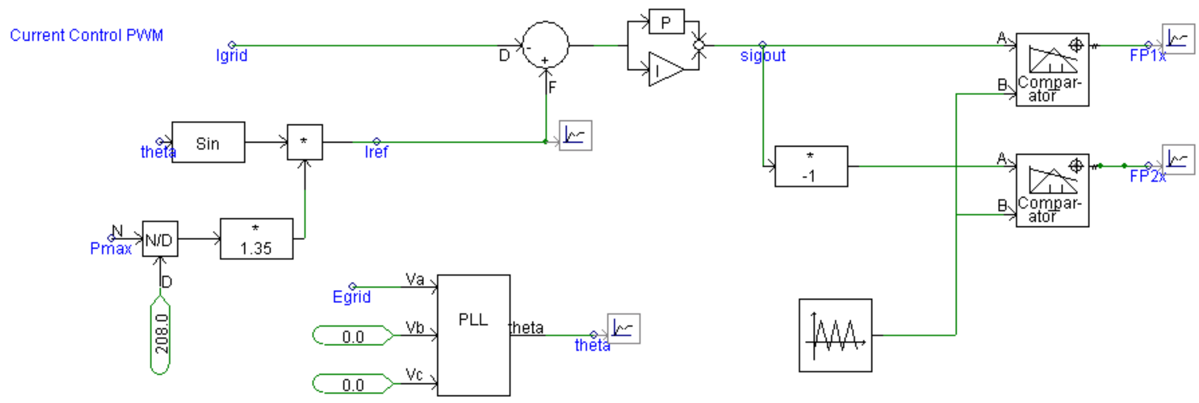

Figure 5-C.7: Maximum Power Point Module in PSCAD

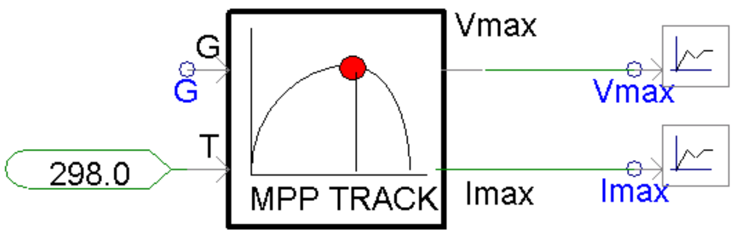

Figure 5-C.8: MPPT Subsystem

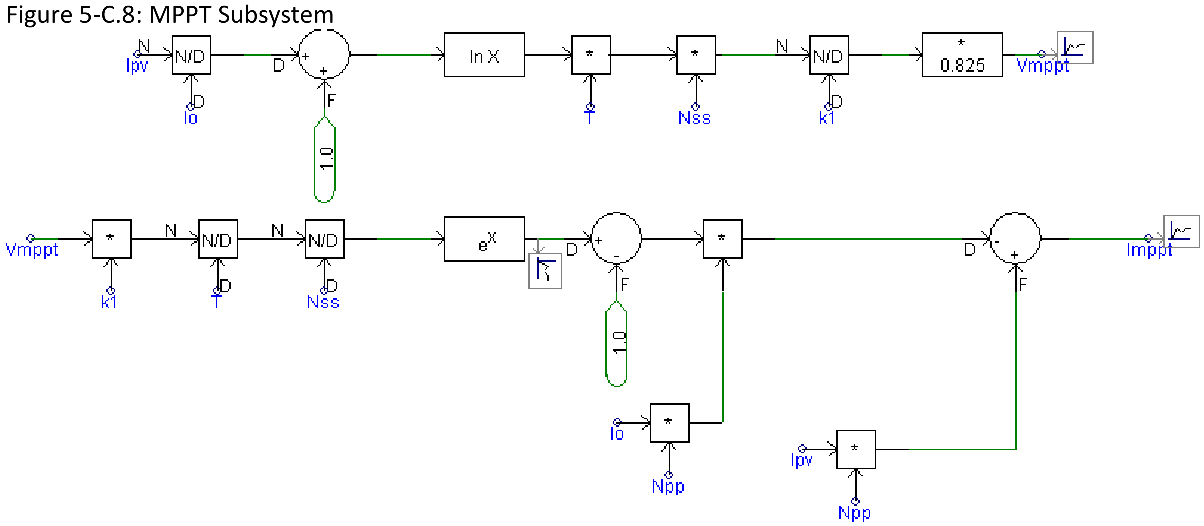

Figure 5-C.9: SCHOTT ASE-270 Electrical Parameters

Current/voltage characteristics with dependence on irradiance and module-temperature.

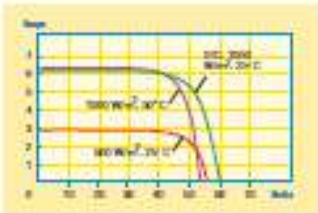

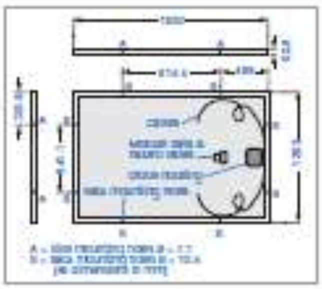

Electrical data

The electrical data applies to standard test conditions (STC):
Irradiance at the module level of 1,000 W/m² with spectrum AM 1.5
and a cell temperature of 25° C.

Power (max.)	P_p (watts)	260 W	270 W
Voltage at maximum-power point	V_p (volts)	48.7 V	49.1 V
Current at maximum-power point	I_p (amps)	5.3 A	5.5 A
Open-circuit voltage	V_{oc} (volts)	60.8 V	61.3 V
Short-circuit current	I_{sc} (amps)	5.9 A	6.1 A

The rated power may only vary by ± 2% and all other electrical parameters by ±10%.
NOCT-value (800 W/m², 20° C, 1m/sec.) = 45° C.

Dimensions and weights

Length mm (in)	1,892.3 (74.5")
Width mm (in)	1,282.7 (50.5")
Weight kg (lbs)	46.6 ± 2 kg (107 ± 5lbs)
Area	2.43 sq meters (26.13 ft sq)

Characteristic data

Solar cells per module	216
Type of solar cell	Semi-crystalline solar cells (EFG process), 10x10 cm²
Connections	10 AWG single conductor, stranded copper with Multi-Contact connector. Junction box comes with 10 built-in bypass diodes.

Cell temperature coefficients

Power	T_K (P_p)	- 0.47 % / °C
Open-circuit voltage	T_K (V_{oc})	- 0.38 % / °C
Short-circuit current	T_K (I_{sc})	+ 0.10 % / °C

Limits

Maximum system voltage	600 VDC U.S.
Operating module temperature	-40 to +90° C
UL certified design load	50 PSF
Equivalent wind resistance	Wind speed of 192 km/h (120 mph)

The right is reserved to make technical modifications. For detailed product drawings and specifications please contact SCHOTT Solar or an authorized reseller.

Certifications and Warranty

The ASE-270-DGF/50 has been independently certified to IEC 61215, IEEE 1262, and UL 1703 (Class A Fire rating). The ASE-270-DGF/50 comes with a 20 year power warranty (see terms and conditions for details).

http://energyoptions-wind.com/docs/Schott%20ASE_270.pdf

Appendix 5-D: Values of MTBF and MTTR Effects on Reduction in Generation

Table 5-D1: Figure Overview

FIGURE	TITLE	MTBF (Days)	Beta_F	MTR(Days)	Beta_R	Impact	OPERATING STATE
5-D1	1 IGBT	90	1	10	1	1	No Failure
5-D2	1 IGBT	100	1	15	1	1	Failure-No power
5-D3	1 IGBT	110	1	5	1	1	Multiple Failures

Graph	Information	Units
1	Watt hours accumulated over one year	KWhr/year
2	Energy injected at the corresponding insolation	Energy Injected
3	Current into the grid at the corresponding insolation	Igrid
4	Input insolation	KW/m^2
5	Loss of energy due to repair	Availability = 0

Figure 5-D1: Watt-Hours/Year, Energy, Irradiance, Current vs. Time, Availability

MTBF=90 and MTTR=10

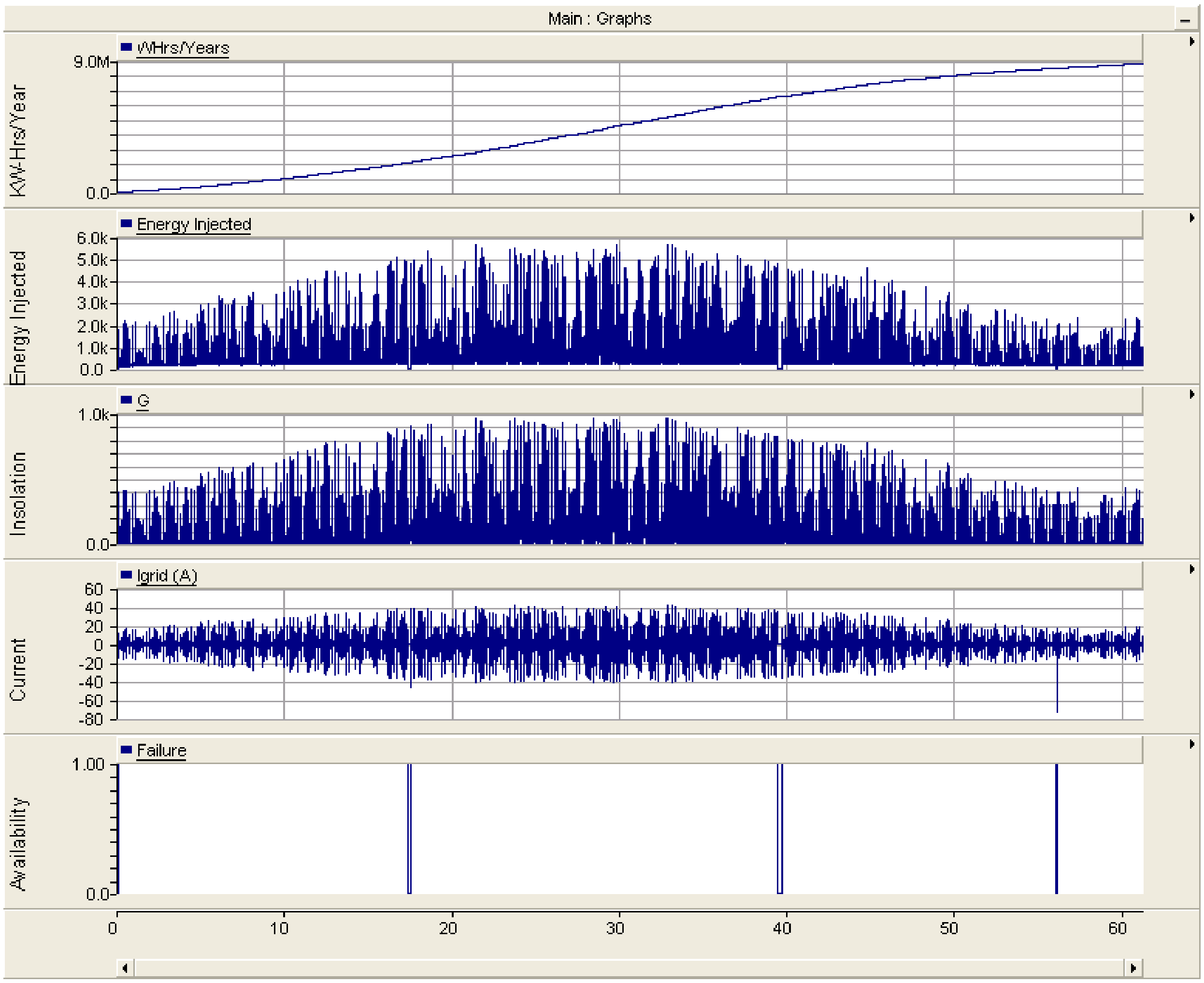

Figure 5-D2: Watt-Hours/Year, Energy, Irradiance, Current vs. Time, Availability

MTBF=100 and MTTR=15

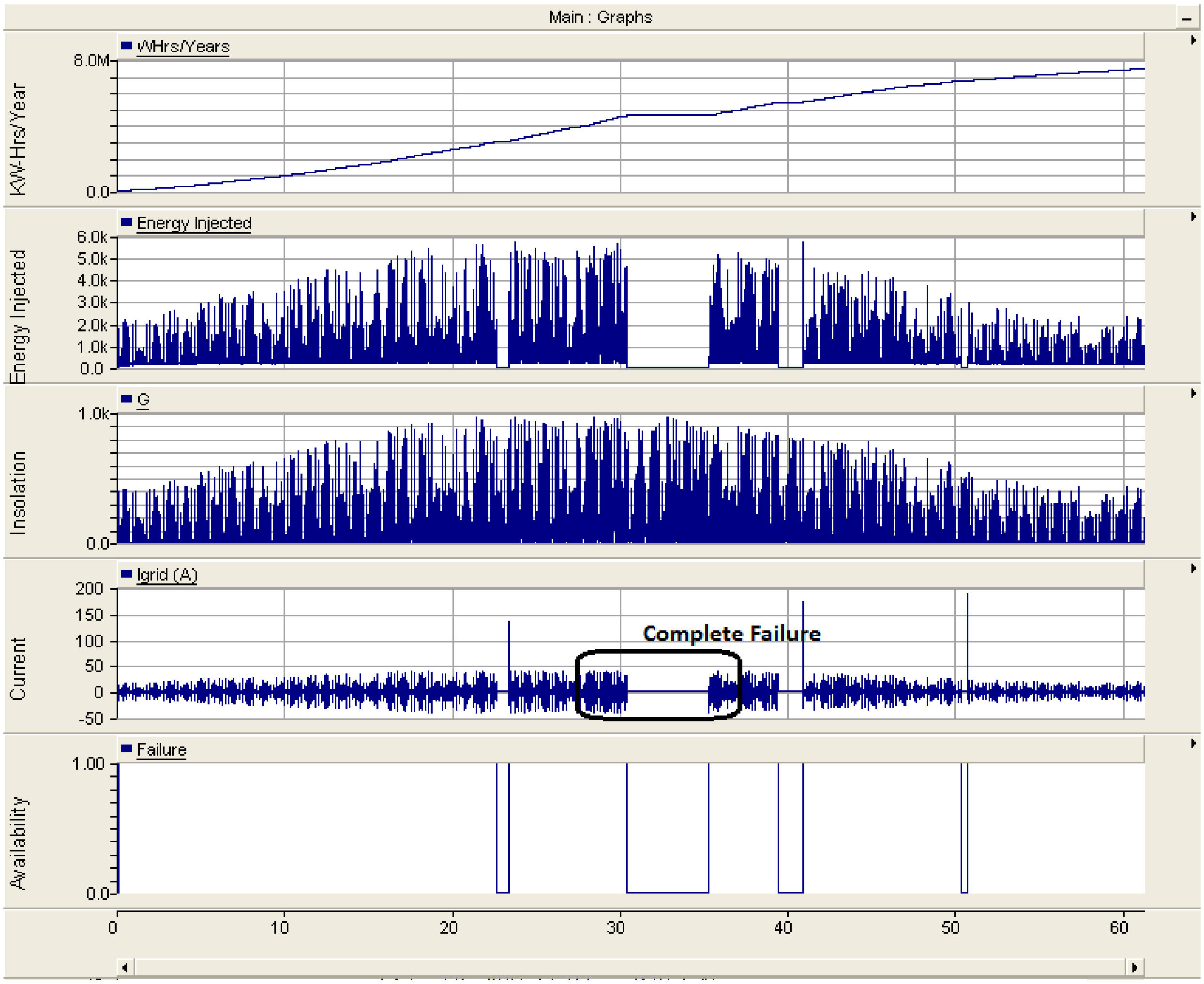

Figure 5-D3: Watt-Hours/Year, Energy, Irradiance, Current vs. Time, Availability

MTBF=110 and MTTR=5

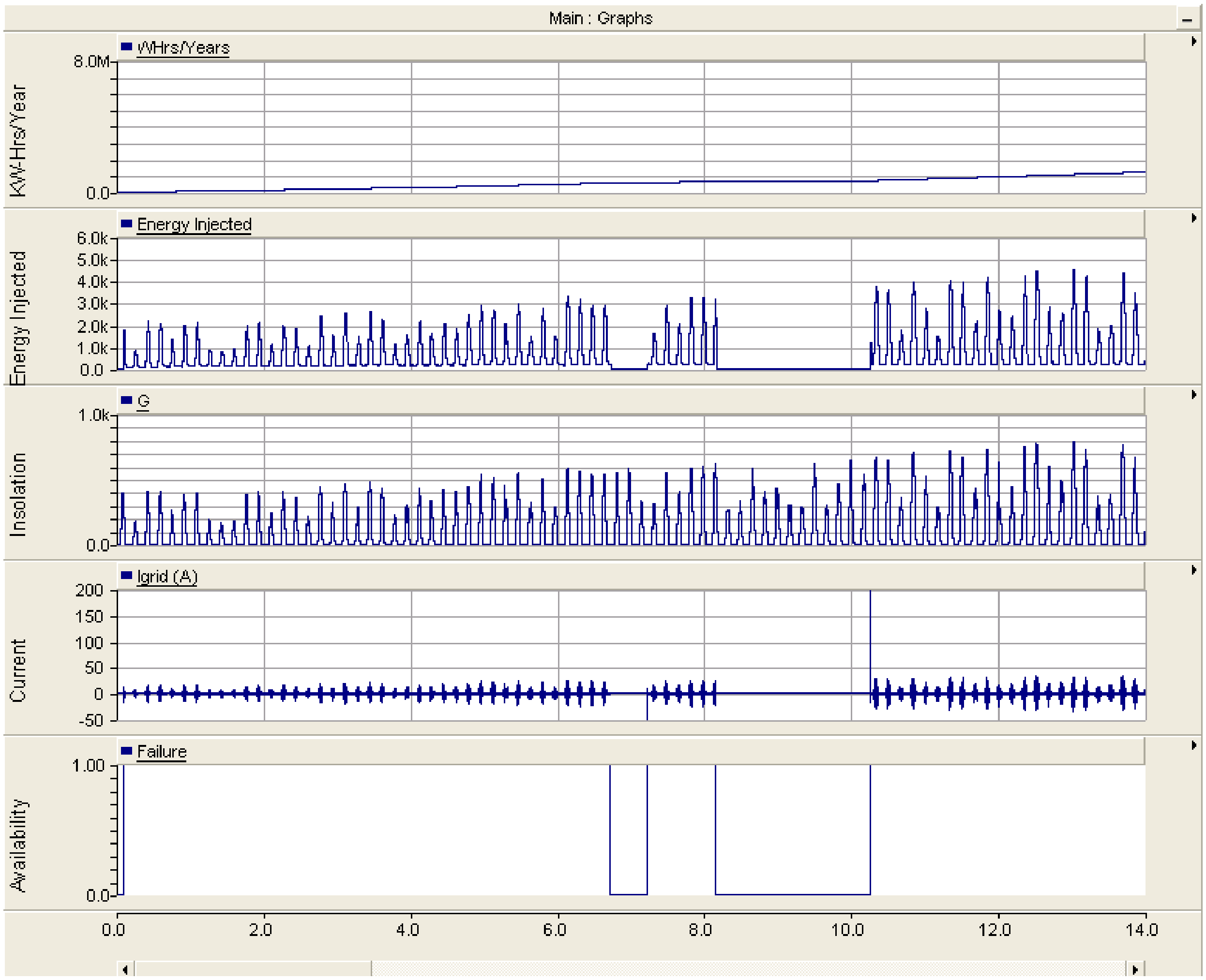

Appendix 5-E: DC-AC Frequency Control

An inverter converts DC into AC. The inverter can be either single-phase or three-phase. Figure 5-E1 shows a single-phase inverter topology. It contains 4 switches (IGBTs) in which two IGBTs are connected in series with each other. The switching devices can be BJTs, MOSFETs or IGBTs. The inverter also contains 4 freewheeling diodes across each IGBT. The purpose of the freewheeling diodes is to provide a path for the load current to flow when the two IGBTs in series are turned off.

The main function of the inverter is to give a pure as possible sinusoidal output in the desired phase, voltage, and frequency.

Figure 5-E1: Simple DC to AC inverter Schematic

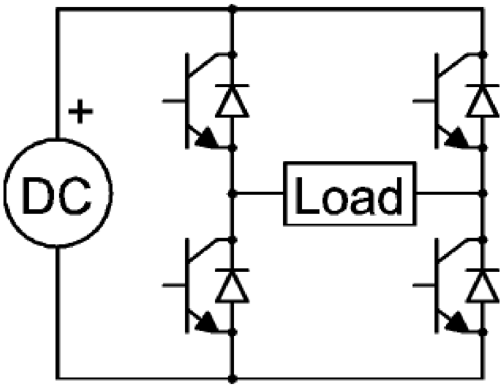

Source: http://upload.wikimedia.org/wikipedia/en/2/2c/H-bridge_inverter_cjc.png

Pulse Width Modulation (PWM): In pulse width modulation, a triangular wave of high frequency is compared with a sinusoidal wave of the same frequency as the output voltage of the inverter. The result is a gating signal as shown in Figure 5-E2.

Figure 5-E2: Sinusoidal Pulse Width Modulation

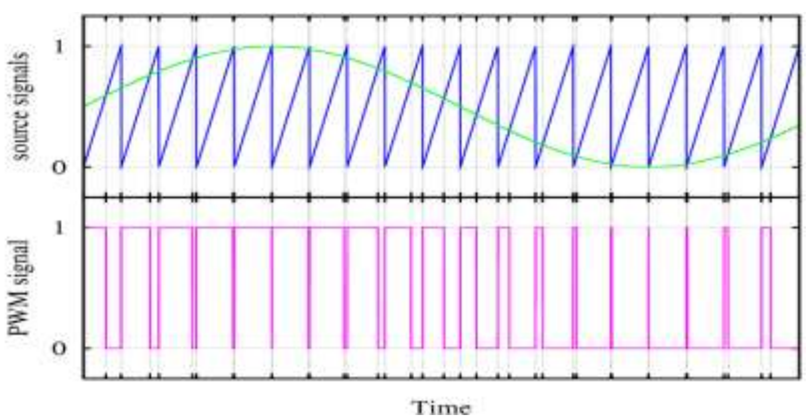

Source: http://upload.wikimedia.org/wikipedia/commons/7/72/Pwm.svg

The peak value of the reference sine wave is A_{sine} and the peak value of the reference triangular wave is A_{tri} with a desired frequency of f_0. The frequency of the reference sinusoid has to be the same as the desired output voltage. The modulation m_a index is the ratio between the amplitude of the reference sinusoidal wave and the amplitude of the rectangular wave.

$$m_a = \frac{A_{sine}}{A_{tri}}$$

During the positive half-cycle of the modulating signal, switches S1 and S4 are turned on and the other two switches are turned off and +Vac voltage appears across the load. During the 2nd half-cycle, switches S2 and S3 are turned on while switches S1 and S4 turn off and –Vac voltage appears across the load. This output is shown in Figure 5-E3.

Figure 5-E3: Inverter Output Using PWM

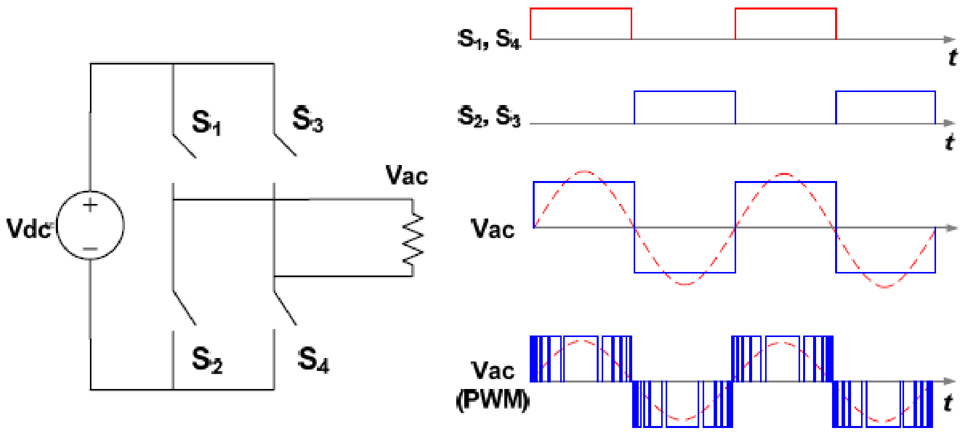

Source: http://upload.wikimedia.org/wikipedia/commons/8/8e/PWM%2C_3-level.svg

Phase Locked Loop (PLL): In the case of grid-connected inverters and a current control scheme, the injected current must be in phase with the grid voltage. This is achieved by a phase locked loop (PLL). PSCAD provides a built-in phase locked loop module to find the phase of the signal and use it for different calculations.

Filter Design: Since the output of the H-Bridge inverter using a PWM technique is a square wave, a filter is needed to reduce the harmonics and get a nearly sinusoidal signal from the inverter. Figure 5-E4 shows the circuit for a low-pass filter. Using a low-pass filter with an appropriate cut-off frequency removes the harmonic content present at the output wave from the inverter. The resulting wave is nearly sinusoidal. The cut-off frequency of a LC filter is given as:

$$f = \frac{1}{2\pi\sqrt{LC}}$$

Figure 5-E4: A Simple LC Filter

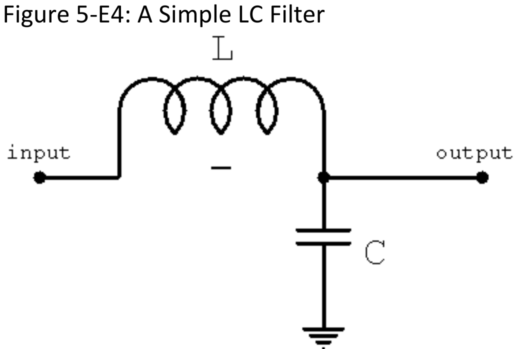

Source: http://static.rcgroups.net/forums/attachments/3/1/1/7/8/2/t3522975-37-thumb-LC-lowpass.gif

Appendix 5-F: Energy Loss and Availability

Table 5-F1A: Partial Failures, Energy Loss, and Availability: IBGTs 1/2

Energy Generation, Energy Loss & Availability Due to Failure of IGBT 1/2 (pair)						
Year	Energy Loss			Availability		
	Watts Hours / Year	Watts Hours / Year	Energy Loss	TTR	TBF	Availability
	Without Failure	With Failure	KW-Hours	Repair=0	Failure=1	A=TBF/[TBF+TTR]
Year 1	8.89E+06	8.57E+06	320.38	1131	7629	0.87
Year 2	8.89E+06	8.46E+06	425.63	1020	7740	0.88
Year 3	8.89E+06	8.55E+06	335.08	665	8095	0.92
Year 4	8.89E+06	8.41E+06	477.22	1013	7747	0.88
Year 5	8.89E+06	8.57E+06	321.08	690	8070	0.92
Year 6	8.89E+06	8.50E+06	388.7	784	7976	0.91
Year 7	8.89E+06	8.69E+06	194.78	717	8043	0.92
Year 8	8.89E+06	8.23E+06	660.5	1704	7056	0.81
Year 9	8.89E+06	8.49E+06	396.34	1109	7651	0.87
Year 10	8.89E+06	8.40E+06	490.06	894	7866	0.9
Year 11	8.89E+06	8.73E+06	162.48	338	8422	0.96
Year 12	8.89E+06	8.17E+06	719.83	1603	7157	0.82
Year 13	8.89E+06	8.83E+06	58.76	126	8634	0.99
Year 14	8.89E+06	8.41E+06	483.11	909	7851	0.9
Year 15	8.89E+06	8.26E+06	626.26	1233	7527	0.86
Year 16	8.89E+06	8.53E+06	354.55	801	7959	0.91
Year 17	8.89E+06	8.63E+06	261.22	710	8050	0.92
Year 18	8.89E+06	8.89E+06	0	0	8760	1
Year 19	8.89E+06	8.52E+06	371.88	860	7900	0.9
Year 20	8.89E+06	8.52E+06	367.59	679	8081	0.92
TOTALS	**1.78E+08**	**1.70E+08**	**7.42E+03**	**1.70E+04**	**1.58E+05**	**0.903**
Units	**Watts Hours**	**Watts Hours**	**KWatt Hours**	**Hours**	**Hours**	**Availability**

Table 5-F1B: Partial Failures, Energy Loss, and Average Availability, IGBTs 1/2

Energy Generation, Loss & Average Availability due to Failure of IGBT 1/2; 20 Years of Operation					
INVERTERS	**A**	**B**	**C**	**Total**	**Units**
Operating	1.78E+05	1.78E+05	1.78E+05	5.33E+05	KWatt-hrs
Failed IGBT	1/2				-
Availability	0.903	1	1	*	-
Generation	1.61E+05	1.78E+05	1.78E+05	5.16E+05	KWatt-hrs
Lost Generation	1.72E+04	0.00E+00	0.00E+00	1.72E+04	KWatt-hrs

5-F1C: Partial Failures, Energy Loss, and Availability: IBGTs 3/4

Energy Generation, Energy Loss & Availability due to Failure of IGBT 3/4 (pair)						
Year	Energy Loss			Availability		
	Watts Hours	Watts Hours	Energy Loss	TTR	TBF	Availability
	Without Failure	With Failure	KW-Hours	Repair=0	Failure=1	A=TBF/[TBF+TTR]
Year 1	8.89E+06	8.76E+06	130.59	257	8503	0.97
Year 2	8.89E+06	8.57E+06	317.99	778	7982	0.91
Year 3	8.89E+06	8.21E+06	679.33	1444	7316	0.84
Year 4	8.89E+06	8.81E+06	79.37	173	8587	0.98
Year 5	8.89E+06	8.67E+06	217.9	414	8346	0.95
Year 6	8.89E+06	8.61E+06	282.65	703	8057	0.92
Year 7	8.89E+06	8.46E+06	434.08	1336	7424	0.85
Year 8	8.89E+06	8.89E+06	0	0	8760	1
Year 9	8.89E+06	8.88E+06	12.28	86	8674	0.99
Year 10	8.89E+06	8.57E+06	317.3	728	8032	0.92
Year 11	8.89E+06	8.29E+06	599.6	1488	7272	0.83
Year 12	8.89E+06	8.44E+06	451.2	1280	7480	0.85
Year 13	8.89E+06	8.15E+06	742.32	1387	7373	0.84
Year 14	8.89E+06	8.17E+06	718.96	1452	7308	0.83
Year 15	8.89E+06	8.66E+06	233.5	465	8295	0.95
Year 16	8.89E+06	8.62E+06	267.32	515	8245	0.94
Year 17	8.89E+06	8.72E+06	173.69	454	8306	0.95
Year 18	8.89E+06	8.51E+06	380.61	948	7812	0.89
Year 19	8.89E+06	8.89E+06	0	0	8760	1
Year 20	8.89E+06	8.62E+06	272	571	8189	0.93
TOTALS	**1.78E+08**	**1.71E+08**	**6.31E+03**	**1.45E+04**	**1.61E+05**	**0.917**
Units	**Watts Hours**	**Watts Hours**	**KWatt Hours**	**Hours**	**Hours**	**Availability**

5-F1D: Partial Failures, Energy Loss, and Average Availability, IGBTs 3/4

Energy Generation, Loss & Average Availability due to Failure of IGBT 3/4; 20 Years of Operation					
INVERTERS	**A**	**B**	**C**	**Total**	**Units**
Operating	1.78E+05	1.78E+05	1.78E+05	5.33E+05	KWatt-hrs
Failed IGBT	3/4				-
Availability	0.917	1	1		-
Generation	1.63E+05	1.78E+05	1.78E+05	5.19E+05	KWatt-hrs
Lost Generation	1.48E+04	0.00E+00	0.00E+00	1.48E+04	KWatt-hrs

5-F1E: Partial Failures, Energy Loss, and Availability: IBGTs 5/6

Energy Generation, Energy Loss & Availability due to Failure of IGBT 5/6 (pair)						
Year	Energy Loss			Availability		
	Watts Hours	Watts Hours	Energy Loss	TTR	TBF	Availability
	Without Failure	With Failure	KW-Hours	Repair=0	Failure=1	A=TBF/[TBF+TTR]
Year 1	8.89E+06	8.45E+06	435.18	1397	7363	0.84
Year 2	8.89E+06	8.74E+06	146.59	296	8464	0.97
Year 3	8.89E+06	8.54E+06	344.76	1038	7722	0.88
Year 4	8.89E+06	8.82E+06	69.46	166	8594	0.98
Year 5	8.89E+06	8.51E+06	380.42	857	7903	0.9
Year 6	8.89E+06	7.65E+06	1238.54	3115	5645	0.64
Year 7	8.89E+06	8.05E+06	840.54	1895	6865	0.78
Year 8	8.89E+06	8.57E+06	323.75	1009	7751	0.88
Year 9	8.89E+06	8.38E+06	507.5	1158	7602	0.87
Year 10	8.89E+06	8.38E+06	509.76	1198	7562	0.86
Year 11	8.89E+06	8.87E+06	22.6	60	8700	0.99
Year 12	8.89E+06	8.59E+06	296.38	696	8064	0.92
Year 13	8.89E+06	8.75E+06	144.06	435	8325	0.95
Year 14	8.89E+06	8.53E+06	361.45	741	8019	0.92
Year 15	8.89E+06	8.65E+06	236.89	519	8241	0.94
Year 16	8.89E+06	8.54E+06	351.7	1374	7386	0.84
Year 17	8.89E+06	8.35E+06	536.27	1176	7584	0.87
Year 18	8.89E+06	8.89E+06	0	0	8760	1
Year 19	8.89E+06	8.36E+06	529.59	1102	7658	0.87
Year 20	8.89E+06	8.36E+06	529.59	1338	7422	0.85
TOTALS	**1.78E+08**	**1.70E+08**	**7.81E+03**	**1.96E+04**	**1.56E+05**	**0.888**
Units	**Watt Hours**	**Watt Hours**	**KW hours**	**Hours**	**Hours**	**Availability**

5-F1F: Partial Failures, Energy Loss, and Average Availability, IGBTs 5/6

Energy Generation, Loss & Average Availability due to Failure of IGBT 5/6; 20 Years of Operation					
INVERTERS	A	B	C	Total	Units
Operating	1.78E+05	1.78E+05	1.78E+05	5.33E+05	KWatt-hrs
Failed IGBT	5/6				-
Availability	0.888	1	1		-
Generation	1.58E+05	1.78E+05	1.78E+05	5.13E+05	KWatt-hrs
Lost Generation	1.99E+04	0.00E+00	0.00E+00	1.99E+04	KWatt-hrs

5-F1G: Partial Failures, Energy Loss, and Availability: IBGTs 7/8

Energy Generation, Energy Loss & Availability due to Failure of IGBT 7/8 (pair)						
Year	Energy Loss			Availability		
	Watts Hours	Watts Hours	Energy Loss	TTR	TBF	Availability
	Without Failure	With Failure	KW-Hours	Repair=0	Failure=1	A=TBF/[TBF+TTR]
Year 1	8.89E+06	8.23E+06	657.7	1613	7147	0.82
Year 2	8.89E+06	8.48E+06	404.61	844	7916	0.9
Year 3	8.89E+06	8.36E+06	530.09	1162	7598	0.87
Year 4	8.89E+06	8.07E+06	822.66	2002	6758	0.77
Year 5	8.89E+06	8.48E+06	408.68	1184	7576	0.86
Year 6	8.89E+06	8.65E+06	243.39	626	8134	0.93
Year 7	8.89E+06	7.81E+06	1082.12	2706	6054	0.69
Year 8	8.89E+06	8.34E+06	546.34	1315	7445	0.85
Year 9	8.89E+06	8.61E+06	282.09	702	8058	0.92
Year 10	8.89E+06	8.58E+06	308.91	815	7945	0.91
Year 11	8.89E+06	8.64E+06	253.62	626	8134	0.93
Year 12	8.89E+06	7.58E+06	1304.29	3144	5616	0.64
Year 13	8.89E+06	8.63E+06	262.09	823	7937	0.91
Year 14	8.89E+06	8.89E+06	0.06	0	8760	1
Year 15	8.89E+06	8.70E+06	185.15	833	7927	0.9
Year 16	8.89E+06	8.78E+06	113.95	525	8235	0.94
Year 17	8.89E+06	8.56E+06	327.53	810	7950	0.91
Year 18	8.89E+06	8.87E+06	14.76	72	8688	0.99
Year 19	8.89E+06	8.72E+06	167.06	658	8102	0.92
Year 20	8.89E+06	8.57E+06	316.3	696	8064	0.92
TOTALS	**1.78E+08**	**1.70E+08**	**8.23E+03**	**2.12E+04**	**1.54E+05**	**0.879**
Units	**Watts Hours**	**Watts Hours**	**KWatt Hours**	**Hours**	**Hours**	**Availability**

5-F1H: Partial Failures, Energy Loss, and Average Availability, IGBTs 7/8

Energy Generation, Loss & Average Availability due to Failure of IGBT 7/8; 20 Years of Operation					
INVERTERS	**A**	**B**	**C**	**Total**	**Units**
Operating	1.78E+05	1.78E+05	1.78E+05	5.33E+05	KWatt-hrs
Failed IGBT	7/8				-
Availability	0.879	1	1		-
Generation	1.56E+05	1.78E+05	1.78E+05	5.12E+05	KWatt-hrs
Loss of Generation	2.15E+04	0.00E+00	0.00E+00	2.15E+04	KWatt-hrs

Table 5-F2: Energy Generation and Loss Based on Failure Categories

	Generation based on Inverter Operation & Failure Categories					Lost Generation Based on Failure		
	No Failures	1 Failure	Sometimes Fail	Always Fail		None	Sometime	Always
Inverters	1+2+3	2+3	(2+3)+1*[1-(DT/365)] Time	(1+2+3)*[1-(DT/365)]Time		Lost	Lost energy	Lost
YEAR	KWh/yr	KWh/yr	KWh/yr	Down Time	KWh/yr	KWh/yr	KWh/yr	KWh/yr
1	2.67E+04	1.78E+04	2.55E+04	12.64%	2.33E+04	0.00E+00	1.12E+03	3.37E+03
I2	2.67E+04	1.78E+04	2.56E+04	11.65%	2.36E+04	0.00E+00	1.04E+03	3.11E+03
3	2.67E+04	1.78E+04	2.60E+04	7.59%	2.46E+04	0.00E+00	6.75E+02	2.02E+03
4	2.67E+04	1.78E+04	2.56E+04	11.58%	2.36E+04	0.00E+00	1.03E+03	3.09E+03
5	2.67E+04	1.78E+04	2.60E+04	7.88%	2.46E+04	0.00E+00	7.00E+02	2.10E+03
6	2.67E+04	1.78E+04	2.59E+04	8.96%	2.43E+04	0.00E+00	7.97E+02	2.39E+03
7	2.67E+04	1.78E+04	2.59E+04	8.19%	2.45E+04	0.00E+00	7.28E+02	2.18E+03
8	2.67E+04	1.78E+04	2.49E+04	19.45%	2.15E+04	0.00E+00	1.73E+03	5.19E+03
9	2.67E+04	1.78E+04	2.55E+04	12.66%	2.33E+04	0.00E+00	1.13E+03	3.38E+03
10	2.67E+04	1.78E+04	2.58E+04	10.21%	2.39E+04	0.00E+00	9.07E+02	2.72E+03
11	2.67E+04	1.78E+04	2.63E+04	3.86%	2.56E+04	0.00E+00	3.43E+02	1.03E+03
12	2.67E+04	1.78E+04	2.50E+04	18.30%	2.18E+04	0.00E+00	1.63E+03	4.88E+03
13	2.67E+04	1.78E+04	2.65E+04	1.44%	2.63E+04	0.00E+00	1.28E+02	3.84E+02
14	2.67E+04	1.78E+04	2.57E+04	10.38%	2.39E+04	0.00E+00	9.23E+02	2.77E+03
15	2.67E+04	1.78E+04	2.54E+04	14.09%	2.29E+04	0.00E+00	1.25E+03	3.76E+03
16	2.67E+04	1.78E+04	2.59E+04	9.14%	2.42E+04	0.00E+00	8.13E+02	2.44E+03
17	2.67E+04	1.78E+04	2.59E+04	8.11%	2.45E+04	0.00E+00	7.21E+02	2.16E+03
18	2.67E+04	1.78E+04	2.67E+04	0.00%	2.67E+04	0.00E+00	0.00E+00	0.00E+00
19	2.67E+04	1.78E+04	2.58E+04	9.82%	2.40E+04	0.00E+00	8.73E+02	2.62E+03
20	2.67E+04	1.78E+04	2.60E+04	7.75%	2.46E+04	0.00E+00	6.89E+02	2.07E+03
Average=	**2.67E+04**	**1.78E+04**	**2.58E+04**	**9.68%**	**2.41E+04**	**0.00E+00**	**8.61E+02**	**2.58E+03**
Units=	**KWh/yr**	**KWh/yr**	**KWh/yr**	**%**	**KWh/yr**	**KWh/yr**	**KWh/yr**	**KWh/yr**

6 ECONOMIC ANALYSIS

6.1 INTRODUCTION

The University of Hartford has a grid-connected photovoltaic system (GCPVS) on the roof of the Lincoln Theater that provides some portion of the theater's energy needs. The economic model discussed in this section aims to determine the revenue that will accrue from the PV system at the end of 20 years, given the investment and other costs. Using the model for the University installation as a starting point, we wish to determine the effects of failures on larger systems that consist of 500 kW arrays. This 5-MW system is considered to be a large scale project, and its net present value is investigated at the end of 20 years. More specifically, we use the economic models to assess differences in net revenues over a 20-year period when considering failures vs. ignoring them (or assuming they do not occur).

The existing research was used to develop economic and engineering models to identify economic benefits that accrue from distributed generation using PV technology. The failures in the system show the effect of "performance on profits." The economic model links the performance figures of the engineering PSCAD simulation model (such as mean time before failure, mean time to repair and performance ratio) to the bottom line figure expressed in dollars.

6.2 OBJECTIVE

The objective is to determine the effect of downtime (defined as the time between failure and the start and completion of onsite or offsite repair, installation, and return of the system or subsystem containing the failed component to operation) on the "balance sheet" for the present and for future years of operation.

While certain costs may be fixed, replacement power to maintain the mandated reserves, purchased on the open market, will vary with seasonal use, plants down for maintenance, and the failure of components not part of the PV systems. Depending on atmospheric conditions, this replacement power may be required to meet demand and capacity requirements. This, as well as fixed and fluctuating costs related to transmission and distribution investment, and financial instruments used to finance plant construction, need to be factored into the bottom line for the current year and projected for the remaining years in the plants, and in the GCPVS.

This analysis will be accomplished using, where possible, published figures on various costs, e.g., transmission and distribution expansion to meet increased demand, or, when these data are not documented, estimates from utility[19]employees serving on the project's Advisory Board.

6.3 SOCIETAL BENEFITS

The societal benefits of PV systems are often underappreciated, underestimated, and usually not included in economic analyses of energy options. This exclusion is understandable in that the benefits themselves are difficult to capture completely, and different experts are unlikely to come up with identical or even similar lists. A quick survey of the literature, however, yields a large sample of cited benefits, and nearly all of these can be assigned an economic value [6-1]. In addition, regular meetings with utility managers provided information on the societal benefits that utility managers believed were acceptable. Our economic model includes the following economic values for societal benefits, with the benefits captured dollars per kilowatt-hour (kWh). The actual value assignments used in this model include: generation O&M ($10/kW/yr), network O&M ($16/kW/yr), minimum load power plant dispatch ($28/kW/yr), transmission investment ($45/kW/yr), transmission congestion relief ($30/kW/yr), generation capacity ($33/kW/yr), and reactive power ($15/kW/yr).

One difficulty in properly assessing a comprehensive economic value for the societal benefits of PV is that the cost penalties of fossil fuels are unlikely to be paid directly by the current consumers of fossil fuels, but more likely by

[19] Northeast Utilities and United Illuminating Companies, the two utilities serving Connecticut

future generations. Similarly, many economic benefits of PVs (outside of those utility-based savings listed above) are not realized by the current PV users. The situation is not unlike the current overuse of antibiotics. Present users enjoy health and economic advantages by using strong antibiotics to annihilate every germ that crosses their path. But the longer-term effect of this overuse is a strengthening of the strains, which entails far greater hardships and costs to fight these hardened germs in future generations.

In recent years, many in industry have begun to use the term “whole life cycle costing” [6-2]; and “life cycle cost analysis” [6-3] when addressing the actual costs of their products or infrastructure. With the growing costs of energy and further expected increases as rapidly developing nations use more of their share of the world’s energy supply, costs such as operating expenses now play a much larger role in the decisions to purchase one product over another. In addition, many nations impose end-of-life take-back policies on manufacturers, or the purchaser themselves must bear the costs of disposal. Hence a life cycle cost is well above the “sticker price” of an item, a concept and practice already well entrenched in many industries. Our observations and analysis show there are a number of credible societal benefits for PV systems that provide real economic value both to present and future generations, and, conversely, there are a multitude of hidden or life cycle costs associated with fossil fuels. With proper explanation and publicity more utilities, utility regulatory bodies, and government agencies may support the application of these benefits to PV and life cycle costs to all energy sources. In many cases this model will result in assigned costs that more properly reflect the true life cycle cost of fossil fuels. Some of these “societal value” considerations include:

Rising carbon dioxide levels in the atmosphere: The additional carbon dioxide caused by the burning of fossil fuels and its relation to global warming, still viewed with skepticism in some circles, can carry a significant price tag. Unfortunately, the societal costs of carbon dioxide in the atmosphere are difficult to quantify. Some estimates claim that the costs of increasing carbon dioxide levels include rising ocean levels, increased storm activities, weather and agricultural pattern changes, real estate losses, and the overall effects of creeping desertification.

One source [6-4] estimates that if the levels of atmospheric carbon dioxide are left unchecked, the costs of just these directly attributable effects will be $271 billion as early as 2025, rising to $1.8 trillion in 2100 (all in constant 2006 dollars). This figure represents approximately 2% of U.S. GDP or close to $1,000 per person in the United States. Other effects (ocean acidification, ocean oxygen decreases and the effect on the oceanic food chain, overall temperature increases and other related human health effects) have not been included in this projection from 2008. Results reported in a 2003 study [6-5] indicate that $100 billion of life cycle costs attributable to gasoline, if added to the U.S. economy, would increase the price of gasoline by about $0.76 per gallon.

Acid rain: One of the major problems with fossil fuels is the amount of acid precursors they emit upon burning. Power plants using coal produce large volumes of sulfur compounds that are converted to sulfuric acid upon exposure to water. Internal combustion engines produce nitrous oxides that become nitric acid. These and other chemical processes of fossil fuel combustion have led to acid rain in multiple locations around the world. The impact of this acidic rain has been documented as significant alterations in aquatic life and in soil acidity levels.

A 2010 EPA study [6-6] concluded that the annual cost benefit of significant reductions in acid rain would be $122 billion, against an annual cost of only $3 billion. This would result in annual cost savings per US person of approximately $400 in 2010 dollars. Acid-free energy sources such as PV would be able to claim this societal benefit. Life cycle costs for acid rain add approximately $1.00 to the cost of a gallon of gasoline used in the United States.

Political cost: It is not surprising that the demand for and supplies of fossil fuels have led to political instabilities and conflicts throughout the world. Many political analysts conclude that the overemphasis on events and governments in the Middle East and some countries in Africa is a direct result of the vast stores of fossil fuels that reside there, and their availability for export. Some responsibility for the U.S. War on Terrorism can also be attributed to issues surrounding the supply of fossil fuels.

The political instability in the oil-rich regions and the need for the United States to keep substantial military resources there to assure access to the oil add directly to the cost of oil imports. According to the National Defense Council Foundation, "The economic penalties of America's oil dependence total $297.2 to $304.9 billion annually. If reflected at the gasoline pump, these 'hidden costs' would raise the price of a gallon of gasoline to over $5.28 or a $1.85 increase over winter 2012 gasoline prices of $3.43 per gallon of regular" [6-5].

Trade imbalance cost: The Department of Energy estimates that each $1 billion of U.S. trade deficit costs the United States 27,000 jobs [6-7]. Oil imports account for approximately one-third of the U.S. trade imbalance, and more than $1.16 trillion of wealth has been transferred out of the United States in the past 30 years. This adds approximately $0.10 to the cost of a gallon of gasoline [6-5].

Volatility of an inelastic market: Economists describe the demand for fossil fuels and particularly crude oil as "inelastic," meaning that demand is relatively insensitive to price. Industry, which uses approximately 40% of the energy in the United States, would have a difficult time reducing usage even in the face of significant price increases. Likewise, car commuters do not go out and buy homes closer to work when gas prices spike upward. This cost is carried as an uncertainty in the business case because the price of fossil fuels has varied widely in response to very small changes in supply, a manifestation of inelastic demand. Fossil fuels are further unique in that supplies are also relatively inelastic, that is, it is difficult to reduce or increase supplies substantially when demand rises or ebbs.

Elastic markets are relatively and quickly self-correcting, whereas inelastic markets deliver strong shocks as stable demand quickly bids up the price in the face of even slightly reduced supplies. The volatility of energy costs has been cited as contributing to several economic downturns in the United States and other industrialized nations, and these downturns have enormous costs associated with them. The contribution of even a small amount of PV-generated power to the nation's energy supply would make markets more elastic and prices more tolerant of supply variability. For inelastic markets, even a single-digit contribution can confer significant downward pressure on prices and thus serve to reduce volatility substantially.

Feed streams for critical materials: Fossil fuels play a critical role as the low-cost feed streams of many commercially and socially important materials such as high performance plastics, medical devices, implants, adhesives, seals, and impact-resistant elastomers. As these nonreplaceable materials are used up and their prices continue to rise, higher costs and less effective alternatives will have to be developed. It is not unreasonable to assume that when fossil fuels begin to run out or increase dramatically in value, there will be a premium on all products containing plastics and composites that rely on fossil fuel feed streams. It is nearly impossible to place an economic value on this very real problem of feed stream supplies.

Accumulation of chemical pollutants: Fossil fuels contain trace elements that are slowly building up in the ecosystem. These elements are present in the fuels as naturally occurring compounds or as additives to modulate energy release, such as the lead that was used in gasoline for many years. In addition, uranium and thorium occur naturally in fossil fuels, and these radioactive elements are being released into the environment, especially in the vicinity of power plants, due to these heavy elements' low volatility. Reducing the accumulation of these elements is one of the more difficult economic benefits to quantify, but the model would be similar to the costs of chemical waste related to chemical plants.

New Jersey has justified a societal benefit charge [6-8] on utility bills to boost alternative energy options, among several other issues funded. The state claims, "Every dollar invested in the energy efficiency program returns $4.00 in savings for the residential customer and $11.00 in savings for the commercial and industrial customer." The 3.8% charge on NJ utility bills is not intended to price utility power at its true value or full stream cost, but rather to use the societal benefit tax to promote clean energy alternatives.

Comments: Note that we have elected **not** to incorporate these nonutility societal valuations listed above into the economic model, as we prefer that this model remain realistic and somewhat conservative. If the costs of the above effects were reflected in the true or life cycle cost of a gallon of gasoline, the referenced estimates of just the first four effects would add $3.70 to the price of a gallon of gasoline. We believe that the Department of Energy and other state agencies and regulatory bodies could and should use these valuations to shift the national debate on PV systems, informing key decision makers and the general public of the hidden costs of fossil fuels and the intrinsic societal benefits of PV that can be both quantified and justified.

Applying similar logic to the fuel cost for electrical generation, the estimated cost impact on the use of fossil fuels in power generation can be calculated. Based on the above analysis, the societal value costs added to the price of gasoline would more than double the price per gallon at winter 2012 prices. A similar assumption about the cost of fuel for electrical power generation can also be made, since much electrical power depends on the use of fossil fuels. However, not all the effects applied to the life cycle costs of gasoline apply to electric power generation since it uses a far greater fraction of domestic fuel supply (for example, coal). The fuel used for electrical power generation in the United States is less than 10% of imported crude oil. Thus the hefty price placed on political instability for the cost of a gallon of gasoline (+$1.40/gallon) would be reduced to only $0.10. The added cost related to societal benefits is still an addition, but it is reduced to a 58% increase for electrical power fuel, compared to a 108% for gasoline.

A “green econometrics” reference [6-9] reports that the cost for fuel per kWh of electrical energy produced varies from $0.025 for coal, to $0.048 for natural gas, to $0.052 for oil. A rough weighted average for a Northeast Utility property discounted for the larger lot sizes of power plant deliveries would lead to a mixed fuel cost of approximately $0.03/kWh. If the life cycle costs of this fuel were assigned, they would add approximately $0.02 to each kWh of electrical power. In many states this amount is 10%-15% of the overall electrical power delivery price of $0.15-$0.20/kWh. A societal benefit charge of approximately $0.02/kWh thus would be a proper benefit for PV systems. This could be either levied on electric bills and/or provided to owners of PV assets.

6.4 SUMMARY OF RESEARCH ON ECONOMIC “VALUES”

Contreras, et al. [6-10] present an overview of 19 different values that should be taken into account when assessing PV values. The two most important drivers are location and “timing of the power output of the system.” They note that locating PV where gasoline prices are high, transmission and distribution (T&D) is congested, and “high insolation to increase production of the PV system” are all important. The authors assess 12 U.S. case studies (6 of which are residential, one a municipal building, and 4 commercial) and determine the PV values, along with the “stakeholder total” (the difference between the benefits and costs) for each case study.

Given their emphasis on the importance of location as a driver of PV values, the most relevant case studies for our purposes are the ones in the Northeast part of the U.S. In two of these particular case studies in the Northeast (Cambridge, MA and Kingston, NY), the study found negative net values. One apparent key factor for the negative net values appeared to be high equipment costs of 31.4 cents/kWh, leading to net benefits of -29.4 cents/kWh and -8.6 cents/kWh, respectively. On the other hand, two case studies in New York City (one residential and one commercial) found positive net values for stakeholder totals, in the amounts of 6.9 and 7.4 cents/kWh, respectively. A major difference between these cases and the two with negative net values is that in the two New York City cases, equipment costs were only 14.7 cents/kWh. So, clearly, equipment is one cost that could potentially determine whether PV systems in the northeastern U.S. have a positive net value.

Marshall and Ruegg [6-11] outline a life-cycle costing approach to determine values from solar energy. Even though the numbers for their particular example are somewhat outdated, their approach remains relevant. Since they assume the expected life of a building is 25 years and a solar system would need to be replaced in 15 years, it is important to treat costs incurred in the future differently from costs incurred in the present. In particular, costs incurred (or benefits received) in the future are not valued as much as those that are incurred or received today. This is because if the savings were realized today, they could be invested and would be worth more in the future. So, it is crucial to discount values expected to be received in the future, to state these values in terms of “present worth” or “present value.”

The values that the Marshall and Ruegg describe as necessary to consider are the initial investment cost, the present value of the “salvage” value of the solar equipment (the value of the equipment at the end of its lifetime), the present value of its replacement costs, present value of operation and maintenance (O&M) costs, and the present value of energy savings. These costs are then added together to obtain the overall life cycle costs. While this framework is clearly too simplistic for our model, the basic life cycle costing model may be helpful in building our own economic model for PV values.

Robertson and Cliburn [6-1] also discuss the sources of value from PV. Their key criteria are “location,” “scale,” “timing,” “orientation,” and “maintenance.” They describe sources of value for utility-driven distributed PV, breaking these values into utility values, policy values, business model values, and risk management issues and their impacts on values. The utility values are broken down as peak-load and intermediate-load values. The tables in Robertson and Cliburn provide a detailed presentation of the benefits in each of these two categories, which are summarized below.

Peak load values: These include distribution investment deferral, transmission congestion relief, transmission investment deferral, generation capacity, generation O&M, generation reserve capacity and O&M, natural gas supply utilization, purchased power, minimum load power plant dispatch, environmental, line losses, reactive power, voltage support, and network O&M.

These include natural gas, environmental, and line losses. The policy values the authors describe are net metering payments, customer rebate payments, and solar renewable energy credits. The business model values include customer revenue retention, peak-period distributed photovoltaics (DPV) revenue, tax investor participation, PV system portability, and payment to PV host site. Several risk-management issues also should be factored in, including grid reliability and outage prevention; natural gas availability; financial, regulatory, carbon, insurance, share price, and fiduciary duty; and generation portfolio cost and risk.

Understanding the sources of distribution costs is crucial for an accurate assessment of avoided distribution costs resulting from PV. Shirley [6-12] looked at average and marginal distribution costs for 124 utilities over a 5-year period in the late 1990s. The study defines each of the cost components within one of 14 different categories and then groups these categories into 4 different aggregate groups: “Transformer & Substation investments” (T&S), “Lines and Feeders investments” (L&F), “Customer-specific investments,” and “street lighting and signal systems.” The study also analyzes O&M by grouping operations costs into 10 different categories, and maintenance into 9 different categories. This study found a high correlation between investment in “Transformers and Substations” and in “Lines and Feeders” and system peak and number of customers.

The correlation (R^2) measure between system peak and each category of “Transformers and Substations” and “Lines and Feeders” is about 0.9. Correlations of customers with T&S and L&F are even higher, at about 0.96. System size and investment per MW were virtually uncorrelated, implying that distribution costs can be high, regardless of the size of the utility. Also, the study found little evidence of economies of scale for “investment efficiency, at least in terms of system peak and system energy.” For L&F plant investment, when “utilities get larger in terms of number of customers, their investment per customer tends to rise.”

The Pernick and Wilder study [6-13], also referred to as the Utility Solar Assessment (U.S.A.) Study, provides a roadmap for electric utilities to accelerate the growth of solar energy. The study interviewed more than 30 industry experts to show how correctly coordinated efforts among regulators, the solar industry, and utilities can allow solar generation to reach 10% of U.S. electrical generation by 2025.

The study showed projected costs for a decade from 2008 (the time of the study) for crystalline silicon PV systems to be approximately $3.00 per peak W compared to $7.00 in 2008. Thin-film PC systems are projected to drop from $5.50 per peak W to $3.00 in 2015, and to less than $1.50 in 2025. Estimations provide information on how PV will cost less than standard grid power in most U.S. markets by 2025. The investments needed to reach 10% solar-based power generation by 2025 will be expensive, but it is comparable to the costs needed to pay for coal and natural gas fired plants. It is also believed that the cost for solar power generation will be considerably less than for a similar amount of nuclear power or coal power. As a result, PV-generated energy will be much less costly than standard grid power by 2025.

Perez and Hoff [6-14] present an analysis of the utilities' values. They note the key values as "energy production value, generation capacity value, transmission and distribution (T&D), system capacity deferral value, loss savings, environmental value, and fuel price hedge protection." Their paper focuses on the first two of these values, finding that generation capacity value ranges between $180 and $250 per kW in New York state, or about $0.045/kWh. Also, the energy production value is about $0.109/kWh, while the residential retail rates in the Long Island region are about $0.20/kWh, implying that the energy production and generation capacity values alone comprise a substantial portion of the current retail electricity rates.

The purpose of the Evans [6-15] project was to demonstrate a methodology that would (a) assess and quantify the benefits of distributed energy resources (DER) for the performance of a power transmission and distribution system, (b) determine the location and attributes of beneficial DER projects, and (c) quantify their network benefits.

For this project DER is defined as:

- Distributed power generation embedded in the network at customer sites (DG)
- Demand response that could be dispatched by the network operator (DR)
- Distributed, switchable reactive sources such as capacitors

Successful network benefit indicators are:

- Real power loss reduction,
- Reduced reactive power consumption,
- Improved voltage profile,
- Reduction in network "stress,"
- Increase in the load-serving capability of the network under contingency conditions, and
- System capacity provided by DER measures.

In terms of the economic benefits, Evans was able to directly estimate the economic value of network benefits such as reduced losses, reactive capacity, and system capacity, and found that the value of network benefits from these projects might approach $450/kW if system capacity is taken into account. Additional quantifiable network benefits such as increased load-serving capability, improved voltage profile, and reduced system stress might have significant value in dollar terms, but they are not as readily priced.

Overall, the studies surveyed in this literature review show clear benefits of distributed PV. A key common theme, however, is that the benefits vary widely depending on the region of the country where the PV system is located, the time of year, and the day. Specifically, the ability to alleviate peak load demand is one key determinant of PV value generation. Other important determinants of value include T&D distribution upgrade deferrals, savings from potential outages, fuel savings from decreased need to run gas turbines to meet peak load demand, and environmental benefits.

6.5 ECONOMIC MODEL

The model is a series of spreadsheets representing inputs such as costs, benefits, and expenses, as shown in Figures 6-1 through 6-4. Installation KW at the top of the model represents the power supplied by the University of Hartford Lincoln Theater PV array, which has a 17kW capacity. The economic model starts with calculating the system's yearly KWh generation, by feeding 17kW into the assumed yearly system generation of 1,300 KWh/KW/yr.

The bulleted information below describes the elements of the economic spreadsheet models, including income, expenses, values, and values to society.

Income (see Figure 6-1):

- The federal investment tax credit (ITC) is 30% of the turnkey system cost for year one only. After a 50% tax on the ITC, the net cost basis is the turnkey system cost minus 50% of ITC.
- The number of renewable energy credits (RECs) is found by dividing KWh/yr system generation by 1,000. Market values of RECs are found by multiplying the number of RECs and an assigned dollar amount. The salvage value of the PV after 20 years is also added to the revenues. After a 35% tax on RECs, the income is calculated by adding all the revenues and subtracting the costs. The dollar per KW value for RECs is found by dividing the market value by the installation kW.
- Income is offset through a tax on the depreciation credit, which is a 35% tax on the depreciation value.

Figure 6-1: Input/Output Charts, Income

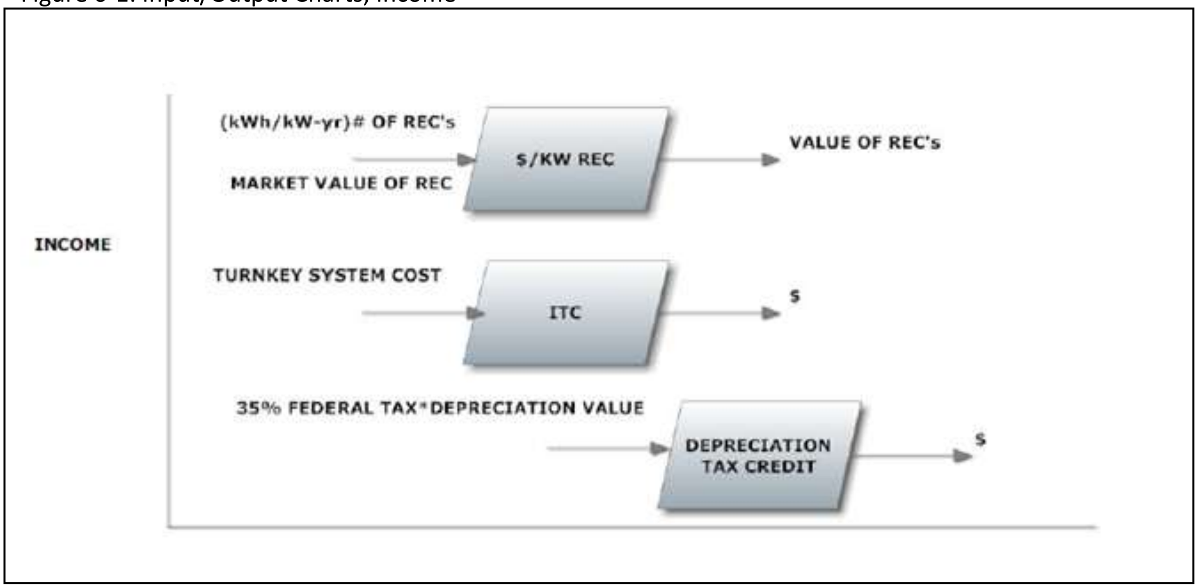

Expenses (see Figure 6-2):

- The costs that start with the turnkey system cost is $6,000 (cost of installing the PV) multiplied by the installation KW. This estimate of $6,000/kW was provided to us from engineers at United Illuminating.
- State of Connecticut rebate value of $4,500 on the installation is also multiplied by the installation KW and subtracted from the costs, although a federal tax of 35% on rebate is added back to the costs, resulting in a net system cost of $94,775.
- Carryover from previous year is added to the costs for each year, that is, the negative net cash flow resulting from the early years because of the lump installation cost. Business operating costs are assumed to be 3% of the net system cost.

Total cost is the sum of business operating costs and the net cost. Net cash flow, the I\income minus the total costs, is negative for the first several years in the startup case models described in the following sections, which is expected due to the up-front turnkey system costs.

Figure 6-2: Input/Output Charts, Expenses

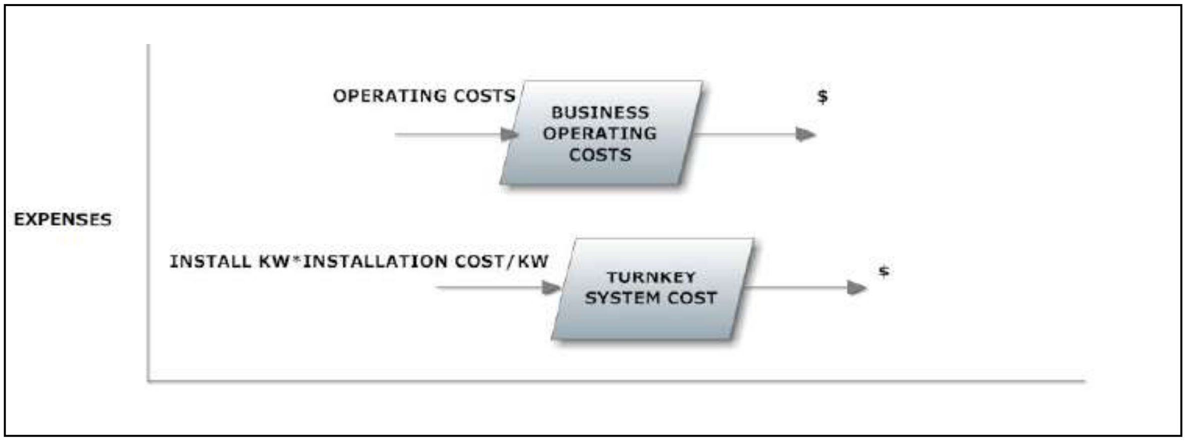

Values (see Figure 6-3):

- Average dollar amount per KWh generated is at a rate of 17 cents, assumed to remain constant through 20 years. Revenue for energy generation is the sum of the monthly KWh generation multiplied by the rate of $0.17, for 12 months, where escalation rates remain at zero.
- Depreciation values are derived from the depreciation rate (MARC) times the net cost basis.
- The state of Connecticut rebate is $4,500/kW.
- Salvage value is the benefits the PV owner can reap through alternative uses of the solar panels and other components at the end of the PV life cycle. We assume this value is zero, due to the rapidly declining prices of new PV components, although there may be some minimal benefits from scrap values.
- Carbon credits revenues are distributed through funds received by the state through auctions with the Regional Greenhouse Gas Initiative (RGGI), an initiative consisting of all the New England states, plus New York and Maryland. The values of carbon credits through RGGIs vary [6-16]. So, we chose to allow for a value of $0.014/kWh from pollutant and greenhouse gas emissions savings. This value was suggested in Robertson and Cliburn [6-12]. Alternatively, this value could be classified as one of the societal values.

Depending on whether the PV is owned by utilities, one could include the benefits to utilities in a model similar to ours. These utility benefits consist of central power generation cost (which could benefit rate payers), central power capacity cost, avoidance of lost revenue from system losses, and deferred T&D costs (not depicted in the Input/Output flow charts because Lincoln Theater's PV is owned by the University of Hartford; however, the T&D values are discussed below).

Figure 6-3: Input/Output Charts, Values

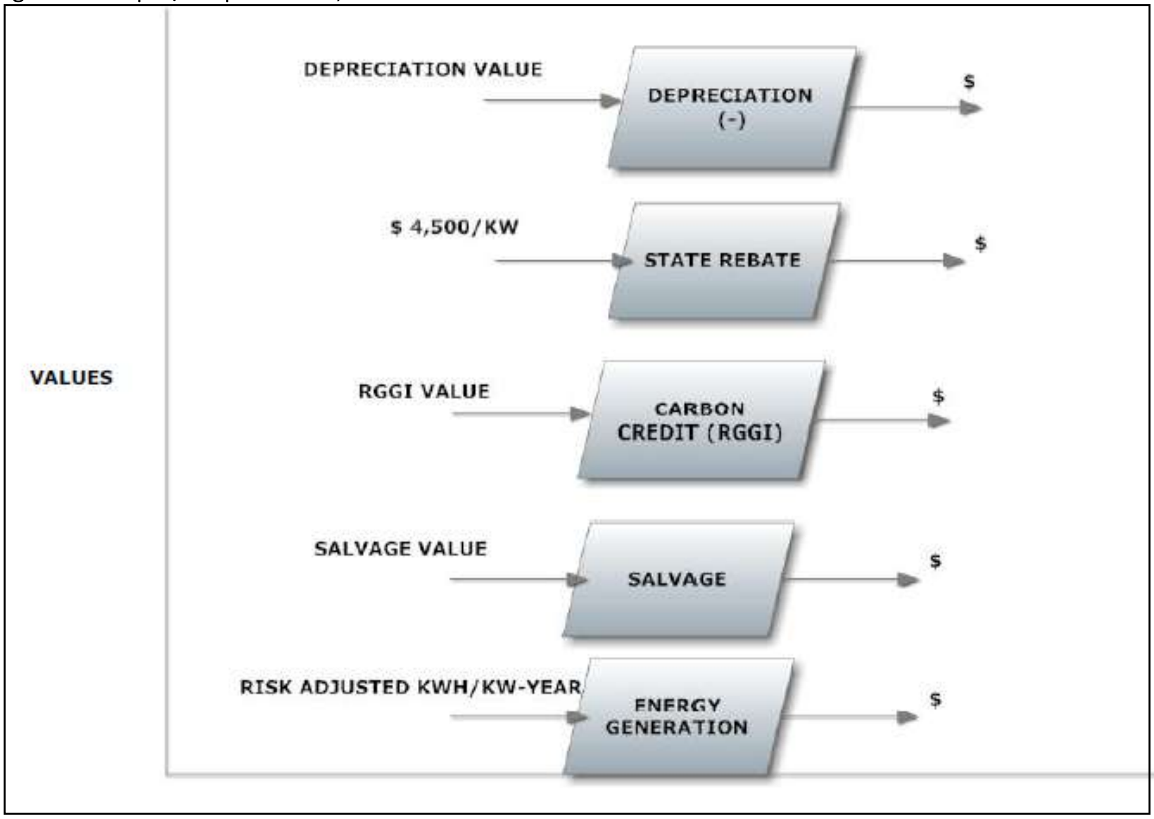

Values for Society (see Figure 6-4)

Note: Not all societal values discussed here are depicted in Figure 6-4.

- Environmental: Decrease in pollutants and greenhouse gas emissions, increase in regional greenhouse gas initiative (RGGI), or "carbon credit" value.
- Electric rates: Generation reserve capacity and O&M (peak), generation O&M of $10/kW/yr; network O&M, $16/kW/yr; rates range from $16-$88/kW/yr, minimum load power plant dispatch, $28/kW/yr.
- Land use: Reduced transmission investment, $45/kW/yr; transmission congestion relief, $30-$50/kW/yr; generation capacity, $33/kW/yr; reactive power, $15/kW/yr.
- Land values: Higher property values from less pollution; higher property taxes (reflecting higher value) may be induced (these values would require more detailed analysis, which are beyond the scope of this project).
- Health: Value of longer human lifespan and fewer health problems due to less pollution.
- Direct job creation: PV cost * (10.9 job-years/$million spent on PV)*(average annual salary of PV-related employees of $40,000).
- Indirect job creation: Benefits, based on the concept that when a new job is created because of PV, those new employees earn income and spend part of it, which becomes additional income to other people and therefore creates even more jobs that otherwise would not have been created without the PV startup investment.

These indirect job creation benefits, obtained from the Connecticut Clean Energy report [6-17] are given by the formula: PV cost *(14.1/$million spent on PV)*(estimated average annual salary of other employees of $40,000). These benefits are added for year 1 only because the startup costs are incurred for the first year of installation. The total value is calculated both with and without job creation benefits.

Figure 6-4: Input/Output Charts, Selected Values for Society

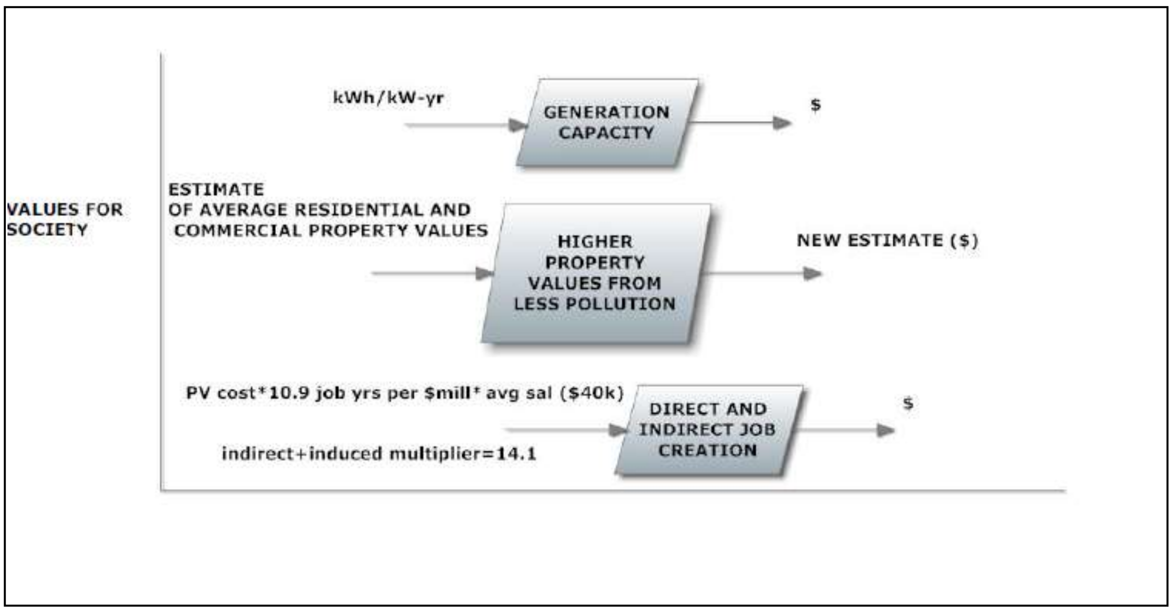

Transmission and Distribution (T&D)

T&D values may vary due to the size of PV and different ownership and location scenarios, as described in Table 6-1.

Table 6-1: Transmission and Distribution Values

PV owned and located at customer	If PV system is installed at the customer site, the utility provides service and ma able to defer upgrading T&D
PV utility owned and located at customer	If the utility owns the PV system and locates it at the customer, utility may still be able to defer upgrade, but the same power losses may be associated with it.
PV utility owned and installed at load	The optimal solution is the PV installed at the load where customers avoid power losses and lost revenue.

6.6 NET PRESENT VALUE

Net present value (NPV), also referred to as present value, of annual income is found in our analysis with discount rates of 1% and 3%. The discounted value of benefits is found by $B = \Sigma B_j /(1+i)^j$ where the summation is for each future period j, with j going from 1 to 20 because of the 20-year expected lifetime of the PV system. This type of present-value analysis is described in section 6.4 above and elaborated upon by Marshall and Ruegg [6-11].

One of the most effective ways to account for benefits from GCPV electricity generation and these legitimate but hard to quantify societal benefits is to use the NPV model.

$$NPV = B_t / (1 + i)^t - C_0$$

where t is the time in years (t=1, 2,…, 20 in our analysis), i is the discount rate (the cost of capital, or the expected return on money if funds are available to invest upfront instead of in some future period t), B_t is the benefits expected to be received at some future time t, and C_0 is the initial cost of the investment. This type of NPV calculation is described by Baye [6-18] and is a commonly accepted way to account for the fact that benefits to be received in the future are worth less than benefits received today.

6.7 BENEFITS AND COSTS

Figure 6-5 illustrates the PV system's benefits and costs. If net benefits add up to be greater than zero, the investment in PV generates positive economic value.

To obtain the net costs in the PV system allowing for failures, first the availability is multiplied by the sun radiation data throughout the year, which gives the available kWh for the year, which will likely be less than 100% efficiency. The system's efficiency depends on the components' mean time before failure (MTBF) and mean time to repair (MMTR), as discussed in sections 2 and 4 of this report.

Two scenarios are taken into account when determining the effect of PV system failures. The economic model was set to run with kWh produced where failures are not seen. Then the failure-adjusted kWh production is substituted into the economic model, and the net benefits compared to the no-failure case.

The cost of electricity is an important factor that determines the value of energy produced by the PV. This number is taken from the International Organization for Standardization (ISO) data, which gives the real-time marginal locational price/kWh. Typical meteorological year (TMY) data, the hourly sun radiation, is correlated with the ISO data to exclude the hours without radiation (sunset to sunrise). Large variations in the monthly ISO New England pricing are seen throughout the years. Data between 2004 and 2010 show the peaking of prices in August, December, and January due to high demand. For the high variations for the remaining months, prices for fuel or other energy sources are the possible reasons. The yearly generation of energy is taken from PSCAD program simulation (see section 4 of this report) and fed into the economic model.

Figure 6-5: Benefits and Costs of a GCPVS

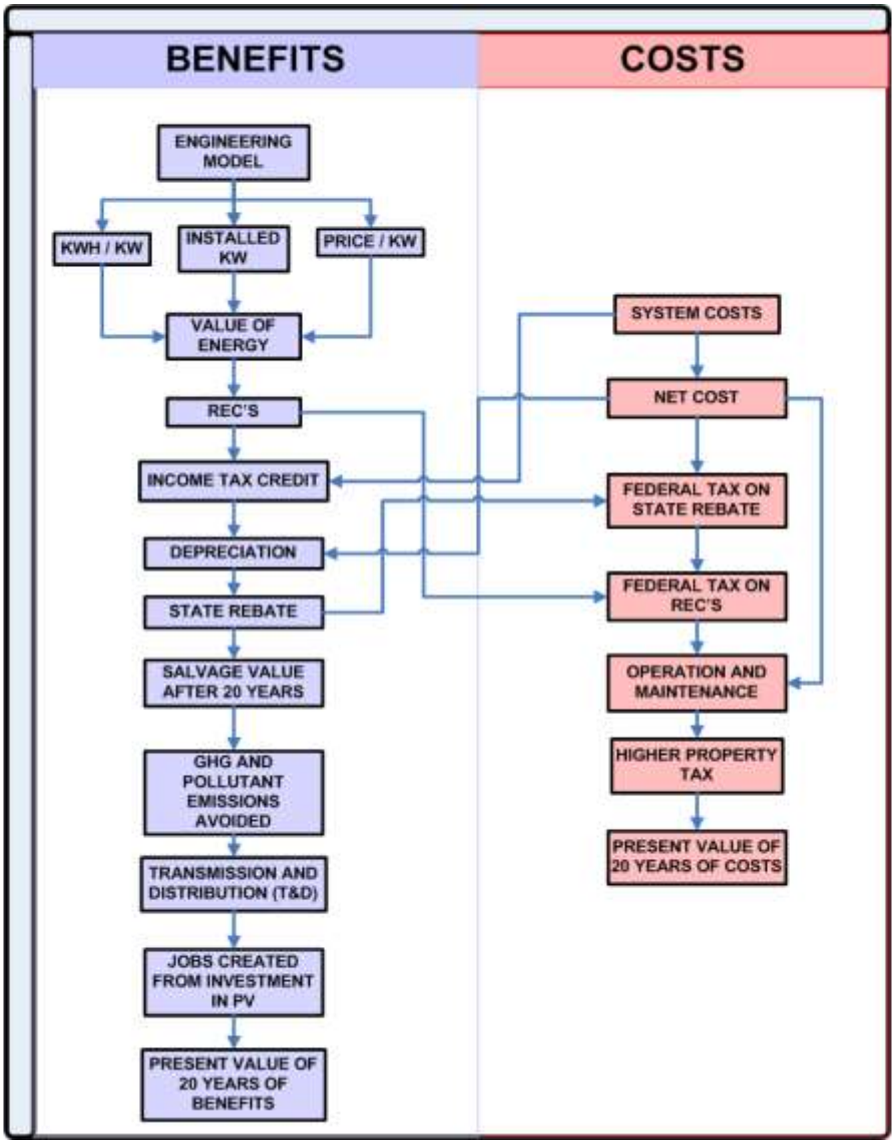

The kWh/yr for the University of Hartford's Lincoln Theater PV array was entered into the economic spreadsheet (SEMS) models, first for the case with no failures and then again for the case with failures. This model depends on the monthly kWh generation, which needs to be input month by month for the failure and no-failure cases. For instance, if there is a failure in x% of the unit every 3.5 years for 25 days, then the electricity generated by the PV needs to be adjusted to be (100-x)% for that downtime. This can be done on a monthly basis, so that if the system is down for 25 days, is entered as approximately 1 month.

The difference in net benefits between the failure model and the no-failure model reveals the value of avoiding failures for a certain kW system.

6.8 DEMONSTRATION CASES

A Power System Computer Aided Design (PSCAD) simulation model is used to calculate the energy generated based on the University of Hartford's GCPVS, rated at 17kW power. As of this date there have been no indications of interruptions of operation, including the most common cause of failures, the inverter components. It is possible that for the system's 6 years of operation, failures occurred while the data collection software was offline (the better part of one year of the 6).

A PSCAD simulation model is used to calculate the energy generated through the PV array located on the roof of Lincoln Theater, with and without failures. The energy without failures is 8899.16 kWh/yr, and the simulation with failures results in an average value of 8517.11 kWh/yr.

These numbers are entered into the SEMS models, reflecting a number of different scenarios such as:

6.8.1 Using No Failures kWh/yr as the Baseline

No Failures
Defined as the energy generated with all three inverters (A, B, and C) operational.

No Startup Cost Case: This case assumes that the PV array is already built and no initial investment is needed to buy and assemble the system. In this case, investment tax credits (ITCs) are not included since they are given to compensate for initial costs. Also, job creation benefits are not included because no labor is needed to install the PV. No startup case is run twice, as we feed the kWh/yr for the "no fail" and "fail" cases. Moreover; each model shows earnings/loss for each year, one including the societal benefits and one excluding them, as well as varying discount rates for calculating the NPV at the end of 20 years.

Startup Cost Case: This case assumes the PV system is built within the first year; therefore, there will be a cost for installing the PV, but ITCs are given for the first year, and direct and indirect job creation benefits help compensate for the initial costs. Similar to the No Startup Cost Case, the SEMS model is run with and without PV failures, and with societal benefits included and then excluded. All these scenarios are also duplicated with the rather high discount rate used to calculate the NPV.

6.8.2 Using Sometimes Have Failures as the Baseline

Sometimes Fail
Defined as the generation from 1 of the 3 inverters is reduced by the average values of availability[20]. The two other inverters are operating as designed.

Sometimes Fail Cases: These cases compare the startup cost and no startup cost cases using the same model from the previous scenario: startup cost with failure, which results in 8672.5 kWh/yr, and the same with no startup cost case.

6.8.3 Using Always Have Failures as the Baseline

Always Fail
In this case, there are both startup cost and no startup cost models with reduced or partial power generated. In the startup cost case, there are both direct and indirect job creation benefits and ITCs. The no startup cost case net present value always exceeds the break-even point throughout the 20 years of operation. Figure 6-6 compares the values totals for each of these failure conditions. As expected, the values decrease with an increase in failures.

[20] As calculated in Section 4, the average value of availability 0.893 ≈ .90

Figure 6-6: Total Energy Generated and Lost, for Failure Categories (Over 20 Years)

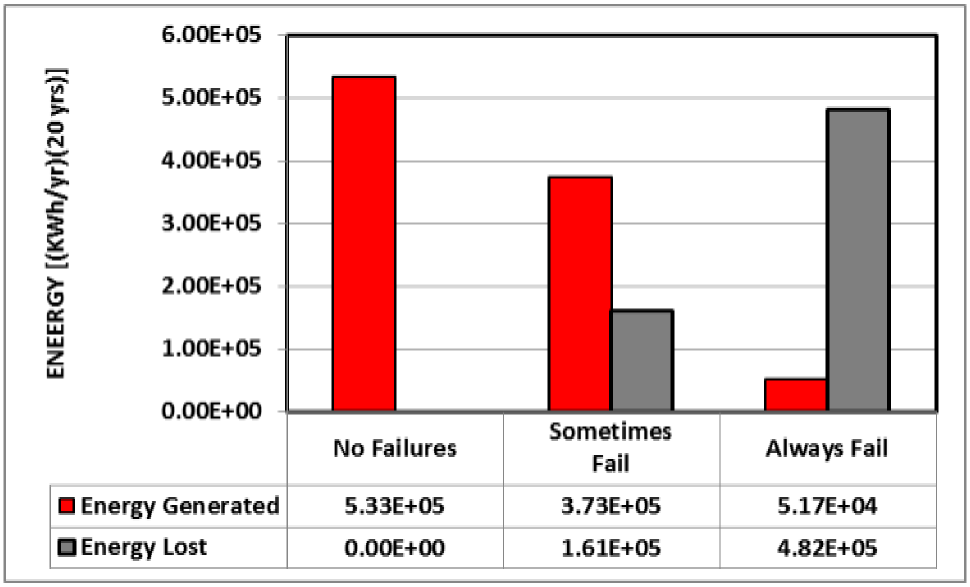

Values of energy generated and energy lost for the failure categories noted above are detailed in Table 6-2, below.

Table 6-2: Energy Generated and Energy Lost, by Failure Categories							
	No Failures		Sometimes		Always		Downtime=DT
	Generation	Lost Energy	Generation	Lost Energy	Generation	Lost Energy	(Days/365)
INV	(1+2+3)	(1+2+3)-(1+2+3)	2+3+(1*DT)	(1+2+3)-(2+3+1*DT)	(1+2+3)*(DT)	(1+2+3)*(1-DT)	IGBT 1/2
YEAR	kWh/yr	kWh/yr	kWh/yr	kWh/yr	kWh/yr	kWh/yr	Downtime
1	2.67E+04	0.00E+00	1.89E+04	7.77E+03	3.37E+03	2.33E+04	0.1264
2	2.67E+04	0.00E+00	1.88E+04	7.85E+03	3.11E+03	2.36E+04	0.1165
3	2.67E+04	0.00E+00	1.85E+04	8.21E+03	2.02E+03	2.46E+04	0.0759
4	2.67E+04	0.00E+00	1.88E+04	7.86E+03	3.09E+03	2.36E+04	0.1158
5	2.67E+04	0.00E+00	1.85E+04	8.19E+03	2.10E+03	2.46E+04	0.0788
6	2.67E+04	0.00E+00	1.86E+04	8.09E+03	2.39E+03	2.43E+04	0.0896
7	2.67E+04	0.00E+00	1.85E+04	8.16E+03	2.18E+03	2.45E+04	0.0819
8	2.67E+04	0.00E+00	1.95E+04	7.16E+03	5.19E+03	2.15E+04	0.1945
9	2.67E+04	0.00E+00	1.89E+04	7.76E+03	3.38E+03	2.33E+04	0.1266
10	2.67E+04	0.00E+00	1.87E+04	7.98E+03	2.72E+03	2.39E+04	0.1021
11	2.67E+04	0.00E+00	1.81E+04	8.55E+03	1.03E+03	2.56E+04	0.0386
12	2.67E+04	0.00E+00	1.94E+04	7.26E+03	4.88E+03	2.18E+04	0.1830
13	2.67E+04	0.00E+00	1.79E+04	8.76E+03	3.84E+02	2.63E+04	0.0144
14	2.67E+04	0.00E+00	1.87E+04	7.97E+03	2.77E+03	2.39E+04	0.1038
15	2.67E+04	0.00E+00	1.90E+04	7.64E+03	3.76E+03	2.29E+04	0.1409
16	2.67E+04	0.00E+00	1.86E+04	8.08E+03	2.44E+03	2.42E+04	0.0914
17	2.67E+04	0.00E+00	1.85E+04	8.17E+03	2.16E+03	2.45E+04	0.0811
18	2.67E+04	0.00E+00	1.78E+04	8.89E+03	0.00E+00	2.67E+04	0.0000
19	2.67E+04	0.00E+00	1.87E+04	8.02E+03	2.62E+03	2.40E+04	0.0982
20	2.67E+04	0.00E+00	1.85E+04	8.20E+03	2.07E+03	2.46E+04	0.0775
Sum	5.33E+05	3.56E+05	1.78E+05	1.61E+05	5.17E+04	4.82E+05	-
Units	[kWh/yr]*20 yrs	[kWh/yr]*20 yrs	[kWh/yr]*20 yrs	[kWh/yr]*20 yrs	[kWh/yr]*20 yrs	[kWh/yr]*20 yrs	fraction

6.9 CALCULATION OF NET PRESENT VALUE

The net present value (NPV) represents the positive or negative value of the project at any point in time.

The NPV given in each case is shown in Tables 6-3 and 6-4 (located at end of this section) and Figures 6-7 through 6-14 show the cumulative NPV at each year over the assumed 20-year timeframe, using discount rates of 1% ("low") and 3% ("high"). Figures 6-15 and 6-16 show the estimates of societal benefits, for the start-up cost case and no-start-up cost case, also using the 1% and 3% discount rate assumptions.

6.10 EVALUATION OF RESULTS

As Table 6-3 details, the case where there are startup costs and no failures generates about $157,000 in NPV benefits over the 20-year life cycle, assuming a 1% discount factor for the NPV calculations. Excluding societal benefits and job creation benefits, the corresponding NPV benefits estimates is only about $44,000. Assuming a 3% discount rate for the NPV calculations, the net benefits are only about $131,000 for the cases with startup costs and no failures. All of the other values are lower as well, because a higher discount rate implies that money received in the future is worth less today than it would be with a lower discount rate (see sections 6.3 and 6.6 above for more details on net present value calculations).

The case of no startup costs and no failures leads to a NPV of approximately $156,000 for the 1% discount rate. The small difference here between this case and the case of startup costs and no failures can be attributed to several factors that essentially neutralize each other. On the one hand, the lack of startup costs should lead to higher net benefits, but since the PV system is assumed to already be in place it is also assumed there are no job creation benefits, depreciation, or ITCs to be considered. On the other hand, the no societal benefits column for the no startup cost case is nearly twice that of the startup cost case, because in the former the startup costs are not included, which increases the NPV benefits by the amount of the startup costs.

Figure 6-7 shows the cumulative net benefits for several scenarios where the startup costs are included and no failures are assumed. For the scenarios that do not include societal benefits, losses are incurred in the first few years, and it takes several years before the cumulative net benefits become positive. Specifically, for an entity such as the University of Hartford that installs a 17kW PV system at a given point in time, it would take about 10 years before the break-even point is reached, when the societal benefits are ignored. This time frame is a year or two longer when there are at least some PV failures, as can be seen in Figures 6-8 and 6-9.

Figure 6-7: Cumulative Present Value of Net Benefits, Including Start-up Costs and No Failures

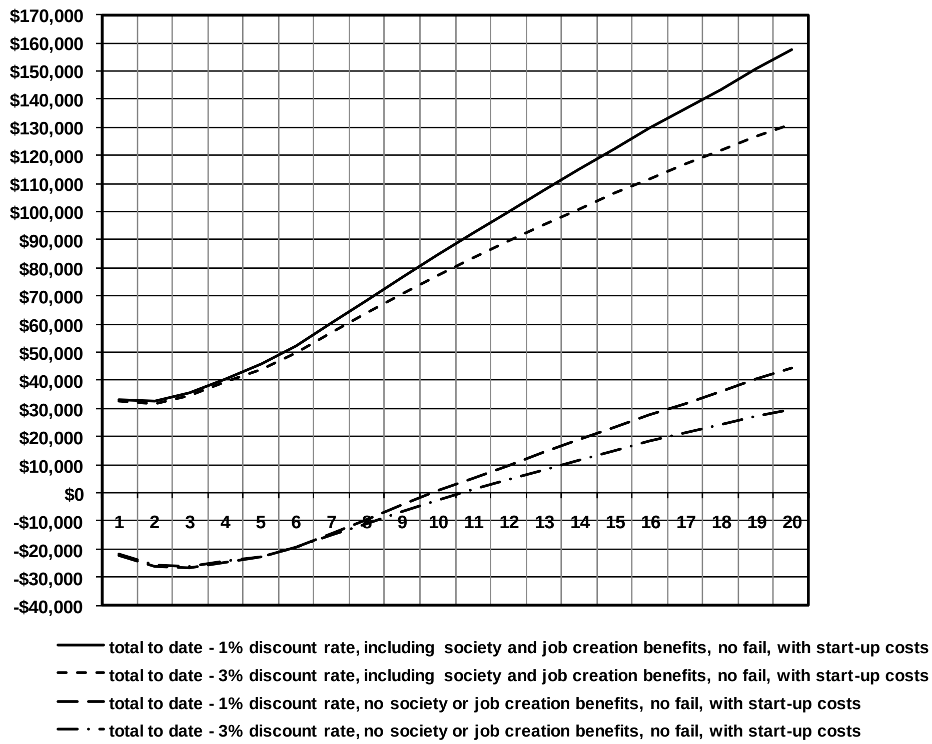

Figure 6-8: Cumulative Present Value of Net Benefits, Including Start-up Costs and Some Failures

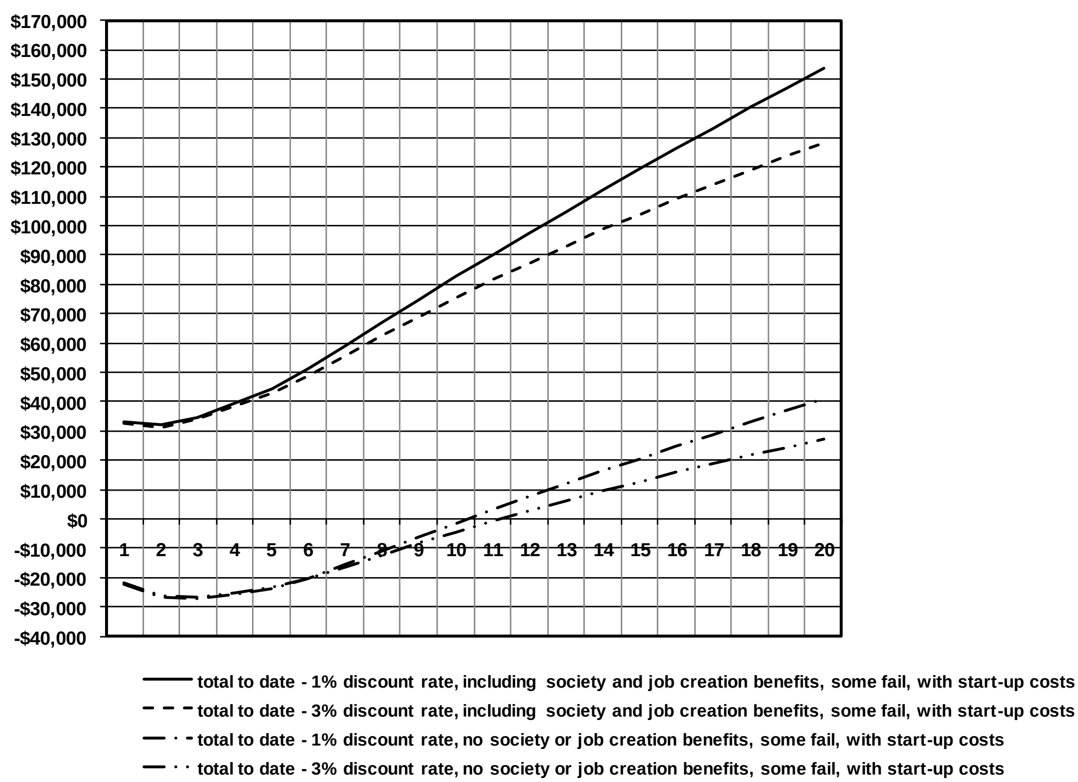

Figure 6-9: Cumulative Present Value of Net Benefits, Including Start-up Costs and All Fail

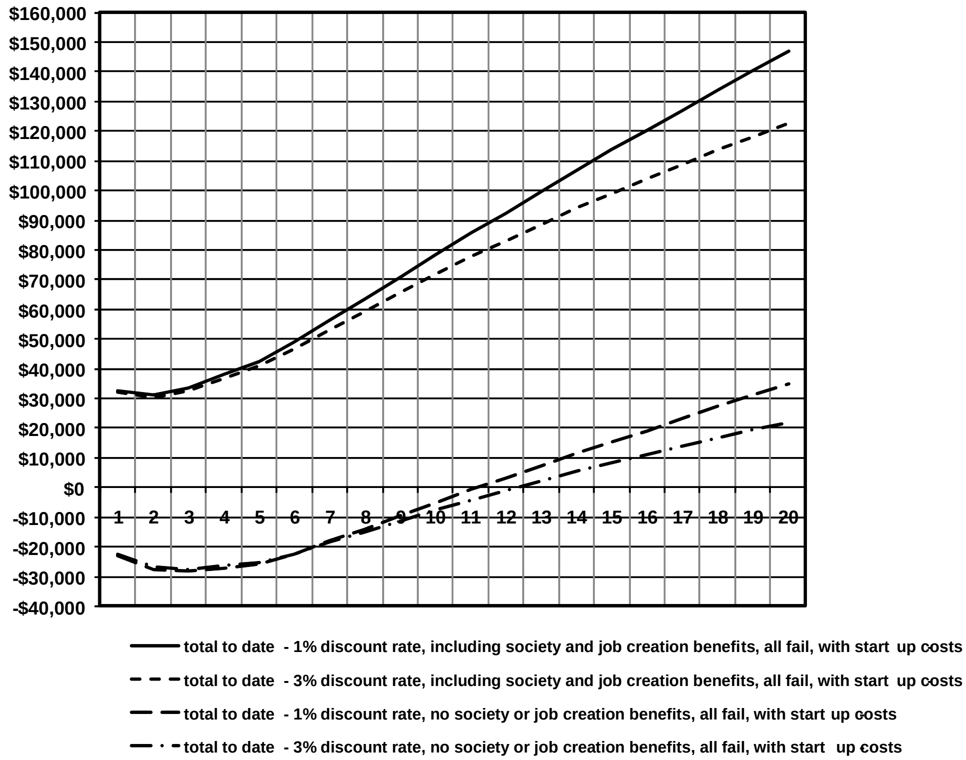

As shown in Figures 6-10, 6-11, and 6-12, when startup costs are excluded, the cumulative NPV is always positive. So, moving forward, given that the startup costs have already been incurred (i.e., when the startup costs are considered a "sunk cost"), the PV is expected to have positive net benefits to the University of Hartford, regardless of whether the estimates include societal benefits and/or the financial effects of failures.

Figure 6-10: Cumulative Present Value of Net Benefits, Including No Start-up Costs and Some Failures

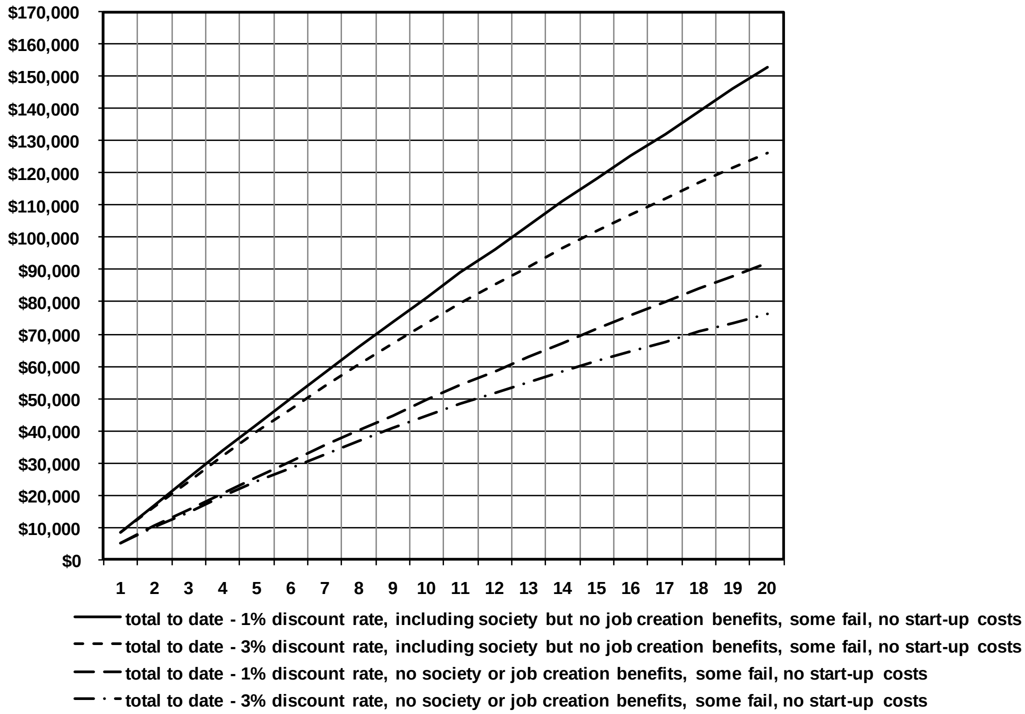

Figure 6-11: Cumulative Present Value of Net Benefits, Including No Start-up Costs and No Failures

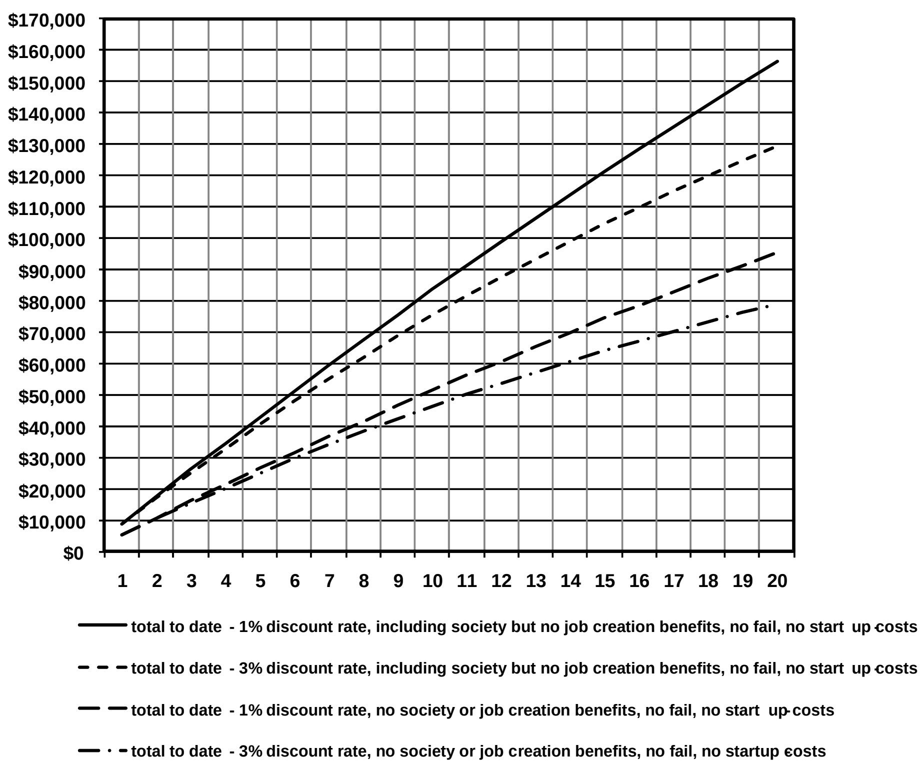

Figure 6-12: Cumulative Present Value of Net Benefits, Including No Start-up Costs and All Fail

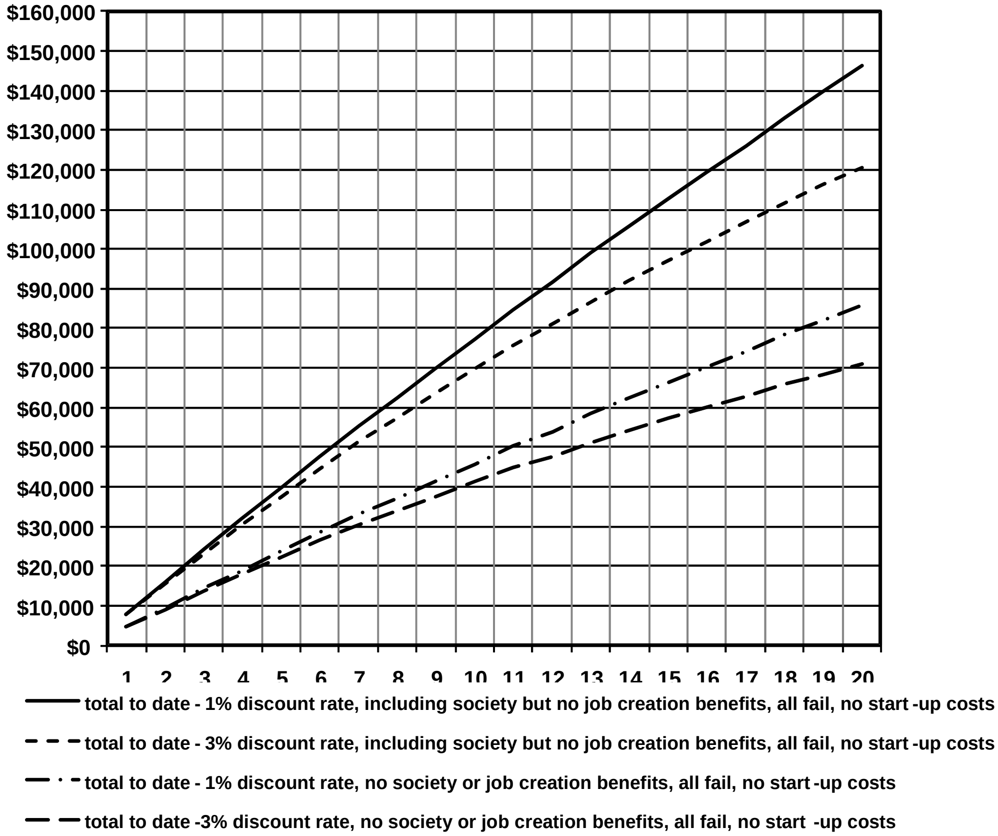

Figure 6-12 compares several scenarios in which startup costs are included, assuming a 1% discount rate for the present value. The general trend shows that excluding societal and job creation benefits lowers the cumulative NPV benefits for the entire 20-year lifespan by about $100,000, with and without considering failures.

Figure 6-13: Cumulative Net Present Value, Including Start-up Costs, 1% Discount Rate

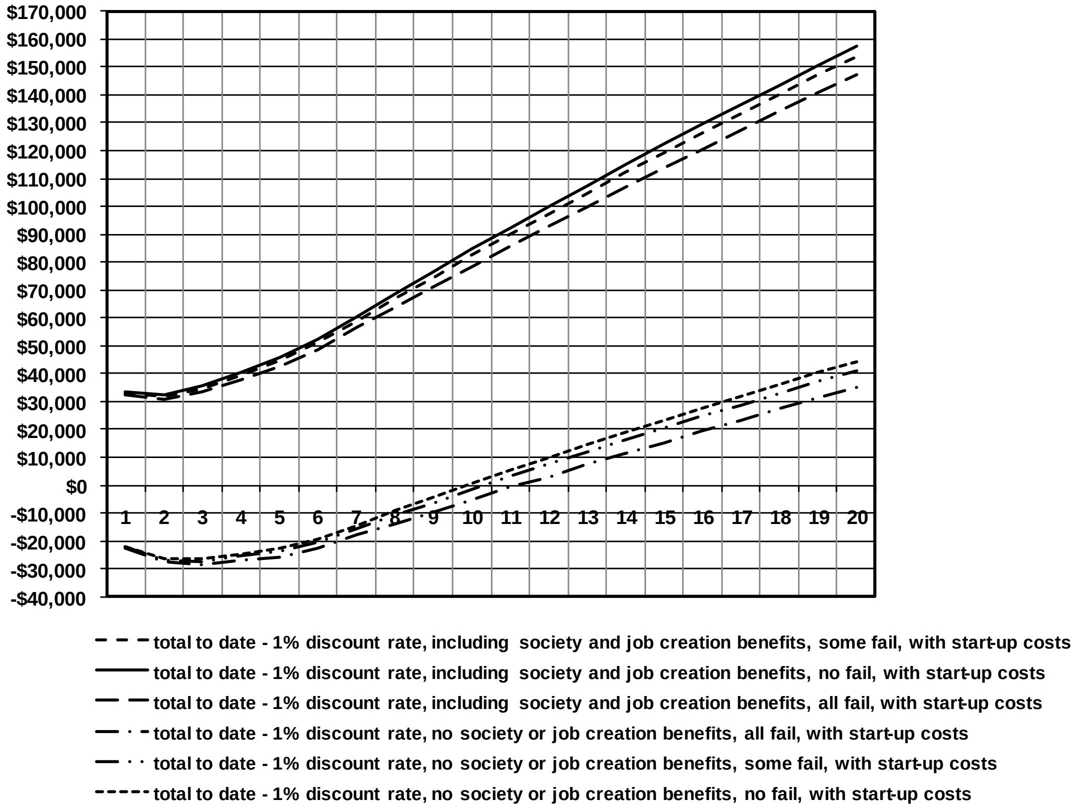

Figure 6-14 shows several cumulative NPV benefits for the situation where startup costs are ignored. Accordingly, job creation benefits are excluded regardless of whether other societal benefits are considered, because it is assumed that the job creation benefits in these models accrue only in the first year, at the time of installation. This exclusion enables us to disentangle the effects of other societal benefits. The NPV of these societal benefits over a 20-year period moving forward is expected to be approximately $50,000.

Figure 6-14: Cumulative Net Present Value, Including No Start-up Costs, 1% Discount Rate

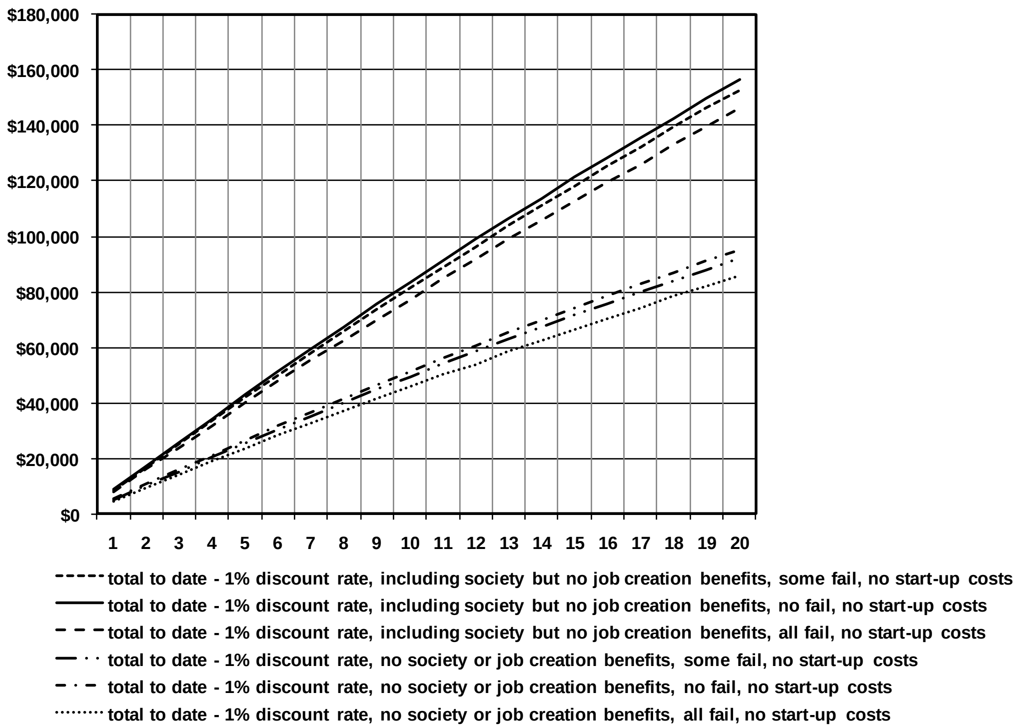

The economic impacts of failures appear to be quite small. As can be seen in Figures 6-15 and 6-16, in all cases the value of the difference between the no failure cases and the corresponding all fail cases are, at most, about $1,000 over the 20-year life cycle.

Figure 6-15: Net Present Value of Societal and Job Creation Benefits

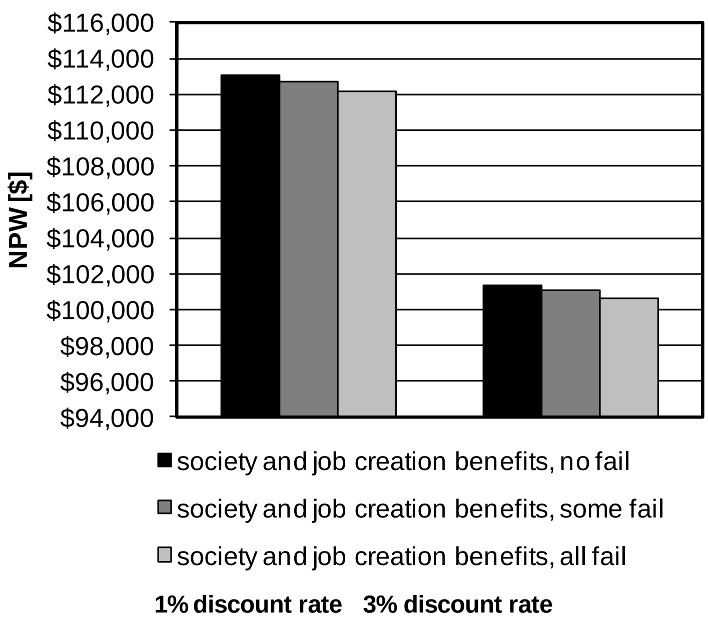

Figure 6-16: Net Present Value of Societal Benefits, with No Start-up Costs

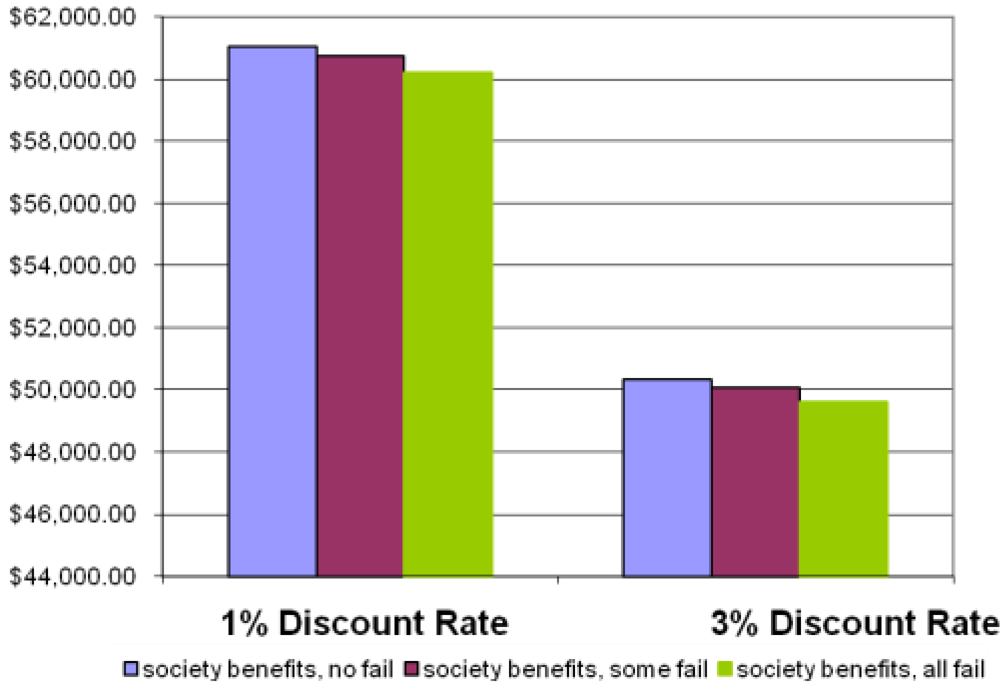

6.11 CONCLUSIONS

The effect of performance on profits was investigated through different scenarios and failures. The engineering model using PSCAD is linked to the economic model SEMS, and the economic benefits that accrue from distributed generation using PV technology are identified. The energy generated per year with and without failures is taken from PSCAD as kWh/yr and entered into the economic model to derive the monetary value in dollars. The economic model aims to show how beneficial or profitable the PV investment will be after 20 years. The net present value (NPV) is taken in each year and totaled to calculate the final value.

6.12 REFERENCES: ECONOMIC ANALYSIS

6-1. Robertson, C. and Cliburn, J.K. "Utility-Driven Solar Energy as a Least Cost Strategy," American Solar Energy Society (ASES) Solar Conference, 2006.

6-2. Whole Life Cost: http://en.wikipedia.org/wiki /Whole-life_cost.

6-3. Life Cycle Costing Analysis. US Dept. of Transportation, Federal Highway Administration, Asset Management, http://www.fhwa.dot.gov/infrastructure /asstmgmt/lcca.cfm.

6-4. National Resources Defense Council, "Facts on Global Warming, http://www.nrdc.org/globalwarming/cost /contents.asp.

6-5. Institute for the Analysis of Global Security, "Energy Security," citing an October 30, 2003 National Defense Council Foundation Report, "The Hidden Cost of Imported Oil," http://www.iags.org/n1030034.htm.

6-6. Environmental Protection Agency, "Acid Rain Program Benefits Exceed Expectations, http://www.epa.gov/ capandtrade/documents/benefits.pdf.

6-7. Institute for the Analysis of Global Security, "How Much Are We Paying for a Gallon of Gas?" http://www.iags.org/costofoil.html.

6-8. New Jersey's Clean Energy Program, "Societal Benefits Charge," http://www.njcleanenergy.com/main/about-njcep/societal-benefits-charge/societal-benefits-charge-sbc.

6-9. greenecon.net/how-to-measure-fuel-efficiency-energy-costs-and-carbon-emissions-for-home-heating/energy_economics.html)

6-10. Contreras, J.L., Frantzis, L., Blazewicz, S., Pinault, D, and Sawyer, H. "Photovoltaics Value Analysis", 2008: NREL/SR-581-423003.

6-11. Marshall, H.E. and Ruegg, R.T. "Simplified Energy Design Economics: Principles of Economics Applied to Energy Conservation and Solar Energy Investments In Buildings", NBS Special Publication 544, U.S. Department of Commerce, NBS: 1980.

6-12. Shirley, W. AEMPFAST Analysis, Optimization, Management. Optimal Technologies International Inc.: 2001.

6-13. Pernick, R. and Wilder, C. (2008). "Utility Solar Assessment (USA) Study: Reaching 10 Percent Solar by 2025," Clean Edge Inc., Co-op America Foundation: 2008.

6-14. Perez, R. and Hoff, T.E. "Energy and Capacity Valuation of Photovoltaic Power Generation In New York," Solar Alliance and the New York Solar Industry Association: 2008.

6-15. Evans, Peter B. "Optimal Portfolio Methodology for Assessing Distributed Energy Resources Benefits for the Energynet." California Energy Commission, April 2005.

6-16. Regional Greenhouse Gas Initiative, http://rggi.org.

6-17. "CT Renewable Energy/Energy Efficiency Baseline Study: Phase I Deliverables," Connecticut Clean Energy Fund (CCEF), http://www.ctcleanenergy.com/Portals/0/Phase%201%20Deliverable%20Final%20Full.pdf, March 2009.

6-18. Baye, M. *Managerial Economics and Business Strategy*, McGraw-Hill: 2010.

Tables 6-3 and 6-4: Net Present Value, with Different Variables

Table 6-3	**1% discount rate**		
	including societal benefits	no societal benefits	Notes
startup cost, no fail	$157,416.46	$44,350.18	no societal benefits case is lower here than for no startup b/c of startup costs
no startup, no fail	$156,369.77	$95,325.27	no job creation, no ITC, no depreciation or tax on depreciation
startup cost, some fail	$153,829.67	$41,078.44	no societal benefits case is lower here than for no startup b/c of startup costs
no startup, some fail	$152,794.86	$92,053.52	no job creation, no ITC, no depreciation or tax on depreciation
startup cost, all fail	$147,074.99	$34,901.34	no societal benefits case is lower here than for no startup b/c of startup costs
no startup cost, all fail	$146,061.96	$85,876.43	no job creation, no ITC, no depreciation or tax on depreciation

Table 6-4	**3% discount rate**		
	including societal benefits	no societal benefits	Notes
startup cost, no fail	$131,193.30	$29,854.13	no societal benefits case is lower here than for no startup b/c of startup costs
no startup, no fail	$129,187.13	$78,859.61	no job creation, no ITC, no depreciation or tax on depreciation
startup cost, some fail	$128,189.03	$27,111.45	no societal benefits case is lower here than for no startup b/c of startup costs
no startup, some fail	$126,194.51	$76,116.93	no job creation, no ITC, no depreciation or tax on depreciation
startup cost, all fail	$122,536.76	$21,938.76	no societal benefits case is lower here than for no startup b/c of startup costs
no startup cost, all fail	$120,563.59	$70,944.24	no job creation, no ITC, no depreciation or tax on depreciation

7.0 Conclusions

7.1 Introduction

We have conducted an applied research program to assess the true costs of a grid connected photovoltaic system (GCPVS). To focus our efforts, we have concentrated on mid-size installations in the 10 to 50 kW range and were able to obtain data from a 17 kW grid-connected working system at the University of Hartford. We have developed performance and economic models for such systems using realistic assumptions and the actual data from our own 17kW installed system. We also assembled an advisory board that included management from the electric power utilities serving our region as well as other participants from industries and companies that work in electric power. Finally, we conducted several site visits of medium-sized PV installations in Connecticut to collect information on the important considerations in GCPVS installation and operation.

We have concentrated our attention on several economic effects that we believe have been underemphasized in previous analyses of PV installations. These effects largely address the relatively new concept in industry of “life cycle costing” [7-1, 7-2] or “whole Life costing.” In many industrial sectors, life cycle costs must be used in the business case analysis and reflected in pricing of products that result from these business cases. In brief, life cycle costing reflects all of the associated costs of ownership of a product from “cradle to grave” including purchase price, operating expenses, maintenance costs, repair costs over the expected lifetime, and disposal and recovery costs after that lifetime has been reached.

In applying the logic of life cycle analysis, we have focused on two important types of economic impact that are often neglected in PV economic models. These are societal benefits and cost of failures. For societal benefits, we identified two distinct benefit types. Results show that one can be easily integrated in the model and confidently justified, whereas other less tangible benefits—though in the end no less real—are more difficult to capture.

7.2 Class I Societal Benefits

In general, we applied societal benefit value streams when we felt they could be reduced to a dollar amount realized by a public utility as an increment to their cost per kilowatt hour. Project members from the utilities helped us to understand and quantify these benefits. These are realistic cost-saving benefits and cost avoidances that can be captured on a balance sheet and would stand up to stockholder, auditor, and public utility commission scrutiny. The benefits to the utility often involve avoidance costs (the cost for adding the next incremental unit of electricity, and not the cost of the mix of sources that a utility may be using for its rate base) [7-3]. For the purpose of these conclusions, we term these the Class I societal benefits.

7.3 Class II Societal Benefits

The Class II societal benefits include those benefits related to the effects of greenhouse gases, acid rain, political instabilities, energy price fluctuations and other ill effects of fossil fuels that are very real but difficult to capture on a balance sheet in way that stands up to generally accepted accounting practices. We do, however, provide assigned values to each effect in a comprehensive list of these intangible benefits. Studies like these will help government agencies and the electric utility industry quantify and explain these benefits. Ultimately, they must be factored into the economics of energy. The accurate economic models of the type our research has developed this can help to move this process toward the ultimate goal of a more comprehensive accounting for these intangible costs.

7.4 Bases of Present Model

The present model is based on three independent, computer-based procedures developed in the course of this research program. The first is the random simulation treatment, MultiC_Risk, which is used to predict time to failure and time to repair for GCPVS. The second is PSCAD software for the modeling of GCPVS that, using the repair times, can calculate the loss of or reduction in power related to the component failures identified from the Multi_CRisk models. We used Weibull distribution functions with failure rate constants gleaned from the limited data of PV failures to develop realistic failure and loss/reduction of power models. The third procedure developed is a series of Excel[R]-based calculations that use accounting categories such as expenses and income, and include the cost and performance of the GCPVS from PSCAD. These are then factored into a calculation of the net present value over the 20-year lifetime of a hypothetical 17kW PV system intended to represent the University of Hartford's Lincoln Theater before its construction (see #4 below). The results from these mathematical models are realistic and we are confident that they can be extended to systems of 5MW that might be used as supplementary power in generation plants for electric power. The three software packages are a valued addition to the toolset that can be applied to analyze and justify investment in PV arrays.

Our conclusions fall into three major areas: **economic/financial** (see conclusions in 1-8), **engineering/optimization** (see conclusions 7-10), and **recommendations for follow-up work** (see conclusions 9-12).

1. Price of Installation vs. Price of PV Panels

Our cost analysis concludes that the price of an installed PV array is now dominated by the price of the installation rather than by the price of the PV panels themselves. The term "cost" means the actual cost for an item, whereas the term "price" reflects the amount paid for a good or service, which is usually much greater than the cost for a product to be viable. Near the end of our program, we found ample evidence that PV array prices had been reduced to the \$1.00-\$2.00/kW range, depending on technology and efficiency ratings. However, the most accepted prices for <u>installed</u> PV arrays are still in the \$6.00-\$7.00/kW range, meaning that installation is now dominating the overall prices. This is a situation that should be addressed.

The PV industry clearly needs to develop accepted best practices for mounting PV arrays that can be widely accepted as low cost standards. The DOE can and should play a role in this standardization. Like any large outdoor installation, a PV array has many safety and reliability criteria that must be met. There are important legal liabilities for installations of this size in proximity to buildings, roads, cars, and pedestrians; hence there is a tendency to overbuild. It appears that many installations involve substantial and custom mounting fixtures in either a ground or roof installation. And although the cost of the panels themselves has been extensively studied and optimized with excellent results, the mountings remain custom-built and expensive. As a result, even if the PV panels themselves were made available free of charge, the total cost of a PV installation could still not be competitive with MW fossil fuel plants.

As construction of the mounts are labor intensive, the price of PV installation will generally rise faster than the cost of living since in its current manifestation it offers little in the way of economies of scale built into its cost structure. The DOE can play an important role in addressing this inconvenient reality by endorsing and funding studies that determine the installation guidelines for different latitudes. This could entail finite element models of low cost and modular structures that could withstand gale force winds and other natural phenomena that provide reliability and safety risks in PV arrays. There could be unconventional solutions that can lead to overall cost reductions such as constructing a wind deflection wall around or among the array panels to allow a far less expensive mounting solution to be used. Similarly, there could be a series of baffles throughout the array that would control the "boundary layer" winds near the surface or even provide downward drafts to help hold the panels in place in the face of gale force shearing winds. These are engineering problems that are well known in aerodynamics, and they could be readily applied to lowering the cost of installed PV arrays around tested best practices. Such solutions would provide the important economies of scale of an industry standard. With DOE endorsement, a supplier base for these standard mountings would quickly develop and the United States would have a distinct advantage if it were tied to special software or algorithms that help select the standard equipment to be used.

2. Class I Societal Benefits and PV Array Costs

Neglecting the Class I societal benefits, those directly captured as a cost increment per kW hour generated by the utility, can have a very large impact on the net benefits estimates, even for a small PV array (17kW) such as that on UH's Lincoln Theater. In this context, we have shown that ignoring these societal benefits can make the difference between whether the net present value of the array (benefits) is positive or negative. While we have included the Class I societal benefits, further research and the suggested costs provided in our current research could help quantify a more comprehensive set of these societal benefits, many of which are currently considered to be "intangible."

3. Societal Benefits: Individual or Societal?

An important consideration regarding the societal benefits is that the majority of those benefits accrue to individuals other than the owners of the PV array. This is important because it implies that there may be under-investment in PV systems because the owners of PV compare only the benefits to themselves against the costs to themselves when determining whether PV is a viable investment. This is a form of market failure where the free market does not lead to the most efficient solution. Economists term this an externality [7-4] since the effects of a decision are largely felt by others and not the person who makes the decision, because the effects are not reflected in the market price. Accordingly, there may be a greater role for state and/or federal government to subsidize PV further to help private PV owners realize or "internalize" the true net benefits to themselves as well as to society when they are considering whether to undertake the investment. In other words, should they be compensated for the societal benefits that accrue to the society and not directly to themselves?

4. Life Cycle Costs and Benefits

We have introduced the concept of life cycle costs in the consideration of benefits associated with fossil fuels and demonstrated that calculating the life cycle costs of a gallon of gasoline would add about $3.70 to the cost of a gallon of regular at the pump. Using similar logic and data, the life cycle costs of fuel used to generate electrical power would add $0.02/kWh. The 17kW installation discussed in this work would therefore accrue approximately $3,000 of societal value per year. Although this is not a particularly large number, it is a real and effective estimate of the life cycle costs that a PV system holds vs. a partly fossil fueled electrical power system. Although it is premature to actually collect and transfer this 2 cents per kWh cost, it could be developed into a form of carbon trading, allowing companies with small- to medium-size PV installations to capture these societal benefits and place a definite dollar amount on them that would then appear in their own business case.

5. Relatively Small Dollar Impact of Failures

With regard to failures in power generation from PV arrays, our models showed that allowing for failures and the reduction or loss of generation had a relatively small dollar impact on the net benefits for a small PV array such as the one on Lincoln Theater. A further area of research could be to explore if this conclusion holds up for larger PV arrays as well, using failure data that is specific to those larger arrays. We strongly encourage the collection of these data to further the development of accurate economic models for large utility scale PV arrays.

6. Net Benefits Moving Forward

The Lincoln Theater PV array that we analyzed had been installed and in operation for quite some time before our analysis began. So in this case, we really were addressing the net benefits moving forward. This situation is different from that of a proposed PV array under consideration for purchase and installation, since in the latter case a decision to install the PV must include considering the full installation and other startup costs. We have addressed both scenarios in the economic models for the Lincoln Theater PV array. For the post-installation analysis, assuming a 1% discount rate, we find much smaller net benefits when societal benefits were not included (that is, the net benefits when excluding societal benefits was about 61% of the net benefits when societal benefits were included). The corresponding percentage was also about 61% when we assumed a 3% discount rate. Although this had no effect on the decision to install since that decision was made years ago in the absence of the economic analysis we developed in this research, such knowledge would have had a profound effect on the pre-purchase decision. In the 1% discount rate scenario including startup costs, the net present value when excluding societal benefits is only about 28% of the net present worth including the societal benefits. Similarly, with a 3% discount rate, in the scenario with startup costs, the net present value when excluding societal benefits is only 22% of the net present value when including these societal benefits. This indicates that more realistic economic models will not necessarily encourage the greater implementation of PV arrays unless the societal benefits to the utility are properly recognized and considered. A summary of the benefits we found under a variety of representative conditions is provided in the tables below:

Table 7-1	**1% discount rate**		
	including societal benefits	no societal benefits	Notes
startup cost, no fail	$157,416.46	$44,350.18	no societal benefits case is lower here than for no startup b/c of startup costs
no startup, no fail	$156,369.77	$95,325.27	no job creation, no ITC, no depreciation or tax on depreciation
startup cost, some fail	$153,829.67	$41,078.44	no societal benefits case is lower here than for no startup b/c of startup costs
no startup, some fail	$152,794.86	$92,053.52	no job creation, no ITC, no depreciation or tax on depreciation
startup cost, all fail	$147,074.99	$34,901.34	no societal benefits case is lower here than for no startup b/c of startup costs
no startup cost, all fail	$146,061.96	$85,876.43	no job creation, no ITC, no depreciation or tax on depreciation

Table 7-2	**3% discount rate**		
	including society benefits	no society benefits	Notes
startup cost, no fail	$131,193.30	$29,854.13	no societal benefits case is lower here than for no startup b/c of startup costs
no startup, no fail	$129,187.13	$78,859.61	no job creation, no ITC, no depreciation or tax on depreciation
startup cost, some fail	$128,189.03	$27,111.45	no societal benefits case is lower here than for no startup b/c of startup costs
no startup, some fail	$126,194.51	$76,116.93	no job creation, no ITC, no depreciation or tax on depreciation
startup cost, all fail	$122,536.76	$21,938.76	no societal benefits case is lower here than for no startup b/c of startup costs
no startup cost, all fail	$120,563.59	$70,944.24	no job creation, no ITC, no depreciation or tax on depreciation

7. Summary Discussion of Economic Values

There are a variety of reasons why the net benefits differ under the various scenarios presented in Tables 7-1 and 7-2. First, in Table 7-1, in the startup costs case where there are no failures, the net benefits estimate is about $157,000 when societal benefits are included, opposed to only about $44,000 when societal benefits are excluded. This implies a net present value for the societal benefits of about $113,000. These societal benefits include the job creation benefit estimates, among the others discussed above. The job creation benefits are assumed to accrue in the first year at the time of installation. When startup costs are ignored in the scenario where there are no failures, the net benefits estimate is only slightly less (about $156,000) when societal benefits are included, while amounting to about $95,000 when societal benefits are ignored.

It is interesting to note that while the case including societal benefits in the no-startup costs case has lower net present value than the corresponding scenario in the startup costs case ($157,000 opposed to $156,000), the case excluding societal benefits in the no-startup costs case has much higher net present value than the corresponding scenario in the startup costs case ($95,000 opposed to $44,000). When including societal benefits, the reason for the small discrepancy between the startup and no-startup cases is that there are no job creation benefits, investment tax credits (ITC), depreciation or depreciation taxes in the no-startup case, while this is offset by the lack of startup costs when the system is already in place. But the no societal benefits case in Table 7-1 has higher net benefits with no-startup costs than with startup-costs, because of the approximately $100,000 of avoided startup costs, although the lack of these startup costs imply no job creation benefits (which have an approximate value of $50,000).

When we consider failures, the economic values are even smaller for each scenario. For instance, there is approximately a 2.5% discrepancy (about $4,000) between the net present value benefits in the no failure vs. some failure cases, when startup costs and societal benefits are included in both situations. The corresponding discrepancy is about 4% (or $6,000) between the same scenarios for the “some failures” and “all fail” cases. This finding implies that as the number of IGBT failures rises, the impact on the net present value benefits rises as well. In other words, when 1 inverter fails in the “some failures” case, a 200% rise in the number of inverter failures (from 1 to 3) leads to a difference in net present value benefits by about 50% (from $4,000 to $6,000 in the startup costs including societal benefits scenario).

With startup costs and no societal benefits, the discrepancy between present value benefits for no failure vs. the some failure cases is only about $3,000 but it is higher in percentage terms (6.8%). On the other hand, moving from some failures to all failures in the same scenario leads to a $6,000 difference (nearly 15%). So the cost of failures is higher in percentage terms when societal benefits are excluded, because the starting net benefits are less due to no society benefits in the initial net benefits. But the higher cost of failures is still less than proportional to the number of inverter failures (that is, moving from 1 to 3 failures—a 200% increase—leads to a 15% loss in economic value). The magnitude of the respective net present value differences are comparable in the no-startup cases.

8. Understanding Actual Net Present Value

Our realistic economic model, which accounts for value contributions of realistic failures and defensible Class I societal benefits, is an important first step in understanding actual net present values of PV systems. The results confirm the need to include societal benefits that can be realized by the utility as a direct contribution to cost per kW. Without societal benefits, the benefits are marginal and PV installations would not progress without continued government subsidies. With societal benefits that can be realized by the utility, the case for PV installations becomes far stonger and is far more justified.

9. Quantifying Net Present Value Benefits

We encourage the DOE, other state/local government and regulatory bodies, and nonprofits to continue this work attempting to quantify the life cycle costs of fossil fuels as measurable net present value benefits to PV and other clean energy alternatives. By collecting and analyzing referenced estimates for just four of the intangible or Class II societal benefits (rising CO_2 levels, acid raid, political instability, and trade imbalance costs), we estimate that nearly $3.70 should be added to the life cycle cost of a gallon of gasoline in the United States. The situation for electric power generation is not as compelling since the fuel source is far more domestic based and also contains an appreciable fraction that is not fossil fuel. The Class II benefits that apply to electric power generation (global warming, acid rain) also have an economic impact, but these are more difficult to justify, and are far below the value of PV installations to the utility. However, they do appear to be at least 10% of the standard utility bill, and if added to the subsidy funds for PV and other renewable sources, they would make an immediate and positive effect. These benefits were not included in the results provided in Tables 7-1 and 7-2. We recommend continued work to quantify and drive acceptance of these costs into the electric power rate base. Only then will electric power generation be aligned with other industry sectors that have moved to life cycle costing in assessing business case values.

10. Suggested Calculation Improvements

With regard to the models themselves, we believe the following improvements would make the calculation stream more user-friendly, reduce the manual calculations necessary, provide results in a more useable form, and raise the overall confidence in the model by allowing it to be applied more readily and to a wider variety of arrays.

- ***Seamless Calculation:*** The three separate software modules should be written in a one code language such as MATLAB, C++, or other advanced language. Each calculation should include Input-Calculations-Output, both in tabular and graphic formats.

- ***Solar Insolation***: Currently, the TMY2 database is used to calculate insolation, in this case, for Hartford, Connecticut. Since TMY2 is a statistical combination of 30 years of NOAA data, it may not provide accurate values when compared to present local solar and atmospheric conditions. For design purposes, a pyrometer can be used to measure insolation and transmit this in real time to a database. For operating performance and effect on the financial results, most installations have means to measure and document real time values of insolation. This capability should be considered in the seamless calculation model.

11. Options for Monitoring Arrays

There have been numerous efforts to monitor current, voltage and power, for indications of failures of module and inverter components. However, performance is still dependent on actual failures and reduction in the generated power. As units go from W to kW to MW and higher, the number of solar cells, modules and arrays as well as inverters, connections, and cabling all increase. Thus, it may become far more difficult to determine if failures in one or a few components have reduced power, normalized to some baseline value. While the task may be daunting, we strongly support pursuing technical options to detect both the "signatures" of incipient failures, and to develop the means to detect occurred failures in large arrays where the incremental impact may be small. The alternative is a slow degradation of power (and economic value) by accumulated component failures that may be attributed to various other effects including fouling of the PV surfaces, insolation variability, and other nonfailure causes.

12. PSCAD and RAM

PSCAD is a state-of-the-art code for modeling the dynamic behavior of electro-magnetic circuits. The code was used to model the Lincoln Theater GCPVS, including the solar modules, the control systems and, most importantly, the inverters. The one shortcoming noted was not the code itself but the availability of sufficient RAM to be able to simulate failures and repair times for the 20 years of warranteed life. Due to lack of RAM, we used 20 one-year operating period calculations performed by MultiC_Risk. Then, after altering the output format, the year had to be scaled to the 60 seconds of run time that could be supported by the available RAM. This was not only time consuming but also presents a problem when time before failure (TBF) and time to repair (TTR) extended over the limit of one-minute of computation. While RAM can be increased, it is not clear that this alone is the cause of the time limitations. The potential influence on results for both TBF and TTR places a high priority on addressing this limitation.

13. Database Availability for Research
Both the NREL and the SNL under the DOE have collaborated on establishing a database to document operational occurrences for component failures [7-5]. This computerized database is available to OEMs that are manufacturing, installing, maintaining, and operating GCPVS. There is no cost for participating. Active participation involves OEMs entering data into the database, which then allows the vendors access to experiences and data of other participants. In addition, the participants and DOE are party to a nondisclosure agreement to protect participants' proprietary and confidential information.

One drawback that affected our program was that this database is not available to noncommercial institutions, such as colleges, universities, and non-profit, non-competing research organizations. This lack of access to key data significantly inhibits their ability to investigate topics, ranging from more efficient solar cells to improved inverters, with the actual data that has been collected. Ongoing research and other studies by these non-profit organizations that could resolve technical or policy issues also are impeded by this lack of access. We recommend that access to this extremely valuable database be allowed without identifying the participants, but with prior approval of the participants, and agreement of the DOE, NREL and SNL.

7.5 REFERENCES

7-1. Whole life cost. http://en.wikipedia.org/wiki/Whole-life_cost

7-2. "Life Cycle Cost Analysis," U.S. Department of Transportation, Federal Highway Administration, Asset Management: http://fhwa.gov/infrstructure/asstmgmt/lcca.cfm.

7-3. "Economic Modeling of Avoided Costs: A Basis for Renewable Energy Financing in Challenging Times," Financing Renewable Energy Symposium, University of Maryland: September 22, 2009.

7-4. Heller, W.P., Starrett, D.A. "On the Nature of Externalities," in S. Lin (ed.), Theory and Measurement of Economic Externalities, New York: Academic Press, 1976: 10; as found in http://en.wikipedia.org/wiki/Environmental_externalities.

7-5. Collins, E., et al. "Reliability and Availability Analysis of a Fielded Photovoltaic System," IEEE 978-1-2950, Sept. 2009: 002316-2321.

8.0 BIBLIOGRAPHY

ELCC Values

Garver, L.L. Effective Load Carrying Capability of Generating Units. *IEEE Transactions on Power*, v85, n8: 1966.

Hoff, T., Perez, R. "Photovoltaic Capacity Valuation Methods." SEPA Report 02-08: May 2008.

Perez, R., Margolis, R. "Update: Effective Load Carrying Capability of Photovoltaics in the United States." NREL/CP-620-40068: June 2006.

Values

Contreras, J.L., et al. "Photovoltaics Value Analysis." NREL/SR-581-42303: February 2008.

Robertson, C., Cliburn, J.K. "Utility-Driven Solar Energy as a Least-Cost Strategy to Meet RPS Policy Goals & Open New Markets." ASES Solar Conference: 2006.

Costs

NREL. "National PV Cost Values." NSTUC-7 Member Consortium for PV Resource Characterization.

Reliability

Bosco, N. "Reliability Concerns Associated with PV Technologies." NREL.

CANMET Energy, Report 2010-122 (RP-TEC) 411-IEARES; March 31, 2010 (Canadian Centre for Mineral and Energy Technology).

Chan, F., et al. "Grid Connected PVB Systems: A Reliability-Based Comparison." IEEE/ISIE 2006, Montreal, Quebec, Canada. 2006: 1583-88.

Collins, E., et al. "Field Data Collection for Quantification of Reliability &Availability for PV Systems and Availability for Photovoltaic Systems." 35th IEEE Photovoltaic Specialist Conference: June 10, 2010. SAND2010-3362-C.

Granata, J.E., et al. "Long-Term Performance and Reliability Assessment of 8 PV Arrays at Sandia National Laboratories." 34th IEEE PVSC, Philadelphia, PA. June 2009: SAND2009-3485C.

Kurtz, S., et al. "Photovoltaic-Reliability R&D Toward a Solar-Powered World." NREL/CP-520-44886: August 2009.

Lee. S.W., Lee, H.K. "Reliability Prediction System Based on Failure Rate Model for Electronic Components." *Journal of Mechanical Science & Technology*, v22, 2008: 957-64.

Loescher, D.H. "Predicting the Reliability of Electronic Circuits." SAND-2004-2377 C.2: 2005.

Maish, A.B., et al. "Photovoltaic System Reliability." 26th IEEE Photovoltaic Specialist Conference, Anaheim, CA. 1997: 1049-54.

Osterwald, C.R. *History of Accelerated & Qualification Testing, Progress in Photovoltaic Research and Applications*. Wiley Interscience: November 2008.

Pecht, M.G., et al. "Predicting the Reliability of Electronic Equipment." *Proceedings of the IEEE*, v82, n7. July 1994: 992-1004.

Pregeli, A. ,Begovic, M., Rohatgi, A. "Impact of Inverter Configuration on PV System Reliability and Energy Production." Photovoltaic Specialists Conference, 2002. Conference Record of the Twenty-Ninth IEEE. May 2002: 1388-91.

Ristow, A., Begović, M., Rohatgi, A. "Modeling the Effects of Uncertainty & Reliability on the Cost of Energy from PV Systems." 20th European Solar Energy Conference & Exhibition. Barcelona, Spain: June 6-10, 2005.

Wohlgemuth, J.H., et al. "Reliability and Performance Testing of Photovoltaic Modules." Proceedings of the 28th IEEE PV Specialists Conference. Anchorage, Alaska. 2000: 1483-86.

Performance

Barker, G., Norton, P. "Predicting Long-Term Performance of Photovoltaic Arrays Using Short-Term Test Data and an Annual Simulation Tool." Solar 2003 Conference America's Secure Energy. Austin, TX, 2003. NREL/CP-550-33601.

Begovic, M., et al."Four-year Performance Assessment of the 342kW PV System at Georgia Tech." 28th IEEE Photovoltaic Specialists Conference. Anchorage, AK, September 15-22, 2000: 1575-78.

Begovic, M., Ghosh, S.R., Rohatgi, A. "Decade Performance of a Roof-Mounted Photovoltaic Array." Conference Record of the 2006 IEEE 4th World Conference on Solar Energy. May 2006: 2383-86.

King, D.L., et al. "Photovoltaic Module Performance." SAN-098-2112 C: October 1998.

Lashway, C. "Photovoltaic System Testing Techniques and Results." *IEEE Transactions on Energy Conversion*, v3, n3, September 1988: 503-06.

Marion, B., Adelstein, J., et al. "Performance Parameters for Grid-connected PV Systems." Proceedings of 31st IEEE Photovoltaic Specialists Conference. Lake Buena Vista, FL. January 2005: NREL/CP-520-37358.

Moore, L., Post, H. "Power Plant Experience at Tucson Electric Power." *Energy Conversion and Resources*, v2, 2005: 387-394.

Moore L., Post, H., et al. "Five Years of Operating Experience at a Large, Utility-scale Photovoltaic Generating Plant." *Progress in Photovoltaics: Research and Applications*, v13, 2008: 249-59.

Simulation

Firth, S.K., Lomas, K.J., Rees, S.J. "A Simple Model of PV System Performance and Its Use in Fault Detection." *Solar Energy*, v84, 2010: 624-35.

Kuei, H., et al. "Modeling and Fault Simulation of Photovoltaic Generation Systems Using Circuit-based Model." Sustainable Energy Technologies,2008 ICSET-2008, Singapore. January 2009: 290-94.

Kim, Seul-Ki, et al. "Modeling and Simulation of a Grid-connected PV Generation System for Electromagnetic Transient Analysis." *Solar Energy*, v83, n5, 2009: 664-78.

Marion, B. "Comparison of Predictive Models for Photovoltaic Module Performance." 33rd IEEE Photovoltaic Specialists Conference. San Diego, CA, May 2008: NREL/CP-520-42511.

Stellbogen, D. "Use of PV Circuit Simulation for Fault Detection in PV Array Fields." 23rd IEEE Photovoltaic Specialist Conference: 1993.

Xuc, J., et al. "Design of PV Array Model Based on EMTDC/PSCAD. 2009 Asia-Pacific Power & Energy Engineering Conference, Wuhan, China: March 2009.

Bibliography

Availability

Collins, E., et al. "Reliability and Availability Analysis of a Fielded Photovoltaic System." Conference Record of the 34th IEEE Photovoltaic Specialists Conference. June 2009: 2316-21.

Du, Y. "Availability Analysis & Design Optimization of Photovoltaic Systems." *Advances in Information Service Sciences*, v3, n2. March 2009: 170-76.

Realini, A. "MTBF: Mean Time Before Failure in PV Modules." Final Report; BBW 99.0579: June 2003.

Ristow, A., Begović, M., Rohatgi, A. "Numerical Approach to Uncertainty and Sensitivity Analysis in Forecasting the Manufacturing Cost and Performance of PV modules." Proc. 19th European Photovoltaic Solar Energy Conference. Paris, France, June 2004: 2178-81.

Reliability

Andrews, J.D., Moss, T.R. *Reliability and Risk Assessment*, 2nd edition. ASME Press: 2002.

Chapter 1: "An Introduction in Reliability and Risk Assessment."

Chapter 5: "Quantification of Component Failure Probabilities."

Chapter 6: "Reliability Networks."

Chapter 11: "Simulation."

Billinton, R., Ringlee, R.J., Wood, A.J. *Power-System Reliability Calculations*. MIT Press Classics: 1973.

Farret, F.A., Godoy-Simoes, M. *Integration of Alternative Energy Sources*. *Wiley*-Interscience: 2006.

Granger, J.J., Stevenson, W.D. *Power Systems Analysis*. McGraw-Hill: 1994.

U.S. Department of Defense. Electronic Reliability Design Handbook. MIL-HDBK-338B: October 1998.

Vose, D. *Risk Analysis: A Quantitative Guide.* 3rd edition. John Wiley & Sons: 2008.

General References

Andrews, J.D., Moss, T.R. *Reliability and Risk Assessment*. ASME Press: 2002.

Barker, G., Norton, P. "Predicting Long-Term Performance of Photovoltaic Arrays Using Short-Term Test Data and an Annual Simulation Tool." Solar 2003 Conference America's Secure Energy, Austin, TX, 2003: NREL/CP-550-33601.

Begovic, A, Rohatgi, M. "Impact of Inverter Configuration on PV System Reliability and Energy Production." Photovoltaic Specialists Conference, 2002. Conference Record of the Twenty-Ninth IEEE, May 2002: 1388-91.

Begovic, M., et al. "Four-year Performance Assessment of the 342kW PV System at Georgia Tech." 28th IEEE Photovoltaic Specialists Conference, Anchorage, AK, September 15-22, 2000: 1575-78.

Begovic, M., Ghosh, S. R., Rohatgi, A. "Decade Performance of a Roof-Mounted Photovoltaic Array." Conference Record of the 2006 IEEE 4th World Conference on Solar Energy, v2, May 2006: 2383-86.

Billinton, R., Ringlee, R.J., Wood, A.J. *Power-System Reliability Calculations*. MIT Press Classics: 1973.

Bosco, N. Reliability Concerns Associated with PV Technologies. NREL.

CANMET Energy. Report 2010-122 (RP-TEC) 411-IEARES. March 31, 2010.

Chan, F, et al. "Grid Connected PVB Systems: A Reliability-Based Comparison." IEEE/ISIE 2006, Montreal, Quebec, Canada, 2006: 1583-88.

Bibliography

Collins, E., et al. “Field Data Collection for Quantification of Reliability &Availability for PV Systems and Availability for Photovoltaic Systems.” 35th IEEE Photovoltaic Specialist Conference, June 10, 2010: AND2010-3362.

Collins, E, et al. “Reliability and Availability Analysis of a Fielded Photovoltaic System.” Conference Record of the 34th IEEE Photovoltaic Specialists Conference, June 2009: 2316-21.

Contreras, J.L., et al. “Photovoltaics Value Analysis.” NREL/SR-581-42303. February 2008.

Du, Y. “Availability Analysis & Design Optimization of Photovoltaic Systems.” *Advances in Information Service Sciences*, v3, n2, March 2008: 170-76.

Firth, S.K., Lomas, K.J., Rees, S.J. “A Simple Model of PV System Performance and Its Use in Fault Detection.” *Solar Energy*, v84, 2010: 624-35.

Garver, L.L., “Effective Load Carrying Capability of Generating Units.” IEEE Transactions on Power, v85, n8: 1966.

Granata, J.E., et al. “Long-Term Performance and Reliability Assessment of 8 PV arrays at Sandia National Laboratories.” 34th IEEE PVSC, Philadelphia, PA, June 2009: SAND2009-3485C.

Granger, J.J., Stevenson, W.D. *Power Systems Analysis*. McGraw-Hill: 1994.

Hoff, T., Perez, R. “Photovoltaic Capacity Valuation Methods.” SEPA Report 02-08. May 2008.

Kim, S.K., et al. “Modeling and Simulation of a Grid-connected PV Generation System for Electromagnetic Transient Analysis.” *Solar Energy*, v83, n5, 2009: 664-78.

King, D.L., et al. “Photovoltaic Module Performance.” SAN-098-2112 C: October 1998.

Kuei, H., et al. “Modeling and Fault Simulation of Photovoltaic Generation Systems Using Circuit-based Model.” Sustainable Energy Technologies,2008 ICSET-2008, Singapore, January 2009: 290-94.

Kurtz, S., et al. “Photovoltaic-Reliability R&D Toward a Solar-Powered World.” NREL/CP-520-44886: August 2009.

Lashway, C. “Photovoltaic System Testing Techniques and Results. IEEE Transactions on Energy Conversion, v3, n3, September 1988: 503-06.

Lee, S.W, Lee, H.K. “Reliability Prediction System Based on Failure Rate Model for Electronic Components.” *Journal of Mechanical Science & Technology*, v22, 2008: 957-64.

Loescher, D., Pregeli, H. “Predicting the Reliability of Electronic Circuits.” SAND-2004-2377 C.2: 2005.

Maish, A.B., et al. “Photovoltaic System Reliability.” 26th IEEE Photovoltaic Specialist Conference, Anaheim, CA, 1997: 1049-54.

Marion, B. “Comparison of Predictive Models for Photovoltaic Module Performance.” 33rd IEEE Photovoltaic Specialists Conference, San Diego, CA, May 2008: NREL/CP-520-42511.

Marion, B., Adelstein J., et al. “Performance Parameters for Grid-connected PV Systems.” Proceedings of 31st IEEE Photovoltaic Specialists Conference, Lake Buena Vista, FL, January 2005: NREL/CP-520.

Moore, L., Post, H. “Power Plant Experience at Tucson Electric Power.” Energy Conversion and Resources, 2005: 387-94.

Moore, L., Post, H., et al. “Five Years of Operating Experience at a Large, Utility-scale Photovoltaic Generating Plant.” Progress in Photovoltaics: Research and Applications, v13, 2008: 249-59.

NREL. National PV Cost Values. NREL. NSTUC-7 Member Consortium for PV Resource Characterization. December 21, 2009.

Osterwald, C.R. “History of Accelerated & Qualification Testing.” Progress in Photovoltaic Research and Applications. November 2008, 33.

Pecht, M.G., et al. “Predicting the Reliability of Electronic Equipment.” *Proceedings of the IEEE*, v82, n7, July 1994: 992-1004.

Bibliography

Perez, R., Margolis, R. “Update: Effective Load Carrying Capability of Photovoltaics in the United States.” NREL/CP-620-40068. June 2006.

Realini, A. “MTBF: Mean Time Before Failure PV Modules.” Final Report; BBW 99.0579. June 2003.

Ristow, A. Begović, M. Rohatgi, A. “Modeling the Effects of Uncertainty & Reliability on the Cost of Energy from PV Systems.” 20th European Solar Energy Conference & Exhibition. Barcelona, Spain: June 6-10, 2005.

Ristow, A., Begović, M., Rohatgi, A. “Numerical Approach to Uncertainty and Sensitivity Analysis in Forecasting the Manufacturing Cost and Performance of PV Modules.” Proc. 19th European Photovoltaic Solar Energy Conference, Paris, France, June 2004: 2178-81.

Robertson, C., Cliburn, J.K. “Utility-Driven Solar Energy as a Least-Cost Strategy to Meet RPS Policy Goals & Open New Markets.” ASES Solar 2006 Conference.

Stellbogen, D. “Use of PV circuit Simulation for Fault Detection in PV Array Fields.” 23rd IEEE Photovoltaic Specialist Conference, 1993.

U.S. Department of Defense. *Electronic Reliability Design Handbook*. MIL-HDBK-338B: October 1998.

Wohlgemuth, J.H., et al. “Reliability and Performance Testing of Photovoltaic Modules.” Proceedings of the 28th IEEE PV Specialists Conference, Anchorage, AK, 2000: 1483-86.

Xuc, J., et al. “Design of PV Array Model Based on EMTDC/PSCAD2009.” Asia-Pacific Power & Energy Engineering Conference, Wuhan, China: March 2009.